# ANNIC 2016

## Applied NANOTECHNOLOGY and NANOSCIENCE International Conference

# BOOK OF ABSTRACTS

University Pompeu Fabra, Barcelona

Nov 9–11, 2016

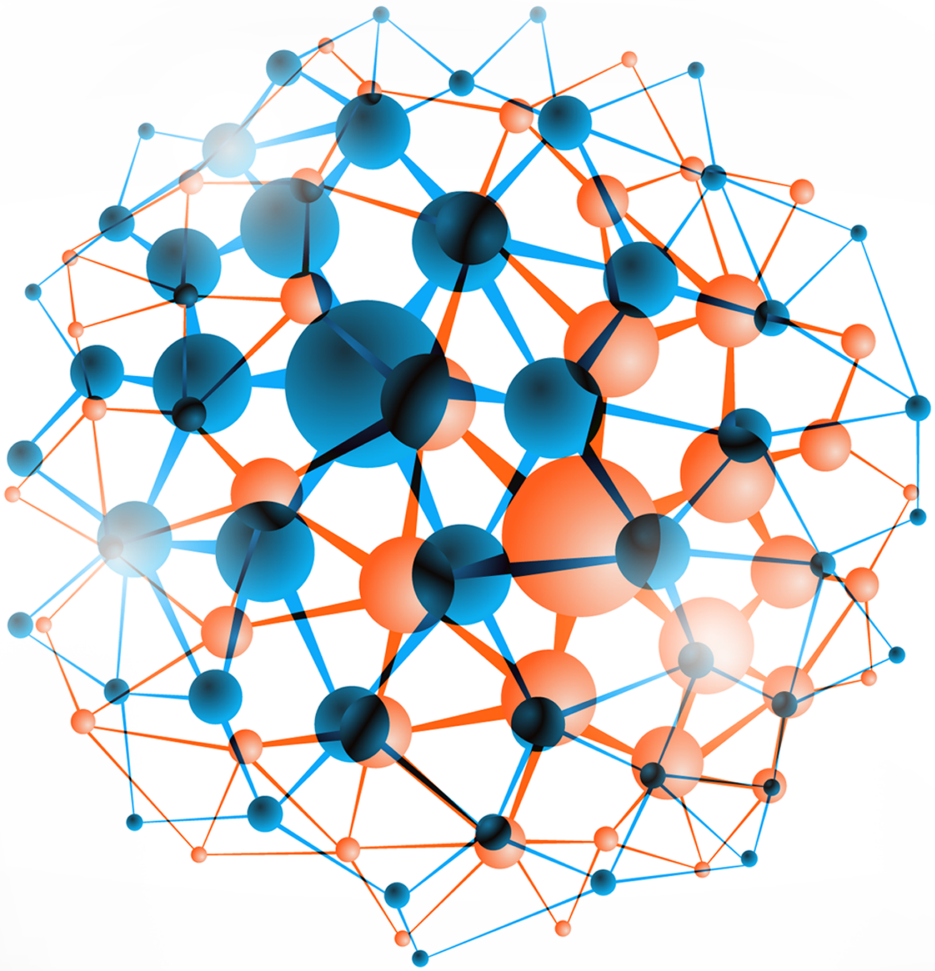

PremC

premc.org/annic2016

# Table of Contents

**Surface chemical reactions at self-heated metal oxide nanowires** 1
Prof. Joan Ramon Morante

**Composite nanostructures for high-efficiency excitonic solar cells** 2
Prof. Alberto Vomiero

**A close look to the atoms: a journey to the nanoworld through advanced electron microscopy** 3
Prof. Jordi Arbiol

**Catalytic Nano-and Micro-bots: What for?** 4
Prof. samuel sanchez

**Cluster particle's deposition on rough surfaces; Effects of diffusion and cluster's shape** 5
Dr. Amir Ali Masoudi, Dr. Leila Hedayatifar, Dr. Foroogh Hassani, Dr. Shadi Esmaily, Dr. Danial Khorsandi, Ms. Zahra Madadi

**A RNA nanotechnology platform for a simultaneous two-in-one siRNA delivery and its application in synergistic RNAi therapy** 7
Dr. Hyung Jun Ahn

**Preparation of a Highly Porous Carbon Nitride by a Facile Post-Synthetic Method** 8
Mr. Tomoyuki Iwamoto, Prof. Yoichi Masui, Prof. Makoto Onaka

**Investigation of porous Si, formed by metal-assisted chemical etching with Au as catalyst** 9
Mrs. Olga Pyatilova, Prof. Sergey Gavrilov, Mr. Andrey Savitskiy, Dr. Alexander Pavlov, Mr. Alexandr Dudin

**Nanotubular anodic TiO2 initial layer morphology evolution under controlled hydrodynamic and temperature conditions** 11
Dr. Alexey Dronov, Mr. Ilya Gavrilin, Prof. Sergey Gavrilov, Prof. Herman Terryn, Dr. Jon Ustarroz, Mr. Oscar Steenhaut

**Preparation and testing of collagen-based nanocomposite scaffolds for tissue engineering and bone implantology** 12
Dr. Martin Braun, Dr. Tomas Suchy, Dr. Monika Supova, Dr. Pavla Sauerova, Dr. Martina Verdanova, Dr. Zbynek Sucharda, Dr. Sarka Ryglova, Dr. Margit Zaloudkova, Dr. Radek Sedlacek, Dr. Marie Hubalek Kalbacova

**Preparation and optimization of vitamin E TPGS-functionalized PLGA nanoparticles for carboplatin encapsulation** 13
Mr. Daniel Profirio, Prof. Pedro Corbi, Prof. Francisco Pessine

**Electrospun Nanocomposite Materials, A Novel Synergy of Polyurethane and Bovine Derived Hydroxyapatite** 15
Dr. Yahya BOZKURT, Mr. Ahmet ŞAHİN, Mr. Akın SUNULU, Mr. Mehmet Onur AYDOGDU, Prof. Faik Nüzhet OKTAR, Dr. Nazmi EKREN, Dr. Oğuzhan GUNDUZ

**Nanostructured titania doped with silver nanoparticles for photocatalytic water disinfection** 16
Ms. Evelína Polievková, Ms. Kateřina Přikrylová, Dr. Jana Drbohlavová

**Understanding 2D Nanoflake-like Heterostructures for Energy Storage and Conversion Applications at the Atomic Level** 18
Mr. Peng-Yi Tang, Dr. María De La Mata, Ms. Li-juan Han, Prof. Aziz Genç, Dr. Yong-min He, Mr. Xuan Zhang, Mr. Lin Zhang, Prof. José Ramón Galán-mascarósc, Prof. Joan Ramon Morante, Prof. Jordi Arbiol

**Remote control of small particles modified with azobenzene derivatives by light irradiation** 20
Dr. Yutaka Kuwahara, Prof. Yoshihiro Yamaguchi, Prof. Seiji Kurihara

**Optically Transparent Polymer-Tungstophosphoric Acid Composite Films with High Refractive Index** 22
Mr. Shuichi Matsumoto, Dr. Thiraporn Ishii, Ms. Mutsumi Wada, Dr. Shoji Nagaoka, Dr. Yutaka Kuwahara, Dr. Makoto Takafuji, Prof. Hirotaka Ihara

**Poly(L-lysine) functionalized Eu-doped NaGd(MoO4)2 Nanophosphors for Optical and MRI Imaging** 24
Prof. Manuel Ocaña, Dr. Nuria Ofelia Nuñez, Mr. Mariano Laguna, Dr. Jesús M De La Fuente, Dr. Eugenio Cantelar, Dr. Maria L Gracia

**Poly(vinylidene fluoride-co-hexafluoropropene) nanocomposite membranes for water purification** 26
Ms. Lutendo Rananga, Dr. Kgabo Moganedi, Prof. Takalani Magadzu

**CO2 gas sensor based on quartz crystal microbalance coated with vanadium oxide thin film** 27
Dr. MALIKA BEROUAKEN, Dr. Lamia Talbi, Prof. Rezak Alkama, Mr. Hamid Menari, Dr. Noureddine Gabouze, Dr. Sabrina Sam

**Electrochemical sensor of organics pollutants based on polythiophene and silicon nanowire** 28
Dr. Samia Belhousse, Dr. Fatma Zohra Tighilt, Dr. Sabrina Sam, Mrs. Kahina Lasmi, Prof. Naima Belhaneche-bensemra, Dr. Noureddine Gabouze

**The correlations between the crystal structure and the photocatalytic performance of the NaNbO3 and KNbO3** 29
Mr. Ryo Sasaki, Dr. Takuya Suzuki

**A site replacement of AxTiyOz of perovskite photocatalyst and their performance** 31
Mr. Koki Saito, Dr. Takuya Suzuki

**Impedance Spectroscopy of Heterojunction Solar Cell a-SiC/c-Si with ITO Antireflection Film Investigated at Different Temperatures** 32
Prof. Vladimír Šály, Dr. Milan Perný, Prof. František Janíček, Dr. Jozef Huran, Dr. Miroslav Mikolasek, Dr. Juraj Packa

**Catalytic oxidation of selected alcohols using gold covered with TEMPO functionalized C60 fullerene as a catalyst.** 34
Dr. Piotr Piotrowski, Prof. Andrzej Kaim

**PMMA polymer modified with SiO2 nanocapsules, possible applications against microbiologically influenced corrosion.** 35
Mr. Paulo Molina, Dr. Lisa Muñoz, Dr. Laura Tamayo, Dr. Maritza Páez

**Poly(L-arginine) surface functionalized manganese oxide nanocomplex for NO-based anticancer immune responses and MR imaging** 37
Ms. Ga-Yun Kim, Mr. Myeong-Hoon Kim, Dr. Hye-Young Son, Prof. Yong-Min Huh, Prof. Seungjoo Haam

**Thermal and Optical Properties of Paraffin-mixed CNTs Nanofluids** 39
Prof. Seok Pil Jang

**Gradient multi-walled carbon nanotubes-based scaffold for cartilage tissue engineering** **40**
Dr. Magdalena Richter, Dr. Jakub Rybka, Mr. Eser Akinoglu, Dr. Tomasz Trzeciak, Prof. Michael Giersig, Prof. Jacek Kaczmarczyk

**Production of β-Chitin Nanofibers from Squid Pen Using a Water Jet Machine** **41**
Prof. Mitsumasa Osada, Mr. Shin Suenaga, Prof. Kazuhide Totani, Prof. Yoshihiro Nomura, Ms. Kazuhiko Yamashita, Prof. Iori Shimada, Prof. Hiroshi Fukunaga, Prof. Nobuhide Takahashi

**Synthesis of Nano Composites from Ti-Al-B-C powders by Adiabatic Explosive Compaction** **42**
Dr. Mikheil Chikhradze, Prof. Nikoloz Chikhradze, Prof. George Oniashvili

**Electrical properties and thermal stability in stack structure of HfO2/Al2O3/InSb by atomic layer deposition** **43**
Mr. Min Baik, Prof. Mann-ho Cho, Mr. Hang-kyu Kang, Mr. Kwang-sik Jeong, Mr. Dae-kyoung Kim, Mr. Chang-min Lee, Prof. Hyoung-sub Kim, Dr. Jin-dong Song

**Study of performance improvement of single-electron associative memory circuit** **44**
Mr. MAKOTO TAKANO, Prof. Takahide Oya

**RGO and TiO2 Nanotube Matrix based Binary Hybrid Device for Reliable Detection of Methyl Acetate Vapor** **45**
Mr. Debanjan Acharyya, Dr. Partha Bhattacharyya

**A Study on the Correlations between Dark Count and Photon Detection Efficiency According to P-Well Structure in GM-APD** **46**
Mr. Hyun Yoo, Dr. Woo-Suk Sul, Mr. Hae-Chul Hwang, Mr. Kwang-Hee Kim, Mr. Gi-Sung Lee, Dr. Young-Su Kim

**Optical properties of GaAs-AlGaAs core-multishell nanowire quantum structures grown by MOVPE** **47**
Dr. PAOLA PRETE, Ms. Roberta Rosato, Mrs. Elena Stevanato, Dr. Fabio Marzo, Prof. Nico Lovergine

**Layer dependent direct optical transitions at Γ-point in synthesized large area MoSe2** **49**
Mr. Jae-Hun Jeong, Mr. Yoon Ho Choi, Mr. Kwang-sik Jeong, Prof. Mann-ho Cho

**Effect of Li co-doping on highly oriented sol-gel Ce-doped ZnO thin films properties** **50**
Prof. Azeddine CHELOUCHE, Dr. Tahar Touam, Mr. Mohand Tazerout, Prof. Djamel Djouadi, Mr. Fares Boudjouan

**NFFA Europe Presentation** **51**
Dr. Flavio Carsughi

**Hydrogen Anti-diffusion Methods for Poly-Si Quenching Resistor in Silicon Photomultipliers** **52**
Dr. Woo-Suk Sul, Mr. Hyun Yoo, Mr. Sang-Hyun Park, Mr. Dong-Eun Yoo, Mr. Dong-Wook Lee, Dr. Boung-Ju Lee

**Frequency selective alcohol sensing performance of Pd/TiO2 nanotube array/Ti (MIM) devices in capacitive mode** **53**
Dr. Partha Bhattacharyya

**Effect of Pressure on Crystal Structure and Optical Properties of Bi2O3 Nanoparticles** **55**
Ms. Melanie White, Ms. Rethika Kumar, Mr. Howard Yanxon, Prof. Ravhi kumar, Prof. Andrew Cornelius

**Characterization of nanometre-scale compositional variations in CMSX-4 superalloy subjected to high temperature annealing and creep deformation using analytical electron microscopy** **56**
Dr. Beata Dubiel, Dr. Paulina Indyka, Dr. Adam Kruk, Dr. Tomasz Moskalewicz

**Plasmonic Ga nanoparticle arrays for phase change memory** **58**
Dr. Oral Ualibek, Mr. Murat Baisariyev, Prof. Igor Shvets, Dr. Gulnar Sugurbekova

**Blue emission of Cerium doped Aluminum (oxy)-nitride thin films prepared by reactive sputtering technique** **59**
Mr. Alaa eldin Giba, Mr. Philippe Pigeat, Dr. Stéphanie Bruyere, Prof. Hervé Rinnert, Dr. Flavio Soldera, Prof. Frank Mücklich, Prof. Raul Gago-fernandez, Prof. David Horwat

**Gold nanoparticles assembly on 1D, 2D and 3D microstructures** **61**
Mr. Ali ISSA, Dr. Irene Izquierdo-Lorenzo, Prof. Fawaz Elomar, Prof. Joumana Toufaily, Dr. Safi Jradi

**Mutual Coupling mitigation of Terahertz antenna by using Graphene based metasurface** **63**
Dr. DEBASIS MITRA, Mr. Jeet Ghosh

**Pseudo-Hall effect in graphite on paper based four terminal devices for stress sensing applications** **65**
Mr. Afzaal Qamar, Mrs. Tuba Sarwar, Mr. Toan Dinh, Mr. A.r.muhammad Foisal, Dr. Hoang-phuong Phan, Dr. Dzung Dao

**Mode control in SOI microring resonators through sub-wavelength modifications** **66**
Mr. Armandas Balcytis, Mr. Darius Urbonas, Mr. Martynas Gabalis, Mr. Konstantinas Vaškevičius, Prof. Saulius Juodkazis, Dr. Raimondas Petruškevičius

**Electrospray Deposition of Antimicrobial Nano-Powder/Bioactive Glass Composites on Ti6Al4V Implants** **68**
Dr. Ceren Peksen, Dr. Mevlut Gurbuz, Prof. Aydın Dogan

**Green Synthesis of ZnO Nanoparticles by an Alginate Mediated Ion-Exchange Process and a case study for Photocatalysis of Methylene Blue Dye** **69**
Mr. Choo Cheng Keong, Ms. Yamini Sunitha Vivek, Dr. Babak Salamati, Dr. Bahman Amini Horri

**Reversible and dynamic micro-topographic pattern on azo-polymers substrates to investigate cell behavior in real-time.** **70**
Ms. Lucia Rossano, Dr. Carmela Rianna, Prof. Maurizio Ventre, Dr. Silvia Cavalli, Prof. Paolo Antonio Netti

**ZnO Nanowires in Surface-Acustic-Wave Sensors** **71**
Dr. Aurelian Marcu, Dr. Cristian Viespe, Mr. Bogdan Butoi, Mr. Paul Dinca, Ms. Liga Avotina, Dr. Cristian Lungu

**PVC and PES waste/nanoclay mixtures, their preparation and properties** **72**
Prof. Dagmar Merinska, Mrs. Alice Tesarikova, Dr. Lubomir Benicek

**Diffusion of nanoparticles in solution through elastomeric membrane** **73**
Mr. Mohamed Zemzem, Dr. Ludwig Vinches, Prof. Stéphane Hallé

**Preparation and evaluation of mechanical properties of filled PVC/ PVB blends/clay and calcium carbonate** **74**
Mrs. Alice Tesarikova, Prof. Dagmar Merinska, Dr. Michael Tupy

**Influence of multi walled carbon nanotubes and silica nanoparticles on tensile properties of polyurethane** 76
Mr. Amir Navidfar, Mr. Alkan Sancak, Mr. Kemal Baran Yildirim, Prof. Levent Trabzon

**Poly (vinylidene fluoride)/Polyaniline/MWCNT Nanocomposite Ultrafiltration Membrane for natural organic matter removal** 78
Mrs. Banan Hudaib, Prof. Vincent Gomes, Dr. Jeffrey Shi, Prof. Dianne Wiley, Prof. Zongwen Liu

**Ca (OH) 2 Nanoparticles Based on Acrylic Copolymers for the consolidation and protection of Ancient Egypt Calcareous Stone Monuments.** 80
Mr. Sayed Mansour, Prof. Sawsan Darwish, Dr. Mahmoud Abd Elhafez, Prof. Nagib Elmarzugi, Prof. Mohammad AlDosari

**Sorting various pluripotent state of iPSCs via magnetization of nanoclusters in microfluidic magnetophoresis devices** 81
Mr. Byunghoon Kang, Ms. Seungmin Han, Mr. Moo-kwang Shin, Dr. Jeong-ki Min, Dr. Hye-Young Son, Prof. Yong-Min Huh, Prof. Seungjoo Haam

**Adsorption of globin proteins in mesoporous (designed) titania for biosensors development.** 82
Mr. stefano loreto, Prof. Karolien De Wael, Prof. Vera Meynen

**Tumor-activated prodrug nanoparticles sensing endogenous levels of matrix metallo-proteinase 2 in 3D tumor spheroids for the on-demand release of doxorubicin** 83
Mrs. Martina Profeta, Dr. Daniela Guarnieri, Dr. Valentina Belli, Dr. Marco Biondi, Dr. Marco Cantisani, Dr. Luca Raiola, Prof. Paolo Antonio Netti

**Hydrogel Micropattern Incorporating Nanostructures for Fluorescence-based Biosensing** 85
Prof. Won-Gun Koh, Mr. Minsoo Kim, Mr. Sang Won Han, Prof. Kangwon Lee

**Fluorescent nano-switch probes: Monitoring of microRNA level in induced pluripotent stem cells without affecting pluripotency** 86
Ms. Seungmin Han, Dr. Hye-Young Son, Dr. Eunji Jang, Mr. Byunghoon Kang, Ms. Jisun Ki, Mr. Moo-kwang Shin, Mr. Byeonggeol Mun, Dr. Jeong-ki Min, Prof. Seungjoo Haam

**Nanoparticle-mediated delivery of supramolecular drugs and biomolecules into cells** 88
Dr. Viktoriya Sokolova, Dr. Olga Rotan, Mr. Patrick Gilles, Mr. Som Dutt, Prof. Thomas Schrader, Prof. Matthias Epple

**New routes to exotic nanomaterials** 90
Prof. Clément Sanchez

**Atomic collapse in graphene** 91
Prof. Francois Peeters

**Complex dynamic multicomponent supramolecular nanomaterials: tailoring low dimensional multifunctional nanostructures** 92
Prof. Paolo Samori

**Solution Processing of Thermoelectric Materials, Devices and Systems** 93
Dr. Andreu Cabot

**Synthesis and characterization of reduced graphene oxide films by aqueous electrochemical reduction** 94
Dr. Alina Pruna, Prof. J.A. Zapien, Prof. A. Ruotolo, Dr. A.M. Mocioiu, Ms. Paulina Dobosz

**CVD-growth of MWCNT arrays on Me-Ct-N-(O) thin films** **96**
Dr. Sergey Dubkov, Prof. Dmitry Gromov, Prof. Sergey Gavrilov, Prof. Sergey Bulyarskii, Dr. Alexey Trifonov, Mr. Eugene Kitsyuk, Dr. Alexander Pavlov, Dr. Paweł Mierczyński, Prof. Tomasz Maniecki

**Electrochemical properties of LiNi0.85Co0.10Al0.05O2 synthesized using AAO(Anodic Aluminum Oxide) template** **97**
Prof. JongTAe SON, Ms. mira shin, Mr. ji-woong shin, Prof. Taewhan Hong, Mr. Do-man Jeon

**Fenton-Like oxidation of Orange II solution using heterogeneous catalysis with bionanocatalyst from fique fiber and iron nanoparticles** **98**
Mrs. Karen Bastidas, Prof. Cesar Sierra, Prof. Hugo Ricardo Ramirez

**Effects of Ag/TiO2 nanoparticles developed for leather surface finishing on human keratinocytes cells** **100**
Dr. Daniela Stan, Ms. Cristina Ana Constantinescu, Dr. Carmen Gaidau, Dr. Madalina Ignat, Dr. Aurora Petica, Dr. Manuela Calin

**Controlled synthesis of Ag-Au-S ternary nanostructured semiconductors** **101**
Mrs. Mariona Dalmases, Mr. Albert Vidal, Dr. Albert Figuerola, Mr. Pau Torruella, Dr. Sonia Estrade

**Peroxidase-like Activity of Apoferritin Paired Copper(II) Nanoparticles and Its Biomemory Applications** **102**
Mrs. Şükriye Nihan KARUK ELMAS, Dr. Remziye Guzel, Prof. Rıdvan Say, Prof. Arzu Ersoz

**FILTERING PIGMENTS FROM HONEY BY NANOFIBER MEMBRANE** **103**
Mrs. farzaneh azizzadeh, Dr. Filiz Lokumcu

**Cantilever-enhanced photoacoustic spectroscopy in the research of natural and synthetic calcium phosphate** **105**
Mrs. Agnese Brangule, Prof. Karlis Gross

**Biocompatible and thermoresponsive polymer synthesis: A facile method for a controlled polymerization** **106**
Dr. Teresa Alejo, Mr. Martín Prieto, Mr. Hugo García-Juan, Dr. Víctor Sebastián, Dr. Manuel Arruebo

**Very efficient and rapid degradation of Congo red dye with TiO2 based nano-photocatalysts** **107**
Prof. Himanshu Narayan, Prof. Hailemicheal Alemu

**NMR investigation of domain wall dynamics and hyperfine field anisotropy in magnets by the magnetic video-pulse excitation method** **108**
Prof. Tsisana Gavasheli, Dr. Grigor Mamniashvili, Dr. Tatiana Gegechkori

**Straightforward etching of ZnO nanostructures for optical sensor application** **109**
Dr. Dong Jin Lee, Dr. Sung Ryong Ryu, Prof. Yong Deuk Woo, Prof. Tae Won Kang, Prof. Deuk Young Kim

**Mechanical behavior of precipitation strengthened nanostructured bulk materials produced by inhomogeneous severe plastic deformation** **110**
Prof. Janusz Majta, Prof. Michal Krzyzanowski, Mr. Marcin Kwiecien, Mr. Szymon Bajda

**Study on the Growth of Carbon Microspheres via Hydrothermal Process of Nano-Crystalline Cellulose (NCC)** **112**
Ms. Lim Hui Hui, Dr. Bahman Amini Horri, Dr. Babak Salamati

**Core-shell nanostructured metal oxides for high performance supercapacitors** **113**
Prof. Hao Gong

**Avidin-conjugated calcium phosphate nanoparticles as modular system for the attachment of biotinylated molecules** 114
Ms. Selina Beatrice van der Meer, Prof. Matthias Epple

**Influence of Exposure with Xe Radiation on Heterojunction Solar Cell a-SiC/c-Si Studied by Impedance Spectroscopy** 116
Dr. Juraj Packa, Dr. Milan Perný, Prof. Vladimír Šály, Dr. Miroslav Mikolasek, Dr. Michal Váry, Dr. Jozef Huran, Dr. Ladislav Hrubčín, Dr. Vladimir Skuratov, Dr. Juraj Arbet

**Self-Assembled 3D Flowerlike Bi2O3 Microspheres and Its Visible Light Driven Photocatalytic Activity** 117
Mrs. Arini Nuran Zulkifili, Prof. Akira Fujiki

**Synthesis and characterization of surface coated fluorescent carbon dot for visible-responsive photocatalytic effect** 119
Mr. Young Kwang Kim, Mr. Kim Sung Han, Prof. Sung Young Park

**Deposition of silicon carbide thin films with RF and DC magnetron sputtering** 120
Mr. Mohand Arezki OUADFEL, Dr. Aissa Keffous, Prof. Mohamed Kechouane, Dr. Noureddine Gabouze, Mr. Hamid Menari, Dr. Maha Ayat

**Memory effect in electroformed nanocrystal silicon nitride based thin film LED** 121
Dr. Tamila Anutgan, Dr. Mustafa Anutgan, Prof. Ismail Atilgan

**Femtosecond Laser Induced sp3 Bonds and Nanodiamonds Formation in Carbon Materials** 123
Dr. Aurelian Marcu, Ms. Liga Avotina, Dr. Corneliu Porosnicu, Dr. Alexandru Marin, Dr. Cristiana Grigorescu, Mrs. Razvan Ungureanu, Mrs. Gabriel Cojocaru, Dr. Daniel Ursescu, Mrs. Mihail Lungu, Dr. Nicola Demitri, Dr. Cristian Lungu

**Comparison of negative capacitance phenomenon in ordinary amorphous and electroformed nanocrystalline silicon based LEDs** 124
Dr. Mustafa Anutgan, Dr. Tamila Anutgan, Prof. Ismail Atilgan

**Dyanmic behavior of water droplet on water repellent surface with low contact angle hysteresis** 126
Prof. Takahiro Ishizaki, Mr. Keisuke Sasagawa, Mr. takuya furukawa

**Refractive index sensing with electrochemical sensor** 128
Mr. Hans Dyrnesli

**Design and Synthesis of Macromolecular Scaffolds for Carbon Monoxide Delivery in Biological Systems** 129
Ms. Diep Nguyen, Prof. Cyrille Boyer

**New Aptamer-Based Biosensor -- Design Study** 130
Dr. Radu Tamaian, Mrs. Nadia Paun, Dr. Violeta Niculescu

**A new serie of phosphat catalysts based on Copper and Zinc: chemical preparation and physicochemical study** 131
Dr. Asmaa AJARROUD

**Relaxation dynamics of multilayer networks modeled with Husimi cacti** 132
Mr. Liviu Bogdan Chiriac, Dr. Aurel Jurjiu, Prof. Mircea Galiceanu, Mr. Alexandru Stefan Farcasanu, Dr. Flaviu Turcu

**Relaxation dynamics of Sierpinski hexagon fractal polymer** 133
Dr. Aurel Jurjiu

**Gardenia jasminoides extract-capped gold nanoparticles reverse hydrogen peroxide-induced premature senescence** 134
Ms. seon yeong chae, Dr. Sun young Park, Mr. Jin Oh Park, Mr. Kyu Jin Lee, Prof. Geuntae Park

**Immobilization of enzyme on porous silicon for electrochemical detection of organophosphorous compounds** 135
Dr. Maha Ayat, Dr. Chafiaa Yaddaden, Dr. Amina Kermad, Dr. Noureddine Gabouze, Prof. Mohamed Kechouane

**Meyer-Neldel temperature on carrier transport of C70 molecular solid** 136
Mr. Sezaimaru Kouki, Mr. Nakashima Fumihiro, Prof. Yong Sun, Dr. Koichi Onishi

**Programmable artificial micro-swimmer** 138
Prof. Jinyao Tang

**Saponin/lipid nanoparticles as an efficient adjuvant and delivery system for mucosal immunization** 139
Prof. Vladimir Berezin, Prof. Andrey Bogoyavlenskiy, Dr. Pavel Alexyuk, Dr. Aizhan Turmagambetova, Ms. Irina Zaitceva, Ms. Madina Alexyuk, Ms. Elmira Omirtaeva

**Optical and electrochemical immunoassay for detection of superoxide dismutase 2 employing biocatalytic formation of quantum dots on the surface of microbeads** 141
Ms. Ruta Grinyte, Dr. Javier Barroso, Dr. Laura Saa, Dr. Valery Pavlov

**Mussel Inspired Nanowire Platforms for siRNA delivery** 142
Dr. Baiju Govindan Nair, Prof. Yoshihiro Ito

**Biodegaradable nanoporous microspheres by RAFT polymerization** 143
Prof. Ildoo Chung, Mr. Taeyoon Kim, Ms. Sorim Lee

**Synergy of radiotherapy and chemotherapy delivered via gold nanostructures in glioblastoma multiforme** 145
Ms. Alexandra Vaideanu, Ms. Astrid Wendler, Dr. Colin Watts, Prof. Mark Welland

**Activatable T1/T2 dual-mode MR imaging nanoplatform for enhancing accuracy by Fe/Mn oxide heteronanocrystals** 147
Mr. Myeong-Hoon Kim, Dr. Hye-Young Son, Ms. Ga-Yun Kim, Prof. Yong-Min Huh, Prof. Seungjoo Haam

**Structural Investigation of the HS to LS Relaxation Dynamics in Spin Crossover compounds** 149
Ms. Teresa Delgado Pérez, Dr. Antoine Tissot, Dr. Céline Besnard, Dr. Laure Guénée, Prof. Andreas Hauser

**Resistive switching in TiO2 nanocolumn arrays electrochemically grown** 151
Mr. Marian Marik, Dr. Alexander Mozalev, Dr. Jaromir Hubalek, Dr. Maria Bendova

**SiAlON thin films on silicon and formation of nanofilaments with memristive properties** 152
Mr. Eduardo Marino, Prof. Blas Garrido, Dr. Sergi Hernandez, Mr. Oriol Blazquez

**Comparative study of inorganic and hybrid ionogels as electrolyte for supercapacitors** 153
Ms. Ronak Janani, Dr. Heming Wang, Dr. Nicolas Farmilo, Dr. Alexander Roberts

**Fabrication and characterization of ZnO/p-Si light-emitting devices by electron beam evaporation** 155
Mr. Pablo Vales, Mr. Oriol Blazquez, Dr. Julian López-vidrier, Dr. Sergi Hernandez, Prof. Blas Garrido

**NATIVE FLUORESCENCE DETERMINATION OF TETRACYCLINE RESIDUES IN MILK PRODUCTS FOLLOWED BY SILICA-MODIFIED MAGNETIC NANOPARTICLES** **156**
Mrs. Olena Khainakova, Prof. Vladymir Zaitsev, Dr. Natalia Kobylinska, Prof. Marta Elena Diaz Garcia

**Magnetoresistance Aharonov--Bohm oscillations in type-II InAsSbP ellipsoidal quantum dots** **157**
Prof. Karen Gambaryan

**The synthesis of N-doped TiO2/CdS nanocomposites for quantum dots-sensitized solar cells** **158**
Ms. Cahyorini Kusumawardani

**A Study on the Properties of Pure SnO2 Gas Sensors** **159**
Dr. TARIK ASAR, Ms. Emine BOYALI, Mr. Burak KORKMAZ, Dr. Saime Şebnem ÇETİN, Prof. Süleyman ÖZÇELİK

**Fully Developed Mixed Convection Flow of a Nanofluid in a Vertical Channel** **161**
Dr. Fahad Al-Amri

**Application of Graphene Based Nanoadsorbents in Produced-water Treatment for Removal of Dissolved Oil** **162**
Mr. Ahmad Diraki, Dr. Ahmed Abdala

**CTAB-coated magnetic nanoparticles for removal of direct yellow 12 from aqueous solutions** **163**
Dr. Alex Fabiano Campos, Mr. Paulo Henrique Michels Brito, Dr. Renata Aquino, Dr. Franciscarlos Gomes da Silva, Dr. Jerome Depeyrot

**Heavy metal adsorption by mercapto and amine functionalized silica aerogel-like materials** **164**
Mr. João Vareda, Prof. Luisa Durães

**Design and fabrication of printed Graphene paper based micro-supercapacitor device with a Redox-active electrolyte** **165**
Ms. Bhawna Nagar, Dr. Deepak Dubal, Mr. Luis Pires, Prof. Arben Merkoçi, Prof. Pedro Gomez-romero

**Effect of confinement inside CNTs for improving dehydrogenation from MXH4 clusters where M = Na, Li and X = Al, B** **167**
Dr. Hitesh Sharma, Mrs. Meenakshi Malhotra, Mrs. Kiranjeet Bedi

**Effect of Undensified Silica Fume on the Dispersion of Carbon Nanotubes Within a Cementitious Composite** **168**
Mr. Salam Alrekabi, Prof. Andy Cundy, Dr. Andreas Lampropoulos, Prof. Raymond Whitby, Dr. Irina N Savina

**Colloidal Au-Ag-Chalcogen-Based Ternary Nanocrystals for Energy Conversion Applications** **169**
Dr. Albert Figuerola, Ms. Mariona Dalmases, Dr. Maria Ibáñez, Mr. Pau Torruella, Dr. Víctor Fernàndez-Altable, Mr. Luis López-Conesa, Ms. Doris Cadavid, Ms. Laura Piveteau, Dr. Maarten Nachtegaal, Prof. Jordi Llorca, Prof. Maria Luisa Ruiz-González, Dr. Sonia Estrade, Prof. Francesca Peiró, Prof. Maksym V. Kovalenko, Dr. Andreu Cabot

**Electrochemical Reduction of Carbon Dioxide on Nano-Copper Films Modified with Polymer of Intrinsic Microporosity** **170**
Mr. Sunyhik Ahn, Dr. Mariolino Carta, Prof. Neil Mckeown, Prof. Frank Marken, Prof. Andrew Barron, Dr. Enrico Andreoli

**Plasmonic nanostructures for catalysis and sensing** **171**
Prof. isabel pastoriza-santos

**Growth of nanowires with periodic morphologies via the vapor-liquid-solid mechanism** 172
Prof. Chun-Sing Lee

**Chemical, Structural and Surface Transformations in Nanocrystals** 173
Prof. Liberato Manna

**Nanobiosensors for diagnostics** 174
Prof. Arben Merkoçi

**Some Features of Pressure Evolution in Systems ``Non-Wetting Liquid - Nanoporous Medium'' at Impact Intrusion** 175
Dr. Victor Byrkin, Dr. Anton Belogorlov, Mr. Daniil Paryohin

**Complex defects in AlN/GaN interface** 176
Dr. Yahor Lebiadok, Mr. Dzmitry Kabanau

**Powerful Laser Diode Matrixes based on AlGaAs/GaAs heterostructures for Active Vision Systems** 177
Dr. Yahor Lebiadok, Mr. Denis Shabrov, Mr. Dzmitry Kabanau

**Removal of azo dye Orange II using nZVI catalyst supported on a natural fiber (Fique).** 178
Mr. David Barinas, Mrs. Karen Bastidas, Prof. Hugo Ricardo Ramirez, Prof. Cesar Sierra, Mrs. Anamaria Barrera Bogoya

**Viscosity and thermal conductivity of aluminum nitride - ethylene glycol (AlN-EG) nanofluids** 179
Dr. Gaweł Żyła

**Associative properties of diblock copolymers used in nanoparticle formation by Flash Nanoprecipitation.** 180
Dr. Walid Saad, Prof. Robert Prud homme

**Simulation and Visualization of Chirality-Dependent Thermal Conduction Phenomena in Carbon Nanotubes** 181
Prof. Vadim A. Shakhnov, Prof. Lyudmila A. Zinchenko, Dr. Vladimir V. Makarchuk, Dr. Elena V. Rezchikova, Mr. Vadim Kazakov

**Influence of post-deposition annealing on the properties of nanostructured TiO2 thin films grown by RF magnetron sputtering for photonic applications** 182
Dr. Tahar Touam, Prof. Azeddine CHELOUCHE, Mrs. Ilham Hadjoub, Mr. Djamel DJOUADI, Mr. Hammiche Laid

**Investigation of Morphological and Optical Properties of Stain Etched Silicon** 183
Dr. Maha Ayat, Dr. Sabrina Sam, Dr. Noureddine Gabouze, Dr. Rabah Boukherroub

**Silicon Nanoparticles Coated with Chitosan for Using Anode of a Lithium Secondary Ion Battery** 184
Ms. SUN MI JIN, Dr. Jong Sung Jin, Prof. Nam-ju Jo

**Microanalysis of DDS Nanoparticle by Polarization Interferometric Nonlinear Confocal Microscopy** 185
Prof. Chikara Egami

**CARBONIC ANHYDRASE INHIBITORS : 2-Substituted-1,3,4-Thiadiazole-5-Sulfamides act as powerful and selective inhibitors of the mitochondrial isozymes VA and VB over the cytosolic and membrane-associated carbonic anhydrases I, II AND IV** 186
Dr. Fatma-Zohra SMAINE, Dr. Jean-Yves Winum

**Synthesis of zirconia-based Pyrochlore type photocatalysts** 187
Mr. Yuta Kawakami, Dr. Takuya Suzuki

**Peptide-functionalized Ultrasmall Gold Nanoparticles for Integrin Receptor Targeting** 188
Ms. Usoa Aguilera Peral, Dr. Tom Coulter, Dr. Yao Ding, Ms. Cristina Espinosa Garcia, Dr. Sarah Hale, Mr. Alessandro Pace, Dr. Ketan Patel, Mrs. Angela Robinson, Dr. Dan Palmer, Dr. Phil Williams, Dr. Meike Roskamp

**Microwave assisted hydrothermal synthesis of magnetite based nanoparticles for hyperthermia therapy** 190
Mr. Milos Ognjanovic, Dr. Biljana Dojcinovic, Dr. Yue Ming, Dr. Hongguo Zhang, Dr. Bostjan Jancar, Dr. Sanja Vranjes Djuric, Dr. Bratislav Antic

**Recent Advances In Nano-Technology In Domain Of Agricultural Sciences And Food Industry** 191
Mr. pejman ghelich, Mr. Ashkan Mohammadali Fam, Ms. Marjan Khorshidizadeh

**A soluble and fluorescent new type thienylpyrrole based conjugated polymer: optical, electrical and electrochemical properties** 193
Ms. Tugba Soganci, Dr. Hakan Can Soyleyici, Dr. Metin Ak

**Nanomaterials obtained by ruthenium immobilization on mesoporous** 194
Dr. Violeta Niculescu, Dr. Radu Tamaian, Dr. Viorica Pirvulescu

**Eco-toxicity of nanostructured ZnO, TiO2, Ce and Zr doped TiO2 developed for photocatalytic applications to Lemna minor and Sinapis alba** 195
Dr. Ivana Troppová, Dr. Hana Sezimova, Prof. Stanislav Daniš, Dr. Pavlína Peikertová, Dr. Lenka Matějová

**Smart window application of a new hydrazide type SNS derivative** 196
Mr. Ogun Gumusay, Ms. Tugba Soganci, Dr. Metin Ak, Dr. Hakan Can Soyleyici

**Synthesis and Fluorescence Properties of Novel Asymmetric Star Shaped Polymer Containing Carbazole** 197
Dr. Metin Ak, Dr. Erhan Karatas

**Processable Amide Substituted 2,5-Bis(2-thienyl)pyrrole Based Conducting Polymer and its Fluorescent and Electrochemical Properties** 198
Mr. Yasin Abduloglu, Ms. Tugba Soganci, Dr. Hakan Can Soyleyici, Dr. Metin Ak

**Organic/inorganic nanoplatform for detection of cancer** 199
Ms. Nikola Bugárová, Dr. Matej Mičušík, Dr. Zdenko Špitálsky, Dr. Peter Šiffalovič, Dr. Mária Omastová

**A GREEN CHEMISTRY APPROACH TO SYNTHESIS OF Ce(IV) NANOPARTICLES USING ORIGANUM SYRIACUM** 200
Dr. Birsen Öztürk, Mrs. Gozde Mediha Kamer, Dr. Dilek Ozyurt, Prof. Reşat Apak

**Porous Gold Nanoparticles for Nonresistant Inactivation of Influenza A Virus** 202
Mr. Jinyoung Kim, Dr. Taeksu Lee, Ms. Minjoo Yeom, Ms. Aram Kang, Prof. Daesub Song, Prof. Seungjoo Haam

**Homogeneous crystal nucleation kinetics in small closed systems** 203
Dr. Zdenek Kozisek, Prof. Pavel Demo, Dr. Alexei Sveshnikov, Mr. Jan Kulveit

**Mechanical, electrical and antibacterial properties of polycrystalline ZnO films passivated with ZnS** 204
Dr. Anna Baranowska-Korczyc, Dr. Mikołaj Kościński, Dr. Emerson L. Coy, Dr. Bartosz Grześkowiak, Dr. Małgorzata Jasiurkowska-Delaporte, Dr. Barbara Peplińska, Prof. Stefan Jurga

**Large-scale silver-modified nanofluorapatite -- bactericidal/cytotoxicity evaluation and physical characterization** **205**
Dr. Małgorzata Kus-Liśkiewicz, Mrs. Renata Wojnarowska-Nowak, Dr. Adriana Barylyak, Dr. Ganna Nechyporenko, Prof. Viktor Zinchenko, Prof. Danuta Leszczynska, Prof. Yaroslav Bobitski

**Microstructural investigation of hexagonal multilayered MoS2 nanoplatelets and their exposed edges role in gas-sensing** **206**
Dr. Geetanjali Deokar, Dr. Raul Arenal, Prof. Eduard Llobet, Dr. Dominique Vignaud, Mr. Jonathan Dervaux, Dr. Jean-Francois Colomer

**Platinum-free catalysts for low temperature fuel cells** **207**
Dr. Tatiana Lastovina, Ms. Julia Pimonova, Dr. Andriy Budnyk

**V2O5 nanorods as CO2 gas sensing devices** **208**
Ms. Ayouz katia, Mrs. Tala-Ighil Razika, Ms. Kawther Mhammedi, Dr. Sabrina Sam, Dr. Noureddine Gabouze

**An Amide Substituted Dithienylpyrrole Based Copolymer: Its Electrochromic Properties** **209**
Ms. Simge Durur, Ms. Tugba Soganci, Dr. Hakan Can Soyleyici, Dr. Metin Ak

**Modified Denatured Lysozyme Effectively Solubilises Fullerene C60 Nanoparticles in Water** **210**
Ms. Marialuisa Siepi, Ms. Jane Politi, Ms. Angela Amoresano, Ms. Paola Giardina, Mr. Luca De Stefano, Ms. Daria Maria Monti, Mr. Eugenio Notomista

**Gold nanoparticles as biocompatible surface for lipase adsorption: Physical-chemical study of the ``nano-bio'' interface** **211**
Ms. Heloise Ribeiro de Barros, Prof. Leandro Piovan, Prof. Izabel Riegel-vidotti

**Periodical Surface Nanostructures Induced by Femtosecond Laser** **212**
Ms. Bogdan Calin, Ms. Catalina Albu, Dr. Laura Ional, Dr. Ekaterina Iordanova, Dr. Georgi Yankov, Dr. Aurelian Marcu

**Statistically optimized preparation of catalase immobilized magnetic nanoparticles** **213**
Dr. Sandeep Kumar, Dr. Asim K Jana

**Pd2Sn vs. Au-Pd2Sn NPs: catalytic study for hydrogenation and Sonogashira coupling reactions** **214**
Dr. Raquel Nafria, Mr. Zhishan Luo, Dr. Michaela Meyns, Prof. Jordi Llorca, Dr. Maria De La Mata, Ms. Sara Marti, Prof. Jordi Arbiol, Dr. Guillermo Muller, Dr. Arnald Grabulosa, Dr. Andreu Cabot

**Water-Free Synthesis of Monodisperse Nickel(0) Nanoparticles** **216**
Ms. Koyel Bhattacharyya, Prof. Nicolas Mézailles

**Supported gold based bimetallic nanoparticles catalyzed oxidation and C-C coupling reactions** **218**
Prof. Redouane Bachir, Dr. Nawel Ameur, Dr. Amina Berrichi, Prof. Sumeya Bedrane, Prof. Abderahim Choukchou-braham

**Shape- and size-controlled synthesis of ligand free CeO2 nanoparticles and their catalytic performances: From nanospheres to nanostars** **219**
Ms. Taisiia Berestok, Dr. Pablo Guardia, Dr. Raquel Nafria, Dr. Massimo Colombo, Dr. Sonia Estrade, Prof. Francesca Peiró, Dr. Andreu Cabot

**Simple approach towards few layers MoS2 nanorods/nanoflowers and their potential for piezo-photocatalytic rapid degradation activity** **221**
Mr. Neeraj Kumar, Dr. Vyom Parashar, Prof. Suprakas Sinha Ray, Prof. Jane Catherine Ngila

**Formation of nanostructured AlOOH film on Al alloys by steam coating toward corrosion protection** 222
Dr. Ai Serizawa, Prof. Takahiro Ishizaki

**Resizable nanopores** 224
Ms. Clemence Briosne-frejaville, Mr. Adrien Mau, Mr. Armandas Balcytis, Dr. Xijun Li, Prof. Saulius Juodkazis

**The surface microstructure of SiC epitaxial films, grown by atom replacement.** 226
Mrs. Dina Bakranova, Prof. Sergey Kukushkin, Prof. Kair Nussupov, Dr. Andrey Osipov, Dr. Nurzhan Beisenkhanov

**Study and analysis of composition variation influence for chemical reactions sequence and thermal effects in Al-Ni multilayered thermite materials** 227
Mr. Egor Lebedev, Prof. Dmitry Gromov, Mr. Yuri Shaman, Ms. Anna Presnukhina, Prof. Sergey Gavrilov

**Modelling of grain refinement around highly reactive interfaces in processing of nanocrystallised multilayered metallic materials** 228
Mr. Szymon Bajda, Prof. Dmytro Svyetlichnyy, Prof. Delphine Retraint, Prof. Michal Krzyzanowski

**Ions irradiation induced damage profile of metal nanowires** 229
Ms. Shehla Honey, Dr. Shahzad Naseem, Dr. Ishaq Ahmad, Mr. Force Tefo Thema, Dr. Malik Maaza

**Enhancement of electrochemical properties of micro/nano electrodes based on TiO2 nanotube arrays** 230
Mr. Dhurgham Khudhair, Ms. Julie Gaburro, Mr. Sajjad Shafei, Prof. Saeid Nahavandi, Dr. Anders Barlow, Dr. Asim Bahatti

**A Robust Scaffold for Multimodality Using a Plasmonic Gold Core and a Mesoporous Iron Oxide Shell** 231
Ms. Aastha Kukreja, Mr. Byunghoon Kang, Dr. Eunji Jang, Dr. Hye-Young Son, Prof. Yong-Min Huh, Prof. Seungjoo Haam

**Infra-red laser pulse increases the expression of heat-inducible molecular cargo delivered via mesoporous silica nanoparticles** 233
Ms. Lien Davidson, Dr. Natalia Barkalina, Dr. Marc Yeste, Mrs. Celine Jones, Dr. Kevin Coward

**Transparent conductive graphene-coated textile fibres: a platform for wearable electronics** 234
Dr. Ana Neves

**In vitro evaluation of carbon nanotube-based scaffolds for cartilage tissue engineering** 235
Dr. Jakub Rybka, Dr. Magdalena Richter, Mr. Eser Akinoglu, Dr. Tomasz Trzeciak, Prof. Jacek Kaczmarczyk, Prof. Michael Giersig

**Spice-based carbon dots: application to in vitro cancer growth inhibition** 236
Dr. Nagamalai Vasimalai, Ms. Vania Vilas-Boas, Dr. Juan Gallo, Dr. Cerqueira M.F., Dr. Menéndez M, Dr. Costa J.M, Dr. Lorena Diéguez, Dr. Begona Espina, Dr. Maria Teresa Fernandez-arguelles

**Role of hydrogen in affecting the growth trend of CNT on micron spherical silica gel** 238
Dr. Raja Nor Raja Othman, Ms. Amal Izzati Ismadi, Dr. Siti Nooraya Tawil, Dr. Kin Yuen Leong

**High-nitrogen graphene nanoflakes with iron functionalities: a viable catalyst for PEMFCs** 239
Mr. Pierre-Alexandre Pascone, Dr. Dimitrios Berk, Dr. Jean-Luc Meunier

**Magneto-plasmonic-carbon-nanoscrolls with enhanced performances for sensitive biosensing applications** 240
Prof. Maria Benelmekki, Dr. Jeong-Hwan Kim

**Evaluation of a novel tool for the study of early metastasis based in B16F10 murine melanoma cells labeled with Cd-Te Quantum Dots.** **241**
Mr. Víctor Díaz-García, Dr. Simon Guerrero, Dr. Marcelo J Kogan, Dr. Andrew Quest, Dr. José Pérez-donoso

# Surface chemical reactions at self-heated metal oxide nanowires

**Wednesday, 9th November - 09:05 - Plenary Speeches - Auditorium - Oral presentation - Abstract ID: 711**

***Prof. Joan Ramon Morante*** [1]

***1.*** *Catalonia Institute for Energy Research (IREC)*

Current sources applied to metal oxide nanowires dissipate enough heat by Joule effect as function of the used current density and nanowires characteristics. Here, it used to control the nanowire temperature and thus modulate the chemical reactions taking place at the surface as nanowire interacts with the environment. These mechanisms became essential for the future development and implementation of advanced catalysts that will be discussed. Besides, the chemical reactions occurring at the surface, the charge interchanges between nanowire and absorbed molecules constitute by itself a transduction mechanism still available for designing precise chemical sensors converting chemical information into electrical one. As example ammonia gas sensor devices based on these mechanisms will be presented and discussed. Chemical steps followed for the ammonia molecule at the surface of the metal oxide will be described and the final transduction mechanism experimentally verified and assessed. Competitive mechanisms such as those due to the presence of humidity at the ambient will also be discussed. Finally, strategy for implementing this kind of device based on the evolution from the laboratory using individual nanowire towards a parallel multi nanowires based device feasible at industrial level will also presented discussed and evaluated as well as other nano materials or nano devices based alternatives for building fully autonomous nano systems.

# Composite nanostructures for high-efficiency excitonic solar cells

**Wednesday, 9th November - 09:40 - Plenary Speeches - Auditorium - Oral presentation - Abstract ID: 715**

***Prof. Alberto Vomiero*** [1]

***1.*** *Luleå University of Technology*

The typical photoanode in dye- and quantum dot- sensitized solar cells is composed of a wide band gap semiconductor, which acts as electron transporter for the photoelectrochemical system. Anatase TiO2 nanoparticles are one of the most used oxides and are able to deliver the highest photoconversion efficiency in this kind of solar cells, but intense research in the last years was also addressed to ZnO and other composite systems. Modulation of the composition and shape of nanostructured photoanodes is key element to tailor the physical chemical processes regulating charge dynamics and, ultimately, to boost the efficiency of the end user device, by favoring charge transport and collection, while reducing charge recombination. We investigated light harvesting, exciton separation and charge injection and transport in several systems: (i) TiO2 nanoparticles / ZnO nanowires; (ii) Multiwall carbon nanotubes (MWCNTs) / TiO2 nanoparticles; (iii) TiO2 nanotubes; (iv) Hierarchically self-assembled ZnO sub-microstructures. Both dye molecules and semiconducting quantum dots were applied as light harvesters. Possible tailoring of structure and morphology of the photoanodes and of the quantum dots, and their implication in improving the functional properties of these kinds of excitonic solar cells will be discussed in detail.

# A close look to the atoms: a journey to the nanoworld through advanced electron microscopy

**Wednesday, 9th November - 10:55 - Plenary Speeches - Auditorium - Oral presentation - Abstract ID: 701**

***Prof. Jordi Arbiol*** [1]

***1.*** *ICREA & Institut Català de Nanociència i Nanotecnologia (ICN2), CSIC and BIST*

New materials for future applications are nowadays being synthesized at nanoscale (ultrathin interfaces, nanoparticles, nanowires and quantum structures, all functionalized for novel applications). As developments in Materials Science are pushing to the size limits of physics and chemistry, there is a critical requirement for identifying and manipulating the atoms at the nanoscale. There is a serious need in advanced nanomaterials to determine their structure, composition and morphology at atomic scale in order to correlate these results with the physical and chemical properties and functionalities they have. In this way, a worldwide increasing interest for advanced electron micro/nanoscopy is emerging. Imagine being able to hold an electron beam over a single atom for 1 entire second in order to actually directly SEE and acquire information. The advent of aberration-corrected transmission electron microscopy technology is now giving resolutions below 0.05 nanometers enabling single atoms to be directly viewed and nano and quantum structures to be optically and electrically analyzed in-situ. We will be able to see single atoms and fancy nanostructures, and we will explain how simple changes at atomic scale can make a great difference when looking at the material properties from the macroworld (photonics and electronics). There is a way to paint the nanoworld with colors, obtaining the intrinsic properties of the atoms themselves, while 3D atomic models obtained from accurate structural analyses will help to understand the growth mechanisms at the nanoscale.

# Catalytic Nano-and Micro-bots: What for?

**Wednesday, 9th November - 11:30 - Plenary Speeches - Auditorium - Oral presentation - Abstract ID: 706**

***Prof. samuel sanchez*** [1]

***1.*** *Insitute for Bioengineering of Catalonia (IBEC), Insitutció Catalana de Recerca i Estudis Avançats (ICREA) and Max Planck Institute for Intelligent Systems*

Engineering tiny nano-bots that actively and autonomously act for desired applications is envisioned to be part of future nanotechnology. Mimicking biomotors, scientists use catalytic reaction to power artificial nano-devices and nano-machines. Self-powered micro-nano-bots can be fabricated from multiple materials, shapes and by various methods, and have demonstrated several proof-of-concept applications in robotics, Lab-chip biosensing, nanomedicine, and environmental field [1]. We fabricate nano-bots from mesoporous silica nanoparticles, microcapsules, electrodeposited microtubes and rolled-up thin films into microtubular jets. Very recently, we have found that hybrid micro-bio-bots combine the best from the two worlds, biology and nano-materials providing very promising bio-related applications [2]. What can nano-microbots do for us? Here, I will present our recent developments in this fascinating field focusing on two applications, i.e. towards nanomedicine [2,3,4] and water remediation[5,6]. Keywords: nanomotors, nanotechnology, drug delivery, active matter, self-propulsion, bots. References [1] S. Sanchez, Ll. Soler and J. Katuri. Angew.Chem.Int.Edit. 54,1414-1444 (2015) [2] M. M. Stanton et al. Adv. Mat. Interf (2015 )DOI: 10.1002/admi.201500505 [3] X. Ma, K. Hahn and S. Sanchez. J. Am. Chem.Soc. 137 (15), 4976--4979 (2015); X. Ma et al. ACS Nano 10 (3), 3597-3605 (2016); X. Ma et al. NanoLett. 15 (10), 7043-7050 (2015) [4] S. Sanchez et al, Chem. Commun., 47, 698. (2011) [5] D. Vilela et al. Nano Letters 16 (4), 2860-2866 (2016) [6] Soler, Ll. et al., ACS Nano, 7, 9611 (2013); Gao, W., Wang, J., ACS Nano, 8, 3170 (2014); Soler, L. Sanchez, S. Nanoscale, 6, 7175 (2014); J. Parma et al. Adv. Funct. Mat. (2016) DOI: 10.1002/adfm.201600381

# Cluster particle's deposition on rough surfaces; Effects of diffusion and cluster's shape

**Wednesday, 9th November - 13:30 - Poster Session - Gallery - Poster presentation - Abstract ID: 470**

***Dr. Amir Ali Masoudi*** [1]***, Dr. Leila Hedayatifar*** [2]***, Dr. Foroogh Hassani*** [3]***, Dr. Shadi Esmaily*** [4]***,***
***Dr. Danial Khorsandi*** [5]***, Ms. Zahra Madadi*** [6]

***1.*** *Department of Physics, Alzahra University, Tehran, Iran,* ***2.*** *AGH University of Science and Technology,* ***3.*** *AGH University of Science and Technology,Faculty of Metals Engineering and Industrial Computer Science, A. Mickiewicza Ave. 30, 30-059 Kraków,* ***4.*** *Department of physics, Virginia Polytechnic Institute and State University, Blacksburg, Virginia, 24061, USA,* ***5.*** *Harvard-MIT's Division of Health Science and Technology,* ***6.*** *Islamic Azad University, North Tehran Branch*

The significance role of thin films in manufacturing electronic, magnetic and optical devices has led to technological advances in surface growth under none equilibrium conditions. To fabricate the desired surfaces, various techniques have been introduced to manage the rate of involved mechanisms such as deposition, evaporation, and diffusion of particles. In recent years, increasing the application of surfaces deposited by clusters in magnetic storage and solar cells has brought about new methods of producing cluster particles and depositing them on surfaces. The controllability of parameters in cluster sources such as, the kinetic energy of particle beam; particle size distribution function and density of clusters in the presence of substrates with specified properties have led to produce a wide variety of thin films. Researches show that deposition of particles with low kinetic energy does not change shapes of particles and substrate, which consequently leads to porous media. In the other hands, deposition of clusters with higher kinetic energy can lead to the deformation of particles and surfaces which can construct smoother surfaces. We use Monte Carlo simulation to study the spatial-temporal behavior of thin films generated by low kinetic energy cluster particles. To this end, two models are considered in order to investigate the effects of clusters' shapes and their diffusion ability on the surface. In the first model, clusters are considered as a string of particles with unit height and non-unit length. The growth process in this model is implemented based on Random Deposition with Surface Relaxation (RDSR) model where particles can diffuse on the surface until reaching the minimum state of energy. In the RDSR model for particles with unit size, the model with specific critical exponents is categorized in Edward- Wilkinson (EW) universality class. The second model studies deposition of porous clusters with different shapes according to Random Deposition (RD) model. Our results reveal that using cluster particles with non-unit size leads to a non-Markovian process with a porous medium which changes the universality class of models to Kardar-Parizi-Zhang (KPZ) by scaling exponents B = 0:3 and a = 0:5.

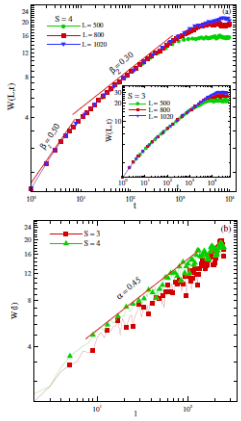


FIG. 3: For the first model, the log-log plot of a) surface width versus time for particles with length $S = 4$. The inset shows the same results for particles with the size of $S = 3$. b) The value of surface width for saturated surfaces. The values of growth exponents are indicated in the figure

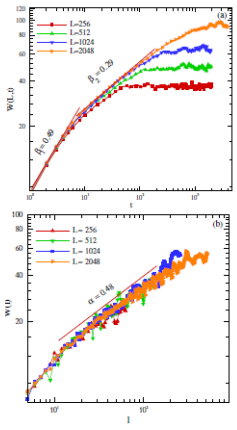


FIG. 4: For the second model, the log-log plot of a) surface width versus time for clusters with different shapes. b) The value of surface width for saturated surfaces. The values of growth exponents are indicated in the figure.

Fig3.png

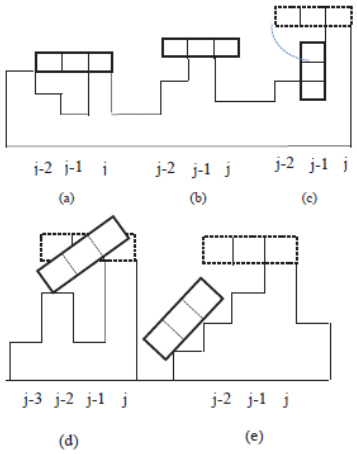


FIG. 1: First model, deposition of cluster particles according to the Random Deposition with Surface Relaxation model (RDSR). Various landing conditions during the simulation; (a)the maximum height under the particle, is the particle's midpoint (b)the neighbor's height does not allow the particle to rotate (c)rotation with radius $S - 1$ (d)tilt (e)diffusion.

Fig1.png

# A RNA nanotechnology platform for a simultaneous two-in-one siRNA delivery and its application in synergistic RNAi therapy

**Wednesday, 9th November - 13:30 - Poster Session - Gallery - Poster presentation - Abstract ID: 17**

***Dr. Hyung Jun Ahn*** [1]

***1.*** *Korea Institute of Science and Technology*

Incorporating multiple copies of two RNAi molecules into a single nanostructure in a precisely controlled manner can provide an efficient delivery tool to regulate multiple gene pathways in the relation of mutual dependence. Here, we show a RNA nanotechnology platform for a two-in-one RNAi delivery system to contain polymeric two RNAi molecules within the same RNA nanoparticles, without the aid of polyelectrolyte condensation reagents. This strategy densely packs and co-delivers polymeric RNAi molecules, leading to the simultaneous silencing of two targeted mRNAs, of which biological functions are highly interdependent. In addition to assembly of polymeric, two types of RNAi molecules within single RNA nanoparticle, combination therapy for multi-drug resistance cancer cells, studied as a specific application of our two-in-one RNAi delivery system, demonstrates efficient synergistic effects for cancer therapy. This RNA nanoparticles approach has an efficient tool for a simultaneous co-delivery of RNAi molecules in the RNAi-based biomedical applications, and our current studies for its RNAi-based therapy present an efficient strategy to overcome multi-drug resistance caused by malfunction of genes in chemotherapy.

# Preparation of a Highly Porous Carbon Nitride by a Facile Post-Synthetic Method

**Wednesday, 9th November - 13:30 - Poster Session - Gallery - Poster presentation - Abstract ID: 42**

***Mr. Tomoyuki Iwamoto*** [1], ***Prof. Yoichi Masui*** [1], ***Prof. Makoto Onaka*** [1]

**1.** *The University of Tokyo*

Graphite-like carbon nitride (g-C3N4) is a potential material for use as photocatalysts, catalyst supports, electrodes, and so force. g-C3N4 is easily made from cheap CN compounds like melamine by pyrolysis. However, it was hard to prepare C3N4 materials with a large surface area. We found a facile method for the preparation of highly porous carbon nitride[1]. Our porous carbon nitride labelled as ``nanoC3N4'' works as a suitable photocatalyst support[2]. In this presentation, we report the effect of each step for the preparation of nanoC3N4 on its porosity and the structural analysis of nanoC3N4. We prepared nanoC3N4 in the following three steps. Step 1: Treating g-C3N4 with concd H2SO4 and washing it with water completely. Step 2: Treating it with aqueous NaOH solution and washing it with water completely. Step 3: Soaking it with EtOH twice. The obtained carbon nitride materials were finally dried in vacuo at 120 ˚C. We changed conditions for each step and measured the BET surface area and DH pore volume. The results are shown in the attached table. NanoC3N4 has more than 20 times a BET surface area than conventional g-C3N4 (Entry 5). In this preparation, the treatments with H2SO4 in Step 1 and EtOH in Step 3 are essential for preparing nanoC3N4. We analysed the structure of the nanoC3N4 by 13C solid-state MAS NMR, IR, XRD, and so force. We found that the polymeric structure of g-C3N4 was maintained even after the treatment with H2SO4. However, a graphite-like layered structure of g-C3N4 is exfoliated. Therefore, we estimate that Step 1 is necessary to exfoliate the polymeric CN layers, and Step 3 is needed to remove water molecules which connect polymeric CN compounds by hydrogen bonds. [1] T. Iwamoto, Y. Masui, J.-C. Wang, M. Onaka Chem. Lett. 2013, 42, 247. [2] K. Mori, T. Itoh, H. Kakudo, T. Iwamoto, Y. Masui, M. Onaka, H. Yamashita Phys. Chem. Chem. Phys. 2015, 17, 24086.

| Entry | Step 1 | Step 2 | Step 3 | BET Surface area / $m^2\ g^{-1}$ | DH Pore Volume / $cm^3\ g^{-1}$ |
|---|---|---|---|---|---|
| 1 | | | | 8 | 0.04 |
| 2 | ✓ | | | 5 | 0.01 |
| 3 | | ✓ | ✓ | 10 | 0.06 |
| 4 | ✓ | | ✓ | 148 | 0.45 |
| 5 | ✓ | ✓ | ✓ | 170 | 0.39 |

Attached image v100 160506 le.png

# Investigation of porous Si, formed by metal-assisted chemical etching with Au as catalyst

**Wednesday, 9th November - 13:30 - Poster Session - Gallery - Poster presentation - Abstract ID: 70**

***Mrs. Olga Pyatilova*** [1]***, Prof. Sergey Gavrilov*** [1]***, Mr. Andrey Savitskiy*** [1]***, Dr. Alexander Pavlov*** [2]***, Mr. Alexandr Dudin*** [3]

***1.*** *National Research University of Electronic Technology,* ***2.*** *Institute of Nanotechnology of Microelectronics of the RAS,* ***3.*** *Institute of Nanotecnology of Microelectronics of the RAS*

Straight pores formed in silicon (Si) have attracted attention for their applications in various fields such as membranes, photo- and betavoltaics devices, bio- and chemical sensors and many others. Metal-assisted etching (MACE) has been studied as a novel method for production of a porous structure in Si. Metal films or particles loaded on Si wafers are used as catalysts for etching of Si in aqueous solutions of HF and H2O2 without external electrical power. This abstract describes a method of porous layers formation using no continuous gold film as a catalyst in the aqueous solution of HF and H2O2 during 10, 30 and 50 minutes. The solution temperature was in the range of 25 °C to 70 °C. Initial substrate was p-(100) type Si with resistivity 0,01 Ohm•cm. In the work were calculated growth rate of the porous layer thickness (Vh) and pore diameter (Vd) at various temperatures solution. The plot of 1/T vs. lnVh and lnVd showed a good straight in the range of 25 ˚C to 70˚C (Fig.1). The growth rate of the porous layer thickness is described by the following equation: Vh=2,6•10ˆ10•exp (-0,54/kT), where Eah=0,54 eV - the activation energy of growth, A1=2,6•10ˆ10 nm/min is pre-exponential factor at Eah. The increase rate of the pore diameter is described by the following equation: Vd=1,01•10ˆ12•exp (-0,66/kT), where Ead=0,66 eV, A2 =1,01•10ˆ12 nm/min at Ead. Accordingly, an activation energy (Ea) and pre-exponential factor (A) were calculated, using the Arrhenius equation. The etching rate of single-crystal silicon increases due to the increase of chemical reaction rate with temperature. Moreover the temperature increase is lead to reducing the hole-injection barrier between the Au and Si and carrier injection into semiconductor. It leads to growth of total hole current. Figure 1 - Arrhenius plot of the growth rate of the porous layer thickness (Vh) and pore diameter (Vd) versus reciprocal temperatures solution. The reported study was funded by RFBR according to the research project No 16-33-00712 мол_а.

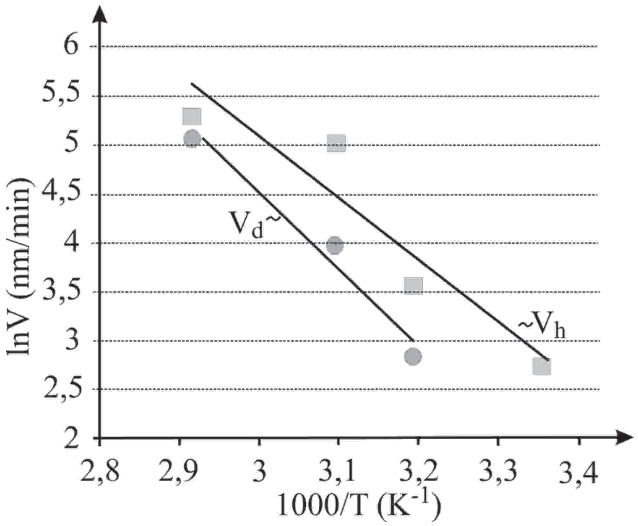


Plot.jpg

# Nanotubular anodic TiO2 initial layer morphology evolution under controlled hydrodynamic and temperature conditions

**Wednesday, 9th November - 13:30 - Poster Session - Gallery - Poster presentation - Abstract ID: 89**

***Dr. Alexey Dronov*** [1], ***Mr. Ilya Gavrilin*** [1], ***Prof. Sergey Gavrilov*** [1], ***Prof. Herman Terryn*** [2], ***Dr. Jon Ustarroz*** [2], ***Mr. Oscar Steenhaut*** [2]

***1.*** *National Research University of Electronic Technology,* ***2.*** *Vrije Universiteit Brussel*

Self-organized anodic TiO2 nanotubular (TNT) layers are highly interesting materials among valve metal oxides, because of the combination of a regular and controllable nanoscale geometry with the various functional properties of titania, which make the material suitable for applications in electro- and photocatalysis, solar energy conversion, sensing, biomedical devices and Li-ion batteries [1]. Over the past few years, various research groups have published a number of works devoted to the study of morphology, chemical, electrical and optical properties of the TNT layers. However, until now some TNT morphology evolution aspects during the electrochemical oxidation were not studied well. In particular the formation, evolution and properties of TNT initial layer, formed at the beginning of anodization process on titanium surface [2], from various anodizing process conditions, which is an important factor for design, manufacture and efficiency increasing of TNT based devices. In this paper, the origin nature concept and geometric parameters evolution studies are presented as well as the chemical and structural properties of initial TNT layer which is formed during the anodizing process of titanium substrates in non-aqueous fluorinated electrolytes under controlled hydrodynamic conditions and electrolyte temperature. During the research it was found that the thickness of the initial layer is almost independent from titanium anode rotation speed and electrolyte temperature, however with increasing of electrode rotation speed and the temperature thinning of the initial porous layer cell walls was observed. Further increase of temperature and anodization process duration leads to the main nanotubular titanium oxide layer etching that eventually leads to detachment of the upper layer from the rest of the oxide layer. X-ray diffraction and XPS analysis showed the presence of crystalline phases in the initial layer and amorphous phase of nanotubular layer underneath it, which may serve as an explanation of such behavior of TNT initial layer. The work was supported by RFBR grant for young scientists № 31 16-33-60217 «mol_a_dk».

# Preparation and testing of collagen-based nanocomposite scaffolds for tissue engineering and bone implantology

**Wednesday, 9th November - 13:30 - Poster Session - Gallery - Poster presentation - Abstract ID: 110**

***Dr. Martin Braun*** [1], ***Dr. Tomas Suchy*** [1], ***Dr. Monika Supova*** [1], ***Dr. Pavla Sauerova*** [2], ***Dr. Martina Verdanova*** [2], ***Dr. Zbynek Sucharda*** [1], ***Dr. Sarka Ryglova*** [1], ***Dr. Margit Zaloudkova*** [1], ***Dr. Radek Sedlacek*** [3], ***Dr. Marie Hubalek Kalbacova*** [2]

***1.*** *Institute of Rock Structure and Mechanics, Academy of Sciences of the Czech Republic,* ***2.*** *Institute of Inherited Metabolic Disorders, 1st Faculty of Medicine, Charles University in Prague,* ***3.*** *Faculty of Mechanical Engineering, Czech Technical University in Prague*

Introduction Nanotechnologies represent a perspective approach which enable regeneration or substitution of an impaired connective tissues. In our study we focused on preparation and testing of biocompatible nanocomposite scaffolds which can imitate a bone matrix and could be potentially applied in bone surgery and implantology. Methods Our scaffolds are based on natural collagen matrix isolated from fish skin supplemented with sodium hyaluronate and natural calcium phosphate nano-particles (bioapatite) isolated from bovine bone and reinforced by poly(DL-lactide) electrospun nanofibers. Structure, degradation, and chemical properties of the scaffolds were characterized using infrared spectrometry (FTIR), scanning electron microscopy (SEM), by means of the determination of mass loss, swelling ratio and pH. We tested three different cross-linking agents to improve the mechanical properties and stability of the scaffolds: N-(3-dimethylaminopropyl)-N'-ethylcarbodiimide hydrochloride and N-hydroxysuccinimide in an ethanol solution (EDC/NHS/EtOH), EDC/NHS in a phosphate buffer saline solution (EDC/NHS/PBS) and genipin. To find out the most suitable scaffold for cell adhesion and tissue engineering application we monitored the effect of these cross-linkers and preparation conditions on the pore size, structure and mechanical properties of the scaffolds. The swelling ratio and also the pH of the scaffolds were assessed using their immersion in a cell culture medium. Moreover, we measured the metabolic activity of human mesenchymal stem cells (hMSCs) cultivated in scaffold infusions for 2 and 7 days as well as cell adhesion, proliferation and cell penetration into our scaffolds using confocal microscopy visualization. Results and Discussion Based on these tests we found out that EDC/NHS/PBS and genipin formed the most effectively cross-linked and stable biomaterials. The scaffolds cross-linked with EDC/NHS/PBS embodied a low degradation together with a low swelling ratio. The genipin cross-linked scaffold has shown the best conditions for hMSC cultivation. No cytotoxicity was proved in infusions from all the tested scaffolds. The results of our experiments suggest that our collagen-based scaffolds cross-linked by both genipin and EDC/NHS/PBS are perspective biomaterials for further in vivo testing and bone surgery applications. Acknowledgments: This study was supported by a grant project provided by the Ministry of Health of the Czech Republic (NV 15-25813A).

# Preparation and optimization of vitamin E TPGS-functionalized PLGA nanoparticles for carboplatin encapsulation

**Wednesday, 9th November - 13:30 - Poster Session - Gallery - Poster presentation - Abstract ID: 153**

***Mr. Daniel Profirio*** [1]***, Prof. Pedro Corbi*** [1]***, Prof. Francisco Pessine*** [1]

***1.*** *Universidade Estadual de Campinas - UNICAMP*

Carboplatin, a platinum-based antineoplasic drug, represents an excellent chemotherapeutic agent for newly diagnosed malignancies and it is effective for testicular, ovarian, bladder, head and neck cancers [1]. However, low uptake of carboplatin by tumor cells is considered a key reason for its limited therapeutic efficacy [2]. In this work nanoparticles composed of poly(D-L-lactic-co-glycolic) acid (PLGA) were prepared to produce nanocarriers for carboplatin. The carboplatin loaded PLGA nanoparticles were formulated by nanoprecipitation method and experimental design, using TPGS (D-α-tocopheryl polyethylene glycol succinate) as stabilizer [3]. Briefly, PLGA was dissolved in acetone while an aqueous solution of carboplatin was prepared. Drug solution was added to the PLGA solution and the biphasic mixture was sonicated to give a primary w/o emulsion. This emulsified mixture was added to a solution containing TPGS and sonicated again to give a double emulsion (w/o/w). Following evaporation of acetone, a suspension of NPs was obtained and purified by ultracentrifugation (20,000 rpm for 15 min and 2 washes with distilled water) or dialysis (membrane with 3500 Da MWCO for 24 h). The results showed that average hydrodynamic diameter is dependent of time, amplitude of sonication, volume and concentration of TPGS aqueous solution (according to a linear model), while polydispersity index and zeta potential are constants (0.10-0.30 and -30 mV). Encapsulation of carboplatin was confirmed by UV-Vis spectroscopy using a derivatization technique with o-phenylenediamine. Dialysis was chosen as purification method because higher values were obtained for entrapment efficiency (5%) and nanoparticle yield (77%) in comparison to ultracentrifugation. Moreover, the optimized formulation (mean particle size = 121.0 nm, PDI = 0.120 and zeta potential = -34.0 mV) was stable over a period of 60 days when stored at 10°C. REFERENCES - [1] S. Jose et al, Colloids and Surfaces B: Biointerfaces 142 (2016) 307-314. [2] T. Sadhukha and S. Prabha, AAPS PharmSciTech 15 (2014) 1029-1038. [3] N. A. Peppas et al, Journal of Controlled Release 190 (2014) 29-74.

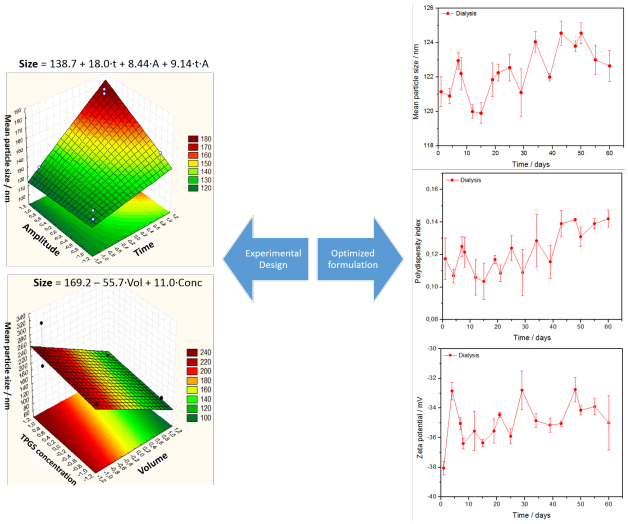
Size = 138.7 + 18.0·t + 8.44·A + 9.14·t·A
Mean particle size / nm
Amplitude
Time
Size = 169.2 – 55.7·Vol + 11.0·Conc
Mean particle size / nm
TPGS concentration
Volume
Experimental Design
Optimized formulation
Dialysis
Mean particle size / nm
Time / days
Dialysis
Polydispersity index
Time / days
Dialysis
Zeta potential / mV
Time / days

Figure.png

# Electrospun Nanocomposite Materials, A Novel Synergy of Polyurethane and Bovine Derived Hydroxyapatite

**Wednesday, 9th November - 13:30 - Poster Session - Gallery - Poster presentation - Abstract ID: 197**

***Dr. Yahya BOZKURT*** [1], ***Mr. Ahmet ŞAHİN*** [2], ***Mr. Akın SUNULU*** [3], ***Mr. Mehmet Onur AYDOGDU*** [4], ***Prof. Faik Nüzhet OKTAR*** [5], ***Dr. Nazmi EKREN*** [6], ***Dr. Oğuzhan GUNDUZ*** [1]

***1.*** *Marmara University, Department of Metallurgy and Materials Engineering, Faculty of Technology Goztepe Campus 34722, Kadikoy-Istanbul,* ***2.*** *Marmara University, Advanced Nanomaterials Research Laboratory, Department of Metallurgical and Materials Engineering, Goztepe Campus 34722 Istanbul,* ***3.*** *Marmara University, Bioengineering Department, Bachelor's Degree, Faculty of Engineering, Istanbul 34722, Turkey,* ***4.*** *Marmara University, Department of Metallurgical and Materials Engineering, Master of Science, Institute of Pure and Applied Sciences, Goztepe Campus 34722 Istanbul, Turkey,* ***5.*** *Marmara University, Bioengineering Department, Faculty of Engineering, Istanbul 34722,* ***6.*** *Marmara University, Advanced Nanomaterials Research Laboratory, Department of Metallurgical and Materials Engineering, Goztepe Campus 34722 Istanbul,*

Introduction: Polyurethane (PU) is one of the most reliable accompanying synthetic polymers that is used for construction of the scaffolds in tissue engineering applications in order to obtain desirable mechanical, physical and chemical properties like elasticity, durability and biocompatibility. Bovine derived hydroxyapatite (BHA) is a ceramic based natural polymers that is used as the most preferred implant material in orthopaedics and dentistry due to the chemically and biologically similarity to the mineral phase found in the human bone structure. As bone repair material, PU or PU scaffold loaded with nano-hydroxyapatite particles could enhance its bone-bonding bioactivity and mechanical properties [1] Methods: In this study, PU and bovine derived hydroxyapatite (BHA) solutions with different concentrations were prepared with dissolving polyurethane and BHA in dimethylformamide (DMF) and Tetrahydrofuran (THF) solutions. Blended PU-BHA solutions in different concentrations were used for electrospinning technique to create nanofiber scaffolds and new biocomposite material together. Results and Discussion: SEM, FTIR and physical characterization tests such as viscosity, electrical conductivity, density and tensile strength measurements were carried out after production process. In Figure 1, SEM images of the PU-BHA fibers were observed together as a scaffolds and bead like structures. Scaffolds were originated from the PU and reason of the bead like structures is the presence of the BHA. Results are found to be promising for bone tissue engineering applications due to the characteristics of the composite nanofiber materials that possess both beneficial properties of two different material (PU and HAp) in same material. Reference: [1] Du JJ, Zou Q, Zuo Y, Li YB. Int J Surg 2014;12:404--7

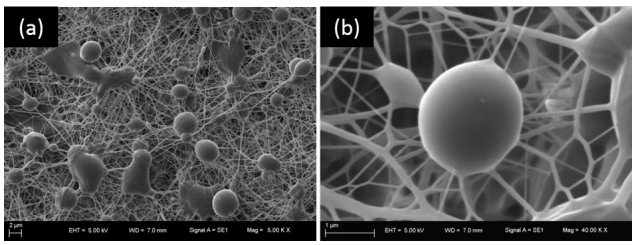


Figure 1 - sem images of the pu-bha nanocomposite fiber structure a low magnification and b high magnification.png

# Nanostructured titania doped with silver nanoparticles for photocatalytic water disinfection

**Wednesday, 9th November - 13:30 - Poster Session - Gallery - Poster presentation - Abstract ID: 201**

***Ms. Evelína Polievková*** [1], ***Ms. Kateřina Přikrylová*** [2], ***Dr. Jana Drbohlavová*** [1]

***1.*** *Central European Institute of Technology-Brno University of Technology,* ***2.*** *Brno University of Technology*

This research presents simple, reproducible and efficient technology of fabrication of TiO2/Ag NPs photocatalytic system for degradation of microbial pollutants from water, namely Candida glabrata. This type of yeast was considered as relatively non-pathogenic fungi for a long time. However, recently with increased usage of immunosuppressive agents combined with antimycotic therapy, systemic infections at individuals with immunodeficiency caused by this fungi have significantly increased as well. Nowadays, occurrence of Candida glabrata is very enlarged which increases the risk of fungal diseases, tooth decay and various infections of mucosal tissues, urogenital system or digestive tract. This work presents fabrication of highly effective TiO2/Ag NPs photocatalytic system active in visible spectrum which was created via anodization of Ti thin film and subsequently doped with silver nanoparticles via in situ UV-assisted synthesis and electrochemical deposition process. Its photocatalytic antimicrobial efficiency was tested on model organism Candida glabrata in different irradiation periods employing fluorescent tubes as light source. The efficiency of TiO2/Ag NPs photocatalytic system was evaluated by fluorescence microscopy using acridine orange dye as indicator of yeast cell viability. The morphology characterization of TiO2 with and without doping was provided by scanning electron microscopy.

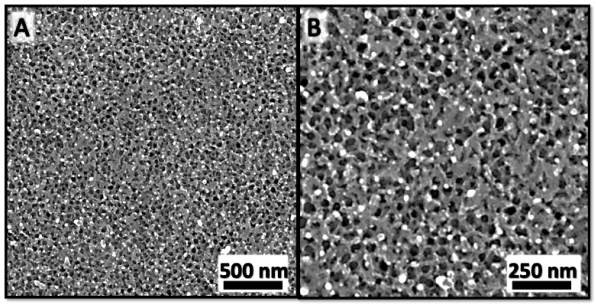


Uv deposited ag nps.png

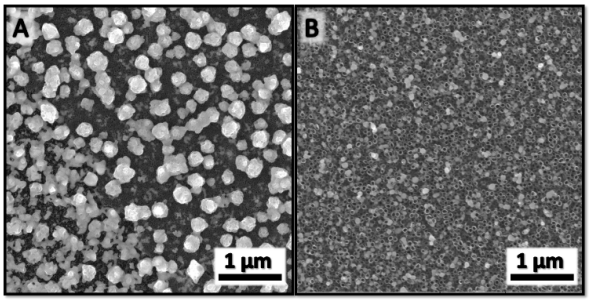


Electrochemically deposited ag nps.png

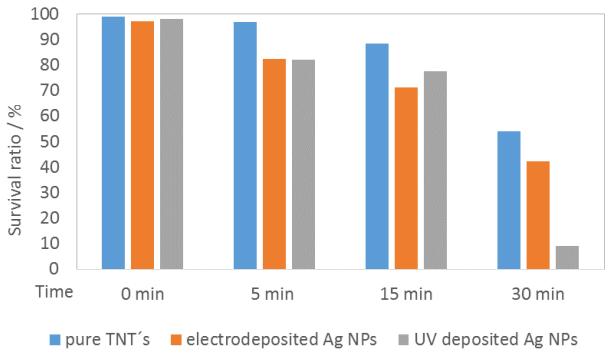


Survival ratio of c.glabrata graph.png

# Understanding 2D Nanoflake–like Heterostructures for Energy Storage and Conversion Applications at the Atomic Level

**Wednesday, 9th November - 13:30 - Poster Session - Gallery - Poster presentation - Abstract ID: 223**

***Mr. Peng-Yi Tang*** [1], ***Dr. María De La Mata*** [1], ***Ms. Li-juan Han*** [2], ***Prof. Aziz Genç*** [1], ***Dr. Yong-min He*** [3], ***Mr. Xuan Zhang*** [4], ***Mr. Lin Zhang*** [5], ***Prof. José Ramón Galán-mascarósc*** [2], ***Prof. Joan Ramon Morante*** [6], ***Prof. Jordi Arbiol*** [7]

***1.*** *Catalan Institute of Nanoscience and Nanotechnology (ICN2), CSIC and The Barcelona Institute of Science and Technology (BIST),* ***2.*** *Institute of Chemical Research of Catalonia (ICIQ), The Barcelona Institute of Science and Technology (BIST),* ***3.*** *School of Physical Science and Technology, Lanzhou University,* ***4.*** *Department of Materials Science (MTM), KU Leuven,* ***5.*** *Department of Integrated System Engineering, The Ohio State University,* ***6.*** *Catalonia Institute for Energy Research (IREC),* ***7.*** *ICN2*

Introduction: The conversion and storage of solar energy into chemical fuel hold promise to meet the increasing demand for global energy and ensure a permanent renewable energy supply for the future. As promising candidates for energy storage and energy conversion, 2-D materials have drawn plenty of researchers´ attention. Despite such a wide spectrum of research on the optimization of nanostructures in various 2D materials, precise relationship between the materials´ structure and physical and chemical properties remains elusive. Methods: Hydrothermal method, electrodeposition etc.. Field emission scanning electron microscope (SEM), transmission electron microscopy (TEM), scanning transmission electron microscopy-electron energy loss spectroscopy (STEM-EELS, with a high angle annular dark field (HAADF)) and geometric phase analyses (GPA). Result: Honeycomb-like hematite nanoflakes/branched polypyrrole nanoleaves heterostructures with a 3D complex structure have been synthesized and employed as high-performance negative electrodes for asymmetric supercapacitors application. Besides, the core-shell MoO2/MoS2 nanoflakes have been synthesized via a step by step process and are utilized as photocathode for water splitting application. Discussion: The detailed TEM-STEM characterization and deep EELS chemical analysis at the nanoscale has been combined to elucidate the mechanisms underlying the formation and morphology evolution of core-branch Fe2O3@PPy heterostructures. In addition, we have studied the mechanism of converting MoO2 nanoflakes into 2D free-standing MoS2 electrode by sulfurization process for water splitting. In this way, the atomic resolution aberration corrected HAADF STEM reveals the sulfurization mechanism in an unprecedented detail, together with EELS chemical maps.

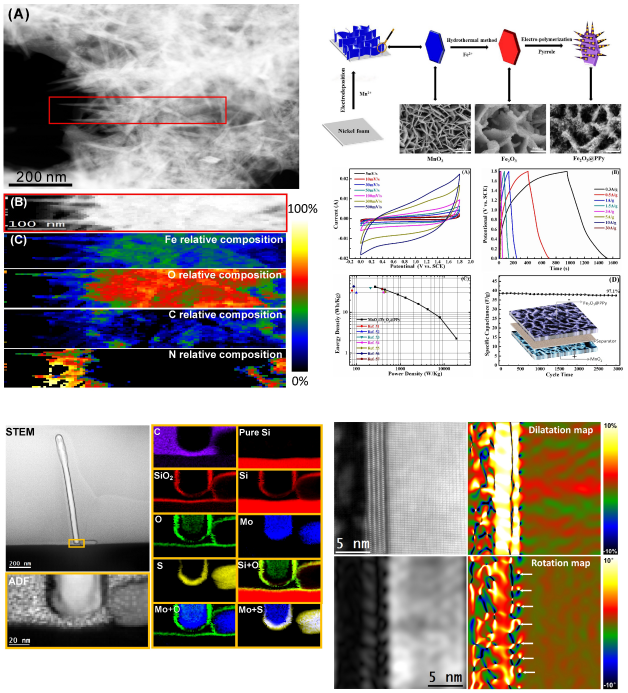


Annic-pengyi tang.jpg

# Remote control of small particles modified with azobenzene derivatives by light irradiation

**Wednesday, 9th November - 13:30 - Poster Session - Gallery - Poster presentation - Abstract ID: 232**

***Dr. Yutaka Kuwahara*** [1], ***Prof. Yoshihiro Yamaguchi*** [1], ***Prof. Seiji Kurihara*** [1]

***1.*** *Kumamoto University*

Introduction: The development of remote-controllable small machines has become important for biotechnology and industrial nanotechnology. We have developed a technique to photo-control silica micro-particles by utilizing distortion of the orientational ordered structure of liquid crystalline (LC) molecules through photo-response of small amount of additive azobenzene (Azo) molecules. In this paper, we have demonstrated remote photo-manipulation of nano-/micro-sized particles (NPs) modified with Azo molecules. Methods: Several kinds of NPs like silica particles and nanosheets of metal oxides were modified by Azo derivatives acting as molecular motor. The resultant Azo-modified NPs (Azo/NPs) were employed in LC systems and model systems of cell membranes. Results and Discussion: UV-visible spectroscopy results reveal that trans-to-cis and cis-to-trans isomerization cycles of Azo groups (top of Figure) could occur continuously by visible light irradiation and rapid thermal reversion. Microscopic observations of the LC system indicate that the Azo/NPs could be transported a few millimeters for ca. 150 s by moving light irradiation at 33 °C (nematic LC phase), as shown in the bottom of Figure. The critical following speed under dragging for a single Azo/NP was evaluated to be at least 10 μm/s at 33 °C. Therefore, the motion behavior appears to be correlated with generation of nano-/micro-sized disorganization regions on the nematic phase caused by photo-induced continuous isomerization of Azo groups. Hence, Azo derivatives can potentially be utilized as a molecular engine in nano-/micro-sized machines by supplying Azo-absorbed light energy and are expected to expand the application of such machines in custom-designed biotechnology and industrial small technology.

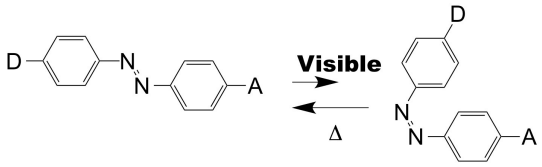


***trans*** form ***cis*** form

Isomerization of azobenzene(**Azo**)

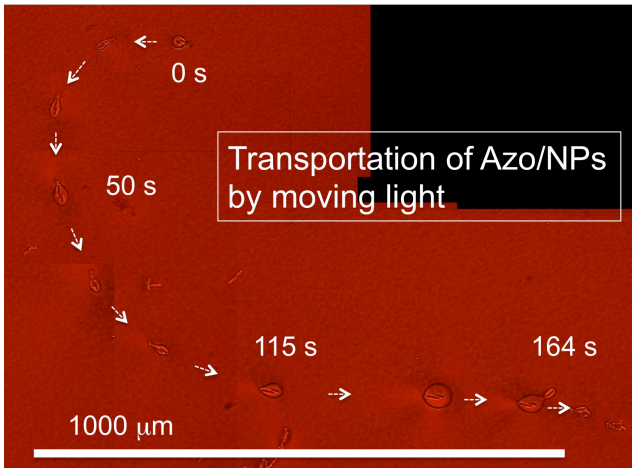


Annicmovs5-2.jpg

# Optically Transparent Polymer-Tungstophosphoric Acid Composite Films with High Refractive Index

**Wednesday, 9th November - 13:30 - Poster Session - Gallery - Poster presentation - Abstract ID: 289**

***Mr. Shuichi Matsumoto*** [1], ***Dr. Thiraporn Ishii*** [1], ***Ms. Mutsumi Wada*** [1], ***Dr. Shoji Nagaoka*** [2], ***Dr. Yutaka Kuwahara*** [1], ***Dr. Makoto Takafuji*** [1], ***Prof. Hirotaka Ihara*** [1]

***1.*** *Department of Applied Chemistry and Biochemistry, Kumamoto University,* ***2.*** *Kumamoto Industrial Research Institute*

Recently high refractive materials have been developed because of their potential uses in optical applications such as optoelectronic device, plastic lenses, fuel cell, etc. Organic-inorganic hybrid materials have been focusing on creating it. Heteropoly acids (HPAs) are a multifunctional material and have interesting properties, including the solubility in aqueous and nonaqueous solutions, the different charges, shapes and sizes, which can induce to novel materials. In this study, a transparent, colorless and high refractive polymer composited with HPAs has been developed. Polyvinyl alcohol (PVA) and poly(methyl methacrylate) (PMMA) were used in this propose. Tungstophosphoric acid (PWA), which is a member of HPAs, was used in this study. The polymer composite films were simply prepared from mixing polymer and PWA then casted on a glass. The schematic illustration exhibits the image of polymer-PWA composite. The optical and structural properties of the obtained composite films were investigated using ultraviolet-visible spectroscopy, a prism coupler and thermogravimetric analyses. The results presented by the both of polymer-PWA (90 wt.%) provided high transparency (90%T) in the visible region (Fig. 1a) and high refractive index (n =1.70). In addition, TiO2 nanoparticles were also used to prepare and study the composite film. Unfortunately, the polymer-TiO2 gave low transparency and turbid film as shown in Fig. 1 (b,d). Therefore, we believe that the optimal combination for creating a colorless and highly refractive polymer films are PVA and PMMA by using PWA 90 wt.%. The observed polymer composited films with PWA should be developed to high refractive and transparent materials for the optical applications.

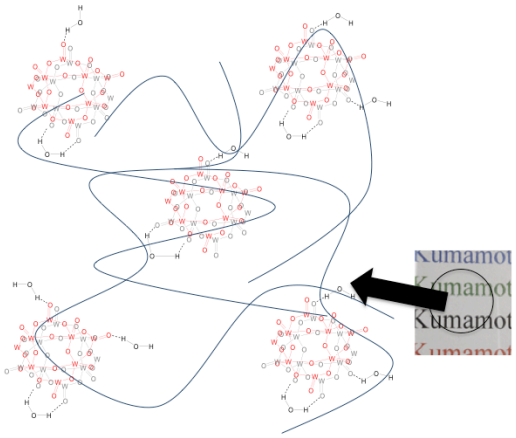

**Schematic illustration of polymer-PWA composite film**

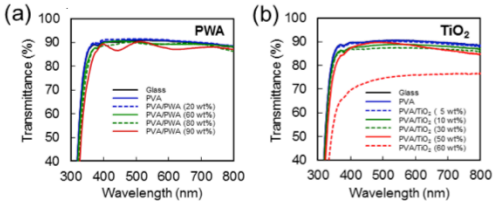


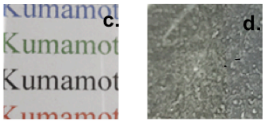


Fig. 1 Transmittance spectra of PVA/PWA (a) and PVA/$TiO_2$ films (b). The images of the obtained films; (c) PVA/PWA and (d) PVA/$TiO_2$.

Abstract fig1018.png

# Poly(L-lysine) functionalized Eu-doped NaGd(MoO4)2 Nanophosphors for Optical and MRI Imaging

**Wednesday, 9th November - 13:30 - Poster Session - Gallery - Poster presentation - Abstract ID: 293**

***Prof. Manuel Ocaña*** [1]***, Dr. Nuria Ofelia Nuñez*** [1]***, Mr. Mariano Laguna*** [1]***, Dr. Jesús M De La Fuente*** [2]***, Dr. Eugenio Cantelar*** [3]***, Dr. Maria L Gracia*** [4]

***1.*** *Institute of Materials Science of Seville (CSIC-US),* ***2.*** *Institute of Materials Science of Aragón (CSIC-UniZar),* ***3.*** *University Autónoma de Madrid,* ***4.*** *Andalusian Centre for Nanomedicine and Biotechnology*

Luminescent rare-earth (RE) based phosphors have attracted recently much attention because of their important applications in several fields including biotechnology (biosensing and bioimaging). Such interest mainly arises from the lower toxicity and higher chemical and optical stability of these phosphors when compared with other luminescent materials (quantum dots, organic dyes-based systems, etc.). The presence of Gd3+ cations in these phosphors is also of high interest since it confers to such materials an additional functionality as contrast agents for magnetic resonance imaging (MRI). For most biotechnological applications, the size and shape of these multifunctional materials are to be controlled since such characteristics affects luminescence and magnetic relaxivity and the circulation behaviour of the nanoparticles in the body, their biodistribution and their excretion pathway. In addition, such nanoparticles must be obviously non-toxic and present high colloidal stability in physiological media. To meet the later criterion, the modification of the nanoparticles surface with ligands having different functional groups is usually required. Among RE-based phosphors, those consisting of a molybdate matrix doped with lanthanide (Ln) cations are of particular interest, since this matrix absorb energy in the UV region which is further transferred to such Ln3+ cations, considerably increasing the intensity of their emissions. Surprisingly, the synthesis of uniform Ln:NaGd(MoO4)2 nanoparticles has not been yet achieved. Herein, we report for the first time in literature a method for the synthesis of non-aggregated and highly uniform Eu3+ doped NaGd(MoO4)2 nanoparticles based on a homogeneous precipitation process in a polyol-based medium. The obtained particles present ellipsoidal shape and their size can be varied by adjusting the experimental synthesis parameters. A procedure for the further functionalization of these nanophosphors with polylisine has been also developed in order to improve their colloidal stability in physiological medium (2-Nmorpholino ethanesulfonic acid, MES). A study of the luminescent dynamics as a function of the Eu doping level has been conducted in order to find the optimum nanophosphors, whose magnetic relaxivity and cell viability have also been evaluated for the first time for this system, in order to assess their suitability as multifunctional probes for optical and magnetic bioimaging applications.

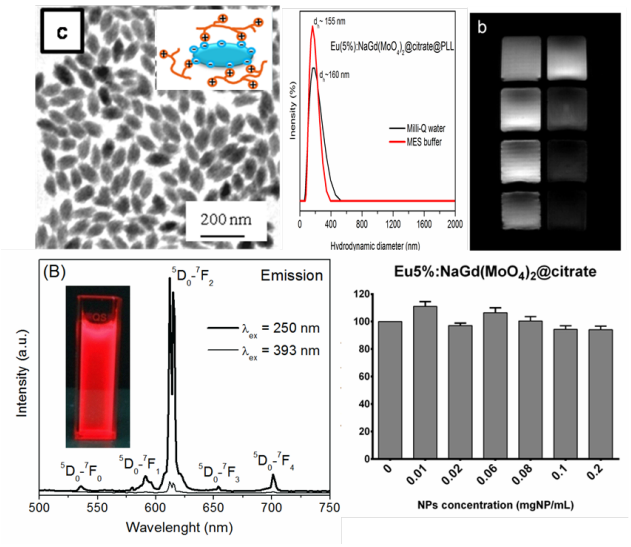


Imagen oca a.png

# Poly(vinylidene fluoride-co-hexafluoropropene) nanocomposite membranes for water purification

**Wednesday, 9th November - 13:30 - Poster Session - Gallery - Poster presentation - Abstract ID: 307**

***Ms. Lutendo Rananga*** [1], ***Dr. Kgabo Moganedi*** [1], ***Prof. Takalani Magadzu*** [1]

***1.*** *University of Limpopo*

Clean drinking water availability is a major problem for developing countries. Membranes technology has become a popular filtration technique and plays a significant role in separation of unwanted constituents such as organic and inorganic pollutants. Herein, the study has focus on the preparation of poly(vinylidene fluoride-co-hexafluoropropene) (PVDF-HFP) doped with multi-walled carbon nanotubes (MWCNTs) and silver nanoparticles. Among various membrane compositions, PVDF-HFP possesses high dielectric constant and good mechanical properties among others. Carbon nanotubes (CNTs) were used as doping material because they display remarkable electrical, thermal and mechanical properties. Silver nanoparticles have been extensively researched due to their high antibacterial activity. The nanocomposite membrane were prepared by a phase inversion method, and characterised by Thermogravimetric analysis, Fourier transform infrared spectroscopy and scanning electron microscopy. The membranes displayed improved porosity, swellability, water content and high salt rejection of NaCl. The membranes were also used to filter contaminated water with E. coli (ATCC 25922) and demonstrated high microbial load reduction and high antibacterial activity. The findings substantiate the reliability of nanocomposite membranes in water purification, which may ultimately safe drinking water for regions of the world stricken by periodic drought or where water contamination is rife.

# CO2 gas sensor based on quartz crystal microbalance coated with vanadium oxide thin film

**Wednesday, 9th November - 13:30 - Poster Session - Gallery - Poster presentation - Abstract ID: 316**

***Dr. MALIKA BEROUAKEN*** [1], ***Dr. Lamia Talbi*** [1], ***Prof. Rezak Alkama*** [2], ***Mr. Hamid Menari*** [1], ***Dr. Noureddine Gabouze*** [1], ***Dr. Sabrina Sam*** [1]

***1.*** *Centre de Recherche en Technologie des Semi-conducteurs pour l'Energétique, Division Couches Minces Surfaces et Interfaces,* ***2.*** *Université A.Mira de Bejaia, Faculté de Génie Electrique .Bejaia*

A gas sensing device based on quartz crystal microbalance (QCM) covered with vanadium oxide thin film has been realized to detect CO2 gas at room temperature. The vanadium oxide thin films were deposited onto QCM substrates by using vacuum thermal evaporation technique. The QCM covered with vanadium oxide film was heated at 200°C for different times. The influence of the annealing time on structural and morphological properties of annealed films was investigated by scanning electron microscopy (SEM). The elaborated structures were tested for CO2 gas sensing behavior. The results show that the increase in the time of annealing increases the sensitive of the sensor. The structure heated at 200°C for 3h exhibited high resonance frequency shift (Δf) to CO2 gas, fast time response (57s), short recovery times (43s), good stability, linearity, reproducibility, and reversibility.

# Electrochemical sensor of organics pollutants based on polythiophene and silicon nanowire

**Wednesday, 9th November - 13:30 - Poster Session - Gallery - Poster presentation - Abstract ID: 341**

***Dr. Samia Belhousse*** [1], ***Dr. Fatma Zohra Tighilt*** [1], ***Dr. Sabrina Sam*** [1], ***Mrs. Kahina Lasmi*** [1], ***Prof. Naima Belhaneche-bensemra*** [2], ***Dr. Noureddine Gabouze*** [1]

***1.*** *CRTSE, Division Couches Minces Surfaces et Interfaces. 2, Bd Frantz Fanon, BP 140 Alger 7-Merveilles,,* ***2.*** *Ecole nationale polytechnique d'alger*

Hybrid devices based on silicon nanowires (SiNW) and polythiophene (PTh) as conductive polymer was prepared by electrochemical way and was used as working electrodes to investigate the redox behavior of para-nitrophenol (p-NPh), phenol and aniline by cyclic voltammetry (CV). p-NPh, phenol and aniline are common organic pollutants found particularly in the effluents from pesticides, pharmaceuticals, petrochemicals and other industries. Owing to their toxicity and reactivity, there is an urgent to develop analytical and simple devices to monitor these pollutants for environmental control and protect human health. SiNW-based sensor devices have gained considerable interest as a general platform for sensors. Metal-assisted chemical etching has successfully been applied for the fabrication of large-area aligned SiNW arrays on single crystal silicon wafers. It is simple and fast method. Hydrogen-passivated surface of SiNW shows a poor stability in water [1]. Surface modification with organic species confers the desired stability and enhances the surface properties. For this reason, this work proposes a covalent grafting of organic conductive polymer such as PTh onto SiNW surface. The choice of conductive polymer allows an improvement of interfacial charge transfer ensuring continuity in the conduction mechanism for a better detection. PTh was covalently grafted on SiNW surface using an electrochemical polymerization which offers several advantages such as simplicity and rapidity. The sensitivity of hybrid structure to different concentration of para-nitrophenol, phenol and aniline was studied by cyclic voltammetry in buffer PBS solution and in p-NPh/PBS, phenol/PBS and aniline/PBS solutions. Figure 1 shows a set of cyclic voltammograms recorded at 50mVs−l, between -1 and 2V in PBS solution for different concentrations from 1.5×10−8 to 1.5×10−4M of p-NPh. In order to check the surface after the electrodetection, the SEM morphology of SiNW/PTh surface was observed after applying a complete cycle.

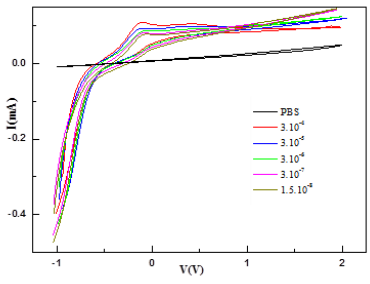


Figure 1.png

# The correlations between the crystal structure and the photocatalytic performance of the NaNbO3 and KNbO3

**Wednesday, 9th November - 13:30 - Poster Session - Gallery - Poster presentation - Abstract ID: 372**

***Mr. Ryo Sasaki*** [1]***, Dr. Takuya Suzuki*** [1]

***1.*** *The University of kitakyushu*

Photocatalyst having a perovskite structure has attracted attention in recent years as the substrate of high performance solar cells. Perovskite structure is an ABO3 chemical composition, and the structure has been actively studied in various fields such as photocatalysts, piezoelectric materials, ceramic dielectric materials and etc. The performance of the photocatalyst is largely changed by substituting elements of A and B sites to the other elements. Our final purpose is to obtain a guiding principle for the synthesis of high performance photocatalysts. In this study, we selected Nb-O based photocatalysts cause they have simple Perovskite structures and would be look forward to high photocatalytic abilities. NaNbO3(NN) and KNbO3(KN) were synthesized by modified solid-state reaction method using Na2C2O4, K2C2O4□H2O and (NH2)2CO. These powders with a molar ratio of [Na2C2O4]:[Nb2O5]:[urea] = 1:1:2 or [K2C2O4□H2O]:[Nb2O5]:[urea] = 1:1:4 were mixed for 1.5 h. The mixed powder was calcined at 560°C for 4 h. Then, we ground the calcined powder and re-calcined at 560°C for 4 h. The sample were analyzed by powder X-ray diffraction (XRD), field emission scanning electron microscopy (FE-SEM), and organic decomposition measurement. Structure refinements were carried out using the Rietveld method by RIETAN-FP (Ver.2.32). The sample was confirmed to be respectively NaNbO3 (PDF-No. 01-72-7753) and KNbO3 (PDF-No. 00-049-453). The photo activities of NN and KN was confirmed by the decomposition of acetic acid to CO2 under simulated solar irradiation(Fig. 2). We select Na8Nb8O24 as an initial structure(space group:Pbcm). As a result, Rwp, RB and RF are shown good values 6.588%, 4.351% and 5.471%, respectively. The structural parameters from this analysis are shown in Table. 1. We select KNbO3 as an initial structure(space group:P4mm). As a result, Rwp, RB and RF are shown good values 9.521%, 4.618% and 2.703%, respectively. This structural parameters are shown in Table. 2. NbO octahedral structure of the NN is distorted and KN show a well-equipped perovskite structure. Difference in photocatalytic performance between NN and KN of organic matter decomposition measurement was not observed. We will carry out the synthesis and analysis of the (Na, K)NbO3 and investigate the correlation between the structure and photo activities.

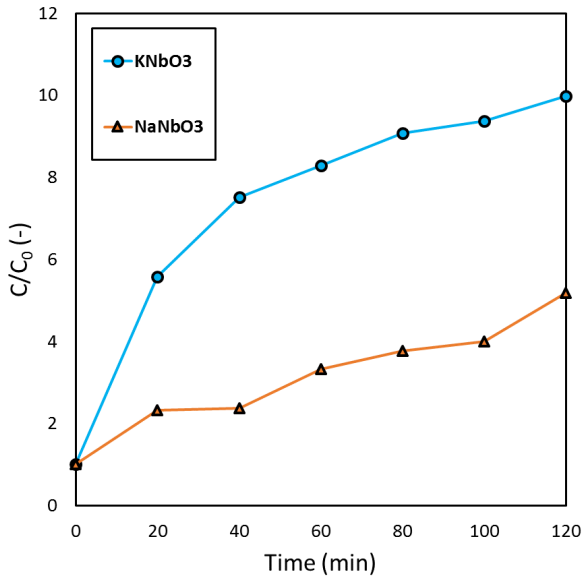


Fig. 1 Decomposition of acetic acid to $CO_2$

Fig1.png

Table. 1 Structural parameters after refinement of NN

| a(Å) | b(Å) | c(Å) | alpha | beta | gamma |
|---|---|---|---|---|---|
| 5.50054 | 5.54701 | 15.49482 | 90 | 90 | 90 |
| **Atom** | **g** | **x** | **y** | **z** | **B** |
| **O4** | 0.8973 | 0.0458 | 0.0062 | 0.1189 | 1.000 |
| **O3** | 0.8481 | 0.5116 | 0.0015 | 0.6466 | 1.000 |
| **O2** | 0.6744 | 0.1490 | 0.8106 | 0.7500 | 1.000 |
| **O1** | 1.1796 | 0.3163 | 0.7500 | 0.0000 | 1.000 |
| **Nb1** | 1.0000 | 0.2554 | 0.7369 | 0.1268 | 1.000 |
| **Na2** | 1.0000 | 0.2118 | 0.2002 | 0.2519 | 1.000 |
| **Na1** | 1.0000 | 0.2586 | 0.2500 | 0.0000 | 1.000 |

Table1.png

Table. 2 Structural parameters after refinement of KN

| a(Å) | b(Å) | c(Å) | alpha | beta | gamma |
|---|---|---|---|---|---|
| 4.01989 | 4.01989 | 4.01989 | 90 | 90 | 90 |
| **Atom** | **g** | **x** | **y** | **z** | **B** |
| **O1** | 0.9257 | 0.5000 | 0.0000 | 0.0000 | 1.000 |
| **Nb1** | 1.0015 | 0.0000 | 0.0000 | 0.0000 | 1.000 |
| **K1** | 0.9480 | 0.5000 | 0.5000 | 0.5000 | 1.000 |

Table2.png

# A site replacement of AxTiyOz of perovskite photocatalyst and their performance

**Wednesday, 9th November - 13:30 - Poster Session - Gallery - Poster presentation - Abstract ID: 380**

***Mr. Koki Saito*** [1], ***Dr. Takuya Suzuki*** [1]

**1.** *The University of kitakyushu*

Recently, photo-catalyst has been widely used as disinfect, antifouling system, solar cell, and etc., cause they are clean and eco-materials without fossil fuel using. Especially, Perovskite photo-catalysts were focused as high performance solar cell, their chemical stability and replace-ability of A and B sites within the structures. In this study, we forced Ti-based Perovskite materials such as ATiO3 (A=metals). Six types Perovskite photo-catalysts synthesized, and A site substituted to K, Rb, Sr, Pb, La, and Pr. Also effects to physical properties of these materials were studied. Ti-TEOA was prepared by mixing Titanium tetraisopropoxide (TIPO) and 2,2',2''-nitrilotriethanolamine (TEOA) in dry air at 1 day. Concentration of Ti--TEOA was adjusted by adding to ion-exchange water. The molar ratio of TEOA/TIPO and concentration of Ti4+ were adjusted to 2/1 and 0.50 mol/L, respectively. Next, each potassium hydroxide, rubidium hydroxide, strontium hydroxide, lead nitrate, lanthanum nitrate, and praseodymium nitrate was added to this mixed solution. The each solution mixing time are 90 min and were heated by hydrothermal method at 140oC for 72h. The gel were washed three time using ion-exchange water and freeze dried. Each Perovskite photo-catalyst were achieved by calcination at 1000 oC for 15h. Products were characterized K2Ti6O13, Rb2Ti6O13, SrTiO3, PbTiO3, La2Ti2O7 and Pr2Ti2O7 by XRD. And physical property of each Perovskite photo-catalyst were measured by FE-SEM, surface area measuring and UV-Vis. SrTiO3 show the largest surface area in all Perovskite photo-catalyst. PbTiO3 had the largest visible light absorption band. Pr2Ti2O7 was had two visible light absorption bands between 400 and 600nm. Photo-activities were measured by oxidation decomposition reaction of acetic acid and reduction dye decomposition reaction of methylene blue. PbTiO3, SrTiO3, and La2Ti2O7 show high acetic acid decomposition because they had visible light absorption band and they could use visible area light. SrTiO3 show highest dye decomposition activity, however this owed its biggest surface area. When we calculated dye decomposition activity par unit surface area, K2Ti6O13 and Rb2Ti6O13 show highest dye decomposition ability. The monovalent metals worked as good electron donor by A site displacement from divalent metal.

# Impedance Spectroscopy of Heterojunction Solar Cell a-SiC/c-Si with ITO Antireflection Film Investigated at Different Temperatures

**Wednesday, 9th November - 13:30 - Poster Session - Gallery - Poster presentation - Abstract ID: 427**

***Prof. Vladimír Šály*** [1], ***Dr. Milan Perný*** [2], ***Prof. František Janíček*** [1], ***Dr. Jozef Huran*** [3], ***Dr. Miroslav Mikolasek*** [1], ***Dr. Juraj Packa*** [1]

***1.*** *Slovak University of Technology,* ***2.*** *Slo,* ***3.*** *Slovak Academy of Sciences*

Progressive smart photovoltaic technologies including heterostructures a-SiC/c-Si with ITO antireflection film are one of the prospective replacements of conventional photovoltaic silicon technology. The main advantages include acceptable efficiency, material savings, environmentally friendly production, acceptable service life and cost [1, 2, 3]. Our paper is focused on the investigation of heterostructures (a-SiC/c-Si) provided with a layer of ITO (indium oxide/tin oxide 90/10 wt.%) which acts as a passivating and antireflection coating. Photolitography and lift off technique was used for Al grid preparation as top contact of solar cell structure. Bottom whole area Al ohmic contact was prepared by Al evaporation. Prepared photovoltaic cell structure underwent the investigation of the temperature on its operation. The investigation of the dynamic properties of heterojunction PV cell was carried out using impedance spectroscopy where the Agilent LCR Meter 4284A was used. An example of the results -- selected impedance spectra -- Nyquist characteristics obtained on sample coated with ITO is shown in Fig. 1. The equivalent AC circuit best approximated the measured impedance data using numerical process was proposed. Assessment of the effect of the temperature on the operation of prepared heterostructure was carried out by analysis of the temperature dependence of AC circuit elements. For a more comprehensive characterization the activation energies and relaxation times were also determined. Impedance spectra were also measured at different DC bias voltages due to a more detailed understanding of transport phenomenon in the heterostructure. Acknowledgement This work was supported by the Slovak Research and Development Agency under the contract No. APVV-15-0326. References [1] I.A. Yunaz, K. Hashizume, S. Miyajima, A. Yamada, M. Konagai, Solar Energy Materials & Solar Cells 93, 1056--1061 (2009). [2] S. Janz, S. Reber, W. Glunz, Proceedings of the 21st EUPVSEC, 660-663 (2006). [3] V.A. Dao, H. Choi, J.Heo, H.Park, K.Yoon, Y. Lee,Y. Kim, N. Lakshminarayan, J. Yi, Current Applied Physics 10, S506--S509 (2010).

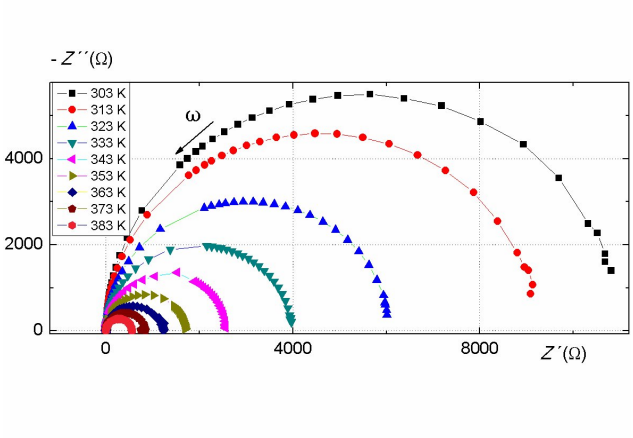


Measured symbol and the fitted solid line impedance spectra for various temperatures in the dark.png

# Catalytic oxidation of selected alcohols using gold covered with TEMPO functionalized C60 fullerene as a catalyst.

**Wednesday, 9th November - 13:30 - Poster Session - Gallery - Poster presentation - Abstract ID: 465**

***Dr. Piotr Piotrowski*** [1], ***Prof. Andrzej Kaim*** [2]

***1.*** *University of Warsaw,* ***2.*** *Univeristy of Warsaw*

Numerous reports revealed that 2,2,6,6-tetramethylpiperidine-1-oxyl (TEMPO) radical and its derivatives are one of the most promising catalysts for selective oxidation of alcohols to their corresponding aldehyde or ketone analogues. Recently, C60 fullerene was applied as a platform for recyclable alcohol oxidation catalyst based on TEMPO malonate derivative [1,2]. Proposed systems turned out to be highly effective. However, reported procedures suffer from several restitution steps, which limit large scale application. In contrast, catalytic system based on insoluble support should allow simple removal of catalytic material from reaction mixture. Taking into account chemical stability and various methods for surface functionalization gold was selected to be material of choice. Deposition of thiolate species has been widely used for the chemisorption of desired groups onto Au surface. We recently reported advantageous procedure for in situ deposition of S-acetyl functionalized fullerenes onto gold surface, leading to systems revealing interesting catalytic properties [3,4]. In this cotribution we present synthesis, characterization and catalytic studies of novel TEMPO functionalized C60 fullerene derivative grafted onto surface of gold powder. Obtained catalyst was characterized using electron spin resonance (ESR) spectroscopy, X-ray photoelectron spectroscopy (XPS), atomic force microscopy (AFM), cyclic voltammetry (CV) and thermogravimetric analysis (TGA). Proposed catalytic system was successfully employed for selective oxidation of selected alcohols to their carbonyl derivatives. [1] H. A. Beejapur, F. Giacalone, R. Noto, P. Franchi, M. Lucarini, M. Gruttadauria, Chem. Cat. Chem. 5 (2013) 2991 --2999. [2] H.A. Beejapur, V. Campisciano, P. Franchi, M. Lucarini, F. Giacalone, M. Gruttadauria, Chem. Cat. Chem. 6 (2014) 2419- 2424. [3] P. Piotrowski, J. Pawłowska, J. Pawłowski, A. Więckowska, R. Bilewicz, A. Kaim, J. Mater. Chem. A 2 (2014) 2353-2362. [4] P. Piotrowski, J. Pawłowska, J. Pawłowski, A. M. Czerwonka, R. Bilewicz, A. Kaim, RSC Adv. 5 (2015) 86771- 86778.

# PMMA polymer modified with SiO2 nanocapsules, possible applications against microbiologically influenced corrosion.

**Wednesday, 9th November - 13:30 - Poster Session - Gallery - Poster presentation - Abstract ID: 469**

***Mr. Paulo Molina*** [1], ***Dr. Lisa Muñoz*** [1], ***Dr. Laura Tamayo*** [1], ***Dr. Maritza Páez*** [1]

***1.*** *Universidad de Santiago de Chile*

Microbiologically influenced corrosion (MIC) of metals, is the corrosion process assisted by the activity of microorganisms attached to a metal surface. Within metal alloys susceptible to MIC, AA-2024 aluminum, is widely used in the aviation industry for its excellent ratio [mechanical strength / weight]. The most used approach to reduce the damage caused by MIC and electrochemical corrosion comprises a multilayer system. One of the layers, can be obtained by two processes; chromate or chromic acid anodized, in both cases chromium (VI) solutions are used, however environmental regulations have placed restrictions on the use of hexavalent chromium, because of its toxic and carcinogenic characteristics (1). A different approach consists to incorporate agents with biocidal properties to the metal surfaces, or the anti-corrosion coatings. Nevertheless, due to the uncontrolled and continuous release of these agents into the environment, their use could damage the ecosystem. From the foregoing, this work proposes to incorporate SiO2 nanocapsules into the polymeric matrix of an anticorrosive coating of polymethyl (methacrylate), allowing encapsulate biocidal agents in its inner, which will be released if the protective coating is damaged. The synthesis of SiO2 nanocapsules was performed using a modified Stöber method, using alkoxysilanes as precursor in the presence of ethyl ether and oleic acid, obtaining particles with a narrow size distribution, less than 100 nm, according to measurements of dynamic light scattering (DLS). To incorporate homogeneously the SiO2 nanocapsules into the polymeric matrix, were superficially modified with methyl methacrylate (MMA) by a transesterification reaction. Figure 1 shown X-ray photoelectron spectrum of SiO2 superficially modified with MMA added into a PMMA film, a signal at 286.27 eV corresponds to the Si-OC bond, would indicate that the surface of nanocapsules were modified with MMA, by the joining the hydroxyl groups of nanocontainers, and the carboxyl group of the molecule of MMA, allowing its incorporation into the PMMA matrix. References (1) J. H. Osborne, K. Y. Blohowiak, S. R.Taylor, Ch. Hunter, G. Bierwagon, B. Carlson , D. Bernard, M. S. Donley, Testing and evaluation of nonchromated coating systems for aerospace applications, Progress in Organic Coatings, 41, (2001), 217--225.

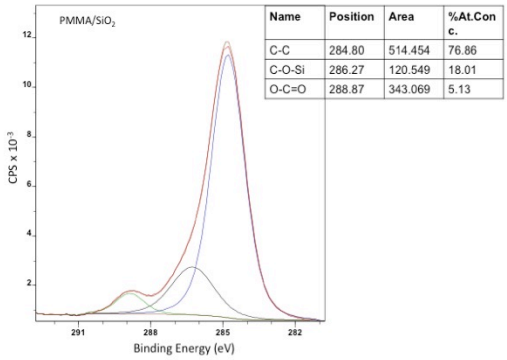


| Name | Position | Area | %At.Conc. |
|---|---|---|---|
| C-C | 284.80 | 514.454 | 76.86 |
| C-O-Si | 286.27 | 120.549 | 18.01 |
| O-C=O | 288.87 | 343.069 | 5.13 |

**Figure 1:** XPS spectrum of $SiO_2$ nanocapsules modified with MMA and incorporated into a PMMA film.

Diapositiva1.jpg

# Poly(L-arginine) surface functionalized manganese oxide nanocomplex for NO-based anticancer immune responses and MR imaging

**Wednesday, 9th November - 13:30 - Poster Session - Gallery - Poster presentation - Abstract ID: 471**

***Ms. Ga-Yun Kim* [1], *Mr. Myeong-Hoon Kim* [1], *Dr. Hye-Young Son* [1], *Prof. Yong-Min Huh* [1], *Prof. Seungjoo Haam* [1]**

***1.*** *Yonsei University*

Poly(L-arginine) surface functionalized manganese oxide nanocomplex for NO-based anticancer immune responses and MR imaging Introduction In this study, we propose a newly designed nanoparticle system for NO-based anticancer immune responses of tumor associated macrophage (TAM). We utilized the interrelation of manganese dioxides nanoparticles (MNPs) with inducible nitric oxide synthase (iNOS) expression and the high reactivity of L-arginine towards iNOS for the NO production. Manganese ions from Folic acid-Poly(L-arginine)-MnO2 nanocomplex (pMNCs) not only help to increase the expression of iNOS but also enhance T1 MRI performance for tumor imaging and detection. Additionally, poly(L-arginine) (PLR) modification enables pro-tumoral M2 phenotype TAMs to polarize into anti-tumoral M1 phenotype macrophage. Methods MnO2 nanoparticles were prepared by reducing MnO4- with reductants. Folic acid and Poly(L-arginine) modified nanocomplexes (pMNCs) were self-assembled by the potential differences between the MNPs surface and substances. M1 and M2 macrophages were prepared by treating RAW 264.7 cells with LPS (1μg/mL) or IL-4 (25 ng/ml) for 24h, respectively. Results The morphology and size of the formed pMNCs were observed by TEM. The crystal structure was characterized using XRD. The presents of PLR and Folic acid on the surface of pMNCs is confirmed by FT-IR, Zeta potential, and TGA. Flow cytometry analysis was performed to quantify the expression of repolarized M1 macrophage. iNOS was chosen as a typical marker for M1 macrophage. We observed that expression of iNOS was increased, suggesting that PLR induced the polarization of the M2 phenotype macrophage to M1. The NO levels of the medium after incubating M2 macrophage with PLR were measured. We observed elevated level of NO concentration after 24h incubation, indicating that PLR supports endogenous NO production. Further studies of anti-tumor activity and Effect on MRI signal of FA-PLR-MNRs are in progress. Conclusion This novel poly(L-arginine) modified MnO2 nanocomplexes (pMNCs) successfully increased NO concentration and killed tumor cells by shifting pro-tumoral M2 phenotype TAM to anti-tumoral phenotype macrophage and improving iNOS expression. In addition, the released Mn2+ ions facilitated highly enhanced T1 MRI performance for tumor imaging and detection. These results are expected to enable the development of a novel anticancer immunotherapy.

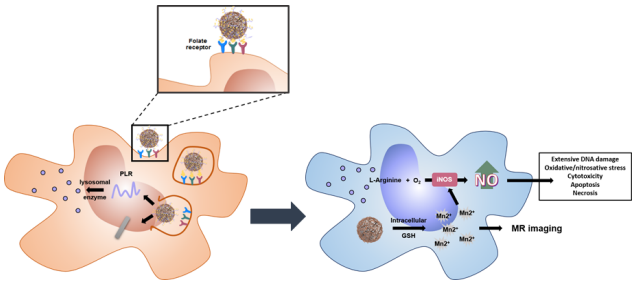


Schematic illustration of fa-plr-mncs mechanisem at tam.png

# Thermal and Optical Properties of Paraffin-mixed CNTs Nanofluids

**Wednesday, 9th November - 13:30 - Poster Session - Gallery - Poster presentation - Abstract ID: 491**

***Prof. Seok Pil Jang*** [1]

***1.*** *Korea Aerospace University*

In this paper, thermal and optical properties such as heat capacity, thermal conductivity and the extinction coefficient of paraffin-mixed CNTs nanofluids, which can dramatically absorb and store the solar thermal energy, are experimentally observed using differential scanning calorimetry (DSC), transient hot wire apparatus and Lambert–Beer law at a fixed wavelength (632.8 nm). Paraffin-mixed CNTs nanofluids are in-house manufactured by two-step method with DI-Water. The specific heat of paraffin-mixed CNTs is enhanced up to 30% compared with DI-water at the temperature range from 50□ to 60□. Also, extinction coefficients of paraffin-mixed CNTs nanofluids are linearly increased with the volume fraction of paraffin-mixed CNTs. Based on the results, we will show the paraffin-mixed CNTs nanofluids have dual functionality of absorption and storage for solar thermal energy.

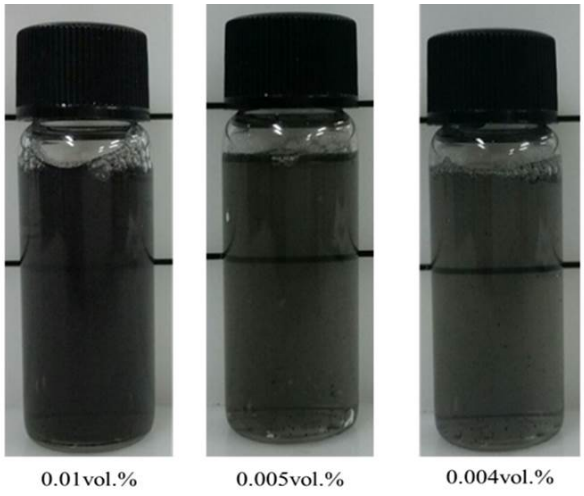


Paraffin-mixed CNTs Nanofluids

Paraffin-mixed cnts nanofluids.jpg

# Gradient multi-walled carbon nanotubes-based scaffold for cartilage tissue engineering

**Wednesday, 9th November - 13:30 - Poster Session - Gallery - Poster presentation - Abstract ID: 504**

***Dr. Magdalena Richter*** [1], ***Dr. Jakub Rybka*** [2], ***Mr. Eser Akinoglu*** [3], ***Dr. Tomasz Trzeciak*** [1], ***Prof. Michael Giersig*** [2], ***Prof. Jacek Kaczmarczyk*** [1]

***1.*** *Department of Orthopedics and Traumatology, Poznan University of Medical Sciences,* ***2.*** *Faculty of Chemistry, Wielkopolska Centre of Advanced Technologies, Adam Mickiewicz University,* ***3.*** *Freie Universität Berlin, Department of Physics*

Introduction. Novel treatment methods of articular cartilage injuries are challenging for scientists. Nowadays, joint degenerative changes resulting from articular cartilage defects are the most common disorder of the musculoskeletal system. Osteoarthritis is now the third most common cause of disability in the world's population. Currently the research has focused on the introduction of new surgical techniques and more advanced biomaterials. Recent investigations include modifications of biocompatible scaffolds, formed by crosslinking of natural and synthetic fibers (hybridization). The ideal scaffold should restore, maintain or improve tissue function, which is the main goal of therapy. In the treatment of articular cartilage defects the scaffold should allow the proliferation of cartilage cells in the site of injury, while preserving the unique properties of chondrocytes. The repaired tissue, in the three-dimensional (3D) form, could therefore more easily integrate with the surrounding cartilage. Methods. The aim of our project was to develop innovative, gradient scaffold for cartilage reconstruction based on multi-walled carbon nanotubes (MWCNTs). In our project, we have created a carbon scaffold for cartilage cell (chondrocytes) growth, composed of three different densities of nanotubes. The physico-chemical and biomechanical features of the biomaterial have been characterized using scanning electron microscope (SEM) and energy dispersive X-ray (EDX) spectroscopy. Next, we investigated the cell growth and expansion on different MWCNTs constructs. Results. Results showed that chondrocytes proliferation was the most effective on the most dense nanotube surface. Moreover, chondrocytes adhered well to the MWCNTs surface and were evenly distributed. The cells were growing separately and displayed multiple cytoplasmic extensions (filopodia). The cell extensions were responsible for bending the nanotubes, resulting in the formation of a 3D structure. The interaction between cell extensions and carbon nanotubes led to the alteration of cell morphology and the direction of their growth. Moreover no toxic effect of MWCNTs towards chondrocytes was observed. Discussion. Most previous studies indicated good properties of carbon fibers as cell carriers. Our study confirmed that the MWCNT-based constructs stimulate and support the growth of articular cartilage cells and therefore are suitable to restore the multi-layered structure of the tissue.

# Production of β-Chitin Nanofibers from Squid Pen Using a Water Jet Machine

**Wednesday, 9th November - 13:30 - Poster Session - Gallery - Poster presentation - Abstract ID: 524**

***Prof. Mitsumasa Osada*** [1], ***Mr. Shin Suenaga*** [1], ***Prof. Kazuhide Totani*** [2], ***Prof. Yoshihiro Nomura*** [3], ***Ms. Kazuhiko Yamashita*** [4], ***Prof. Iori Shimada*** [1], ***Prof. Hiroshi Fukunaga*** [1], ***Prof. Nobuhide Takahashi*** [1]

***1.*** *Shinshu University,* ***2.*** *National Institute of Technology, Ichinoseki College,* ***3.*** *Tokyo University of Agriculture and Technology,* ***4.*** *YAEGAKI Bio-industry, Inc.*

Squid is a popular sea food in many parts of the world. However, squid pen is disposed as waste from processed marine products factories. Squid pen contains beta-chitin. Chitin is structural polysaccharides consisting of beta-(1,4)-linked N-acetyl anhydroglucosamine units. At least two types of chitin crystal are known, alpha- and beta-chitins. Most natural chitins have the alpha-type crystal structure, while the beta-type chitin is present in squid pen. The beta-chitin has parallel molecular chains without significant hydrogen bonds between inter-molecular sheets. Chitin nanofiber has attracted research interest in the field of materials chemistry. When chitin is disintegrated into nanofiber, the hydrophilic surface area increases, enhancing the biochemical significance of the material. In this work, we converted beta-chitin to nanofiber by wet pulverize treatment with a water jet machine just using water. Beta-Chitin nanofiber is expected as functional materials. We obtained the individualized beta-chitin nanofibers 5-10 nm in cross-sectional width and at least a few microns in length, which was confirmed by TEM micrograph. This study showed that a wet pulverize treatment with a water jet machine is a promising method for producing beta-chitin nanofiber.

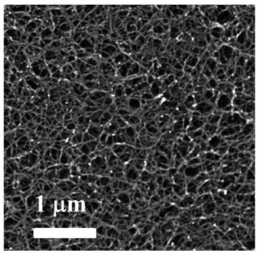


Figs.jpg

# Synthesis of Nano Composites from Ti-Al-B-C powders by Adiabatic Explosive Compaction

**Wednesday, 9th November - 13:30 - Poster Session - Gallery - Poster presentation - Abstract ID: 529**

***Dr. Mikheil Chikhradze*** [1], ***Prof. Nikoloz Chikhradze*** [2], ***Prof. George Oniashvili*** [3]

***1.*** *F.Tavadze Institute of Metallurgy and Materials Science / Georgian Technical University,* ***2.*** *G.Tsulukidze Mining Institute,* ***3.*** *F.Tavadze Institute of Metallurgy and Materials Science*

Recent developments in materials science have increased the interest towards the bulk nano materials and the technologies for their production. The unique properties which are typical for the composites fabricated in Ti-Al-B-C systems makes them very attractive for aerospace, power engineering, machine and chemical applications. In addition, aluminum matrix composites (AMCs) have great potential as structural materials due to their excellent physical, mechanical and tribological properties. Because of good combinations of thermal conductivity and dimensional stability AMCs are found to be also potential materials for electronic application. The methodology and technology for the fabrication of bulk materials from ultrafine grained powders of Ti-Al-B-C system are described in this paper. It includes results of theoretical and experimental investigation for selection of powder compositions and determination of thermodynamic conditions for blend preparation, as well as optimal technological parameters for mechanical alloying and adiabatic compaction. The crystalline coarse Ti, Al, C powders and amorphous B were used as precursors, and blends with different compositions of Ti-Al, Ti-Al-C, Ti-B-C and Ti-Al-B were prepared. Preliminary determinations/selections of blend compositions were made on the basis of phase diagrams. The powders were mixed according the selected ratios of components to produce the blend. Blends were then processed in high energetic planetary ball mills for mechanical alloying, syntheses of new phases, amorphization and production of nano and ultrafine powders. The blends processing time ranged from 1 to 24 hours. The optimal technological regimes of nano blend preparation were determined experimentally. The ball milled nano blends were placed in metallic tubes and loaded by explosive energy for further consolidation and synthesis in adiabatic regime. The effect of the processing parameters on the structure and properties of the nano and ultrafine materials was investigated and is discussed here. For consolidation of the mixtures the explosive compaction technology was applied at room temperatures. The relationship of the ball milling technological parameters and the consolidation conditions on the structure/properties of these materials is presented and discussed in this paper.

# Electrical properties and thermal stability in stack structure of HfO2/Al2O3/InSb by atomic layer deposition

**Wednesday, 9th November - 13:30 - Poster Session - Gallery - Poster presentation - Abstract ID: 534**

***Mr. Min Baik*** [1], ***Prof. Mann-ho Cho*** [1], ***Mr. Hang-kyu Kang*** [1], ***Mr. Kwang-sik Jeong*** [1], ***Mr. Dae-kyoung Kim*** [1], ***Mr. Chang-min Lee*** [2], ***Prof. Hyoung-sub Kim*** [2], ***Dr. Jin-dong Song*** [3]

***1.*** *Yonsei University,* ***2.*** *Sungkyunkwan university,* ***3.*** *Korea Institute of Science and Technology*

We report on changes in the electrical properties and thermal stability of 5nm HfO2 grown on Al2O3-passivated InSb by atomic layer deposition (ALD). The deposited HfO2 on InSb at a temperature of 200 °C was in an amorphous phase with low interfacial defect states. During post deposition annealing (PDA) at 400 °C, the In-Sb bonding was dissociated and diffused through HfO2. X-ray photoelectron spectroscopy (XPS) data indicated the diffusion of In atoms from the InSb substrate into the HfO2 during the PDA at 400 °C. This process generated In-O and Sb-O bonding on HfO2 surface, which degraded capacitance equivalent thickness (CET). We confirmed the generation of In-O and Sb-O bonding by using time-of-flight secondary ion mass spectrometry (TOF-SIMS). The change in the defect states resulted from the diffused In and Sb was also investigated by C-V measurement. 1nm-thick Al2O3 as a passivation layer on InSb substrate reduced the diffusion of In atoms and improved thermal stability. In addition, stress induced leakage current (SILC) data showed that gate leakage current was reduced by the passivation layer. Using the C-V measurement, the change in border traps was investigated: border trap density after the annealing treatment was increased, compared to that of as-grown sample, which is caused by In atoms located between Al2O3 and InSb. As a result, even though border trap density was increased by the Al2O3 layer on InSb substrate, the thermal stability at the interfacial region and gate leakage current could be successfully accomplished by the Al2O3 layer.

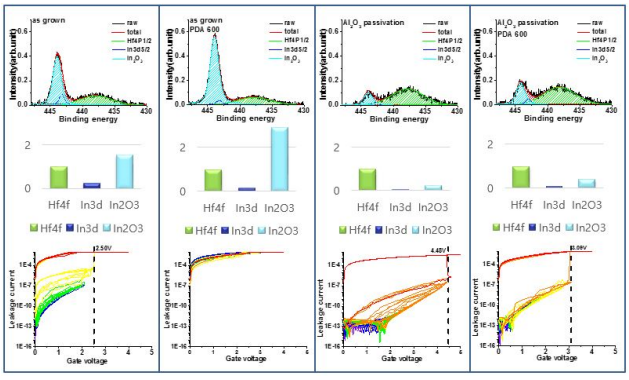


X-ray photoelectron spectroscopy data which is related to ratio of elements in surface of hafnium oxide and stress induced leakage current data.jpg

# Study of performance improvement of single-electron associative memory circuit

**Wednesday, 9th November - 13:30 - Poster Session - Gallery - Poster presentation - Abstract ID: 549**

***Mr. MAKOTO TAKANO*** [1], ***Prof. Takahide Oya*** [1]

***1.*** *Yokohama National University*

The analog neural network (NN) has attracted much attention in the nano-electronics area because of having many advantages such as parallel-processing and noise-harnessing functions. However, it is exceptional challenging to fabricate analog NN circuits. The crucial problem is how to implement the neurons' behavior. It is known that a neuron circuit consisting of CMOS is quite complicated and require a large circuit area. Here we focus on single-electron circuits (SECs). It is the nano-electronic circuit which can control transportation of an individual electron tunneling by harnessing a quantum effect named the Coulomb blockade. In this study, we design the SE Hopfield's competitive NN circuit and confirm that it can perform the associative memory function. The Hopfield network is a NN model known for its ability to perform the associative memory function. It consists of neurons which have binary output value connected each other via the connection weight Wij. The associative memory is the function which stores some patterns and recalls them from given noisy or a related input pattern. We prepare one type of SEC called a ``single-electron box (SEB)'' as a neuron and connect them each other via coupling capacitors (CW) which correspond to the connection weight. The SEB consists of a bias voltage source (Vd), a capacitor (C), a node, and a tunneling junction (Cj) in series. The tunneling junction Cj has a threshold voltage value for the electron tunneling. If the node voltage VN is increased by increasing Vd or the value of an external input and exceeds the threshold value, an electron tunnels through the junction Cj. Then, VN changes sharply. We stored ten kinds of 5×7-pixel black/white patterns on this network by calculating weight parameters Wij using the learning rule called orthogonal leaning. As a result of computer simulation, we could confirm that our circuit could perform the associative memory function. As a next step, to achieve higher performance, we focus on the multi-layer NN model and the back propagation which is the learning algorithm for it. We consider the method to construct the multi-layer NN by using SE circuit and apply backpropagation to it.

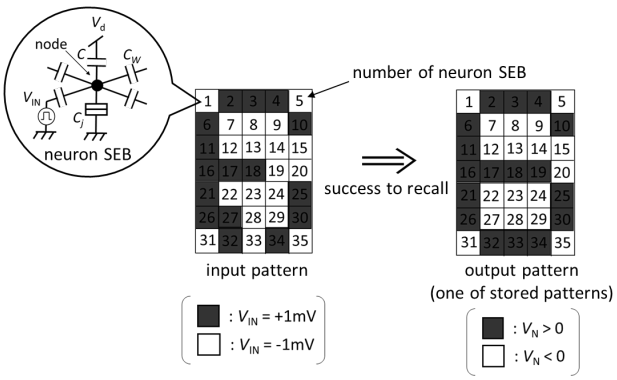


Schematic image of the operation of the single-electron associative memory circuit.png

# RGO and TiO2 Nanotube Matrix based Binary Hybrid Device for Reliable Detection of Methyl Acetate Vapor

**Wednesday, 9th November - 13:30 - Poster Session - Gallery - Poster presentation - Abstract ID: 580**

***Mr. Debanjan Acharyya*** [1], ***Dr. Partha Bhattacharyya*** [1]

**1.** *Indian Institute of Engineering Science and Technology, Shibpur*

This paper demonstrates the development of highly sensitive methyl acetate sensor based on reduced graphene oxide (RGO) decorated TiO2 nanotube (NT) matrix. Methyl acetate is a colorless, volatile liquid, used as a solvent during the preparation of wine, resins, dyes and pharmaceutical products. Inhalation of such acetate vapors (even mild amount) can cause irritation in eye and skin, dyspnea, palpitations, headache, ataxia, asthenia, etc. Therefore, efficient detection of acetate contamination is important to the beverage and pharmaceutical industry for securing the human safety. However, commercial unavailability of such sensors warrants the development of a potential methyl acetate sensor. In this study, RGO decoration on TiO2 NT matrix was performed by two-step electrochemical process. Acetate vapor sensing performance of the device was tested towards methyl acetate, ethyl acetate and n-butyl acetate vapors (in the concentration range of 1-400 ppm). The High mobility RGO clusters on TiO2 NTs facilitates the enhance sensitivity towards methyl acetate at 210°C in a high dynamic concentration range. The response magnitude, response time and recovery time was found to be 85.87%, 30 sec and 90 sec respectively, towards 400 ppm methyl acetate. Fig. 1(f) represents the response magnitude variation with the exposure of three vapors for different concentrations at 210°C. It is worth mentioning that, at the same concentration, response magnitude towards methyl acetate is significantly higher than that of the others. The high sensitivity of methyl acetate at lower temperature attributed to the smaller molecular size and lower bond dissociation energy than that of its counter parts. A transient response characteristic towards exposure of methyl acetate is plotted in Fig. 1(h), which substantiates the RGO decorated TiO2 NTs matrix as an efficient methyl acetate sensor. Response and recovery time with the exposure of methyl acetate are depicted in Fig. 1(i) and found to be very promising. Such highly sensitive phenomenon possibly attributed to the high surface to volume ratio of TiO2 NTs matrix as well as high mobility carriers in RGO. According to the literature review, it is imperative to mention that this is the first report on solid state device based methyl acetate sensor.

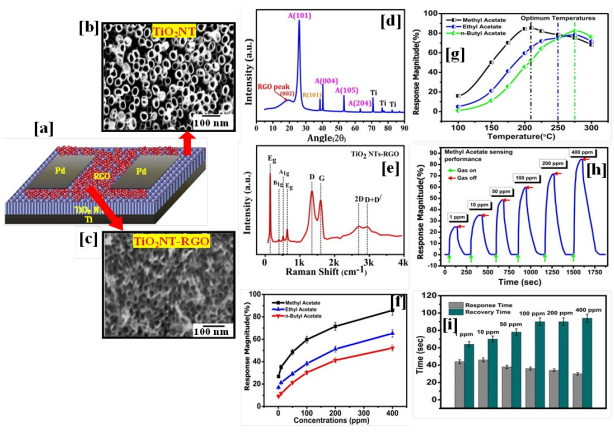


Debanjan acharyya.jpg

# A Study on the Correlations between Dark Count and Photon Detection Efficiency According to P-Well Structure in GM-APD

**Wednesday, 9th November - 13:30 - Poster Session - Gallery - Poster presentation - Abstract ID: 684**

***Mr. Hyun Yoo*** [1], ***Dr. Woo-Suk Sul*** [1], ***Mr. Hae-Chul Hwang*** [1], ***Mr. Kwang-Hee Kim*** [1], ***Mr. Gi-Sung Lee*** [1], ***Dr. Young-Su Kim*** [1]

**1.** *National Nanofab center*

[Introduction] The next-generation radiation device SiPM (Silicon Photomultiplier) is a combination of several hundred to several thousand micro cells comprised of GM-APD (Geiger Mode-Avalanche Photodiode) and quenching resistor. The electric field generated at the pn junction directly influences photon detection efficiency (PDE) and dark count which are key performance indices of GM-APD. The criteria for optimized P-Well structure are presented in this paper. [Methods] When the maximum electric field of GM-APD increases, the PDE increases, but Band to Band Tunneling (BBT) and Trap Assisted Tunneling (TAT) among the causes of dark count increase in proportion to the intensity of the maximum electric field. The intensity of the maximum electric field varies according to the P-Well structure and a proper design of P-Well is critical in the determination of the performance of GM-APD. In this paper, the TCAD simulation of Silvaco was used to set energy and dose of the implantation, and simulation was conducted by varying the P-Well anneal time and temperature. The electric field distribution was extracted from the breakdown voltage based on the simulation results and the PDE and dark count were compared. [Conclusion] When the P-Well anneal time was shorter than 150 minutes, the maximum electric field was high, but the depth of P-Well was shallow, resulting in lower triggering probability and PDE. When the P-Well anneal time was longer than 150 minutes, the electric field decreased, resulting in lower PDE. The higher the P-Well anneal temperature was, the lower the maximum electric field became and the PDE tended to decrease. When the maximum electric field at the pn junction was lower than 5.6E5(V/cm), BBT became lower than TAT and the dark count rapidly decreased. In conclusion, the design of P-Well with 1000°C and 150 minutes will generate the maximum electric field of 5.6E5(V/cm) or lower, and high PDE and low dark count can be expected. [Acknowledgments] This study was funded by the Nano Open Innovation Lab partnership project of NNFC.

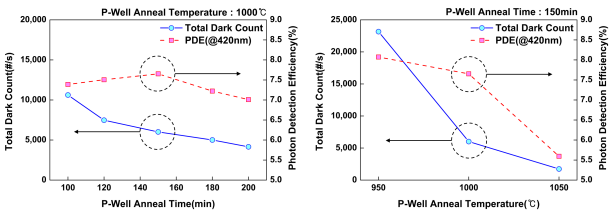


Figure sipm 20160930.png

# Optical properties of GaAs–AlGaAs core–multishell nanowire quantum structures grown by MOVPE

**Wednesday, 9th November - 13:30 - Poster Session - Gallery - Poster presentation - Abstract ID: 698**

***Dr. PAOLA PRETE*** [1], ***Ms. Roberta Rosato*** [2], ***Mrs. Elena Stevanato*** [2], ***Dr. Fabio Marzo*** [2], ***Prof. Nico Lovergine*** [2]

***1.*** *Institute for Microelectronics and Microsystems, CNR, Unit of Lecce,* ***2.*** *Dept. of Engineering for Innovation, University of Salento*

III-V compounds nanowires (NWs) have gathered considerable research interests in recent years, in reason of their potential applications to novel and high-performance nano-scale light emitting diodes, lasers, photodetectors and solar cells. In particular, radial modulation of NW composition in the form of core-(multi)shell heterostructures promises to impact these nano-devices by adding new degrees of freedom to their design. Besides, strict control over the epitaxial self-assembly of such radially heterostructured NWs and detailed insights of their nano-scale (structural, radiative) properties are necessary. We report on the luminescence properties of dense arrays of vertically-aligned GaAs-AlGaAs core-multishell NW quantum heterostructures grown on (111)B-GaAs wafers by metalorganic vapor phase epitaxy. Au-catalysed GaAs NWs were radially overgrown by two AlGaAs shells between which a few-nm thin GaAs shell was introduced to form a quantum well tube (QWT). Besides the GaAs nanowire core emission band peaked at around 1.503 eV, 7K PL spectra showed an additional broad peak in the 1.556-1.583 eV energy interval, ascribed to the transition between electron and hole confined states within the QWT. The emission blue-shifts with the shrinkage of as-grown GaAs well tubes, as the nanowire local (on the substrate) density and height change. High spatial resolution cathodo-luminescence (CL) spectroscopy inside a field-emission scanning electron microscope was performed at low-temperature (7K) on single GaAs-AlGaAs core-multishell NWs and GaAs-AlGaAs QWT structures. CL imaging of single QWT heterostructures allowed us to spatially resolve different contributions found in the CL (and PL) spectra. Furthermore, we show for the first time the occurrence of both large-scale spatial inhomogeneities (along the NW trunk) and nano-scale fluctuations of QWT emissions. Our findings are finally analysed as function of QWT parameters and growth conditions.

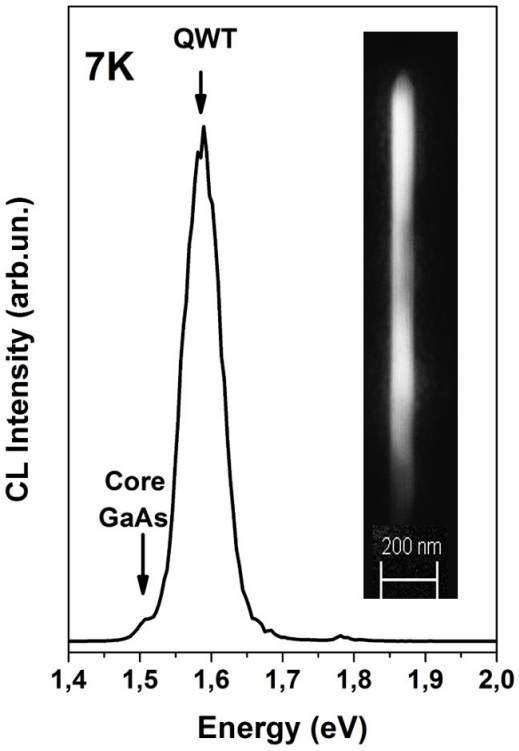


Fig abs annic2016.jpg

# Layer dependent direct optical transitions at Γ-point in synthesized large area MoSe2

**Wednesday, 9th November - 13:30 - Poster Session - Gallery - Poster presentation - Abstract ID: 537**

*Mr. Jae-Hun Jeong* [1], *Mr. Yoon Ho Choi* [1], *Mr. Kwang-sik Jeong* [1], *Prof. Mann-ho Cho* [1]

*1.* *Yonsei University*

Two-dimensional transition metal dichalcogenides (TMDs) have attracted great interest for applications in opto-electronic device. We studied the optical properties of the large area MoSe2 thin film on c-axis sapphire (0001) substrate grown by molecular beam epitaxy (MBE). Photoluminescence (PL), Raman, X-ray diffraction (XRD), and X-ray photoelectron spectroscopy (XPS) were measured to evaluate the film quality. We obtained the optical absorption spectra of mono-, bi- and tri-layer MoSe2 and observed optical critical point which is correspond to the direct transition at Γ-point of the Brillouin zone (BZ) at ~3 eV. Increasing the number of layer, the intensity of the absorption peak at Γ-point was increased and its position was shifted. The changes in peak at Γ-point are caused by the band structure depending on the number of layer, resulting in the modulation of the joint density of state (JDOS). Since the geometrical band shape of conduction band and valance band are similar around Γ-point for few layer MoSe2, both van Hove singularities (VHS) and band nesting contribute to strong absorption peak. Using 3eV optical pump, we can selectively excite the MoSe2 by choosing suitable number of layer. The modulation of band structure and strong photon-electron interaction of 2D material would be widely applied to photonic and optoelectronic devices.

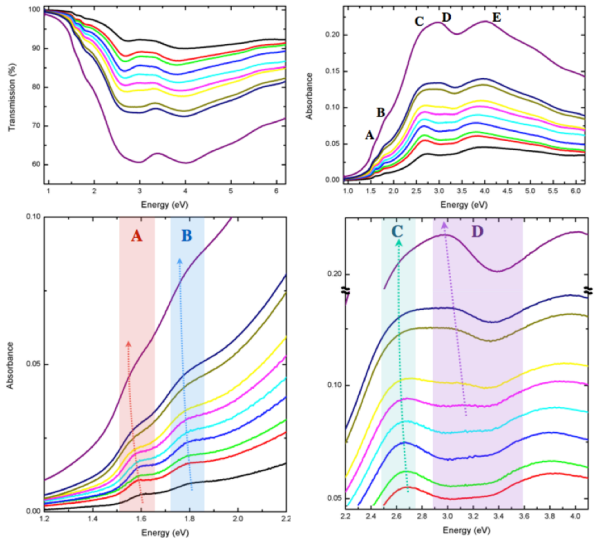


Absorbance of mose2.png

# Effect of Li co-doping on highly oriented sol-gel Ce-doped ZnO thin films properties

**Wednesday, 9th November - 13:30 - Poster Session - Gallery - Poster presentation - Abstract ID: 84**

***Prof. Azeddine CHELOUCHE*** [1], ***Dr. Tahar Touam*** [2], ***Mr. Mohand Tazerout*** [1], ***Prof. Djamel Djouadi*** [1], ***Mr. Fares Boudjouan*** [1]

***1.*** *université de Béjaia,* ***2.*** *Université Badji Mokhtar-Annaba*

Undoped, Ce-doped and Ce--Li co-doped ZnO thin films have been deposited onto glass substrates by sol--gel dip coating method. The effects of Ce--Li co-doping for 0.1 at.% Ce and 0--20 at.% Li on the structural, morphological and optical properties of the ZnO films were investigated by X-ray diffraction (XRD), atomic force microscopy (AFM), UV-Vis-NIR spectrophotometry and photoluminescence spectroscopy (PL). XRD analysis revealed that all the films were highly c-axis oriented and had a hexagonal wurtzite structure. AFM images showed that film morphology and surface roughness were influenced by Li doping concentration. UV-Vis-NIR measurements indicated that the film transmission decreases with increasing Li content and the optical band gap was dependent on the Li concentration. Room temperature PL spectra put into evidence that emission is significantly influenced by Li content. In particular, it was found that the visible emission intensity of the film with 20 at.% Li doping in 0.1 at.% Ce-doped ZnO is approximately 30 times greater than that of the undoped film.

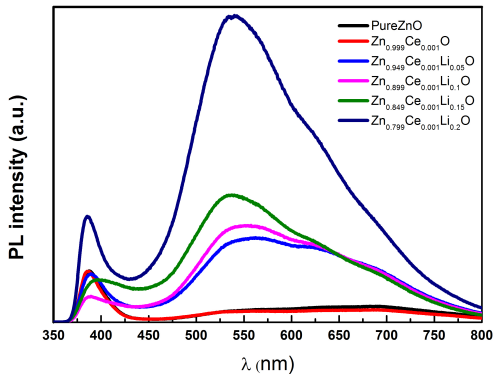


Pl ce-li.jpg

# NFFA Europe Presentation

**Wednesday, 9th November - 13:30 - Poster Session - Gallery - Poster presentation - Abstract ID: 728**

***Dr. Flavio Carsughi*** [1]

***1.*** *Forschungszentrum Jülich*

NFFA•EUROPE sets out a platform to carry out comprehensive projects for multidisciplinary research at the nanoscale extending from synthesis to nanocharacterization to theory and numerical simulation. Advanced infrastructures specialized on growth, nano-lithography, nano-characterization, theory and simulation and fine-analysis with Synchrotron, FEL and Neutron radiation sources are integrated in a multi-site combination to develop frontier research on methods for reproducible nanoscience research and to enable European and international researchers from diverse disciplines to carry out advanced proposals impacting science and innovation. NFFA•EUROPE enables coordinated access to infrastructures on different aspects of nanoscience research that is not currently available at single specialized ones and without duplicating their specific scopes. Website: http://www.nffa.eu/

# Hydrogen Anti-diffusion Methods for Poly-Si Quenching Resistor in Silicon Photomultipliers

**Wednesday, 9th November - 13:30 - Poster Session - Gallery - Poster presentation - Abstract ID: 670**

***Dr. Woo-Suk Sul*** [1], ***Mr. Hyun Yoo*** [1], ***Mr. Sang-Hyun Park*** [1], ***Mr. Dong-Eun Yoo*** [1], ***Mr. Dong-Wook Lee*** [1], ***Dr. Boung-Ju Lee*** [1]

***1.*** *National Nanofab center*

[Aims] Silicon photomultipliers (SiPMs) are prime candidate of solid state photo-sensors for the next generation fusion medical image systems. SiPM is combined by the hundreds ~ thousands microcells with consisting of geiger-mode avalanche photodiode (GM-APD) and poly-silicon quenching resistor. The poly-silicon resistors are affected by the non-uniform inflow of the hydrogen atoms during the semiconductor fabrication. As a result, it causes critical problems such as degradation with resistance and uniformity. In this paper, we present hydrogen anti-diffusion methods to improve stability and uniformity of resistance on the poly-silicon resistors. [Experimental Methods] Generally, the dangling bonds of GM-APD are reduced by the forming gas annealing (FGA, hydrogen contents about 10%) in order to improve the electrical stability. But this method has a problem of losing the resistive site due to the hydrogen recovery of interface trap site in the resistor. In this experiment, we applied two methods to prevent the injection of unwanted hydrogen atoms. The first method is forming the SixN1-x layer in the surface of resistor using the nitrogen ion implantation. The second method is deposition of the thin Si3N4 film on surface of the resistor. [Results] The figure shows uniformity and total resistance of resistors on whole dies of 8 inch wafer. Uniformity of the resistors with nitrogen ion implantation is improved 19 ~ 53% as compared with the reference resistors of only applying FGA. In addition, the resistors of deposited Si3N4 are confirmed that uniformity is a 61% improvement. However, resistance is decreased on nitrogen ion implanted resistors than the reference resistors. This reason is reduced physical resistive sites due to the influence of generated SixN1-x film of surface of the resistor by implanted nitrogen ions. However, Si3N4 film deposited resistors is confirmed that indicates a high resistance than the reference resistors, because it has not lost additional silicon atom. If poly-silicon quenching resistors are applied hydrogen anti-diffusion method of depositing the Si3N4 films considering resistance and uniformity of resistor, it seems to be able to fabricate the more stable poly-silicon quenching resistors. [Acknowledgments] This study is supported by the Nano·Material Technology Development Program of NRF (NRF-2015M3A7B7045446).

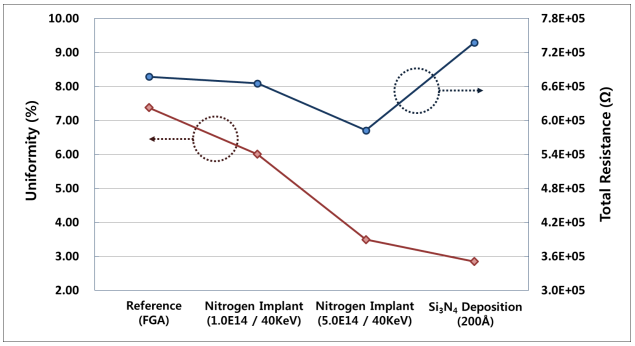


Figure 20160930.png

# Frequency selective alcohol sensing performance of Pd/TiO2 nanotube array/Ti (MIM) devices in capacitive mode

**Wednesday, 9th November - 13:30 - Poster Session - Gallery - Poster presentation - Abstract ID: 486**

***Dr. Partha Bhattacharyya*** [1]

***1.*** *Indian Institute of Engineering Science and Technology, Shibpur*

Optimal gas/vapor sensing performance by adopting either manipulation of the sensing layers or fabricating different device structures like resistive, metal insulator semiconductor (MIS), metal insulator metal (MIM) and thin film field effect transistor (TFET) sensors receives paramount importance since last 3-4 decade. These sensors were operated in resistive mode (current/voltage) and the fractional resistance change resulting from effective change in carrier concentrations under exposure of gases/vapor was used as indexed term to identify the sensor response. As far as price and durability is concerned, the resistive gas sensor is reasonable to commercialize. But, poor selectivity and limited sensor response are the two main bottlenecks which force to sensor researcher to find alternative method for superior gas detection. Earlier studies revealed that, doping or surface functionalization by use of noble metals were mostly used for better selectivity, whereas grain size control found to play a pivotal role for improved sensor response. But, improved results were still far from satisfactory and needs further improvements. In this context, capacitive measurement under exposure of gases/vapor is relatively new and far accurate than the resistive one. The capacitive measurement is predominantly governed by the change in relative dielectric permittivity (□r) of the medium in presence of gases/vapor and is less sensitive to the charge effects. Pd/TiO2 nanotube/Ti (MIM) devices were investigated at the temperature range of 27-200°C and over a frequency range of 0.01-200KHz towards 2-propanol, ethanol and methanol targeting concentrations range of 1-100ppm. From the impedance measurement, the device resonance was found at 2.2 KHz in air ambient and shifted towards lower frequency regime of 0.40 KHz, 0.25 KHz and 0.16 KHz upon exposure to 100 ppm of 2-propanol, ethanol and methanol, respectively (shown in Fig 2 (a)). Selectivity window attributed frequency selective alcohol sensitivity of the TiO2 nanotubes. Adsorption induced shifts in resonance frequency may be attributed to the (i) variation in dielectric permittivity (□r) of the nanotube void region and (ii) change in density of the adsorbed molecules. Further, the sensor showed maximum capacitive response magnitude of 406%, 556% and 669%, towards 100 ppm of 2-propanol, ethanol and methanol, respectively.

**Corresponding author**
* Corresponding author. Tel.: +913326684561, fax: +913326682916
*E-mail: pb_etc_besu@yahoo.com

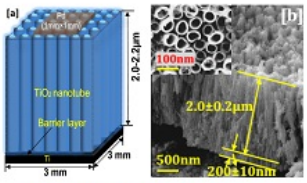


*Figure 1: (a) Schematics of capacitive sensor devices with requisite dimensions (not to scale) (b) Cross sectional FESEM image of the annealed $TiO_2$ nanotube array; inset shows the top view of the same.*

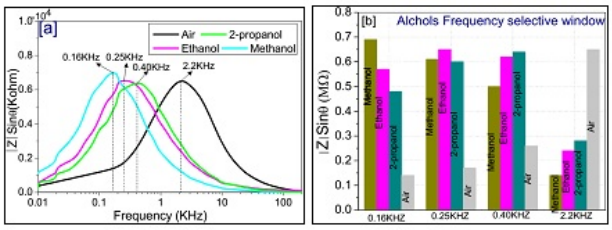


*Figure 2: (a) Imaginary complex impedance (|Z|sinθ) as a function of input signal frequency over the range of 0.01-200KHz upon exposure to air, 2-propanol, ethanol and methanol. (b) Frequency selectivity window of the alcohols at concentrations of 100ppm.*

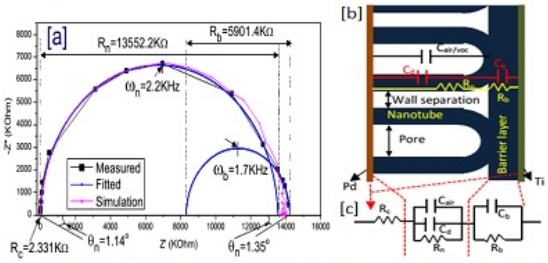


*Figure 3: (a) Cole-Cole plot of the $TiO_2$ nanotube array in air ambient at 100°C temperature (b) schematic illustrations of the $TiO_2$ nanotube based capacitive sensor devices showing individual contribution to the total impedance ($Z=R_s+Z_n+Z_b$), $R_s$=contact resistance, $Z_n$=impedance of the $TiO_2$ nanotubes and void region,*

Partha bhattacharyya.jpg

# Effect of Pressure on Crystal Structure and Optical Properties of Bi2O3 Nanoparticles

**Wednesday, 9th November - 16:00 - Nanophotonics & Nano-optics - Room 1 - Oral presentation - Abstract ID: 560**

***Ms. Melanie White*** [1], ***Ms. Rethika Kumar*** [2], ***Mr. Howard Yanxon*** [1], ***Prof. Ravhi kumar*** [1], ***Prof. Andrew Cornelius*** [1]

***1.*** *University of Nevada Las Vegas,* ***2.*** *Green Valley High School*

Nano materials have gained importance recently in several medical and technological applications due to their unique size-dependent properties that make these materials superior and indispensable. Bi2O3 nanoparticles are used in a number of applications such as fungicidal agent, gas sensor and semiconductor. Recent studies show that bulk Bi2O3 exhibit several polymorphs and the crystal structure is sensitive to external pressure and temperature conditions. Despite the importance of this material, the polymorphs of nanoparticles of Bi2O3 are less known to date when compared to the bulk. In order to understand the new Bi2O3 nanoparticle phases and polymorphs, we have investigated the crystal structure of bismuth oxide (beta-Bi2O3) nanoparticles (average particle size of 100nm) under high pressure conditions up to 50 GPa. The powder x-ray diffraction experiments were performed using high resolution synchrotron x-rays in the angle dispersive geometry with a diamond anvil high pressure cell at the Advanced Photon Source (APS), Argonne National Laboratory. Raman spectroscopy measurements were conducted up to similar pressure ranges to complement the x-ray results. Our experiments clearly indicate that the nanoparticles undergo pressure induced amorphization above 15 GPa. The phase change behavior is found to be comparable with bulk Bi2O3. We will discuses the structural stability and vibrational properties in detail.

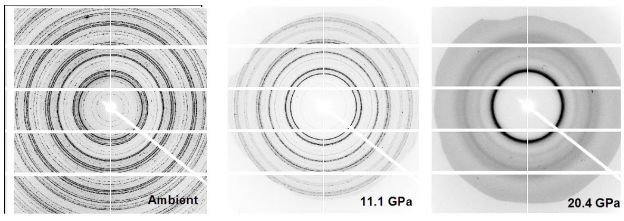


Fig. X-ray diffraction images showing the pressure induced amorphous transition in Bi2O3 nanoparticles

Phase transition.jpg

# Characterization of nanometre-scale compositional variations in CMSX-4 superalloy subjected to high temperature annealing and creep deformation using analytical electron microscopy

**Wednesday, 9th November - 16:17 - Nanophotonics & Nano-optics - Room 1 - Oral presentation - Abstract ID: 457**

***Dr. Beata Dubiel*** [1]***, Dr. Paulina Indyka*** [2]***, Dr. Adam Kruk*** [1]***, Dr. Tomasz Moskalewicz*** [1]

***1.*** *AGH University of Science and Technology, Faculty of Metals Engineering and Industrial Computer Science, A. Mickiewicza Ave. 30, 30-059 Kraków,* ***2.*** *Jagiellonian University, Faculty of Chemistry, Ingardena 3, 30-060 Kraków*

Single crystal nickel-base superalloys are widely used for gas turbine blades application. Their chemical composition contains refractory elements, which provide solid solution strengthening. The presence of heavy elements promotes precipitation of the brittle topologically close packed (TCP) phases after long time exposure at high temperature. Advanced analytical electron microscopy methods are very convenient to investigate the microstructure and the nanoscale fluctuations in chemical composition of TCP phases present in single crystal nickel-base superalloys. CMSX-4 single crystal superalloy subjected to standard heat treatment was delivered by Howmet Ltd, UK. The specimens were annealed at temperature of 1100 °C for 500 h and subsequently creep tested at temperature of 900 °C and stress of 250 MPa. Microstructure and chemical composition were investigated using analytical electron microscopes Jeol JEM-2010 ARP and FEI Tecnai Osiris equipped with Super-X Energy Dispersive X-ray (EDS) system. Scanning-transmission electron microscopy (STEM) imaging was performed in high angle annular dark-field (HAADF) mode. The distribution of the specific chemical elements was determined using STEM images coupled with EDS maps. 3D characterisation was carried out by means of STEM-HAADF and STEM-EDS tomography. TEM microstructural investigation have shown that after two-step high temperature exposure applied the microstructure consists of gamma, gamma prime and TCP precipitates of mi and P phases. Electron tomography investigation revealed the plate-like and lath-like morphology of TCP phases. STEM-EDS tomography analysis have shown that gamma and TCP phases contain mostly Re, W, Co, Cr and Mo, while the gamma prime phase is enriched in Ni, Al, Ti and Ta. STEM-HAADF images revealed the thin platelets of the P phase of the nanometric width embedded in the mi phase. The quantitative EDS line profiles indicated the differences in element concentration in both phases at the nanoscale (Fig. 1). Based on the combination of several analytical electron microscopy methods the compositional differences in the co-precipitates of the mi and P phases were revealed. ACKNOWLEDGMENTS This work was supported by the Polish National Science Centre, project nr 2012/07/B/ST8/03392. The authors also thank Howmet Exeter, UK for providing the CMSX-4 material.

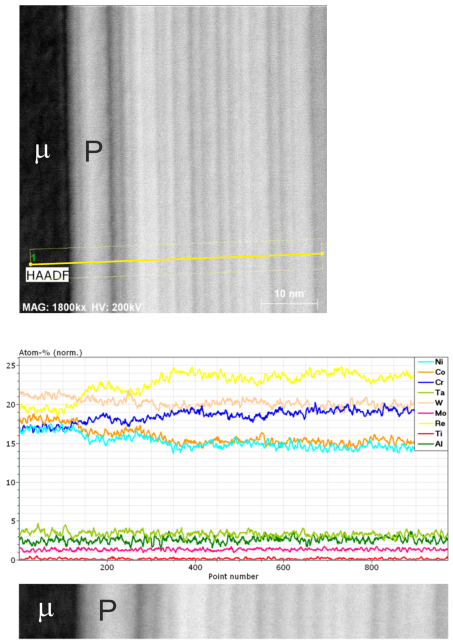


Fig. 1. STEM-HAADF image showing the alternating parallel plates of the P and μ phases and the corresponding STEM-EDS concentration profiles of chemical elements in at. %.

Fig1 v2.png

# Plasmonic Ga nanoparticle arrays for phase change memory

**Wednesday, 9th November - 16:34 - Nanophotonics & Nano-optics - Room 1 - Oral presentation - Abstract ID: 500**

***Dr. Oral Ualibek*** [1], ***Mr. Murat Baisariyev*** [1], ***Prof. Igor Shvets*** [2], ***Dr. Gulnar Sugurbekova*** [1]

*1. National Laboratory Astana, Nazarbayev University, 2. School of Physics, Trinity College Dublin*

Already, novel applications have been demonstrated that rely on the unique optical and material properties of Ga nanoparticles (NPs): UV spectroscopy substrates for simultaneous fluorescence and surface-enhanced Raman spectroscopy (SERS), highly compact solid liquid phase change memory elements, phase transition non-linear substrates, and graphene/plasmon nanocomposites. In this work, we demonstrate for the first time highly ordered spherical Ga NP arrays were fabricated by glancing angle deposition (GLAD) technique. GLAD is very simple, based on self-assembling, and can produce highly ordered one dimensional plasmonic NP chains. A collimated flux of ad-atoms is sent towards the stepped template surface at a glancing angle of incidence resulting in the formation of NP arrays. Optical evolution of Ga nanoparticle plasmon resonance during deposition has been characterized by in-situ real-time reflectance anisotropy spectroscopy. We have observed plasmonic resonance energy difference of Ga NPs at solid and liquid states. This phenomenon can be interesting to make highly compact solid-liquid phase change memory elements with information encoded in the structural phase. As well as, experimental results also reproduced by an analytical simulation. This work has been supported by the Ministry of Education and Science of Kazakhstan under the research founding NU- Berkeley No. 0115PK03029

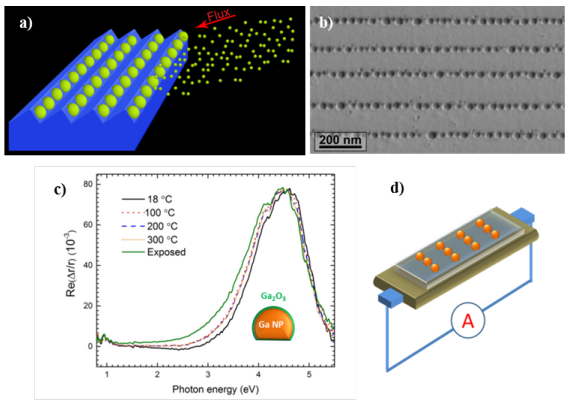


Figure 1. (a) A schematic view of the GLAD technique (b) Scanning Electron Spectroscopy image of Ga NP arrays grown by GLAD technique. Plasmonic resonances of Ga NP arrays at solid and liquid states were measured by RAS (c) and schematic view of substrate heater with silicon (d).

Figure1.png

# Blue emission of Cerium doped Aluminum (oxy)-nitride thin films prepared by reactive sputtering technique

**Wednesday, 9th November - 16:51 - Nanophotonics & Nano-optics - Room 1 - Oral presentation - Abstract ID: 266**

***Mr. Alaa eldin Giba*** [1], ***Mr. Philippe Pigeat*** [2], ***Dr. Stéphanie Bruyere*** [2], ***Prof. Hervé Rinnert*** [2], ***Dr. Flavio Soldera*** [3], ***Prof. Frank Mücklich*** [3], ***Prof. Raul Gago-fernandez*** [4], ***Prof. David Horwat*** [2]

***1.*** *Université de Lorraine and Saarland University,* ***2.*** *Université de Lorraine,* ***3.*** *Saarland University,* ***4.*** *Instituto de Ciencia de Materiales de Madrid*

Recently, blue light emitting solid-state materials received high attention for use in white LEDs and other luminescent applications. In this direction, phosphors- doped nitrides and oxy-nitrides composites attracted much potential due to their thermal, chemical stability and the possibility to tune their electronic structure to adapt to the required applications. In particular, the III-nitrides (e.g. AlN, GaN) have been considered as a suitable host material for phosphors that emit in UV-visible range due to its large bandgap. Thus, the purpose of this study is to sensitize blue emission from rare earth doped AlN as a wide bandgap semiconductor. In the present work, Cerium-doped aluminum nitride (Ce-AlN) thin films were prepared at room temperature using radio frequency (RF) reactive sputtering. X-ray diffraction and high resolution transmission electron microscopy (HRTEM) revealed a well crystalline textured microstructure with single <002> out-of-plane orientation. Strong blue emission from the prepared samples was detected when excited by 325 nm laser. Electron energy loss spectroscopy (EELS) has been used to reveal the dominant oxidation state of Ce atoms, which undergoes a change from of Ce(IV) to Ce(III) ions after annealing. The chemical composition was analyzed by simulation of Rutherford backscattering spectrometry (RBS) and compared to HRTEM images. A clear correlation between microstructure, composition and sample photoluminescence (PL) was established. It was found that surface oxidation during post-deposition annealing plays an important role in the PL response of the samples. We believe that the strong blue emission in this new (oxy)-nitride material holds great potentials for solid state lighting applications due to its thermal and chemical stability as well as the luminescence efficiency. Moreover, the comprehensive approach conducted within this study could serve as a guideline for better understanding and the design of the luminescence behavior in rare earth-doped (oxy)-nitride thin films.

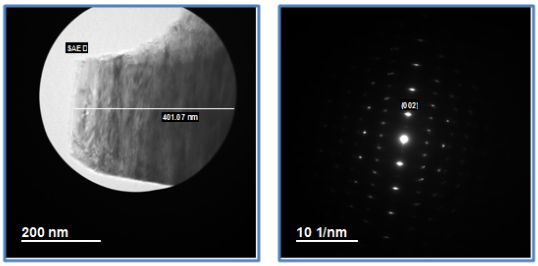


*Bright field TEM image and the corresponding diffraction pattern of AlN prepared at room temperature.*

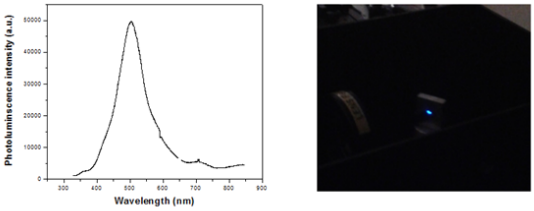


*Photoluminscence of Ce doped AlN excited by 325 nm laser (on left). Photo reveals the blue emission that can be seen by the naked-eye (on right).*

Microstructure of aln and photoluminscence of ce doped aln.png

# Gold nanoparticles assembly on 1D, 2D and 3D microstructures

**Wednesday, 9th November - 17:08 - Nanophotonics & Nano-optics - Room 1 - Oral presentation - Abstract ID: 573**

***Mr. Ali ISSA*** [1], ***Dr. Irene Izquierdo-Lorenzo*** [2], ***Prof. Fawaz Elomar*** [3], ***Prof. Joumana Toufaily*** [3], ***Dr. Safi Jradi*** [2]

***1.*** *University of Technology of Troyes (UTT) and Lebanese University,* ***2.*** *University of Technology of Troyes (UTT),* ***3.*** *lebanese university*

During the last decade, Metallic Nanoparticles (MNPs) attract much attention due to their localized surface plasmon resonance (1). Many considerable efforts have been put forth to align these NPs from colloidal solutions onto patterned substrates in order to obtain extraordinary optical properties. To the date, patterning of plasmonic nanoparticles is an active challenge.(2) In this context we will present a highly versatile approach to control the assembly of gold nanoparticles (GNPs) that present interesting optical properties in the visible region (figure 1). Our new approach is based on the functionalization of polymer micro and nanostructures by the inclusion of an amine molecule in a photopolymerizable mixture used for two-photon photolithography. After laser writing of any desired 1D, 2D and 3D microstructures, the obtained polymer templates are immersed in acetated GNP spheres for several hours resulting in the attachment of these nanoparticles on the polymer surface due to the high attraction towards the functionalized structures. The linear arrangements of our GNPs can be as thin as 2-3 NPs wide for several microns of length, separated down to 400 nm (Figure 1-1D). Nanoparticle aggregation on the surface is rare even in relatively large surfaces: on Figure 1-2D, a 50×50 µm square is showing mainly a single layer arrangement. More interestingly, the colloidal solution can penetrate inside a complex 3D microstructure which can be completely covered by GNPs. In Figure 1-3D, the inclusion inside a woodpile photonic crystal of 20×20×8 µm with a period of 1 µm is shown. SERS and extinction spectra were performed on the GNPs patterns. (1) Aroca, R., Surface-enhanced vibrational spectroscopy, John Wiley & Sons, Chiechester, 2006 (2) Su, B., et al., ``A general strategy for assembling nanoparticles in one dimension'', Adv. Mater., Vol. 26, 2501-2507, 2014

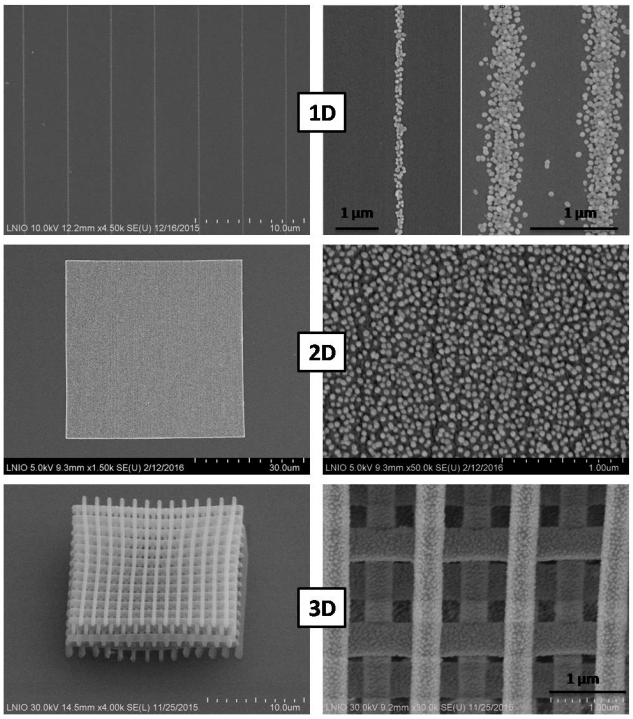


Figure 1 sem images of linear planar and 3d gold nanoparticles arrangements.jpg

# Mutual Coupling mitigation of Terahertz antenna by using Graphene based metasurface

**Wednesday, 9th November - 17:25 - Nanophotonics & Nano-optics - Room 1 - Oral presentation - Abstract ID: 528**

***Dr. DEBASIS MITRA*** [1], ***Mr. Jeet Ghosh*** [1]

***1.*** *Indian Institute of Engineering Science and Technology, Shibpur*

Mutual Coupling(MC) is an inevitable phenomenon for multiple antenna system. Due to the MC effect, the antenna suffers from a tradeoff between array performance and array size [1]. Different types of metasurface are reported in several literatures to reduce MC[2]. Realization of metasurface at the higher frequency is more difficult due to the losses in metal. In this regard, one of the promising materials in THz frequency is graphene[3]. In this paper, an efficient approach is reported to reduce mutual coupling between THz patch antenna arrays by incorporating a graphene metasurface designed on silicon wafer. A 50nm thick polysilicon layer and a 10nm thick SiO2 film are introduced on the top of the substrate successively. The polysilicon layer is used as a gate electrode. Due to the ultrathin thickness, the graphene has been modeled by surface conductivity. The value of surface conductivity is determined by Kubo's formula [4]. Here, electric-field-coupled (ELC) resonator with extended arms is performed as a building block of the graphene metasurface. The extended arm of the ELC is used to bias the graphene properly. The unit cell analysis of graphene metasurface is shown in figure 1(a). The metasurface layer is designed to provide band-stop functionality at 0.47THz. In order to reduce coupling between the patches, a 2×7 array of proposed metasurface is implanted between two patches. It is observed in Figure 1(b) that 7dB isolation improvement is obtained. The H field distribution, shown in Figure 1(c), clearly exhibits the isolation between radiating elements in the proposed design. In addition, radiation pattern of the propose configuration does not degraded and also slight improvement in the cross polar performance has been obtained as shown in figure 1(d) . Acknowledgment: The work funded by Visvesvaraya Young Faculty research fellowship award, under DeitY, Govt. of India. Reference [1]Z. Qamar, et. al., IEEE Trans. Ant. Propag. 7, 1653, (2016). [2]D. Gangwar, et. al., Wireless Personal Communications, Springer. 75, 2747, (2014). [3]G. Moreno, et. al., IEEE Ant. Wireless Propag. Letters. 15, 1533, (2016). [4]G. W. Hanson, et. al., J. Appl. Phys. 103, 064302 (2008)

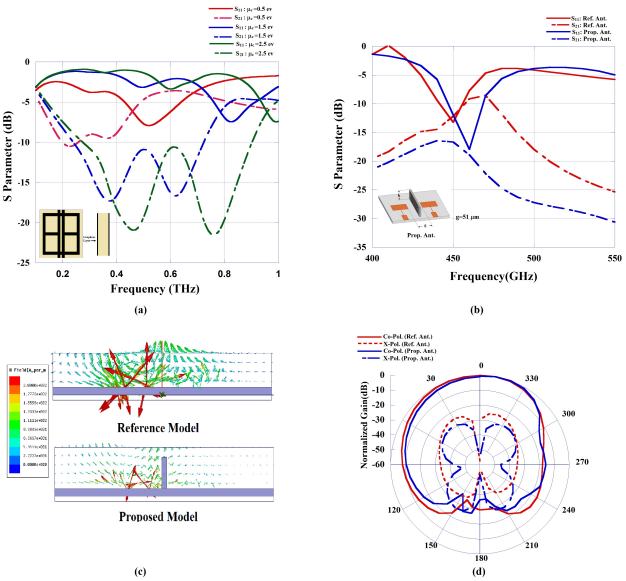


**Figure 1: (a) S parameter analysis of unit cell with variation of chemical potential ($\mu_c$) of graphene; inset: Unit cell of the graphene metasurface (b) The $S_{11}$ and $S_{12}$ response of the two adjacent patch antenna with and without Graphene metasurface; inset: Proposed antenna configuration (c) The H-Field vector distribution in the H Plane of reference and proposed model. (d) Normalized radiation pattern of the proposed and reference antenna array**

Ant figure.jpg

# Pseudo-Hall effect in graphite on paper based four terminal devices for stress sensing applications

**Wednesday, 9th November - 16:00 - Nanofabrication & Nanomanufacturing - Room 207 - Oral presentation - Abstract ID: 547**

***Mr. Afzaal Qamar*** [1], ***Mrs. Tuba Sarwar*** [2], ***Mr. Toan Dinh*** [1], ***Mr. A.r.muhammad Foisal*** [1], ***Dr. Hoang-phuong Phan*** [1], ***Dr. Dzung Dao*** [1]

*1. Queensland Micro- and Nanotechnology Centre, Griffith University, Australia, 2. Pakistan Institute of Engineering and Applied Sciences*

A cost effective and easy to fabricate stress sensor based on pseudo-Hall effect in Graphite on Paper (GOP) has been presented in this article. The four terminal devices were developed by pencil drawing with hand on to the paper substrate. The stress was applied to the paper containing four terminal device with the input current applied at two terminals and the offset voltage observed at other two terminals (called pseudo-Hall effect). The GOP stress sensor showed significant response to the applied stress which was smooth and linear. These results showed that the pseudo-Hall effect in GOP based four terminal devices can be used for cost effective, flexible and easy to make stress, strain or force sensing applications. In recent years, researchers have paid much attention to paper based devices for diagnostics and electronic applications. Flexible and wearable electronics is the fundamental part of flexible appliances which require ultra-thin and flexible navigation modules, force sensing, body tracking, and relative position monitoring systems. Soft robotics and transient electronics are the ultimate beneficiaries of these flexible and wearable electronics. The main advantages of this technology are the low cost, diversity in material choice, disposability and ease of fabrication. Graphite on paper (GOP), in which graphite layers are deposited on paper by either graphite-ink printing techniques, or manual pencil drawing techniques, has been utilized as the sensing element in flexible sensors for strain. Most of the work on GOP based stress/strain sensors is based on the two terminal resistor sensors which suffer several drawbacks. They show high temperature sensitivity relative to stress response and require Wheatstone bridge to detect the signal. On the other hand pseudo-Hall effect device inherently utilizing the high accuracy of four-wire resistance measurement method can overcome the limitations of the conventional resistor sensors. Therefore, in this study we report a GOP based cost effective and flexible stress/strain sensor based on pseudo-Hall effect. We have investigated the response of GOP four terminal devices and results are shown in Fig. 1(i). The smooth and linear behavior of the device against applied stress shows its potential applications in stress/strain and force sensing applications.

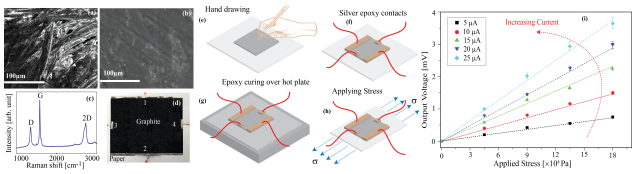


Final.png

# Mode control in SOI microring resonators through sub-wavelength modifications

**Wednesday, 9th November - 16:17 - Nanofabrication & Nanomanufacturing - Room 207 - Oral presentation - Abstract ID: 530**

***Mr. Armandas Balcytis*** [1]***, Mr. Darius Urbonas*** [2]***, Mr. Martynas Gabalis*** [2]***, Mr. Konstantinas Vaškevičius*** [2]***, Prof. Saulius Juodkazis*** [1]***, Dr. Raimondas Petruškevičius*** [2]

***1.*** *Swinburne University of Technology,* ***2.*** *Center for Physical Sciences and Technology*

Silicon-on-insulator (SOI) microring waveguiding structures show significant promise in telecommunications due to their narrowband resonances, and in biosensing due to their sensitivity to external perturbations. Furthermore, all applications can benefit from the strong confinement of optical energy, hence, small footprint, enabled by the large refractive index of silicon as well as compatibility with mature CMOS technology. However, especially in sensing, strong field confinement can be detrimental as it limits optical interaction with the surrounding media. Furthermore, since microrings support multiple resonances the free spectral range available for sensing is limited. These challenges illustrate a clear need to devise ways to control the energy confined within a microring resonator in both the spatial and spectral dimension. The main methods of mode control involve structural modifications of the waveguide-coupled microring resonators on the subwavelength scale. Electron beam lithography (EBL), despite its relatively slow serial scanning mode of operation, offers resolution in excess of 10 nm. This makes it capable of control over minute structural features and also to independently tailor exposure conditions for different patterned components, hence, more flexibly compensate for distortive proximity effects. EBL, combined with finite-difference time domain photonic simulation methods, underlies rapid prototyping of novel designs. In this work both FDTD simulation as well as EBL fabrication of novel SOI based waveguide-coupled microring resonator designs are discussed. Different complimentary approaches to augmenting the performance of microrings in the context of sensing applications are presented. Ring resonators with subwavelength-size annular gratings with finely controlled groove radii ranging from 10 nm to 80 nm have been fabricated using EBL and demonstrate Bragg selection of certain modes as well as slow-light derived dispersion related quality factor enhancement. Numerical simulations show how this principle can be applied to plasmonic nanodisk gratings on ring resonators which lead to a greatly extended free-spectral range and sensing performance. Lastly, EBL fabricated gradient effective refractive index resonators offer strong mode delocalization useful in bulk sensing and also exhibit enhanced Q-factor values. These examples illustrate ways to circumvent known limitations of SOI label-free optical sensors, leading to the increase in sensitivity and a broader utility of such devices.

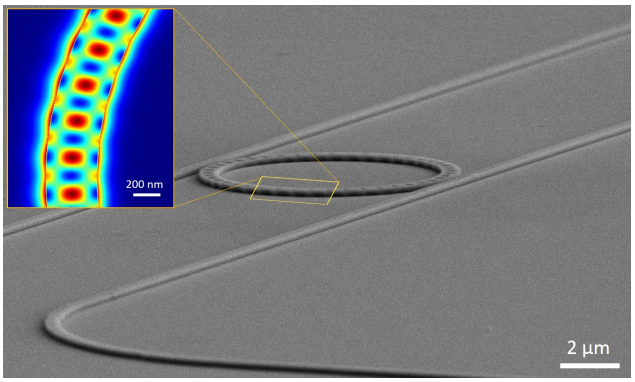


Img1.jpg

# Electrospray Deposition of Antimicrobial Nano-Powder/Bioactive Glass Composites on Ti6Al4V Implants

**Wednesday, 9th November - 16:34 - Nanofabrication & Nanomanufacturing - Room 207 - Oral presentation - Abstract ID: 588**

***Dr. Ceren Peksen*** [1], ***Dr. Mevlut Gurbuz*** [1], ***Prof. Aydın Dogan*** [2]

***1.*** *Ondokuz Mayıs University,* ***2.*** *ANADOLU UNIVERSITY*

Introduction. Bone infections after orthopaedic surgery especially implant releated osteomyelitis still one of the most important problem of Orthopaedics and Traumatology. Several techniques and methods have been developed to prevent infection. In this study, Ti6Al4V implants were electrospray coated by metal ion doped calcium phosphate based antimicrobial nano-powder (ABT) and bioactive glass (BG) to prevent local infections. Methods. Antimicrobial powders were synthesized by using wet chemical method. Calcium oxide and orthophosphoric acid were used as source of Ca2+ ion and PO43- ion, respectively. Ag+ ion was used as antimicrobial agent. Bioactive glass was prepared by mixing and firing the required reagents using a standart procedure. Halo Test Method was used to determine antimicrobial activity of powders. The BG powder was suspended in non aqueous medium. This suspension was deposited on substrates by dip coating. Then a vertical configuration of the ESD set-up was performed to deposit antimicrobial powder on implants. After deposition, electrospray deposited samples were sintered for 20-30 seconds by RF sintering unit under high vacuum. Surface characteristic of coated samples were investigated by Scanning Electron Microscopy (SEM, Zeiss Supra 50VP) and metal ion content of coatings were determined by Energy Dispersive X-Ray Spectroscopy (EDX). The adhesion of the coatings to the substrate was evaluated through the scratch test technique. Results and Discussion. In vitro antimicrobial tests indicate that the synthesized powder provides efficient antimicrobial effect. SEM images showed that the ABT/BG coatings form a continuous coating on Ti6Al4V surface. The result of scratch tests provided that the critical load of ABT/BG coating was indicated a high adhesive strength exists between coating and substrate. The results showed that bioactive glass with antibacterial ceramic powder has better adhesion and mechanical properties. Conclusions. In this study, an antimicrobial nano-powder/bioactive glass coating was successfully prepared on titanium alloy surface. As a surface coating material to host the silver ions, antimicrobial nano-powder and bioactive glass have several advantages that may benefit its usefulness as implants such as good biocompatibility, good mechanical property, easy manufacturability. In conclusion, the ABT/BG coatings may have potential application in Orthopaedics and Traumatology Surgery.

# Green Synthesis of ZnO Nanoparticles by an Alginate Mediated Ion-Exchange Process and a case study for Photocatalysis of Methylene Blue Dye

**Wednesday, 9th November - 16:51 - Nanofabrication & Nanomanufacturing - Room 207 - Oral presentation - Abstract ID: 480**

***Mr. Choo Cheng Keong*** [1], ***Ms. Yamini Sunitha Vivek*** [2], ***Dr. Babak Salamati*** [2], ***Dr. Bahman Amini Horri*** [3]

***1.*** *Monash University Malaysia,* ***2.*** *Monash University Malaysia (MUM),* ***3.*** *University of Surrey*

Photocatalytic degradation has been gaining attention in recent years and the role of Zinc Oxide nanoparticles as a photocatalyst has been investigated due to it wide availability, low cost and favourable gap energy. In this study, ZnO beads were prepared via extrusion-dripping method through an ion exchange mediated process using Sodium alginate as the precursor before drying at 40oC for 24hr. The oven dried samples were calcined at 500 ˚C and 600 ˚C to study the effect of calcination temperature on the synthesized ZnO nanoparticles. The morphology, microstructure and optical activity of the calcined ZnO nanoparticles were analyzed by FESEM and XRD. It was found that ZnO nanoparticles synthesized at 600 ˚C was of higher purity with high crystallinity. To enhance the photocatalytic efficiency of zinc oxide, ZnO/NCC (Nanocrystalline Cellulose) films are synthesized at varying ZnO loading fractions of 10 wt%, 15 wt%, 20 wt% and 25 wt%. Photocatalytic activity of the prepared pure ZnO, ZnO/NCC films and NCC was evaluated by photodegradation of Methylene blue dye. It was observed that the removal efficiency of ZnO-NCC films is increased with higher loadings of ZnO particles. In the presence of UV light irradiation after 30 minutes, the degradation efficiency of ZnO-NCC films were obtained to be 87%, 90%, and 96% for films with ZnO loadings of 15 wt%, 20 wt% and 25 wt% respectively. It was also observed that the films exhibited a higher performance in the presence of UV light. The results of this study help to understand the links between the characteristics and photodegradation capabilities of ZnO nanoparticles in the modified film form with the support of NCC.

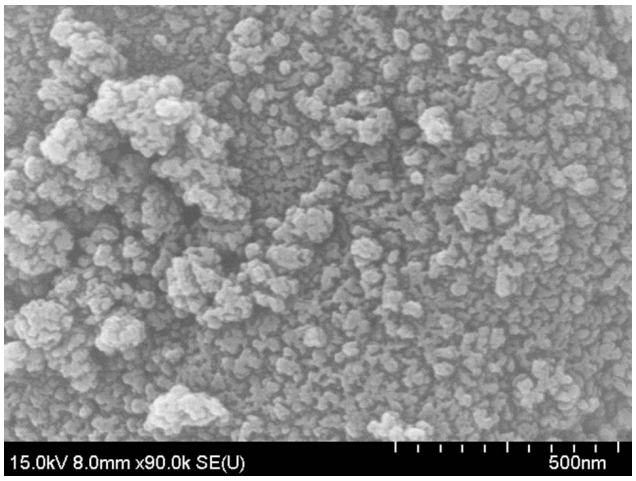


Zno600.jpg

# Reversible and dynamic micro-topographic pattern on azo-polymers substrates to investigate cell behavior in real-time.

**Wednesday, 9th November - 17:08 - Nanofabrication & Nanomanufacturing - Room 207 - Oral presentation - Abstract ID: 353**

***Ms. Lucia Rossano*** [1]***, Dr. Carmela Rianna*** [2]***, Prof. Maurizio Ventre*** [3]***, Dr. Silvia Cavalli*** [1]***, Prof. Paolo Antonio Netti*** [3]

***1.*** *Center for Advanced Biomaterials for Health Care IIT@CRIB, Largo Barsanti e Matteucci 53, 80125 NA, IT.,* ***2.*** *Institute of Biophysics, University of Bremen.,* ***3.*** *Department of Chemical, Materials and Industrial Engineering, University Federico II*

The cellular response to the external environment is a central aspect in tissue engineering and biomedical science. The topographical signals play an important role in cell-material interactions; in particular, in natural tissues there is a dynamical remodeling of topographical features that influence many cells processes, such as migration, orientation and differentiation. The conventional static culturing systems do not allow to understand how cell respond to spatio-temporal changes of signals. In order to overcome the limits of these static systems and to develop versatile platforms, great interest has recently arisen using stimuli-responsive materials as dynamic support to investigate cell response. In this work azo-polymers have been used to realize dynamic light-switchable support. Thanks to the fact that azobenzene molecules undergo a reversible trans-cis-trans isomerization process, when illuminated with a coherent and linear light at a proper wavelength, formation of topographic features is archived with potential use in nanopatterning. In fact, illumination causes a unique and remarkable surface mass-transport on micrometer and sub-micrometer length scale. Here, we report a method to fabricate and characterize many different topographic patterns using a confocal microscope set-up to guide and evaluate cell behavior. This set-up enables a precise spatial and temporal control on the inscription process, exposing dynamic topographical cues to live cells in real-time. This innovative method allows erasing the embossed pattern and eventually rewriting another pattern in the same spot, thus switching on or off topographical signal in live cell condition. This technique may pave the way to an in depth investigation of complex processes involved in cell-topography interactions in a dynamic and biomimetic way, owing to the versatility of confocal set-up and the unique properties of the azobenzene surfaces.

# ZnO Nanowires in Surface-Acustic-Wave Sensors

**Wednesday, 9th November - 17:25 - Nanofabrication & Nanomanufacturing - Room 207 - Oral presentation - Abstract ID: 267**

***Dr. Aurelian Marcu*** [1], ***Dr. Cristian Viespe*** [1], ***Mr. Bogdan Butoi*** [1], ***Mr. Paul Dinca*** [1], ***Ms. Liga Avotina*** [1], ***Dr. Cristian Lungu*** [1]

**1.** *National Institute for Laser Plasma and Radiation Physics*

Gas and liquid sensors development involve more and more nanotechnologies in developing their active surfaces. Nanostructures with controlled morphologies and structural properties are more and more used for building such devices, and their properties control became critical issues in the fabrication processes. Vapor-Liquid-Solid (VLS) technique is one of the approaches in growing nanostructures (nanowires) with controlled morphologies and structural properties. Combining this technique with the pulsed-laser deposition method, we have grown oxide (ZnO) nanowires on the surface-acoustic-wave (SAW) sensors. We have investigated nanostructure morphological and surface patterning influences over SAW sensors performances and we found significant improvements in sensor response on the nanostructures morphologies, with important decreasing of the threshold measurable concentration in comparison with thin film performances. Surface pattern growing is another way of noise reduction and sensibility improvements. Comparisons between different nanostructure patterns and structure morphologies and thin film surfaces are presented and exemplified on the hydrogen and deuterium detection. Acknowledgment: This work was supported by a grant of the Romanian National Authority for Scientific Research, CNCS -- UEFISCDI, project number PN-II-IDPCE- 2011-3-0522 and LAPLAS 3, Cod: PN 09 39.

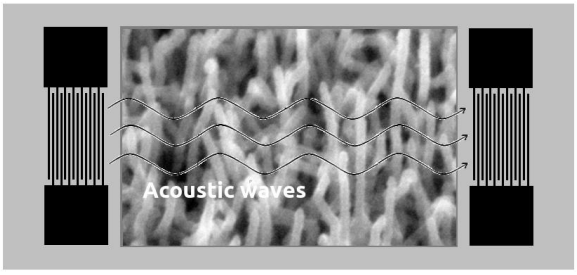


**Nanowire based Surface-Acustic-Wave sensor**

Sensor.jpg

# PVC and PES waste/nanoclay mixtures, their preparation and properties

**Wednesday, 9th November - 16:00 - Polymers & Nanocomposites - Room 412 - Oral presentation - Abstract ID: 369**

***Prof. Dagmar Merinska*** [1], ***Mrs. Alice Tesarikova*** [1], ***Dr. Lubomir Benicek*** [1]

***1.*** *Tomas Bata University in Zlin, Czech Republic*

Mixtures of PVC and PES waste (shredded fibers) were prepared in order to find way how the waste of PES raster used in hydroisolatic foils can be re-used. After the grinding of waste from mentioned foils this waste is divided into three different fractions. The first one is PES shredded material with the rest of plasticised PVC, which is possible to re-work without problems and it is possible to add it into the origin mixture for the production of hydroisolatic foils. The next two fractions obtain significantly less of PVC material and here it is necessary to add PVC and to find the optimal way for their mixing into the material with required properties. In order to find the way of PES waste treatment and other nanofiller synergy, to the prepared samples of PVS/PES waste the montmorillonite in one concentration was added. The influence of it on the observed properties was studied. There exist some studies about the recycling of PVC [1], but none about the combination of PVC and PES shredded material obtained in the form of waste. In our work all three fractions were added into two types of PVC and there were mixed on double roll equipment (to use the conditions and way as close to the practise as possible). Mechanical properties were measured on the prepared samples (bodies were cut from the rolled film) and the values of pure PVC mixture and mixtures wtih different filling of PES shredded material were observed. The same procedure was applied on the samples with nanofiller. One of results is shown in the Graph 1. This work was supported by project of TACR TH01030054.

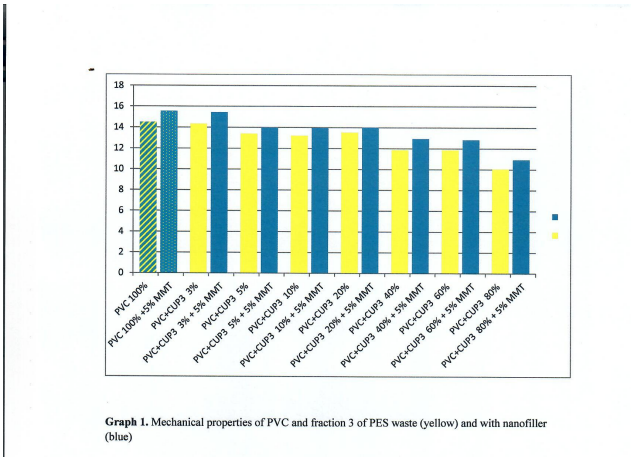


**Graph 1.** Mechanical properties of PVC and fraction 3 of PES waste (yellow) and with nanofiller (blue)

Image barcelona graph 1.jpg

# Diffusion of nanoparticles in solution through elastomeric membrane

**Wednesday, 9th November - 16:17 - Polymers & Nanocomposites - Room 412 - Oral presentation - Abstract ID: 365**

***Mr. Mohamed Zemzem*** [1], ***Dr. Ludwig Vinches*** [1], ***Prof. Stéphane Hallé*** [1]

**1.** *École de Technologie Supérieure*

Nanotechnology is currently one of the most studied branches of science with the number of uses of engineering nanoparticles (ENP) in various fields. The ENP have wide variety of applications including biomedical, energy and agribusiness fields. These ENP are increasingly used in suspension in liquids. In many applications such as in filtration processes or in the production of packaging, ENP in solution are in contact with elastomeric membranes. On the other hand, it's well known that numerous elastomeric membranes are sensitive to certain liquids. This sensitivity results in deterioration by swelling of the mechanical and physical properties of the material in contact with a liquid. In addition, recent studies have already validated the penetration of gold and titanium dioxide nanoparticles through some nitrile membranes. The aim of this work is to evaluate the influence of ENP, as well as additives present in the solutions, on the penetration process of the liquid carrier (water). It will be also assessed the kinetic properties of penetration of the solutions through the elastomeric membrane structure. Gravimetric technique was chosen as the main method quantified swelling phenomena and evaluate equilibrium and kinetic properties. The dynamic liquid uptake measurements were undertaken on gold nanoparticles (5 nm and 50 nm in diameter) in aqueous solutions in contact with elastomeric material. Swelling tests were also conducted with MilliQ water and filtrates (solution in which only the ENP were extracted). Indeed, additives, usually added as stabilizers to avoid ENP agglomeration in the liquid carrier, can impact significantly the swelling of the nitrile sample. Results showed that the diffusion coefficients of the three solutions of ENP are almost identical. However, it should be noted that these coefficients are notably higher for the filtrates, which underscore the effect of the ENP on the liquid penetration process as well as the influence of additives and stabilizers on the penetration of ENP through the membrane structure. These findings allow better understanding of ENP diffusion phenomenon through elastomeric structure and show the influence the elements composing the colloidal solution on the penetration phenomena.

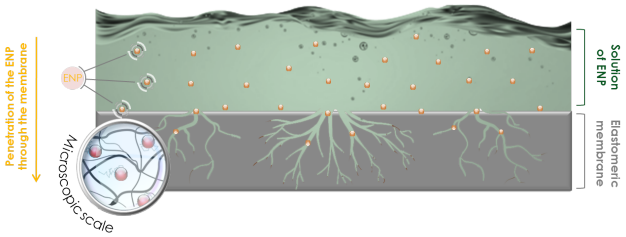


Penetration of nanoparticles in colloidal solution through elastomeric membrane.png

# Preparation and evaluation of mechanical properties of filled PVC/ PVB blends/clay and calcium carbonate

**Wednesday, 9th November - 16:34 - Polymers & Nanocomposites - Room 412 - Oral presentation - Abstract ID: 305**

***Mrs. Alice Tesarikova*** [1], ***Prof. Dagmar Merinska*** [1], ***Dr. Michael Tupy*** [2]

***1.*** *Tomas Bata University in Zlin, Czech Republic,* ***2.*** *Fatra, a.s. Napajedla, Czech Republic*

The comparison of mechanical properties of blends of plasticized poly(vinyl chloride) (PVC) with poly(vinyl butyral) (PVB) was the main aim of this study. The possibility of the re-use of recycled PVB from waste of windshields was studied. Composites of PVC/PVB blends, montmorillonite (MMT) and CaCO3, prepared by melting and mixing in a twin-screw extruder were evaluated. PVC plasticized with 38 % of diisononyl phthalate (DINP), and PVB plasticized with 28 % of triethylene glycol, bis(2-ethylhexanoate) (3GO) and recycled PVB (rec. PVB) were tested. The filler as an organically modified MMT with tradenames Cloisite 93A and 30B and CaCO3 were used. The concentration of all the above-mentioned fillers added to the polymeric matrix was 3, 5, 7 and 9 wt. %. Blends used for the determination of mechanical properties of PVB/PVC mixtures in various ratio were prepared in continual BUSS extruder with two kneading chambers. Process conditions were 160 °C of temperature and rotation speed 55 rpm. The high PVB molecular weight can provide very high tensile strength of material. Measurement showed that fillers do not deteriorate mechanical properties of filled PVC/recycled PVB blends. The same fact was also observed for fillers in virgin PVB. As was shown by TEM analyses - the nanofiller achieves a determinate degree of intercalation, but no full exfoliation (e.g. Image 1). The improvement of mechanical properties in scale from 60% of PVB was probably caused by mentioned high molecular weight of PVB. Further, the comparison showed that the ideal filling is 3 and 5 wt.% of nanofillers. This study seems to clarify a little more efficiency of PVC/PVB composites applications such as flooring, many uses in civil engineering. This work was supported by projects TH 01030054 (TACR--Epsilon) and IGA/FT/2016/009.

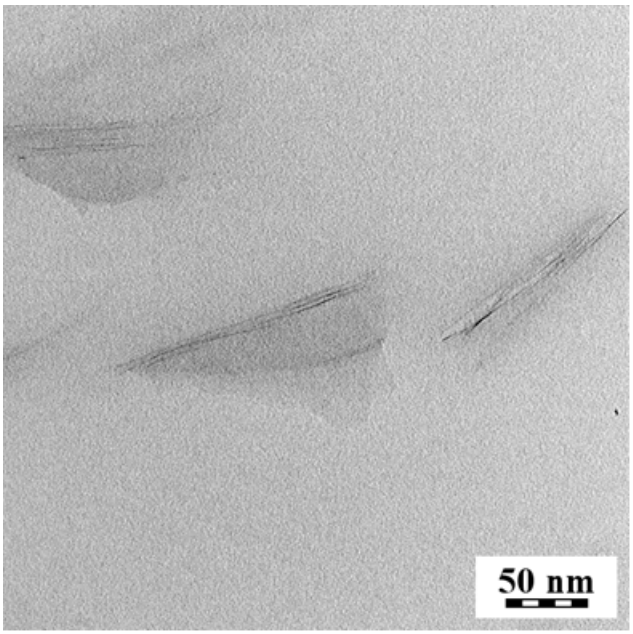


**Image 1:** TEM picture of PVC/recycled PVB 80% with 3% Cloisite 93A

Tem image.png

# Influence of multi walled carbon nanotubes and silica nanoparticles on tensile properties of polyurethane

**Wednesday, 9th November - 16:51 - Polymers & Nanocomposites - Room 412 - Oral presentation - Abstract ID: 83**

***Mr. Amir Navidfar*** [1], ***Mr. Alkan Sancak*** [1], ***Mr. Kemal Baran Yildirim*** [1], ***Prof. Levent Trabzon*** [1]

***1.*** *Istanbul Technical University*

Reinforcing of polymers with nanoparticles can considerably improve the desired properties of the polymeric nanocomposite foams. Carbon nanotubes (CNT) as an interesting additive due to their superior properties such as low density and high aspect ratio make them favorable fillers for reinforcement. In addition, SiO2 (silica) nanoparticles have been widely used with polymers to enhance the heat resistance, radiation resistance, mechanical and electrical properties. Polymeric foams such as Polyurethane (PU) are a group of lightweight materials, which are appropriate for a broad range of applications such as thermal and electrical insulation, shock and sound absorbents. PU foams are produced via the polymerization reaction of a diisocyanate with a polyol. Prior to the synthesis of PU foams, CNTs were functionalized by treating with the hydrogen peroxide (H2O2). In the next step, CNTs or silica nanoparticles were added to polyol and were mixed for 10 min. Then, Isocyanate was added to the composition, which was mixed and poured into wooden mold. Nanocomposites with various content of CNTs, silica A and silica B nanoparticles were produced up to 1 wt%. Molded nanocomposites were cut in turning machine with thickness of 10 mm and test samples were prepared with CNC machine according to ISO 1926. The aim of this work is investigating tensile properties of the nanocomposites with various percentages of CNTs and silica nanoparticles such as 0.25, 0.5, 0.75 and 1 wt %. Tensile tests will carry out and their results will discuss. In addition, the morphology of the nanocomposites will perform using scanning electron microscopy (SEM). As a result, neat PU presents lowest tensile strength, whereas highest strength can be seen in the nanocomposites containing 0.25 wt% Silica-A with 33 wt% improvement, but further Silica-A addition decreased strength of the PU/Silica-A foam. In addition, this phenomenon can be seen in adding of Silica-B and MWCNT into polymer matrix, which adding 0.25 wt% of Silica-B and MWCNT increased the tensile strength about 27% and 16%, respectively. In order to produce nanocomposites with higher CNT content and prevent appearance of large agglomerations, hybrid nanocomposite was produced, which could lessen large agglomerations.

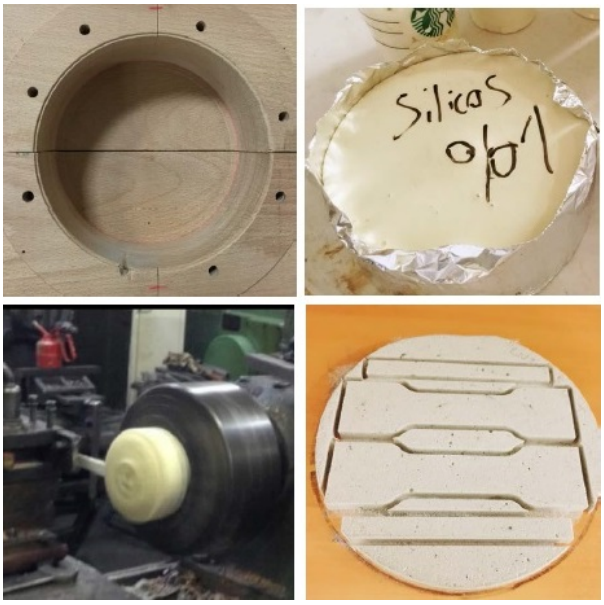


Graphical abstract.jpg

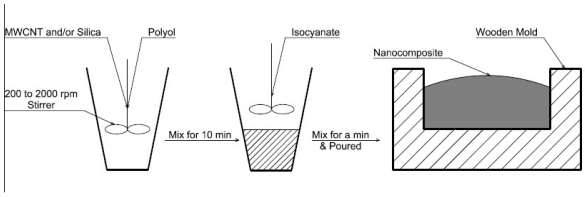


Mixing.jpg

# Poly (vinylidene fluoride)/Polyaniline/MWCNT Nanocomposite Ultrafiltration Membrane for natural organic matter removal

**Wednesday, 9th November - 17:08 - Polymers & Nanocomposites - Room 412 - Oral presentation - Abstract ID: 169**

***Mrs. Banan Hudaib*** [1], ***Prof. Vincent Gomes*** [1], ***Dr. Jeffrey Shi*** [1], ***Prof. Dianne Wiley*** [1], ***Prof. Zongwen Liu*** [1]

***1.*** *Sydney university*

Abstract:The objective of this work was to improve the permeability and the rejection properties of poly (vinylidene fluoride) PVDF ultrafiltration(UF) membrane using multi-wall carbon nanotubes(MWCNTs)/ polyaniline (PANI) composite prepared by phase inversion through in situ polymerization method of PANI, for removal of natural organic matter (NOM) in water. 1. Introduction:PVDF is a promising UF membrane material due to its excellent properties such as high mechanical strength, high thermal stability and chemical resistance to organic solvents[1]. However, its hydrophobicity is considered to be the main drawback that reduces water flux and increases fouling[2]. Modification of the membrane surface by addition of nanoparticles like CNTs increases the membrane hydrophilicity with enhanced specific surface area, chemical stability and ease of functionalization[3]; this improves the permeability and antifouling properties of membranes. 2. Membrane preparation: MWCNT was dispersed in DMF solvent by ultrasonication first, then aniline hydrochloride and ammonium persulphate (APS) were added to the mixture which was stirred for 72 hrs at room temperature to synthesize the MWCNT/PANI nanocomposite by in-situ polymerization.Fixed amount of PVDF was added and stirred at 60 0C for 24 hr. The casting solution was degassed and cast on a glass plate. The cast film was immersed into a pure water bath to achieve in situ polymerization of aniline with different percentage amounts of MWCNT ranging from 0.25wt.% to 2wt.% in PVDF casting solutions. 4. Results and Discussion:The measurements of permeability, NOM rejection, contact angle, porosity, tensile strength, zeta potential and scanning electron microscopy (SEM) were performed. The resultant membrane (of PANI/1.5%MWCNT) showed the highest permeability (1320 LMH/bar) with a 35-fold of permeability improvement in comparison to pristine PVDF membrane; furthermore, the filtration test showed 78% rejection for Suwannee River Humic acid (HA). This significant improvement is due to the inclusion of MWCNT/PANI complex in the PVDF matrix, which increased hydrophilicity and formed more porous areas with well-developed finger like smaller pores under the top layer connected to the larger pores in the underneath layer see Fig.1. Moreover, the MWCNT/PANI increased the adsorption capacity of the membrane by the interaction of the negative NOM and the positively charged membrane surface.

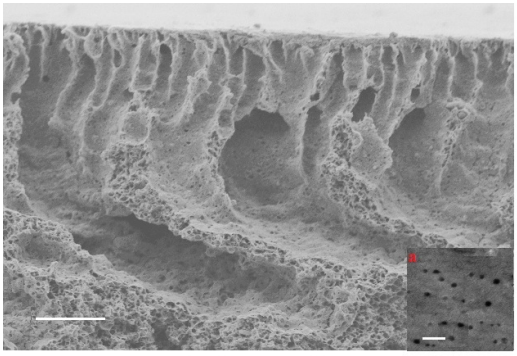

**Fig.1.** SEM images of PVDF/1.5 wt. %cMWCNT/PANI cross-section view; showing the top surface (a). Cross section scale bar: 20 µm, top surface (a) scale bar: 200 nm.

Sem image.jpg

# Ca (OH) 2 Nanoparticles Based on Acrylic Copolymers for the consolidation and protection of Ancient Egypt Calcareous Stone Monuments.

**Wednesday, 9th November - 17:25 - Polymers & Nanocomposites - Room 412 - Oral presentation - Abstract ID: 46**

***Mr. Sayed Mansour [1], Prof. Sawsan Darwish [2], Dr. Mahmoud Abd Elhafez [2], Prof. Nagib Elmarzugi [3], Prof. Mohammad AlDosari [4]***

***1.*** *PhD Student , Cairo university , Egypt,* ***2.*** *Faculty of archaeology , Cairo university , Egypt,* ***3.*** *Faculty of Pharmacy, Tripoli University and BioNano Integration Research Group, Biotechnology Research Center, LARST, Tripoli, Libya,* ***4.*** *National Nanotechnology Research Center, King Abdulalziz City for Science and Technology (KACST), Riyadh, Saudi Arabia.*

The deterioration of lime-based porous materials used in artistic/architectural field (lime-based wall paintings, calcareous stones) is one of the most serious problems facing conservation today. The aim of this study was to evaluate the effectiveness of inorganic compatible treatments, based on nano sized particles of calcium hydroxide (slaked lime) as a consolidation and protection material dispersed in acrylic copolymer, poly ethylmethacrylate/methylacrylate (70:30) (Poly (EMA/MA), for calcareous stone monuments and painted surfaces affected by different kinds of decay, thanks to the conversion of lime into calcium carbonate. Calcium carbonate is, as a matter of fact, very compatible with many carbonatic lithotypes and architectonic surfaces, because its characteristics are very similar to those of the materials to be restored. The synthesis process of Ca (OH)2 nanoparticles/polymer nanocomposites have been prepared by in situ emulsion polymerization system. The prepared nanocomposite containing 5% of Ca (OH)2 nanoparticles showed obvious transparency features and represent nanocomposites coating technology with hydrophobic, consolidating and well protection properties. Some tests are performed in order to estimate the superficial consolidating and protective effect of the treatment; the obtained nanocomposites have been characterized by TEM, while the penetration depth, re-aggregating effects of the deposited phase and the surface morphology before and after aging was examined by Scanning electron microscopy (SEM), Improving of stone mechanical properties were evaluated by compressive strength tests, Changes in water-interaction properties were evaluated by water absorption capillarity measurements and colorimetric measurements were used to evaluate the optical appearance. All the results converged in individuating these nanometric particles of slaked lime as an innovative, completely compatible, and efficient material for the consolidation of artistic (lime-based wall paintings) and architectural (lime stones) surfaces,Ca (OH)2 /polymer nanocomposite enhanced the durability of limestone toward thermal aging and improved the stone mechanical properties compared to the samples treated with pure acrylic copolymer without Ca (OH)2 nanoparticles.

# Sorting various pluripotent state of iPSCs via magnetization of nanoclusters in microfluidic magnetophoresis devices

**Wednesday, 9th November - 16:00 - Nanomedecine & Nanobiology - Auditorium - Oral presentation - Abstract ID: 539**

***Mr. Byunghoon Kang*** [1], ***Ms. Seungmin Han*** [2], ***Mr. Moo-kwang Shin*** [1], ***Dr. Jeong-ki Min*** [3], ***Dr. Hye-Young Son*** [1], ***Prof. Yong-Min Huh*** [1], ***Prof. Seungjoo Haam*** [1]

***1.*** *Yonsei University,* ***2.*** *Yonsei,* ***3.*** *Korea Research Institute of Bioscience and Biotechnology*

iPSCs are prone to randomly differentiate into any cell line, and it is hard to maintain cell population with high pluripotency level. Therefore, it is necessary to isolate homogenous populations of highly pluripotent iPSCs for applying the iPSCs in reprogramming somatic cells into iPSCs or differentiating iPSCs into specific cells. FACS and MACS have been used for sorting specific cells, but both methods have underlying issues in time and efficiency. Therefore, we developed magnetophoresis system with microfluidic channel to overcome abovementioned flaws. It can sort cells with higher quality and faster than conservative methods. We used iPSCs-specific surface marker (A) and differentiated cells-specific surface marker (CD44), and each marker was labelled synthesized 200 nm and 500 nm magnetic clusters (200-A NC, and 500-CD44 NC), respectively. Highly pluripotent iPSCs are tagged with only 200-A NC, and slightly differentiated cells are tagged with 200-A NC and 500-CD44 NC. The cells are multifractionated in magnetophoresis microfluidic system. Consequently, magnetically cell separation in a microfluidic channel system containing five outlets was successfully performed. Cells were deflected and carried out into different outlet channels depending on their magnetization. The magnetization is decided by tagged magnetic particle size and amount, which is related with pluripotency state of iPSCs. The result showed that outlet 1, 3, 5 had non-tagged cells, highly pluripotent iPSCs, and slightly differentiated cells, respectively. This method allows for high-throughput, cell preservation, and successfully overcoming the current flaws of FACS and MACS. A multifractionation method for magnetic cell separation has been presented and evaluated using a stem cell model. Magnetization differences according to size and amount of tagged NC showed remarkable potential for multifractionation of the target cells. The results that we have shown agree with pluripotency state of iPSCs. This system demonstrates the ability to separate various kinds of homogeneous and heterogeneous cells by taking advantage of a range of magnetizations.

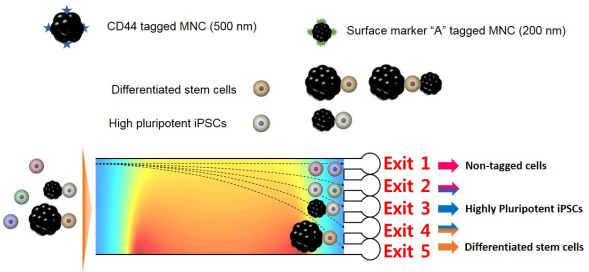


Figure.jpg

# Adsorption of globin proteins in mesoporous (designed) titania for biosensors development.

**Wednesday, 9th November - 16:17 - Nanomedecine & Nanobiology - Auditorium - Oral presentation - Abstract ID: 138**

***Mr. stefano loreto*** [1]***, Prof. Karolien De Wael*** [1]***, Prof. Vera Meynen*** [1]

***1.*** *University of Antwerp*

Mesoporous materials are ideal substrates for the incorporation and immobilizations of proteins due to their high surface area, pore volume and the possibility to obtain a very homogeneous, controllable pore size. Mesoporous TiO2 could be very promising with respect to the possible joined effects of semiconductor properties and redox active proteins. However, the controlled synthesis of titanium dioxide is a challenging step often leading to disordered mesoporous structures and non-uniform pore networks. We successfully synthesised highly ordered mesoporous titania with differnt pore diameters, homogeneous pore size, large surface area and pore volume. The designed mesoporous titanium dioxide with different pore sizes has been used for the adsorption of horse hearth myoglobin (hhMb); a globular shape proteins with a mean diameter of 5 nm. The effect of different parameters (buffer type and concentration, solution pH) on the incorporation and the rate of the adsorption have been studied in depth. The encapsulation rate has been monitored by UV-vis spectroscopy and a kinetic model for the adsorption has been elaborated. TGA/DTG, FT IR, UV DR spectroscopy and electron paramagnetic resonance (EPR) have been used to detect changes in the secondary structure or in the heme center upon the adsorption. The stability of the encapsulated hhMb has been evaluated by its electrochemical activity (Cyclic Voltammetry) and peroxidase like activity in the presence of ABTS. The results clearly show the beneficial effect of the incorporation into the pores. The study of the adsorption of human neuroglobin on both unmodified and functionalized mesoporous titania will be the next step of this work.

# Tumor-activated prodrug nanoparticles sensing endogenous levels of matrix metallo-proteinase 2 in 3D tumor spheroids for the on-demand release of doxorubicin

**Wednesday, 9th November - 16:34 - Nanomedecine & Nanobiology - Auditorium - Oral presentation - Abstract ID: 101**

***Mrs. Martina Profeta*** [1], ***Dr. Daniela Guarnieri*** [1], ***Dr. Valentina Belli*** [1], ***Dr. Marco Biondi*** [2], ***Dr. Marco Cantisani*** [1], ***Dr. Luca Raiola*** [1], ***Prof. Paolo Antonio Netti*** [1]

***1.*** *Center for Advanced Biomaterials for health Care (CABHC), Istituto Italiano di Tecnologia, Centro di Ricerca Interdipartimentale sui Biomateriali (CRIB), Università di Napoli Federico II,* ***2.*** *Dipartimento di Farmacia, Università di Napoli Federico II*

Matrix Metalloproteinases (MMPs) are proteolytic enzymes that play a key role in tumor metastasis progression so a novel approach in nanoparticles (NPs) design may be the one that benefits from MMPs over-expression, in order to realize a stimuli-responsive nanocarrier. To this aim we designed biocompatible and biodegradable NPs made up of a poly(D,L-lactic-co-glycolic acid) (PLGA)--block--polyethylene glycol (PEG) copolymer (namely PELGA), blended with a tumor activated prodrug (TAP) composed by an MMP2-sensitive peptide bound to doxorubicin (Dox) and to a PLGA molecule. The same prodrug was produced without the MMP-sensitive linker as negative control. PELGA-TAP and PELGA-Dox NPs were produced and characterized. DLS results show that NPs diameter is below 100 nm with a PDI< 0.2 and a negative z-potential for both NPs formulations. SEM and Cryo-TEM images show that NPs are spherical and monodispersed. In vitro Dox release from NPs, in presence and absence of free MMP2 enzyme, was tested performing a cleavage assay on both NPs. Release profiles show that PELGA-TAP NPs allow Dox controlled release specifically upon MMP2 cleavage of the TAP while PELGA-Dox NPs drug release is comparable to PELGA-TAP NPs release in absence of the enzyme. To demonstrate PELGA-TAP NPs ability to sense the differences in expression levels of endogenous MMP2 enzyme, U87 and HDF, tumor and healthy cell lines respectively, were used to built up an in vitro spheroidal model. Spheroids were treated with PELGA-TAP and PELGA-Dox NPs. Confocal microscopy images show the presence of a fluorescence signal within U87 spheroids after 24h exposure to PELGA-TAP NPs, inducing spheroids' disaggregation after 48h, while a very low fluorescence signal was observed for U87 spheroids treated with PELGA-Dox after 24h and 48h of incubation. Interestingly, HDF spheroids show a lower fluorescence signal than U87, with little differences between PELGA-TAP and PELGA-Dox NPs treatment. The results presented above suggest that PELGA-TAP NPs can deliver Dox specifically upon enzymatic cleavage and promote drug penetration within 3D tumor spheroids so, starting from these promising results, NPs could be tested on more complex in vitro tissue equivalents to further validate their selective drug release and their efficacy as drug delivery systems.

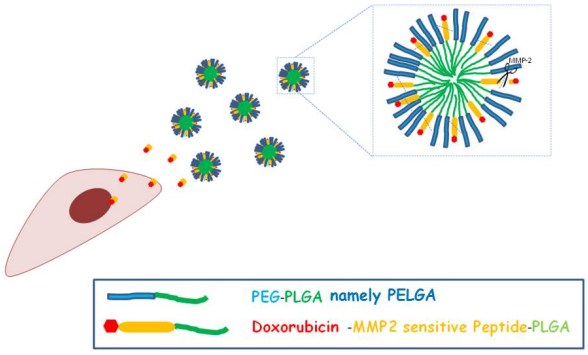


Mmp-2 sensitive nps.jpg

# Hydrogel Micropattern Incorporating Nanostructures for Fluorescence-based Biosensing

**Wednesday, 9th November - 16:51 - Nanomedecine & Nanobiology - Auditorium - Oral presentation - Abstract ID: 281**

***Prof. Won-Gun Koh*** [1], ***Mr. Minsoo Kim*** [1], ***Mr. Sang Won Han*** [1], ***Prof. Kangwon Lee*** [2]

***1.*** *Yonsei University,* ***2.*** *Seoul National University*

Different fluorescence biosensor based on hydrogel microstructures incorporating different nanostructures are introduced in this symposium. First, the quantum dot (QD)--enzyme conjugates were entrapped within the poly(ethylene glycol) (PEG)-based hydrogel microstructures. Glucose oxidase (GOX) and alcohol oxidase (AOX) were chosen as the model oxidase enzymes, conjugated to carboxyl-terminated CdSe/ZnS QDs, and entrapped within the hydrogel microstructures, which resulted in a fluorescent hydrogel microarray that was responsive to glucose or alcohol. The hydrogel-entrapped GOX and AOX were able to perform enzyme-catalyzed oxidation of glucose and alcohol, respectively, to produce H2O2, which subsequently quenched the fluorescence of the conjugated QDs. Second, we developed a novel silver-based MEF biosensing platform that consisted of poly(ethylene glycol)(PEG) hydrogel microstructures entrapping silica-coated AgNPs (Ag@SiO2). AgNPs were coated with different thickness of silica to optimize the MEF effects. As a model system, the fluorescence detection of glucose by a sequential bi-enzymatic reaction was chosen. For this analysis, hydrogel microstructures entrapping glucose oxidase (GOX), peroxidase (POD) and Ag@SiO2 were prepared by a simple photopatterning process. We took advantage of the MEF from Ag@SiO2 within the hydrogel microstructures to improve the performance of the fluorescence detection device. Finally, describes the design and fabrication of a microdevice as a new platform for highly sensitive MMP-9 detection. For enhanced MMP-9 detection, fluorescently labeled MMP-9-specific peptides were immobilized onto an electrospun nanofiber matrix that was framed with hydrogel micropatterns via photolithography. Due to the huge surface area of the nanofiber and small dimensions of the microsystem, a faster response time (30 minutes) and lower detection limit (10 pM) could be achieved.

# Fluorescent nano-switch probes: Monitoring of microRNA level in induced pluripotent stem cells without affecting pluripotency

**Wednesday, 9th November - 17:08 - Nanomedecine & Nanobiology - Auditorium - Oral presentation - Abstract ID: 538**

***Ms. Seungmin Han*** [1], ***Dr. Hye-Young Son*** [2], ***Dr. Eunji Jang*** [1], ***Mr. Byunghoon Kang*** [1], ***Ms. Jisun Ki*** [1], ***Mr. Moo-kwang Shin*** [1], ***Mr. Byeonggeol Mun*** [1], ***Dr. Jeong-ki Min*** [3], ***Prof. Seungjoo Haam*** [1]

***1.*** *Yonsei University,* ***2.*** *Yonsei,* ***3.*** *Korea Research Institute of Bioscience and Biotechnology*

The isolation of highly pluripotent induced pluripotent stem cells (iPSCs) and increasing reprogramming efficiency are goals of reprogramming into iPSCs. It has been studied to isolate highly pluripotent iPSCs without affecting pluripotency. In general, highly pluripotent iPSCs has been isolated by surface markers and morphology of cells with confirming generation embryonic body and teratoma. However, surface markers and morphology do not show endogenous condition. microRNA (miRNA) has been drawn lots of interest as a biomarker, because it has been proved that miRNA plays a role as a regulator in various biological functions; metastasis, proliferation, and especially differentiation state or pluripotency level in iPSCs. Therefore, miRNA expression level can be combined with conservative method (surface markers and morphology) for efficiently distinguish highly pluripotent iPSCs during reprogramming somatic cells into iPSCs. A non-invasive imaging system that can monitor miRNA expression level without affecting pluripotency of iPSCs provides a useful tool to identify and analyze specific cell populations during reprogramming into iPSCs. Herein, we designed a miRNA imaging probe (miP) containing sequences of positively and negatively expressed miRNAs that determine the differentiation status of somatic cells during reprogramming. miP consists of a complementary sequence to target miRNA, a fluorophore and a quencher at the end of each oligonucleotide. When miP meets with target miRNA, quencher is detached from fluorophore and miP has fluorescence signal. Also, polyethylene glycol (PEG)-grafted polyethylene imine (PEI-PEG) was utilized as a non-invasive delivery carrier of a fluorescence imaging probe, which enabled repeated evaluation of miRNA expression. miP loaded PEI-PEG (miP-P) showed ~96 % of miP untake efficiency, and had fluorescence signal within 30 minutes in vitro when it met with endogenous target miRNA. We call it as a fluorescent nanoswicth, because it turns ``ON'' with target miRNA. The fluorescence signal results were corresponded with qRT-PCR analysis. In addition, we confirmed that miP-P system does not affect pluripotency of iPSCs. Consequently, the fluorescent nanoswitch has a potent to isolate highly pluripotent iPSCs without affecting pluripotency of iPSCs. We envisage that this miRNA imaging system could be valuable methodology for identifying and sorting pluripotent stem cells during somatic cell reprogramming.

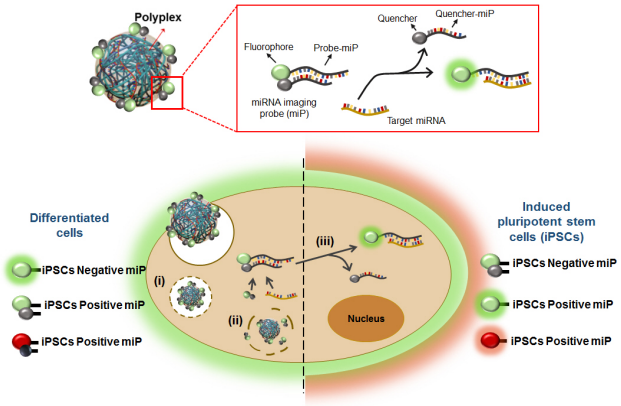


Scheme of fluorescent nano-switch probes for monitoring ipscs.jpg

# Nanoparticle-mediated delivery of supramolecular drugs and biomolecules into cells

**Wednesday, 9th November - 17:25 - Nanomedecine & Nanobiology - Auditorium - Oral presentation - Abstract ID: 436**

***Dr. Viktoriya Sokolova*** [1], ***Dr. Olga Rotan*** [1], ***Mr. Patrick Gilles*** [2], ***Mr. Som Dutt*** [2], ***Prof. Thomas Schrader*** [3], ***Prof. Matthias Epple*** [4]

***1.*** *Inorganic Chemistry and Center for Nanointegration Duisburg-Essen (CeNIDE), University of Duisburg-Essen, Essen,* ***2.*** *Organic Chemistry, University of Duisburg-Essen, Essen,* ***3.*** *Organic Chemistry, University of Duisburg-Essen; Collaborative Research Centre 1093 "Supramolecular Chemistry on Proteins", University of Duisburg-Essen, Essen,* ***4.*** *Inorganic Chemistry and Center for Nanointegration Duisburg-Essen (CeNIDE), Collaborative Research Centre 1093 "Supramolecular Chemistry on Proteins", University of Duisburg-Essen, Essen*

I. Introduction The successful transport of supramolecular drugs and biomolecule into living cells is highly important in biomedicine and pharmaceutics. Molecules alone usually cannot penetrate the cell membrane, therefore, an efficient carrier is needed. Calcium phosphate nanoparticles are well suited as a carrier for such molecules due to their high biodegradability and good biodegradability which is due to the fact that calcium phosphate is the inorganic mineral of human bone and teeth.1-3 II. Methods Calcium phosphate nanoparticles were prepared by rapid precipitation and were loaded either with different artificial protein- and DNA-binders (polyfunctional anionic polymers, cationic calixarene dimers or amphiphilic molecular tweezers) or with fluorescently-labelled small and large biomolecules (nucleic acids, proteins or peptides). All nanoparticle dispersions were characterized by dynamic light scattering (DLS), nanoparticle tracking analysis (NTA), and scanning electron microscopy (SEM). The amount of the fluorescing molecules on the nanoparticles was quantified by quantitative UV spectroscopy. The uptake of such fluorescence-labelled nanoparticles into HeLa cells was monitored by confocal laser scanning microscopy (CLSM). The cell viability was analyzed by an MTT assay. III. Results Functionalized calcium phosphate nanoparticles had a spherical morphology with a diameter between 150 and 200 nm (Figure 1). Neither the nanoparticle dispersions nor the dissolved molecules showed any cytotoxicity. As visualized by CLSM, the nanoparticles were easily taken up by HeLa cells together with their cargo molecules. In contrast, the dissolved molecules alone were not able to penetrate the cell membrane. IV. Discussion Calcium phosphate nanoparticles can serve as versatile carrier for small and large molecules across cell membranes. Such nanoparticles are efficiently taken up by cells where they can exert a biological or pharmaceutical function. Figure 1: Scanning electron micrograph of calcium phosphate nanoparticles, functionalized with oligonucleotides. References: 1. M. Epple et. al., J. Mater. Chem. 2010, 20, 18. 2. V. Sokolova et. al,. J. Nanoparticle Res. 2012, 14, 910. 3. O. Rotan et. al., Mater.-Wiss. u. Werkstofftechn. 2013, 44, 176.

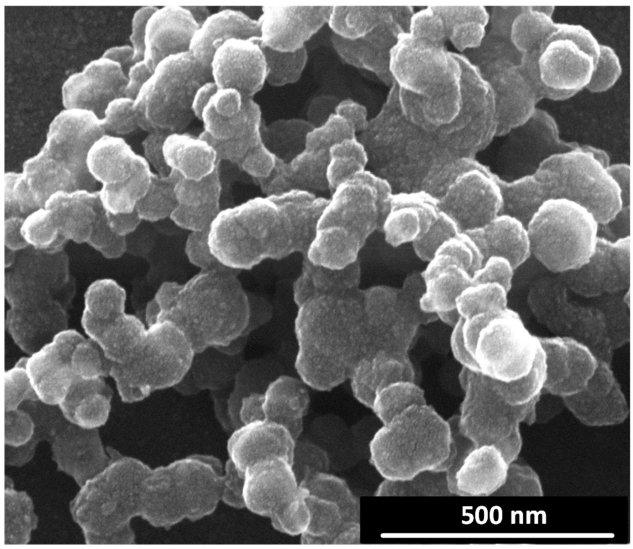


Figure-scanning electron micrograph of calcium phosphate nanoparticles.jpg

# New routes to exotic nanomaterials

**Thursday, 10th November - 09:00 - Plenary Speeches - Auditorium - Oral presentation - Abstract ID: 723**

***Prof. Clément Sanchez*** [1]

**1.** *Collège de France*

Nanomaterials and nanostructured materials can provide new solutions for important societal concerns such as those related to energy, environment and health. Therefore there is an important need to amplify the set of nano-objets found in the ``nanofoundries'' of materials chemistry laboratories. Using innovative and integrative processing approaches and utilizing hybrid molecular metal complex precursors or nanoparticles as precursors, we are trying to push further the limits of the nanochemistry developed with inorganic or hybrid matter. New families of nano-oxides (nanoMagnéli phases, multicationic oxides at nanoscale, core-shell mesoporous silicas) will be presented which might host advanced properties at the nanoscale in various fields, such as, catalysis, energy harnessing and nanomedicine. Moreover the syntheses strategies allowing to obtain covalent nano-alloys such as metal borides and metal phosphides and their mixte alloys will also be discussed. The fabrication of the above-mentioned nanomaterials involve innovative molecular approaches with different stimuli (conventional heating, microwave heating...) and original reaction media, such as ionic solvents, polymers or nano-reactors. Multifunctional nanomaterials can be made via the controlled of multiple inorganic-organic and inorganic-inorganic interfaces. These strategies can also give rise to interesting core-shell mesoporous silicas obtained by double templating, core-shell hybrid Janus nanoparticles obtained via self-assembly driven ``chemical''polarization and inorganic hetero-nanostructures obtained by nanophase segregation or insertion-crystallisation. This conference will described a few of the results we have obtained in this area. We bet that some of the described strategies will open a land of opportunities to create several families of ''exotic nanomaterials''.

# Atomic collapse in graphene

**Thursday, 10th November - 09:35 - Plenary Speeches - Auditorium - Oral presentation - Abstract ID: 721**

***Prof. Francois Peeters*** [1]

***1.*** *University of Antwerp*

The chiral nature of charge carriers in graphene prohibits backscattering and prevents confinement by electrostatic potentials, resulting in high electronic mobility and unusual phenomena such as Klein tunneling. This picture breaks down in the presence of charge impurities exceeding a critical value Zc, where a qualitative change in behavior leads to the capture of electrons akin to atomic collapse in 3D atoms. Although in graphene Zc is substantially lower than in 3D atoms, attaining the supercritical regime is difficult because screening can significantly reduce the effective charge of the impurity. The transition from sub-critical to the supercritical regime is accompanied by trapping of electrons in quasi-bound states which are the condensed matter analogue of the long sought after phenomenon of atomic collapse in super-heavy nuclei. The quasi-bound electron-states show up as a strong enhancement of the density of states within a disc centered on the vacancy site. We find that these states are surrounded by a circular halo of hole states which are interpreted as the analogue of positron production in atomic collapse. We further show that the quasi-bound states at the vacancy site are gate tunable and that the trapping mechanism can be turned on and off, providing a new paradigm to confine, control and guide electrons in graphene.

# Complex dynamic multicomponent supramolecular nanomaterials: tailoring low dimensional multifunctional nanostructures

**Thursday, 10th November - 10:45 - Plenary Speeches - Auditorium - Oral presentation - Abstract ID: 724**

***Prof. Paolo Samori*** [1]

***1.*** *University of Strasbourg*

The development of multicomponent thus multifunctional carbon-based nanomaterials via the full control over the architecture vs function relationship can be further modulated and leveraged by using light-stimuli as a route towards the realization of smart and high performing (opto)electronic (nano)devices, sensors and logic gates. However, their practical use requires the optimization of the self-assembly of multimodular architectures at surfaces using non-conventional methods, their controlled manipulation and responsiveness to external stimuli, and the quantitative study of various physico-chemical properties at distinct length- and time-scales. My lecture will review our recent findings on: (i) The harnessing of the yield of exfoliation of graphene in liquid media by mastering the supramolecular approach via the combination with ad-hoc functional molecules possessing high affinity for the graphene surface, leading ultimately to the bottom-up formation of optically responsive graphene based nanocomposites for electronics. [1] The physisorption of conjugated polymers on already pre-patterned liquid processed graphene nanopatches exhibiting tunable ionization energy obtained with thermal annealing, is a viable strategy to fabricate non-volatile memory devices.[2] (ii) Since the sensing occurs via molecular recognition, the sensitivity in humidity and (heavy) metal sensing can be harnessed by using low dimensional structures exhibiting a high surface area, fully decorated with receptors. Electroactive fibers obtained from an amphiphilic monomolecular dyad showed unique characteristics as resistive humidity sensors combining a response rate as fast as 26 ms with an exponential growth of the current from 0 to, at least, 75% of relative humidity (RH). In this RH range the current changes up to 7 orders of magnitude, i.e. from a few pA to tens mA, demonstrating an extremely high sensitivity to humidity variations.[3] (iii) The tailoring of multicomponent films comprising photochromic systems and semiconducting molecules, and their exploitation to realise multifunctional devices such as optically switchable field-effect transistors and memories. [4] Our approaches provide a glimpse on the chemist's toolbox to generate molecular nanomaterials with ad-hoc properties for the fabrication of high performing multifunctional nanodevices.

# Solution Processing of Thermoelectric Materials, Devices and Systems

**Thursday, 10th November - 11:20 - Plenary Speeches - Auditorium - Oral presentation - Abstract ID: 727**

***Dr. Andreu Cabot*** [1]

***1.*** *Catalonia Energy Research Institute (IREC)*

Breakthroughs in materials hold the key to new generations of products. This breakthrough will be reached through the control over material properties and the understanding of mechanisms and phenomena at the atomic scale. At the same time, industrial innovation will be supported on cost-effective technologies able to transform this control and understanding into optimized and new products. In this scenario, solution-based methods allow production of nanomaterials with unmatched degree of control over size, shape, phase and composition of the crystalline domains. At the same time, the availability of materials in solution or as nano-inks enables the large volume and high yield fabrication of devices and even systems over a variety of substrates by cost-effective printing and coating technologies. I will talk about the potential of solution-based synthesis routes and solution-processing technologies to produce high-efficiency thermoelectric nanocomposites, low-cost thermoelectric devices and autonomous thermoelectric-enabled sensing systems.

# Synthesis and characterization of reduced graphene oxide films by aqueous electrochemical reduction

**Thursday, 10th November - 13:30 - Poster Session - Gallery - Poster presentation - Abstract ID: 9**

***Dr. Alina Pruna*** [1]***, Prof. J.A. Zapien*** [2]***, Prof. A. Ruotolo*** [2]***, Dr. A.M. Mocioiu*** [1]***, Ms. Paulina Dobosz*** [3]

***1.*** *Polytechnic University of Bucharest,* ***2.*** *City University of Hong Kong,* ***3.*** *The Institute of Photonic Sciences*

INTRODUCTION In recent years, the electrochemical synthesis of graphene materials has drawn considerable attention thanks to the negative potentials employed that can overcome the energy barriers to efficiently reduce the oxygen functional groups (OFGs) in graphene oxide (GO), more than it is possible via chemical methods [1, 2]. In this paper, ErGO films were synthesized by a two-step approach involving a spin-coating step of the GO dispersion and subsequent electrochemical reduction. The effects of OFGs in GO and the electrochemical reduction methods based on potential modulation were assessed. EXPERIMENTAL The aqueous dispersions of GO were spin-coated on ITO substrates and dried at 100 °C. The GO films were reduced in aqueous NaNO3 solution by modulated potential approaches in a three-electrode set-up. The structure, morphology and degree of reduction were analyzed by Infrared spectroscopy (FTIR), Raman spectroscopy, X-ray diffraction (XRD), scanning electron microscopy (SE) and electrochemical tools. RESULTS AND DISCUSSION ErGO thin films with controlled residual content of functional groups can be obtained by electrochemical reduction. The analysis of cyclic voltammograms showed that reduction potential and the electroreduction current plateau obtained by chronoamperometric mode are influenced by the initial content of OFGs in GO films. The FTIR spectroscopy results confirmed the partial removal of OFGs by the decrease in peak intensity of corresponding groups. The Raman measurements indicated the defect degree in ErGO films is dependent on the electroreduction approach. As a measure of electroreduction degree, the ErGO films were used as substrate for nucleation of ZnO nanocrystals, since these employ the OFGs as nucleation sites. It was observed that ZnO nucleation and growth decreased on ErGO (figure 1b and 1d) with respect to corresponding GO substrate (figure 1a and 1c). This study shows that electrochemical reduction technique has great potential for providing graphene materials with versatile electrochemistry and applicability in various fields. ACKNOWLEDGMENTS. Financial support from the Romanian National Authority for Scientific Research and Innovation, CNCS -- UEFISCDI (project number PN-II-RU-TE-2014-4-0806) is gratefully acknowledged. REFERENCES 1. H.L. Guo et al., ACS Nano 3, 2653 (2009). 2. A. Pruna et al, J. Nanoparticle Res. 15, 1605 (2013).

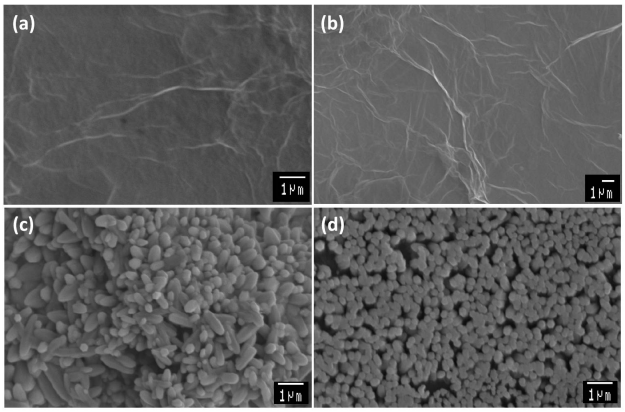


Annic image.jpg

# CVD-growth of MWCNT arrays on Me-Ct-N-(O) thin films

**Thursday, 10th November - 13:30 - Poster Session - Gallery - Poster presentation - Abstract ID: 73**

***Dr. Sergey Dubkov*** [1], ***Prof. Dmitry Gromov*** [1], ***Prof. Sergey Gavrilov*** [1], ***Prof. Sergey Bulyarskii*** [2], ***Dr. Alexey Trifonov*** [3], ***Mr. Eugene Kitsyuk*** [4], ***Dr. Alexander Pavlov*** [2], ***Dr. Paweł Mierczyński*** [5], ***Prof. Tomasz Maniecki*** [5]

***1.*** *National Research University of Electronic Technology,* ***2.*** *Institute of Nanotechnology of Microelectronics of the RAS,* ***3.*** *Scientific Research Institute of Physical Problems named after F.V.Lukin,* ***4.*** *Scientific-Manufacturing Complex "Technological Center",* ***5.*** *Lodz University of Technology*

Carbon nanotubes (CNT) have a number of attractive chemical, physical, electrical, and mechanical properties [1], making their use promising in various devices, such as field emission devices, optical waveguides, solar cells , sensors, fuel cells, supercapacitors, lithium-ion batteries, and others.[2]. CNTs are produced in electric arc discharge between carbon electrodes or laser ablation of graphite [1,2]. However, with regard to the integrated technologies for different devices a catalytic chemical vapor deposition is the preferred method [1,2], since the CNT growth takes place on the surface of the solid phase in this case. Known catalysts for this process are the metals Fe, Co, Ni, Pd, their alloys, and the alloys of these metals with other transition metals, in which, however, the content of the catalyst is always predominant [3]. In this work we have studied the possibility of using thin film alloys Me-Ct as a catalyst for the growth of the CNT, where Me is a transition metal of IV-VII of the Periodic Table of the Elements, and Ct is catalytic metal for nanotube growth (Fe, Ni, Co, Pd), with the addition of a components, such as nitrogen and oxygen. It was revealed that the initial film Me-Ct-N- (O) is in an amorphous state. Heating to synthesis temperature leads to full crystallization of the film and appearance of pure solid catalyst particles on the surface. These particles are a source of CNTs. Wherein the content of Ct in the alloy is <40 at.% the attraction of using this alloy as CNT growth catalyst is the ability to control density and diameter of CNTs; good reproducibility and uniformity of the CNT growth process on the area of the substrate surface, in spite of the serious variation in film thickness of the catalyst. [1] M. S. Dresselhaus et al. Springer-Verlag. (2001). 449 p. [2] Z. Ren et al. Springer-Verlag. (2013). 299 p. [3] E.V. Lobiak et al. J.Alloys &Comp. (2015) 621.

# Electrochemical properties of LiNi0.85Co0.10Al0.05O2 synthesized using AAO(Anodic Aluminum Oxide) template

**Thursday, 10th November - 13:30 - Poster Session - Gallery - Poster presentation - Abstract ID: 74**

***Prof. JongTAe SON [1], Ms. mira shin [1], Mr. ji-woong shin [1], Prof. Taewhan Hong [1], Mr. Do-man Jeon [2]***

***1.*** *Korea National University of Transportation,* ***2.*** *Research groups, EG CORP.*

Recently, among various cathode materials for lithium batteries, LiCoO2 has been still use on the market due to electrochemical stability. However, LiCoO2 cathode materials have low thermal stability, high cost, low capacity. [1-2] Co and Al co-synthesized materials, Li(Ni,Co,Al)O2, are one of the most applicable materials due to the low cost, thermal stability than LiCoO2. Thus, the battery properties of lithium ion cell with LiNi0.85Co0.10Al0.05O2 cathode are better than LiCoO2. But, LiNi0.85Co0.10Al0.05O2 still show that capacity fading. [3] Anodizing method is an effective means of improving electrochemical performance. To improve the electrochemical properties of cathode material LiNi0.85Co0.10Al0.05O2 for a lithium-ion battery, LiNi0.85Co0.10Al0.05O2 cathode powders were prepared by sol-gel method in AAO template followed by heat treatment. The effects of nano-rod samples were more deeply explored through atomic force microscope (AFM), X-ray photoelectron spectroscopy (XPS) and differential capacity vs. voltage (dQ/dV) plots. It is found that nano-rod shaped LiNi0.85Co0.10Al0.05O2 (NCA) cathode shows different characteristics in structural change and cycling voltage plateau that was related to changing of binding energy and surface area. References [1] T. J. Park, J. B. Lim, and J. T. Son, Bull. Korean Chem. Soc. 2014, Vol. 35, No. 2 357 [2] Z. R. Chang, X.Z. Yuan and H. Wang, Powder Technology 207 (2011) 396--400 [3] H. Kondo, T. Kamiyama and Y. Ukyo, J. Power Sources 174 (2007) 1131--1136 Acknowledgement This study was supported by the granted financial resource from the Ministry of Trade program of the Industry & Energy, Republic of Korea (G02N03620000901) and the Global Excellent Technology Innovation of the Korea Institute of Energy Technology Evaluation and Planning (KETEP)

# Fenton-Like oxidation of Orange II solution using heterogeneous catalysis with bionanocatalyst from fique fiber and iron nanoparticles

**Thursday, 10th November - 13:30 - Poster Session - Gallery - Poster presentation - Abstract ID: 97**

***Mrs. Karen Bastidas*** [1], ***Prof. Cesar Sierra*** [1], ***Prof. Hugo Ricardo Ramirez*** [1]

***1.*** *National University of Colombia (Bogota)*

The availability of natural water resources has declined over time, becoming one of the biggest problems today. Advanced oxidation processes with iron nanoparticles applied to azo dyes in aqueous phase is one of the most modern innovative technologies. This work, shows how the combination of cellulosic fibers with iron oxide nanoparticles could provide exceptional biodegradable composite materials for the treatment of organic dyes in wastewater. Likewise, allows an easy separation catalyst-treated water, turning the biocatalyst in a highly recyclable and reusable material. A catalytic wet hydrogen peroxide process was applied for the degradation of an azo dye Orange II (OII). Using as catalyst a bionanocomposite from fique fiber impregnated with iron nanoparticles; nanoparticles were prepared by borohydride reduction of an aqueous iron salt in presence of a support material. To track the impregnation process on the fiber, samples from the precursor solution were taken at different times and its iron concentration was determined by atomic absorption spectrophotometry (AAS). Complementary characterization of the catalyst was performed by SEM, XRD, FTIR, thermal analysis, XPS, XRF and BET surface area. Tests were carried out in a slurry batch reactor, following a long time the OII degradation by UV-VIS spectroscopy. The variables studied for the catalytic activity were pH, percentage of iron, initial concentration of H2O2 and OII in the system. Subsequent to the synthesis process, the catalyst reported 10.9 wt.%,14.9 wt.% and 13.21.5 wt.% of iron as active phase. Catalytic results under pH = 2.5, 10.9 wt. % of iron, 5.5x10-3M and 1.1x10-4M as initial concentrations of H2O2 and OII, respectively, show that this bionanocomposite presents good properties for the degradation of Orange II solutions, allowing to reach after 4h of oxidation 93.23% of dye degradation, using only 800 mg of catalyst per 250 mL of solution. Iron released into the final solution is neglectable. These results suggest that the reduction reaction by iron nanoparticles is potentially a viable in situ treatment of wastewater contaminated with hazardous organic compounds including azo dyes.


Img 7035.jpg

# Effects of Ag/TiO2 nanoparticles developed for leather surface finishing on human keratinocytes cells

**Thursday, 10th November - 13:30 - Poster Session - Gallery - Poster presentation - Abstract ID: 98**

***Dr. Daniela Stan*** [1], ***Ms. Cristina Ana Constantinescu*** [1], ***Dr. Carmen Gaidau*** [2], ***Dr. Madalina Ignat*** [2], ***Dr. Aurora Petica*** [2], ***Dr. Manuela Calin*** [1]

***1.*** *Institute of Cellular Biology and Pathology "Nicolae Simionescu" of Romanian Academy, Bucharest, Romania,* ***2.*** *R&D National Institute for Textiles and Leather (INCDTP)–Leather and Footwear Research Institute (ICPI) Division, Bucharest, Romania*

Introduction. The finishing of leather surface with nanomaterials (NMs) having advanced properties (e.g. antimicrobial, self-cleaning and flame retardant) are priorities for the European leather industry. The impact of NMs on human health is very important for their large scale application in footwear industry. The aim of our study was the investigation of the effects of Ag/TiO2 nanoparticles (NPs) on human skin cells. Materials and Methods. Three formulations of Ag/TiO2 nanoparticles (NPs) were prepared using an electrochemical method for deposition of 0.53% (Ag/TiO2-NP1), 1.14% (Ag/TiO2-NP2) and 1.62% (Ag/N-TiO2-NP3), respectively of Ag on nanosized TiO2 and N-TiO2. The Ag/TiO2 and Ag/N-TiO2 NPs were characterized for i) particle size and Zeta potential (by DLS); ii) powder morphology and elements identification on surface (by SEM, EDX), iii) photocatalytic activity using the method of dye degradation under UV/Vis light. The cytotoxicity studies were performed by MTT assay after exposing human keratinocytes (HaCaT cells) to various concentrations of different Ag/TiO2 NPs (0.01-1mg/ml) for 48 hours. The organization of actin cytoskeleton was visualized by fluorescence microscopy after incubation of cells with Ag/TiO2 NPs, by staining the cells with fluorescently-labeled Phalloidin. The intracellular reactive oxygen species (ROS) levels were quantified using the fluorogenic dye 2',7'dichlorofluorescein diacetate, using a spectrophotometer. Results. 1) the size and Zeta potential for all three formulations was below 90 nm and above -40 mV, respectively; 2) low cytotoxic effect at concentration up to 0.3 mg/ml; 3) IC50 values (concentration of NPs where 50 % of cells are viable) are 0.75 mg/ml, 0.35 mg/ml and 0.81 mg/ml for NP1, NP2 and NP3, respectively; 4) the actin cytoskeleton in HaCaT cells is only slightly modified by exposure to Ag/TiO2 NPs at concentrations up to 0.5 mg/ml, whereas the higher concentrations of Ag/TiO2 NPs (0.5 and 1 mg/ml) induce cell retraction; 5) an increase in intracellular ROS is seen only for cells incubated with 1 mg/ml Ag/TiO2 NPs. Conclusions. The developed Ag/TiO2 NPs have a potential toxic effect at the skin level only at very high concentrations (above 0.5 mg/ml). Acknowledgement. The works were funded by UEFISCDI, project number PNIII_15/2015 under the frame of ERA-NET SIINN program.

# Controlled synthesis of Ag-Au-S ternary nanostructured semiconductors

**Thursday, 10th November - 13:30 - Poster Session - Gallery - Poster presentation - Abstract ID: 102**

***Mrs. Mariona Dalmases*** [1], ***Mr. Albert Vidal*** [1], ***Dr. Albert Figuerola*** [1], ***Mr. Pau Torruella*** [1], ***Dr. Sonia Estrade*** [1]

**1.** *University of Barcelona*

Ternary semiconductors have been attracting great attention recently owing to their interesting properties which make them suitable for many applications such as optoelectronics, photovoltaics, thermoelectrics and photocatalysis. The nanostructuration of these materials could enhance their properties and allows the fine tunning of the latter by the control of the size and shape of the nanomaterial. In this poster, two novel nanostructured Ag-Au-S ternary semiconductors are presented; synthesised by diffusion of gold (I) cations into pre-synthesised Ag2S nanoparticles at room temperature. There are two known crystallographic phases of the Ag-Au-S system with different stoichiometry: Ag3AuS2 which presents a cubic structure and AgAuS, with a monoclinic structure. The method allows the synthesis of both phases separately and it is also adequate for the synthesis of the analogue systems with Se and Te.

# Peroxidase-like Activity of Apoferritin Paired Copper(II) Nanoparticles and Its Biomemory Applications

**Thursday, 10th November - 13:30 - Poster Session - Gallery - Poster presentation - Abstract ID: 157**

***Mrs. Şükriye Nihan KARUK ELMAS*** [1], ***Dr. Remziye Guzel*** [2], ***Prof. Rıdvan Say*** [3], ***Prof. Arzu Ersoz*** [3]

***1.*** *KARAMANOĞLU MEHMETBEY UNIVERSITY,* ***2.*** *DICLE UNIVERSITY,* ***3.*** *ANADOLU UNIVERSITY*

Bionanomaterials are increasingly attracted in recent years due to the unique behaviours in biosensors, bioassays, nanoelectronics, drug delivery system and biomedical imaging. Ferritin, a nature bionanomaterial, is an iron storage and detoxification globular protein, composed of 24 homologous polypeptide subunits of the heavy chain (H-ferritin) and light chain (L-ferritin). Bionanomaterials have been prepared using apoferritin biomolecules embedding of metal atoms into lattice of this protein. These bionanostructures have obtained using photosensitive amino acid-monomers linkage method (ANADOLUCA). In this study, the synthesis of nanoapoferritins has achieved in the presence of bis (2-2'-bipyridil) MATyr-MATyr-rutenyum (II) photosensitive monomers by microemulsion. Then, Cu(II) metal has organised into lattices of apoferritin nanostructures and these multi functional structures have characterised by transmission electron microscopy (TEM). Michaelis-Menten kinetics of bionanomaterials have improved using 3.3',5.5'-tetramethylbenzidine (TMB) which is the substrate of HRP. The effect of pH, temperature and subsrate concentrations on the activity of these bionanomaterials have analyzed. The memory function of the fabricated biodevice has validated using cyclic voltammetry (CV) and chronoamperometry (CA). Key word: Apoferritin, Biomemory, Bionanostructure, Peroxidase Activity

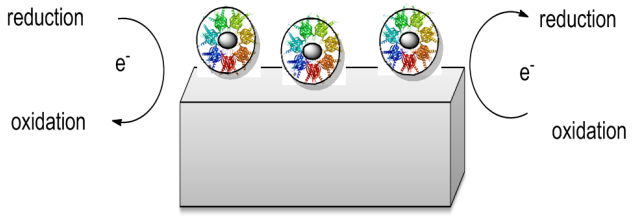


Poster.png

# FILTERING PIGMENTS FROM HONEY BY NANOFIBER MEMBRANE

**Thursday, 10th November - 13:30 - Poster Session - Gallery - Poster presentation - Abstract ID: 174**

***Mrs. farzaneh azizzadeh*** [1], ***Dr. Filiz Lokumcu*** [1]

***1.*** *Istanbul Technical University*

Honey is a natural food product which has various health benefits. It can be consumed either as is or added to other foods as a sweetener. In the latter case, the pigments in honey can cause some off-color problems in the products. For example, when honey is added to jam or jellies as a sweetener, the brown coloring caused by heat treatment during process affect consumer acceptance adversely. In honey carotenoids and anthocyanins are present as pigments, whereas carotenoids are the largest occurring one. Due to fact honey is very sensitive to heat and other process conditions, if the pigments are needed to remove then it must be done without heat or chemical treatments. It is hypothesized that pigments may be removed from honey by using nanofiber membrane. It is predicted that the hydrophilicity of the filter medium is a crucial factor for removing pigments from honey. Electrospun nanofibers as filter membrane appear to be suitable for membrane applications, due to the easiness of modifying the surface of the medium. For instance, the surface characteristics of nanofiber membranes, such as hydrophilicity, porous structure and sizes, can be adjusted according to the filtration needs by electrospinning parameters. In this study, the objectives were two-folds. First, polyacrylonitryle (PAN) nanofibers were obtained by electrospinning. Then, PAN nanofibers used as filter membrane for removing pigments from honey. PAN nanofibers were obtained from the PAN solution in dimethylformamide (DMF) at 10% by using electrospinning. The feed rate, the applied voltage and the distance to the collector plate were 3 ml/hour, 40 kV and 25 cm, respectively. The electrospinning was conducted for 30 min. Contact angle measurements of electrospun samples were conducted. The honey was filtrated through a laboratory set-up containing electrospun PAN nanofiber membrane at 1 bar. The physicochemical properties of filtrate such as viscosity, refractive index, pH, electrical conductivity, dielectric parameters were determined. Outcomes of this study may help to separate sensitive functional ingredients such as pigments, active ingredients without getting damaged from heat or chemical treatments. The electrospun nanofiber membranes seem to have a high potential utilization in food industry in the future.

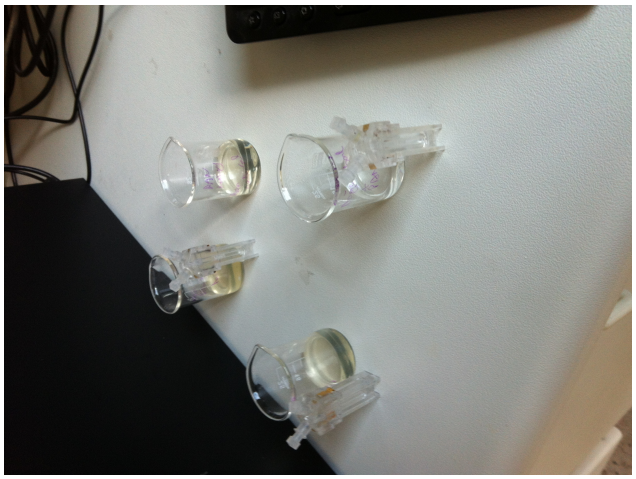

Img 5026.jpg

# Cantilever-enhanced photoacoustic spectroscopy in the research of natural and synthetic calcium phosphate

**Thursday, 10th November - 13:30 - Poster Session - Gallery - Poster presentation - Abstract ID: 175**

***Mrs. Agnese Brangule*** [1], ***Prof. Karlis Gross*** [2]

***1.*** *Riga Technical university, Riga Stradiņš university,* ***2.*** *Riga Technical university*

Introduction. The photoacoustic spectroscopy (PAS) has many applications in different fields of research and industry. PA spectroscopy is a form of spectroscopy, which uses both - light and sound and is based on the absorption of electromagnetic radiation by analyte molecules. In 1997, Rehman and Bonfield were the first to study the structure of carbonated apatite with the FTIR-PAS with the MTech PAS cell. They concluded that PAS provides a sensitive, nondestructive and fast means of analyzing synthesized hydroxyapatite and carbonated apatites. The aim of this study is to find advantages of PA spectroscopy with cantilever detector for the investigation of synthetic nanosized calcium apatite (in powder and on the pellet surface) and in archaeological human bone. Materials and Methods. In this study, we evaluated: -) synthesized nanosized calcium phosphate powders with variable A and B carbonate content and different degree of crystallinity; -) the surface of uniaxially pressed calcium phosphate pellets before and after contact with bacteria; -) archaeological human bones. PA spectra were collected using an FTIR PA cell (Gasera PA301) at 450---4000 cm-1, at a resolution of 4 cm-1, with an average of 20 scans. Results and Discussions. Spectra obtained by PA spectroscopy all show bands characteristic of carbonated calcium phosphates: v2CO3 in region 800---920 cm-1, v3CO3 in region 1400---1600 cm-1. Two processes were simultaneously followed on the pellet surface: identification of calcium phosphate bands and identification of bacteria from amide peaks. Human bones showed overlapping amide and carbonate bands in the region (900---1900 cm-1). Conclusions. PA spectroscopy can be further used for sensitive, non-destructive analysis of synthesized nanosized carbonated calcium phosphate in the form of powder and on the surface and for archaeological bone.

# Biocompatible and thermoresponsive polymer synthesis: A facile method for a controlled polymerization

**Thursday, 10th November - 13:30 - Poster Session - Gallery - Poster presentation - Abstract ID: 274**

***Dr. Teresa Alejo*** [1], ***Mr. Martín Prieto*** [1], ***Mr. Hugo García-Juan*** [1], ***Dr. Víctor Sebastián*** [1], ***Dr. Manuel Arruebo*** [1]

***1.*** *University of Zaragoza*

Introduction: Stimuli responsive copolymers derived from oligo (ethylene glycol) methacrylate are promising biocompatible materials that present thermoresponsive properties which make them suitable as injectable drug delivery systems. These polymers are soluble in water, and undergo a transition to water-insoluble materials over a certain temperature called lower critical solution temperature (LCST). This temperature can be tuned by changing the oligo (ethylene glycol) methyl ether methacrylate (OEGMA) to di (ethylene glycol) methyl ether methacrylate (MEO2MA) monomer ratios [1]. The development of efficient and facile strategies for the synthesis of well-defined polymer architectures is a significant challenge necessary to overcome. Most usual Cu-mediated radical polymerizations present some drawbacks like high sensitivity of the catalyst to oxygen and water, and the requirement of exhaustive polymer purification processes to remove traces of the potentially toxic metal. In the present work, P(MEO2MA-co-OEGMA500) copolymers were prepared through three different synthetic methods with high reproducibility and narrow molecular weight distributions. Methods: Thermoresponsive P(MEO2MA-co-OEGMA500) was obtained via a photochemical controlled ATRP-like polymerization and compared with the common methods of synthesis including atom transfer radical polymerization (ATRP) and atom transfer radical polymerization with activators generated by electron transfer (AGET-ATRP). The ATRP and AGET-ATRP methods use organic complexes derived from copper as catalysts. Conversely, the photopolymerization employs a photocatalyst activated upon UV light irradiation. The polymers obtained were characterized by NMR spectroscopy, cloud point measurement, FTIR, GPC and TGA. Results and Discussion: It was possible to obtain thermoresponsive P(MEO2MA-co-OEGMA500) by photopolymerization, ATRP and AGET-ATRP methods. The LCST of the copolymer was adjusted to the physiological temperature range by changing the OEGMA/MEO2MA monomers molar ratio to be used in biomedical applications. The results showed low-polydispersity and control over the molecular weight and polymer composition under the three methods of synthesis. However, the photocatalized reaction has several advantages compared to the others. By following this method it is possible to produce a reversible activation and deactivation of the polymerization upon UV light irradiation. Moreover, it is a user-friendly method with simple reaction conditions which allows the use of reduced amounts of catalyst. [1] J.F. Lutz, A. Hoth, Macromolecules 2006, 39, 893.

# Very efficient and rapid degradation of Congo red dye with $TiO_2$ based nano-photocatalysts

**Thursday, 10th November - 13:30 - Poster Session - Gallery - Poster presentation - Abstract ID: 290**

***Prof. Himanshu Narayan*** [1], ***Prof. Hailemicheal Alemu*** [1]
*1. National University of Lesotho*

Degradation of Congo red (CR) dye with $TiO_2$ based nano-photocatalyst (NPC) loaded with $Nd^{3+}$ and $Er^{3+}$ ions is reported. The chemical route of synthesis through co-precipitation/hydrolysis (CPH) was employed to produce NPCs with general composition $TiO_2[R_2O_3]_x$, {x = 0.1, 0.2; R ≡ Nd, Er} and particle size within 12 – 16 nm. Characterization of the NPC samples was done using powder x-ray diffraction (XRD), transmission electron microscopy (TEM), diffused reflectance spectroscopy (DRS), Raman spectroscopy and Fourier transform infra-red (FTIR) spectroscopy. Photocatalytic degradation under visible light was measured in terms of the percent degradation of CR in 180 min ($C'_{180}$), time taken to degrade to half of the initial CR concentration ($t_{1/2}$) and apparent rate constant ($k_{obs}$). For both doping types, values of $C'_{180}$ close to 100% were obtained with x = 0.2 NPCs, indicating complete removal of the dye. For the same NPCs, very high values of $k_{obs}$ were found; $2.91 \times 10^{-2}$ $min^{-1}$ and $2.36 \times 10^{-2}$ $min^{-1}$, for $Nd^{3+}$ and $Er^{3+}$ loaded NPCs, respectively, suggesting very rapid degradation. Other NPCs with x = 0.1, also showed reasonably good and fast degradation of CR. The observations may be attributed to the small particle size of the NPCs. Moreover, from the DRS results it is observed that the addition of $Nd^{3+}$ and $Er^{3+}$ ions apparently introduces intermediate energy levels within the band gap of $TiO_2$. Such new levels seem to support photocatalysis because they act as electron traps leading to effective suppression of the undesired $e^-/h^+$ recombination. To some meaningful extent they also facilitate the absorption of visible irradiations required in the process.

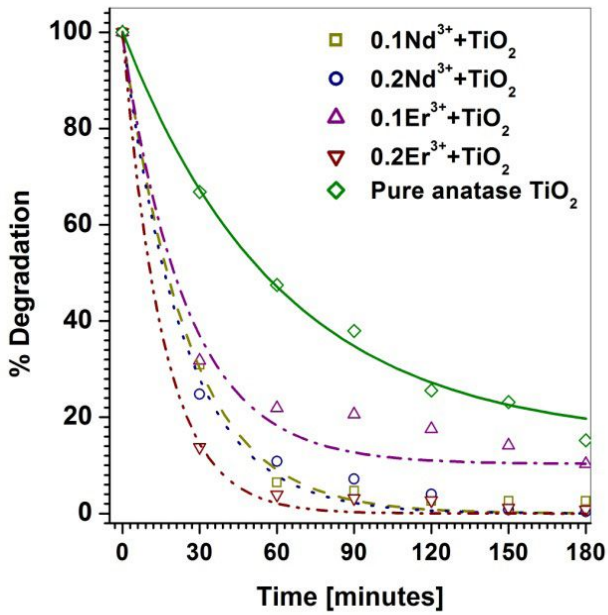


Degradation of congo red dye against time.jpg

# NMR investigation of domain wall dynamics and hyperfine field anisotropy in magnets by the magnetic video-pulse excitation method

**Thursday, 10th November - 13:30 - Poster Session - Gallery - Poster presentation - Abstract ID: 329**

***Prof. Tsisana Gavasheli*** [1], ***Dr. Grigor Mamniashvili*** [1], ***Dr. Tatiana Gegechkori*** [1]

***1.*** *ivane Javakhishvili Tbilisi State University*

Two-pulse nuclear spin echoes were studied experimentally depending on the time of application and pulse amplitudes of the DC magnetic field-magnetic video-pulses (MVP) as well as on the value of the external magnetic field. The measurements were performed with nanopowders and polycrystals of metallic cobalt, in lithium ferrite and half metal Co2MnSi. Two types of dependences of these signals on time of application of MVP with respect to moments of application of exciting radio-frequency pulses were established, which were determined by the degree of anisotropy of local hyperfine fields. The mechanisms of influence of the pinning and mobility of domain walls on the revealed specific features of the signals under study are also discussed. It is shown that temporal spectra of the MVP effect on two-pulse echoes in multidomain magnets are determined by the parameters of domain walls and can be used for qualitative and quantitative characterization of the domain wall dynamics of magnets.

# Straightforward etching of ZnO nanostructures for optical sensor application

**Thursday, 10th November - 13:30 - Poster Session - Gallery - Poster presentation - Abstract ID: 340**

***Dr. Dong Jin Lee*** [1]***, Dr. Sung Ryong Ryu*** [2]***, Prof. Yong Deuk Woo*** [3]***, Prof. Tae Won Kang*** [1]***, Prof. Deuk Young Kim*** [4]

***1.*** *Quantum-functional Semiconductor Research Center, Dongguk University,* ***2.*** *KDePRI, Korea Institute of Radiological & Medical Sciences,* ***3.*** *Department of Mechanical and Automotive Engineering, Woosuk University,* ***4.*** *Quantum-functional Semiconductor Research Center and Department of Semiconductor Science, Dongguk University*

Nano etching could be a feasible top down approach to make the rough surface and sharp tips. Among the several etching methods, there are some disadvantages and limitations like, making masks in the case of wet and dry etching, using toxic or corrosive acids in chemical etching, usage of sophisticated and expensive tools like plasma, reactive ion etc., But the nano-etching mechanism proposed here is facile, using non-toxic and non-corrosive photoresist (PR) through a thermo-chemical reaction. The PR consists of carboxylic (COOH) and cyclopentanone (C5H8O) can react with zinc and oxygen atoms respectively on the surface of the ZnO nanostructure. The thermo-chemical reaction is controllable by varying the PR concentration and the reaction time. The optical sensor were fabricated by using the etched ZnO nanorods and the bare ZnO nanorods. Compared with bare ZnO nanorod, the sensing properties of the etched ZnO nanorod sensor were greatly improved.

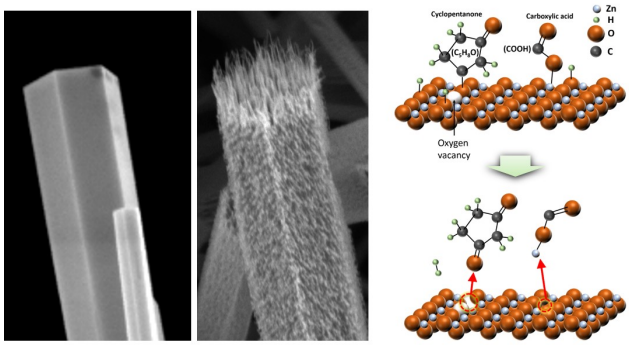


Abstract-figure.jpg

# Mechanical behavior of precipitation strengthened nanostructured bulk materials produced by inhomogeneous severe plastic deformation

**Thursday, 10th November - 13:30 - Poster Session - Gallery - Poster presentation - Abstract ID: 375**

***Prof. Janusz Majta*** [1], ***Prof. Michal Krzyzanowski*** [2], ***Mr. Marcin Kwiecien*** [1], ***Mr. Szymon Bajda*** [1]

***1.*** *AGH University of Science and Technology,* ***2.*** *AGH University of Science and Technology, Birmingham City University*

A product's service life of various power industry components can be extended with application of nanostructured metals and alloys. Implementation of nanomaterials, in particular nanostructured steel, encourages replacement of existing products with new nano-products that are more environmentally friendly throughout their lifecycle. For example, the thermal stability of the modified nanostructured steels will ensure the long-term creep resistance of these popular structural materials by avoiding the growth of coarse grains and precipitates at the expense of fine precipitates. Severe plastic deformation (SPD) offers a new processing alternative to bottom-up conventional nanomaterial's production methods, in spite the currently existing difficulties towards adaptation of the SPD processes to practical use. Interpretation of the mechanical behavior of the nanostructured materials produced by SPD, in which several strengthening mechanisms operate simultaneously, presents a significant challenge. However, the potential benefits are clear. For example, precipitation strengthening can be used to obtain an improved creep resistance, which remains constant even after long-term exposure to high temperature. In this contribution, general findings and some new evidence from different factors affecting mechanical behavior of these materials will be discussed. In particular, we will discuss in more details the role of second phase particles in grain refinement and multilayer nanocrystalline structure formation, predominantly the role of Nb(C,N) in these processes. The structures are produced using top-down approach in the novel metal forming processes. We will demonstrate the new possibilities arising from application of the controlled introduction of inhomogeneous deformation during complex processing, such as recently developed Accumulative Angular Drawing (AAD) and Compression Press Bonding (CPB). These processes are strongly affected by nonlinear strain path changes. It will also be shown that the expected effect of decreasing ductility in nano structured materials, attributed to limited dislocation activity at these length scales, can be effectively minimized by introduction of finely dispersed particles, which effectively increased the work hardening rate according to well-known Considere Criterion for plastic instability. The discussed above phenomena are supported by computer modeling results obtained using the multi-scale numerical approach, and some examples will be presented.

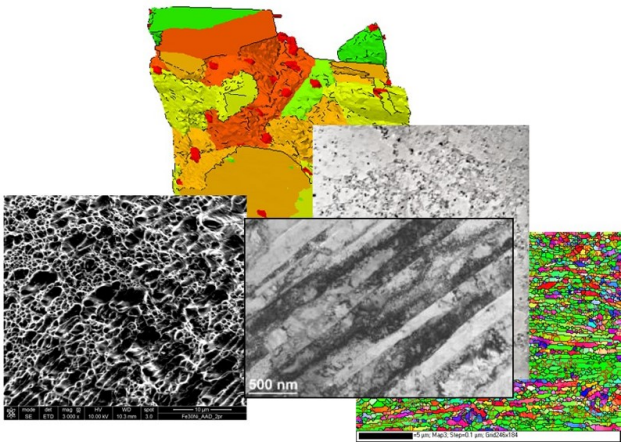


Microstructure evolution in spd - simulation and microscopic analysis.jpg

# Study on the Growth of Carbon Microspheres via Hydrothermal Process of Nano-Crystalline Cellulose (NCC)

**Thursday, 10th November - 13:30 - Poster Session - Gallery - Poster presentation - Abstract ID: 406**

***Ms. Lim Hui Hui*** [1], ***Dr. Bahman Amini Horri*** [2], ***Dr. Babak Salamati*** [1]

***1.*** *Monash University Malaysia (MUM),* ***2.*** *University of Surrey*

Development of carbon microspheres has gained some attentions as it widely used as a material for different applications such as electrode in lithium batteries, supercapacitors, pore forming agent in electrode of Solid Oxide Fuel Cell (SOFC), catalyst support and many more. In this study, the growth of carbon microspheres via hydrothermal process of Nano-Crystalline Cellulose (NCC) which is a green material has been elaborated. Hydrothermal reaction was carried out by using 2.5 wt % of NCC solution in a stainless steel autoclave at a constant temperature of 350 °C by varying reaction durations of 2 h to 20 h. The washed and dried sample were then characterized using various analytical instruments such as Field Emission Scanning Electron Microscopy (FE SEM), Energy-dispersive X-ray Spectroscopy (EDX), Thermogravimetric Analysis (TGA) and Fourier Transform Infrared Spectroscopy (FT-IR). Carbon microspheres synthesized were to be in the size range between 2 µm to 6 µm diameter with high carbon content of > 80 wt% carbon element.

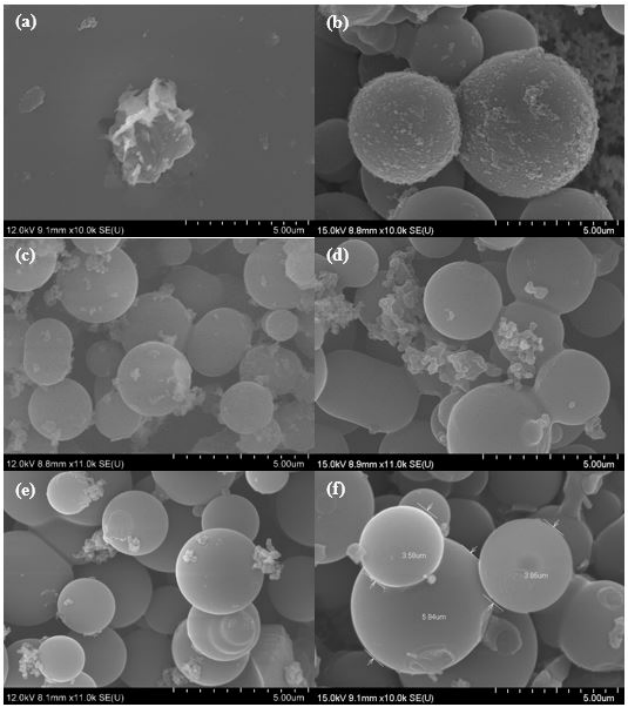


Growth of carbon microspheres.jpg

# Core-shell nanostructured metal oxides for high performance supercapacitors

**Thursday, 10th November - 13:30 - Poster Session - Gallery - Poster presentation - Abstract ID: 407**

***Prof. Hao Gong*** [1]

***1.*** *Department of Materials Science and Engineering, National University of Singapore*

Some nanomaterials with large surface areas can lead to high charge storage in a supercapacitor, and they have attracted great attention. Different materials have been proposed and used for supercapacitors. In this presentation, high performance Ni based oxides and hydroxides supercapacitors will be showing to have very high specific capacitance and energy density. Typically, core-shell structures show not only high specific capacitance but also high total energy per device. Electrochemical performance, microstructure, morphology and BET surface area are found strongly related to Ni, Co and Cu concentration. Due to the high specific capacitance and the much lower price of Ni and Co than Ru, a Ni oxide/hydroxide based supercapacitor has its unique advantage and may be a very promising candidate for the next generation of commercial high capacitance supercapacitors. Full supercpacitor cell prototypes are made, and high energy density is reached. Bulb lighting and fan turning are demonstrated even for a small size supercapacitor device.

# Avidin-conjugated calcium phosphate nanoparticles as modular system for the attachment of biotinylated molecules

**Thursday, 10th November - 13:30 - Poster Session - Gallery - Poster presentation - Abstract ID: 423**

***Ms. Selina Beatrice van der Meer*** [1], ***Prof. Matthias Epple*** [1]

***1.*** *Inorganic Chemistry and Center for Nanointegration Duisburg-Essen (CeNIDE), Collaborative Research Centre 1093 "Supramolecular Chemistry on Proteins", University of Duisburg-Essen, Universitaetsstr. 5-7, 45117 Essen, Germany*

Introduction: Calcium phosphate nanoparticles are biocompatible, biodegradable and bioactive due to their similarity to nanocrystalline hydroxyapatite in hard tissue of the human organism.[1] Avidin is a tetrameric protein that forms a very strong complex with the biomolecule biotin. The avidin-biotin-complex is the strongest known non-covalent bond between a protein and a ligand.[2] In this work, avidin-conjugated calcium phosphate nanoparticles were used for the non-covalent attachment of biotinylated compounds via the avidin-biotin-complex formation. The versatility of the complex formation onto the surface of the nanoparticles was demonstrated with various biotinylated molecules, including fluorescent dyes and antibodies. Methods: Calcium phosphate nanoparticles were first coated with a thin layer of silica and then covalently functionalized with 3-mercaptopropyltrimethoxysilane. This led to a sulfhydryl-terminated nanoparticle.[3] Avidin was then activated with the cross-linker sulfo-SMCC at amino groups and subsequently conjugated to the nanoparticle by the sulfhydryl groups. This resulted in an avidin-terminated nanoparticles. The freshly prepared avidin-conjugated calcium phosphate nanoparticle dispersion was combined with the biotinylated compounds and incubated overnight. After each reaction step the dispersion was purified by centrifugation and the pellet was dispersed by ultrasonication in ultrapure water. (Figure 1) Results: Avidin can be covalently attached to calcium phosphate nanoparticle. The hydrodynamic diameter of this nanoparticles was about 200 nm (DLS). The zeta potential was +21 mV. A spherical morphology of the nanoparticles was found in SEM. After the attachment of the biotinylated molecules, an increased diameter was observed by DLS and SEM. The capacity of biotin binding sites for the conjugated avidin was assessed by a fluorescence quenching assay.[4] Each conjugated avidin molecule on average bound 2.6 biotin molecules. A variety of biotinylated molecules can be loaded on the avidin-conjugated calcium phosphate nanoparticle. Furthermore, different biotinylated molecules can be coupled to the same nanoparticle. Fluorescently labelled avidin-conjugated calcium phosphate nanoparticles were detected intracellularly by CLSM (HeLa cells). The co-localization of fluorescent avidin and fluorescent biotin indicated the stability of the complex during the in vitro studies. The dissolved complex alone (i.e. without nanoparticles) is not taken up by HeLa cells. References: [1]M.Epple,K.Ganesan,R.Heumann,J.Klesing,A.Kovtun,S.Neumann,V.Sokolova, J.Mater.Chem.2010,20,18--23. [2]N.M.Green,Adv.Prot.Chem. 1975,29,85--133. [3]D.Kozlova,S.Chernousova,T.Knuschke,J.Buer, A.M.Westendorf, M.Epple, J.Mater.Chem. 2012,22,396--404. [4]G.Kada,H.Falk,H.J.Gruber,BBA 1999,1427,33--43.

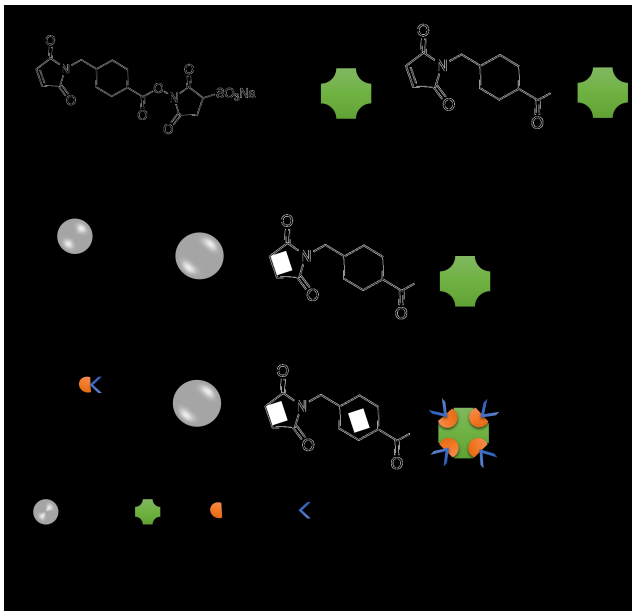

Figure 1 synthesis of avidin-conjugated calcium phosphate nanoparticle including the attachment of biotinylated compounds.jpg

# Influence of Exposure with Xe Radiation on Heterojunction Solar Cell a-SiC/c-Si Studied by Impedance Spectroscopy

**Thursday, 10th November - 13:30 - Poster Session - Gallery - Poster presentation - Abstract ID: 428**

***Dr. Juraj Packa*** [1], ***Dr. Milan Perný*** [1], ***Prof. Vladimír Šály*** [1], ***Dr. Miroslav Mikolasek*** [1], ***Dr. Michal Váry*** [1], ***Dr. Jozef Huran*** [2], ***Dr. Ladislav Hrubčín*** [2], ***Dr. Vladimir Skuratov*** [3], ***Dr. Juraj Arbet*** [2]

***1.*** *Slovak University of Technology,* ***2.*** *Slovak Academy of Sciences,* ***3.*** *Joint Institute for Nuclear Research*

The efficiency of heterostructures a-SiC/c-Si may be the same or even better in comparison with conventional silicon structures when suitable adjustment of technological parameters and adding other suitable layers such as anti-reflective, passivation layers and anti-recombination contacts is done. Recently, the record efficiency of 25.6 % [1] was achieved on similar heterojunction structure, which makes this technology the most efficient among the silicon based solar cells. The main advantages of heterojunction formed amorphous SiC thin film and crystalline silicon compared to standard crystalline solar cell lie in high build-in voltage and thus a high open-circuit voltage [2]. In our previous papers assessment of the impact of neutrons and Xe ions induced damage of a-SiC/c-Si heterostructures without ITO film was done. ITO offers high transmittance and high conductance and simultaneously acts as a passivating and antireflection coating. A deterioration of properties of heterostructures (a-SiC/c-Si) due to irradiation is examined in our paper using impedance spectroscopy method. Irradiation of structures with Xe ions to total fluency (5x1011 cm-2) was performed at room temperature. An example of the results -- deformation of impedance spectra due to the irradiation of sample coated with ITO is shown in Fig. 1. Xe ions induced damage is reflected in changes of AC equivalent circuit elements. AC equivalent circuit was proposed and verified using numerical simulations. Impedance spectra were also measured at different DC bias voltages due to a more detailed understanding correlation between ions induced damage and transport phenomenon in the heterostructure. Acknowledgement This work was supported by the Slovak Research and Development Agency under the contract No. APVV-0443-12 and by the Scientific Grant Agency of the Ministry of Education of the Slovak Republic and of the Slovak Academy of Sciences Project VEGA 1/0651/16. References [1] Masuko K, et al: Achievement of more than 25% conversion efficiency with crystalline silicon heterojunction solar cell. Photovoltaics, IEEE Journal, Vol. 6 20141433-5. [2] S. Janz, S. Reber, W. Glunz, Proceedings of the 21st EUPVSEC, 660-663 (2006).

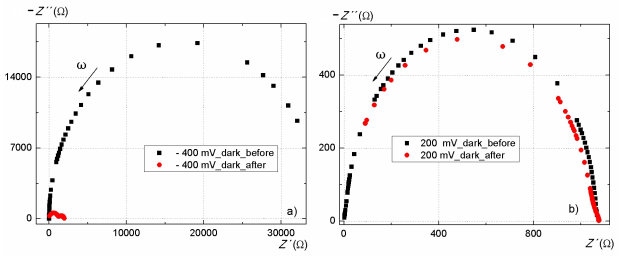


Measured symbol and the fitted solid line impedance spectra before and after irradiation at room temperature.jpg

# Self-Assembled 3D Flowerlike Bi2O3 Microspheres and Its Visible Light Driven Photocatalytic Activity

**Thursday, 10th November - 13:30 - Poster Session - Gallery - Poster presentation - Abstract ID: 447**

***Mrs. Arini Nuran Zulkifili*** [1]***, Prof. Akira Fujiki*** [1]

***1.*** *Shibaura Institute Of Technology*

A three-dimensional (3D) flowerlike Bi2O3 photocatalyst was synthesized by a simple template-free homogeneous precipitation method at 60□ for 24 hours. The purpose of this study is to explore for a low cost and simple method in synthesizing the self-assembled 3D structural in order to enhance the photocatalytic performance under visible light irradiation (λ>420nm). In this study, the morphology, structure and photoabsorption of 3D flowerlike Bi2O3 were characterized, and the effects of the photocatalytic performance were analyzed. The results indicated that the size of the 3D flowerlike hierarchical microspheres was about 2mm to 5mm and composed of several 2D nanosheets. The formation of the hierarchical microspheres has been proposed as the Ostwald ripening process which aid the self-assembled process. The as-obtained samples were then calcined under a different temperature (200□, 300□, 400□, 500□ and 600□) to study the effect of calcination towards the structure and how it affects the photocatalytic performance. The photocatalytic performance was then evaluated by the decolorization of methylene blue (MB) dye under visible-light irradiation. The 3D flowerlike Bi2O3 structure exhibits a higher catalytic activity than the commercial Bi2O3 which is about 5 to 7 times higher.

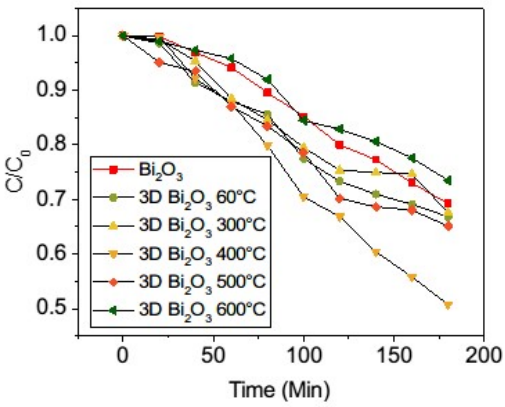


Mb degradation.jpg

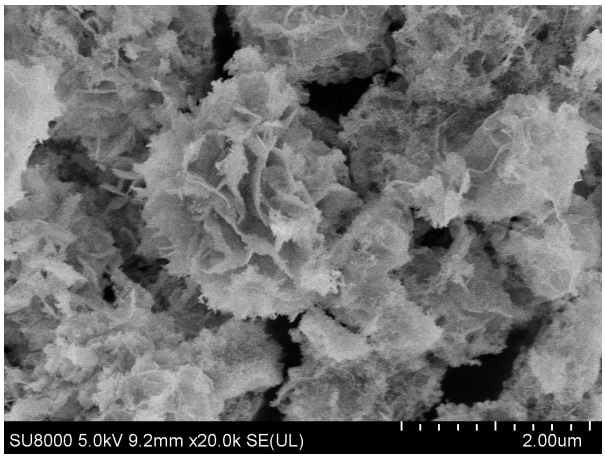


9. 400 20k.jpg

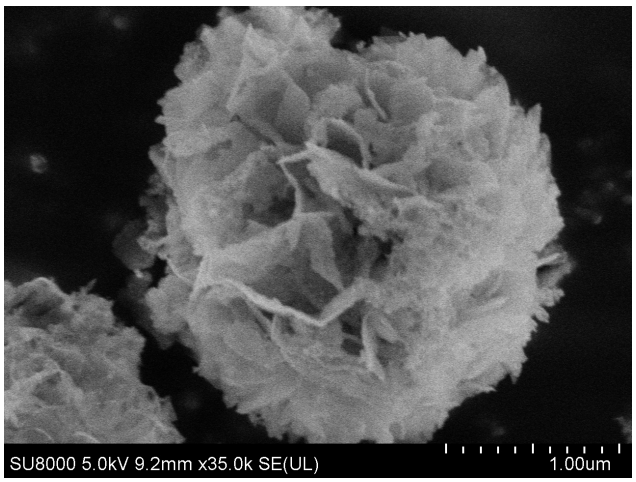


9. 400 35k3.jpg

# Synthesis and characterization of surface coated fluorescent carbon dot for visible-responsive photocatalytic effect

**Thursday, 10th November - 13:30 - Poster Session - Gallery - Poster presentation - Abstract ID: 449**

***Mr. Young Kwang Kim*** [1], ***Mr. Kim Sung Han*** [1], ***Prof. Sung Young Park*** [1]

***1.*** *Korea National University of Transportation*

The field of photo-electrochemical solar energy conversion significantly overlaps with the area of environmental photocatalysis, which requires not only self-cleaning surfaces, but also antifouling ones. Fouling is a phenomenon that occurs when aquatic microorganisms bind to a surface and form a conditioning layer providing an accessible platform for other aquatic species, such as diatoms and algae, to attach, proliferate, and finally degrade it. Titanium dioxide (TiO2) was found to be the most promising candidate for large scale industrial applications. A photocatalytic surface protected from contact with atmospheric biofoulants can possibly overcome the limitations of all currently existing photocatalytic systems Here, new design for surface protection of TiO2 photocatalysts by coating with fluorescence carbon nanoparticles (NPs) were prepared as a material to absorb photons and promotes the decomposition of organic pollutants on various substrates. We fabricated a synthesis of carbonized fluorescence particles by the acidic dehydration of catechol-q-poly (dimethyl aminoethyl methacrylate) (CA-FNPs) that improve the photocatalytic activity of TiO2 under visible light irradiation. We prepared the fluorescent agent using acid treatment (H2SO4) and the presence of catechol group allows FNPs to be bonded to the TiO2 surfaces in a facile way which is using catechol chemistry pH 8.5 (CA-FNPs/TiO2). The carbonized fluorescence NPs (CA-FNPs) exhibit broad UV-vis absorption characteristics, showing identical lattice d-spacings in the TEM images, while the XPS studies clearly indicated structural composites. The adhesive surface coatability of the FNPs was confirmed by the contact angle, SEM, and EDX measurements. The coordination between carbonized CA-FNPs and TiO2 was confirmed by the time-dependent studies of methylene blue degradation under ultraviolet (UV) and visible light irradiation. Moreover, HeLa cell detachments from the CA-FNPs/TiO2-coated surface verify its antifouling properties in the presence of visible light. This approach enhances the utilization of visible light in photocatalytic activity and suggests a new fluorescence coating platform using antifouling properties of the nanocomposites in visible light-mediated photocatalysis can overcome the existing limitations of the currently used materials.

# Deposition of silicon carbide thin films with RF and DC magnetron sputtering

**Thursday, 10th November - 13:30 - Poster Session - Gallery - Poster presentation - Abstract ID: 483**

***Mr. Mohand Arezki OUADFEL*** [1], ***Dr. Aissa Keffous*** [1], ***Prof. Mohamed Kechouane*** [2], ***Dr. Noureddine Gabouze*** [1], ***Mr. Hamid Menari*** [1], ***Dr. Maha Ayat*** [3]

***1.*** *Centre de Recherche en Technologie des Semi-conducteurs pour l'Energétique (CRTSE), Division Couches Mines Surfaces et Interfaces (CMSI).,* ***2.*** *Faculté de Physique, Université Houari Boumediene (USTHB), Bab ezzoaur, Alger.,* ***3.*** *Centre de Recherche en Technologie des Semi-conducteurs pour l'Energétique (CRTSE), Division Couches Mines Surfaces et Interfaces (CMSI)*

Silicon carbide thin films have been deposited by RF magnetron sputtering method in order to observe the effect of the argon flow rate on the properties of the obtained layers. We used à polycrystalline 6H-SiC (99.99 purity) as target, and good cleaned pSi(111) and microscopic glass slides as substrates. The deposition occurred in high vacuum chamber, firstly pumped at 10-5 mbar, with a turbo-molecular pump. Pressure during deposition has been maintained at 2*10-3 mbar. Characterization of the samples has been made by FTIR to observe the different bounds present in the films, and UV-Vis spectrophotometry in order to observe the optical response and measure the thicknesses of the films. As primary observation, we found that all the films obtained by RF sputtering method show a strong presence of oxides, so we decided to elaborate other samples on different substrates by DC magnetron sputtering to compare.

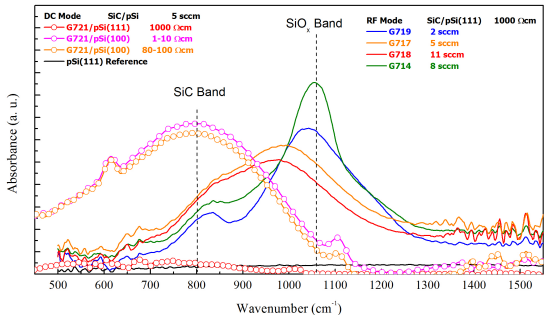


Figure 01 .jpg

| | Ar flow (sccm) | Deposition duration (min) | Distance (Sub. /Targ.) (cm) | Power (w) | DC / RF |
|---|---|---|---|---|---|
| **G718** | 11 | 90 | 08 | 130 | RF |
| **G714** | 8 | | | | |
| **G717** | 5 | | | | |
| **G719** | 2 | | | | |
| **G721** | 5 | 90 | 08 | 130 | DC |

Table 01.jpg

# Memory effect in electroformed nanocrystal silicon nitride based thin film LED

**Thursday, 10th November - 13:30 - Poster Session - Gallery - Poster presentation - Abstract ID: 505**

***Dr. Tamila Anutgan*** [1]***, Dr. Mustafa Anutgan*** [2]***, Prof. Ismail Atilgan*** [3]

***1.*** *Karabuk University, Department of Medical Engineering,* ***2.*** *Karabuk University, Department of Mechatronics Engineering,* ***3.*** *Karabuk University, Department of Metallurgical and Materials Engineering*

In our previous work [1] it was demonstrated that plasma deposited amorphous silicon nitride (a-SiNx:H)-based heterojunction p+in+ diode (Fig.1(a)) was transformed to light emitting diode (LED) after being subjected to Joule-heating assisted electroforming. The electroformed LED exhibited stable light emission easily perceived by the naked eye. The electrical transport and electroluminescence mechanisms of this LED were interpreted via a modified band-tail hopping model, taking into account the formation of Si nanocrystals within the i-layer during electroforming [2]. The low plasma deposition temperature (≤ 523 K), low cost and simple production, compatibility with Si technology, long lifetime and applicability on large surfaces of this thin film diode make it a serious potential competitor to the current crystalline and organic LEDs. In this work, we introduce an additional interesting property of this LED - resistive memory switching, thus extending its applications to light emitting memory (LEM). Unlike the previously proposed LEMs in the literature [3], there is no need for integration of two separate devices (light emitter and memory) since this LED itself exhibits the memory effect. Memory phenomenon was observed via systematically scanning current-voltage (I--V) characteristics and paying attention to their sequence and direction (Fig.1(b)). At forward-bias ('forward-1'), the I--V curve is repeatable, independent of scan direction and visible light emission always accompanies. When reverse-bias I--V ('reverse-2') is taken subsequent to `forward-1', it is similar to the curve `forward-1' below 1 V. Above 1 V, current density increases ~102 times and then follows `reverse-3' which becomes normal reverse I--V independent of scan direction. When it is switched to forward bias, the diode remembers its past: `forward-4' shows almost the same I--V with `reverse-3' and the visible light emission is absent until ~6 V, where the current density suddenly drops down onto the `forward-1' and the visible light emission starts. `Forward-5' reproduces `forward-1' thus verifying the diode's return to its original state. The kinetics of switching from light-OFF to light-ON state was studied by applying 3.5--6.5 V forward-voltage stresses and measuring corresponding time when the switching occurs. Finally, these results on memory effect were explained via energy-band diagram of the electroformed LED.

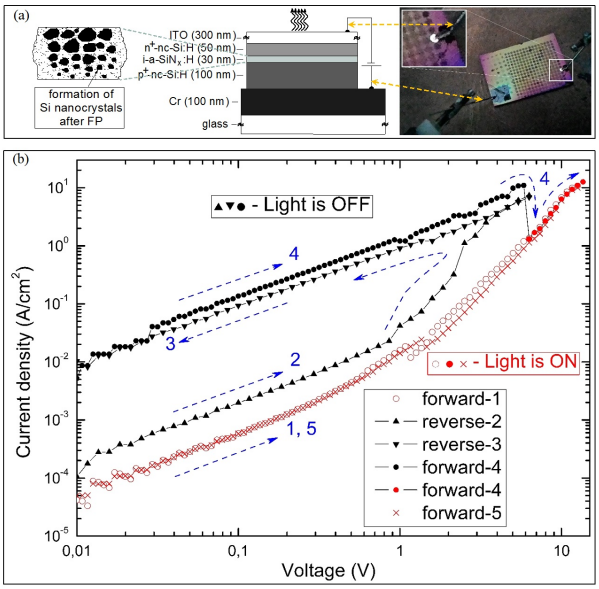


Fig. 1. (a) The cross-sectional a-$SiN_x$:H based diode structure with the schematic indication of nc-Si islands formed in i-layer after electroforming and the photographs of the electroformed diode taken during its light emission under application of forward bias. (b) Forward- and reverse-bias I–V characteristics of the diode after electroforming. The measurement sequence and the directions of the measurements are indicated by the numbers and the dashed arrows, respectively.

Fig 1 figure caption annic 2016 ta.jpg

**References:**
[1] M. Anutgan, T. Anutgan, I. Atilgan, B. Katircioglu, IEEE Transactions on Electron Devices 58 (8) (2011) 2537-2543.
[2] M. Anutgan, T. Anutgan, I. Atilgan, B. Katircioglu, Philosophical Magazine 93 (24) (2013) 3332-3352.

References.png

# Femtosecond Laser Induced sp3 Bonds and Nanodiamonds Formation in Carbon Materials

**Thursday, 10th November - 13:30 - Poster Session - Gallery - Poster presentation - Abstract ID: 509**

***Dr. Aurelian Marcu*** [1], ***Ms. Liga Avotina*** [2], ***Dr. Corneliu Porosnicu*** [3], ***Dr. Alexandru Marin*** [4], ***Dr. Cristiana Grigorescu*** [5], ***Mrs. Razvan Ungureanu*** [3], ***Mrs. Gabriel Cojocaru*** [3], ***Dr. Daniel Ursescu*** [3], ***Mrs. Mihail Lungu*** [3], ***Dr. Nicola Demitri*** [6], ***Dr. Cristian Lungu*** [1]

***1.*** *National Institute for Laser Plasma and Radiation Physics,* ***2.*** *Institute of Chemical Physics, University of Latvia, Kronvalda 4, LV 1010 Riga, Latvia,* ***3.*** *National Institute for Laser, Plasma and Radiation Physics, 077125 Bucharest, Romania,* ***4.*** *"Ilie Murgulescu" Institute of Physical Chemistry, 202 Splaiul Independentei 060021, Bucharest, Romania,* ***5.*** *National Institute R&D for Optoelectronics INOE 2000, 077125 Bucharest, Romania,* ***6.*** *Hard X-ray Beamline and Structural Biology, Elettra-Sincrotrone Trieste, Strada Statale 14 - km 163,5 in AREA Science Park, 34149 Basovizza TS Italy*

A polycrystalline graphite target was irradiated using a pulsed femtosecond laser with 120 fs pulse duration and 800 nm wavelength and different energies per pulse. Were performed `in-depth' and surface investigations and on the sp3 bonds percentage increase and possible diamond crystal formation. X-ray photoelectron spectroscopy investigations have shown an increasing tendency of the sp3 percent in the low power irradiated areas and similarly `in the depth' of the higher power irradiated zones. Multiple wavelength Micro-Raman investigations have confirmed this trend for high laser power densities (tens of J/cm2 ) and accomplish by the crystallite size `in-depth' grow. Synchrotron X-ray diffraction pattern have shown the presence of a diamond peak in one of the irradiated zones. Based on the wavelength dependent photon absorption into graphite, our investigations have shown that sp2-sp3 transitions is depending on the laser fluencies but not on photon adsorption rate per atom. Thus the observed effects are correlated with high density photon per atom and are attributed to the melting and recrystallization processes taking place tens of nanometers below the target surface. The presence of a diamond related peak observed in just one central zone of a multiple pulse irradiated spot, also suggests that diamond bonds formation is rather an accidental process based on the non uniform laser adsorption and respectively on the ablation related processes taking place within the polycrystalline graphite.

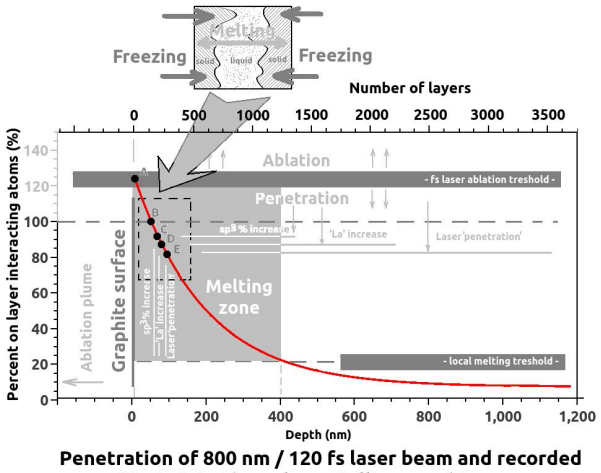


**Penetration of 800 nm / 120 fs laser beam and recorded effects into the polycrystalline graphite**

Nanodiamonds.jpg

# Comparison of negative capacitance phenomenon in ordinary amorphous and electroformed nanocrystalline silicon based LEDs

**Thursday, 10th November - 13:30 - Poster Session - Gallery - Poster presentation - Abstract ID: 531**

***Dr. Mustafa Anutgan*** [1], ***Dr. Tamila Anutgan*** [2], ***Prof. Ismail Atilgan*** [3]

***1.*** *Karabuk University, Department of Mechatronics Engineering,* ***2.*** *Karabuk University, Department of Medical Engineering,* ***3.*** *Karabuk University, Department of Metallurgical and Materials Engineering*

Hydrogenated amorphous silicon p+in+ homojunction LED (Figure 1-a) can be electroformed under a sufficiently high, calibrated forward voltage leading to its instant nanocrystallization at room temperature. This nanocrystallization process is of scientific and technological interest since the electroformed LED exhibits boosted electroluminescence together with a memory effect. Transport and luminescence phenomena in the electroformed LEDs were recently studied and explained by a modified band-tail hopping model where the charge carriers are mainly supplied from the silicon nanocrystallites [1]. In the present work, the electroformed nanocrystalline LED has been analyzed by capacitance spectroscopy and compared with the previous work [2] on the ordinary LED. The depletion regions of both ordinary and electroformed devices disappear above some particular forward bias, which leads to an interesting capacitance-voltage-frequency behavior. When the frequency is decreased at a constant forward voltage, the capacitance of the ordinary LED first increases, passes over a peak and then sharply decreases to relatively huge negative values (Figure 1-b). The peak points in the capacitance spectra are attributed to the condition where the injected charge carriers fill the relevant gap states around the demarcation level (Ed), and further decrease in the frequency at that forward bias results in recombination of the charges below Ed [2]. Compared to the ordinary LED, the capacitance-frequency behavior of the electroformed LED remains almost unaffected at forward voltages below 0.6 V and above 1.4 V (Figure 1-b); whereas, significant differences are observed around 1.0 V and at reverse bias regime (Figure 1-c). These similarities and differences in the capacitance spectra of both LEDs have been discussed within the frame of the modification of the gap states after the formation of Si nanocrystallites. From the circuit analysis point of view, the observed negative capacitance phenomenon has been regarded as an inductive effect since, similar to inductance, recombination also exhibits 180° phase difference with the traditional capacitance. Although this approach can be debated by means of the device physics, inclusion of an inductor in the equivalent circuit has been shown to be fruitful during simulations giving out reasonable parameters such as the frequency dependence of AC hopping conductivity.

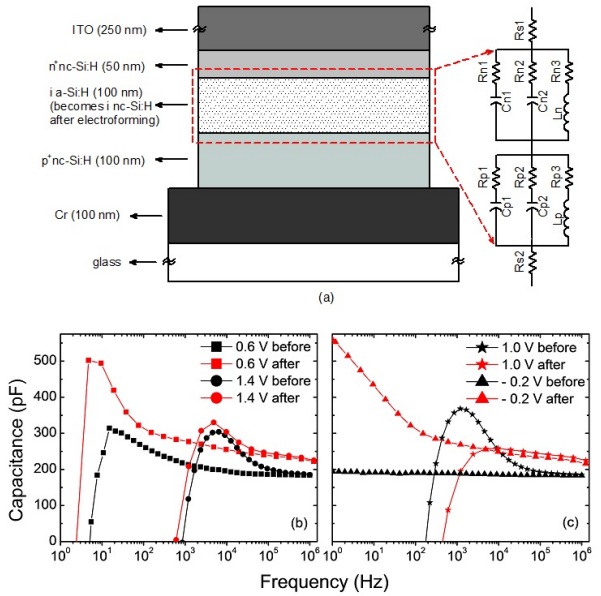


Figure 1: (a) Schematical cross section of the thin film Si-based LED and the corresponding equivalent circuit model used in this work. Comparison of the capacitance spectra of the LEDs before and after electroforming exhibiting (a) more or less similar and (b) quite different behaviors at particular voltages.

Figure1.jpg

**References:**

[1] M. Anutgan, T. Anutgan, I. Atilgan, B. Katircioglu, Philosophical Magazine 93 (24) (2013) 3332-3352.

[2] M. Anutgan, I. Atilgan, Applied Physics Letters, 102 (15) (2013) 153504 pp. 1-4.

References.jpg

# Dyanmic behavior of water droplet on water repellent surface with low contact angle hysteresis

**Thursday, 10th November - 13:30 - Poster Session - Gallery - Poster presentation - Abstract ID: 545**

***Prof. Takahiro Ishizaki*** [1]***, Mr. Keisuke Sasagawa*** [1]***, Mr. takuya furukawa*** [1]

***1.*** *Shibaura Institute Of Technology*

1. Introduction: Surface treatment technology for control of water droplet behavior is indispensable for various applications such as -TAS, automobile, and so on. Superhydrophobic surface with a water contact angle over 150o is known as a surface to extremely repel water. The superhydrophobicity is created by two factors, i.e., low surface energy and nanostructure. In general, the nanostructure is easily damaged by physical contact, resulting in the decrease in the water contact angle. Thus, it is required to create a novel surface that can control wetting behavior of water droplet after physical contact. Hydrophobic surface with a low contact angle hysteresis is considered to be an alternative surface to satisfy the demand due to the dewetting property. Thus, it is very important to develop a technology for creating hydrophobic surface with a low contact angle hysteresis. In this presentation, we report the preparation of water repellent surface showing a low contact angle hysteresis. 2. Experimental: Si wafer was used as substrate. The substrates were ultrasonically and photochemically cleaned. Hydrophobic surface showing low contact angle hysteresis was prepared on the cleaned substrate from a 1,3,5,7-Tetramethylcyclotetrasiloxane or octadecyltrimethoxysilane (ODS) by a chemical vapor deposition at 333 to 443 K for 6 to 72 h. Static and dynamic contact angles of the samples were estimated using a contact angle meter. 3. Results and Discussion: Fig 1 shows the advancing and receding contact angles of the samples prepared at 353 and 443 K. The averaged advancing contact angles of the samples at 353 and 443 K for 24 h were approximately 100 and 160o, respectively. The advancing and receding contact angles of the samples at 353 K increased with an increase in the treatment time. The contact angle hysteresis of the samples were approximately kept constant at 20o. In case of the samples at 443 K, the contact angle hysteresis decreased with an increase in the treatment time and became less than 10o when the treatment time was more than 12 h. Acknowledgement This work was partly supported by Grant-in-Aid for Scientific Research (A) (No. 16H02400) from Japan Society for the Promotion of Science.

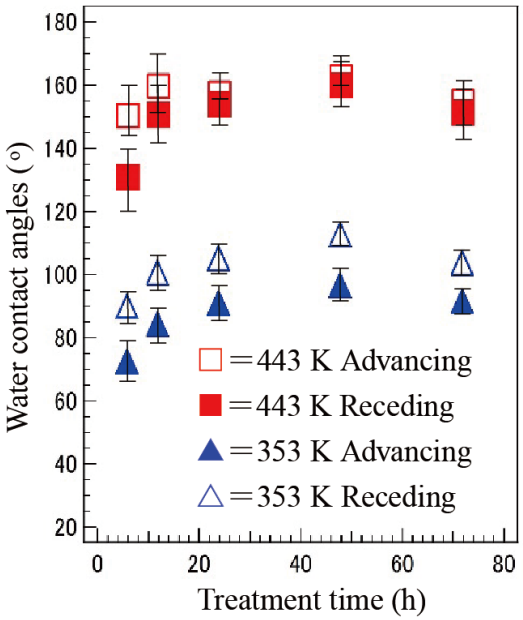
Water contact angles (°)
Treatment time (h)
□=443 K Advancing
■=443 K Receding
▲=353 K Advancing
△=353 K Receding
180
160
140
120
100
80
60
40
20
0
20
40
60
80

Fig1.png

# Refractive index sensing with electrochemical sensor

**Thursday, 10th November - 13:30 - Poster Session - Gallery - Poster presentation - Abstract ID: 553**

***Mr. Hans Dyrnesli*** [1]

***1.*** *Aarhus University*

Introduction Fast, reliable and cheap sensors for biomarker detection have the potential of enabling early diagnosis of severe conditions. Here, a nano-structured optical/electrochemical sensor is presented as a basis for highly specific biomolecule detection. Hole-mask colloidal lithography allow for rapid large-area patterning of sensor surface with plasmonic gold-nanodisks, which function as interface for both optical and electrochemical sensing of analytes. Methods Gold-structured sensor surface was fabricated on indium-doped zinc oxide-coated glass by hole-mask colloidal lithography. A home-made electrochemical flow cell was used for optical/electrochemical proof-of-concept measurements. Results Sensor is able to reliably detect changes in bulk refractive index of less than 0.015, as well as electrochemical reduction of ferricyanide. Discussion By simultaneously measuring different properties of an analyte, multifunctional sensors have the potential of improving fidelity of measurements and provide a means of recognizing false positive detection events. Presented is a proof-of-concept system that is not specific to any particular analyte. Specificity can be achieved by functionalizing the sensor surface with antibodies or molecular imprinted polymers.

# Design and Synthesis of Macromolecular Scaffolds for Carbon Monoxide Delivery in Biological Systems

**Thursday, 10th November - 13:30 - Poster Session - Gallery - Poster presentation - Abstract ID: 623**

***Ms. Diep Nguyen*** [1], ***Prof. Cyrille Boyer*** [1]

***1.*** *CAMD, School of Chemical Engineering, University of New South Wales*

CO has been recognised as a signalling molecule in mammalian organisms and is involved in regulating physiological and pathophysiological pathways. CO has also been demonstrated to have potent anti-inflammatory, anti-proliferative and anti-apoptotic effects. The significant therapeutic effects of controlled CO inhalation have been proven in animal models of disease with the anti-inflammatory activity of CO studied in phase II clinical trials. However, the therapeutic benefits of CO gas administration have remained questionable as a result of its systemic toxicity at high concentrations and difficulties in storing and delivering gaseous CO to the target tissue in a controlled manner. To overcome these limitations, chemists have developed molecules capable of releasing carbon monoxide (CORMs) as pharmaceutical agents for safer, more convenient and controlled CO release. Among CORMs, the commercial CORM-2 and CORM-3 are one of the most common CO-releasing molecules used in biological studies. These compounds exert significant biological properties including anti-inflammatory and antimicrobial activities. However, the clinical use of these compounds as therapeutic agents is limited owing to their short CO-releasing half-life and poor solubility in aqueous solutions. These drawbacks can be addressed by using macromolecular scaffolds as CO carries. Macromolecular carriers, such as polymeric nanoparticles appear to be an ideal vehicle for the transport of drugs because their sizes can be easily tuned, permitting the passive accumulation in a tumor tissue via the enhanced permeability and retention (EPR) effect. Additionally, macromolecular carriers offer a high CO-loading capacity due to the attachment of several CO per macromolecule, resulting in a significant increase in the CO concentration. Furthermore, nanocarriers not only enhance the therapeutic efficacy, but they also reduce the systemic toxicity of drugs, which results in a reduction in side effects. Inspired both by the excellent biological activities of CORM-2/CORM-3 and many advantages of macromolecular materials offering, we aimed to construct novel multifunctional macromolecular systems that possess the features allowing the controlled and selectively delivery of CO. This work opens up new strategy for the development of CO-releasing scaffolds in biological applications.

# New Aptamer-Based Biosensor -- Design Study

**Thursday, 10th November - 13:30 - Poster Session - Gallery - Poster presentation - Abstract ID: 660**

***Dr. Radu Tamaian*** [1], ***Mrs. Nadia Paun*** [1], ***Dr. Violeta Niculescu*** [1]

***1.*** *National Institute for Research and Development for Cryogenic and Isotopic Technologies*

Introduction. Aptamers, either single-stranded oligonucleotide or peptide molecules able to specifically bind a target molecule, are synthetic analogues with a wide range of applications. Their pH and temperature tolerance, unlike the antibodies, combined with a high affinity and specificity in binding of the target molecules, makes them excellent recognition elements for development of novel biosensors. Methods. In this paper we propose a new designed for an aptamer-based biosensor for detection of circulating microRNAs. We based our design study on direct correlations between the aberrations in microRNAs expression and oncogenesis, respectively the metastatic process. Results and discussion. From the human circulating (serum and plasma) microRNAs sequences currently known was targeted as biomarker a 34 microRNA model (predictor) from serum used for the early diagnosis of non-small cell lung carcinomas. As recognition element of the biosensor was designed an aptamers set to specifically bind their targets from the 34 microRNA model. In order to transduce the bio-recognition the aptamer-based assay was designed as single-site binding for each of the 34 targets. According to the signal-harvesting method, an electrochemical format was preferred for the current design. The further development of this type of aptamer-based biosensor for detection of circulating microRNAs may contribute to early non-invasive detection of lung cancer at asymptomatic high-risk individuals. Acknowledgments: this research was financed by The Executive Agency for Higher Education Research Development and Innovation Funding (UEFISCDI), Romania, on the Contract no. 210/2014, Project PN-II-PT-PCCA-2013-4-2075 and 34N/2016 NUCLEU Program, under Project PN 16 36 04 03 „Research on the development of new porous materials with high selective and catalytic properties for the reduction and stabilization of the pollutant concentrations in gaseous and liquid backgrounds".

# A new serie of phosphat catalysts based on Copper and Zinc: chemical preparation and physicochemical study

**Thursday, 10th November - 13:30 - Poster Session - Gallery - Poster presentation - Abstract ID: 690**

***Dr. Asmaa AJARROUD*** [1]

***1.*** *university hassan II- Casablanca*

Phosphate catalysts are of major importance in both industry and in research, especially those based on metal.[1] Hence, for this reason, our main reaserch focus was the chemical synthesis of a set of catalysts with a good catalysis activity and a high selectivity in conjuction with the physicochemical study of those materials. The authenticity of our work lays in the fact that we have eleborated a new serie of copper and zinc based phosphate catalysts.[2] In this novel serie a set of differentes phosphate catalysts (Cu,Zn-P), each one with a different pourcentages of copper and zinc metals were chemically prepared and elaborated. After this, our products were charachterized using various physico chemical technics such as : X ray diffraction (XRD), Scanning electron microscopy (SEM), Transmission electron microscopy (TEM), Infra-red spectroscopy (IR). RAMAN spectroscopy. Finally, we will use this novel serie in the catalysis of various chemical reactions , such as : isomeristaion, alkylation, hydrogenation and hydrogenolysis with the aim that we utilize this set in the field of green chemistry and the environnment protection [1] : M Guisnet. Ideal bifunctional catalysis over pt-acid zeolites. Catalysis today.2013 [2] : S Eriksson. All. Preparation of catalyses from microemulsion and their application in heterogeneous catalysis. Applied catalysis. 2004

# Relaxation dynamics of multilayer networks modeled with Husimi cacti

**Thursday, 10th November - 13:30 - Poster Session - Gallery - Poster presentation - Abstract ID: 707**

***Mr. Liviu Bogdan Chiriac*** [1], ***Dr. Aurel Jurjiu*** [1], ***Prof. Mircea Galiceanu*** [2], ***Mr. Alexandru Stefan Farcasanu*** [1], ***Dr. Flaviu Turcu*** [1]

***1.*** *Babes-Bolyai University,* ***2.*** *Federal University of Amazonas, Manaus*

Monodendrons and dendrimers have been shown to represent some of the most powerful synthetic building blocks that can be employed in the construction of supramolecular and macromolecular systems with well defined shapes and sizes. Among these systems, the cylindrical supramolecular dendrimers have well defined multilayer structure. Recently, multilayered assemblies that are constructed through the layer-by-layer (LbL) deposition of dendrimers have attracted much attention because of their facile preparation and versatility in terms of structure and functionality. We focus on the relaxation dynamics of multilayer polymer structures having as underlying topology the Husimi cactus. The work provides theoretical support to the newly synthesized multilayer polymers. We study the relaxation dynamics of the multilayer network in the framework of Generalized Gaussian Structures model, using both Rouse and Zimm approaches. Such model, in the Rouse-type approach, allows to determine the full dynamical behavior of the polymer system through the diagonalization of its connectivity matrix. Remarkably, for the multilayer structure we develop an analytical method for the determining of the whole eigenvalues spectrum of its connectivity matrix. This fact allows us to study in detail the crossover from a pure Husimi cactus behavior to a predominantly linear chain behavior. For networks with small number of layers the intermediate times/frequencies domain of the dynamical quantities shows a bulk-like behavior, a mixture between the Husimi cactus behavior and linear chain behavior. For the networks with large number of layers intermediate times/frequencies domain decomposes into two regions. The first, located at middle to lower times/frequencies shows a bulk-like behavior and, the second situated at lower times/frequencies displays a linear chain behavior. In the Zimm-type approach, which includes the hydrodynamic interactions, the quantities that describe the mechanical relaxation dynamics do not show scaling, except the limiting case, namely, a very large number of layers and low size of the layer. The theoretical findings are well supported by mechanical relaxation experiments, both with respect to scaling, as well as to the splitting of the intermediate domain.The mechanical experiments were performed on pillared-layered polymers, LbL assembly of dendrimers, supramolecular cylindrical dendrimers, and supramolecular cylindrical micelles.

# Relaxation dynamics of Sierpinski hexagon fractal polymer

**Thursday, 10th November - 13:30 - Poster Session - Gallery - Poster presentation - Abstract ID: 705**

***Dr. Aurel Jurjiu*** [1]

***1.*** *Babes-Bolyai University*

Fractals are of particular relevance in many fields of science. In physics and chemistry the concept of fractals is widely used for describing the disordered systems, growth phenomena, chemical reactions controlled by diffusion, relaxation dynamics of polymer networks, and energy transfer. We extends the theoretical works on relaxation dynamics of polymers with complex architectures by considering a new class of fractal structures, namely the Sierpinski hexagon gaskets. Our work is motivated both, by the outstanding results of G.R. Newkome et al. who succeeded to synthesize the first nondendritic fractal polymer based on Sierpinski hexagonal gaskets and also by the search of scaling in the intermediate time/frequency region of the quantities which describe the relaxation dynamics. We perform our calculations in the framework of the generalized Gaussian structures (GGS) model which represents the extensions of the Rouse and Zimm models, developed for linear polymer chains, to polymer systems with arbitrary topologies and which highlight both the connectivity of the molecules under investigation, as well as the influence of hydrodynamic interactions. The main advantage of GGS model is that, in the Rouse-type approach the quantities which describe the relaxation dynamics can be calculated only by making use of the eigenvalues of the connectivity matrix of the structure. In the Rouse-type approach, based on real-space renormalization transformations, we develop an analytical method for determining of the complete eigenvalue spectrum of the connectivity matrix. Thus, the investigation of the relaxation dynamics of huge fractal structures (N=6ˆ10 monomers) can be easily performed. The general picture that emerges in the Rouse type-approach is that Sierpinski hexagon fractal polymers do obey scaling and the sole fractal parameter of importance for their relaxation dynamics is the spectral dimension. The introduction of hydrodynamic interactions, on the other hand, completely changes the picture. Our use of the Zimm formalism, based on the preaveraged Oseen tensor, does not lead anymore to scaling forms in the intermediate domain of the relaxation quantities. Our theoretical findings with respect to scaling in the Rouse model are well supported by experimental results obtained for physical polymer gels, F-actin solutions, hexagonal liquid crystals, and hexagonal micelles.

# Gardenia jasminoides extract-capped gold nanoparticles reverse hydrogen peroxide-induced premature senescence

**Thursday, 10th November - 13:30 - Poster Session - Gallery - Poster presentation - Abstract ID: 490**

***Ms. seon yeong chae [1], Dr. Sun young Park [1], Mr. Jin Oh Park [1], Mr. Kyu Jin Lee [1], Prof. Geuntae Park [1]***

***1.*** *Pusan National University*

Biological synthesis of gold nanoparticles is ecofriendly and effective for the development of environmentally sustainable nanoparticles compared with existing methods. Here, we developed a simple, fast, efficient, and ecofriendly approach to the synthesis of gold nanoparticles by means of a Gardenia jasminoides extract. These G. jasminoides extract-capped gold nanoparticles (GJ-GNPs) were characterized by UV-Vis, high resolution transmission electron microscopy (HR-TEM), X-ray diffraction (XRD), and Furrier transform infrared spectroscopy (FT-IR). The synthesized GJ-GNPs turned red and showed maximal absorbance at 540 nm. Thus, GJ-GNPs were synthesized successfully, and GJ-GNPs were found to have roughly spherical and hexagonal shapes, and monodispersed, with the diameter of particles 20 nm. The synthesized GJ-GNPs were confirmed to be crystalline in nature. Prematurely senescent cells are known to have characteristics of replicative senescence, such as a loss of the proliferative potential, enlarged and flattened cell shape, irreversible cell cycle arrest, and increased senescence-associated β-galactosidase (SA-β-gal) activity. We hypothesized that GJ-GNPs would protect ARPE19 cells from hydrogen peroxide-induced premature senescence. We tested the effects of hydrogen peroxide (at various concentrations) on ARPE19 cell senescence and showed that low concentrations of hydrogen peroxide induced positive staining of SA-β-gal and arrested cell cycle progression. Thus, hydrogen peroxide treatment induced premature senescence in ARPE19 cells, as indicated by the changed cellular morphology. Treatment with GJ-GNPs restored the hydrogen peroxide-induced morphological changes. SA-β-gal activity was elevated in hydrogen peroxide-treated cells, however, this effect was attenuated by GJ-GNP treatment. Moreover, compared with the normal control, hydrogen peroxide treatment significantly increased lysosome content of the cells and production of reactive oxygen species (ROS). GJ-GNPs effectively attenuated the increase in lysosome content and ROS production in these senescent cells. According to cell cycle analysis, G2/M arrest was promoted by hydrogen peroxide treatment in ARPE19 cells, however, this change was reversed by GJ-GNPs. Western blot analysis showed that treatment with GJ-GNPs increased the expression of p53, p21, SIRT3, HO-1, and NQO1 in senescent cells. Our findings should advance the understanding of premature senescence and may lead to therapeutic use of GJ-GNPs in retina-related regenerative medicine.

# Immobilization of enzyme on porous silicon for electrochemical detection of organophosphorous compounds

**Thursday, 10th November - 13:30 - Poster Session - Gallery - Poster presentation - Abstract ID: 629**

***Dr. Maha Ayat*** [1]***, Dr. Chafiaa Yaddaden*** [2]***, Dr. Amina Kermad*** [2]***, Dr. Noureddine Gabouze*** [1]***, Prof. Mohamed Kechouane*** [3]

***1.*** *CMSI, Centre de Recherche en Technologie des Semi-conducteurs pour l'Energétique,* ***2.*** *Centre de Recherche en Technologie des Semi-conducteurs pour l'Energétique,* ***3.*** *Université des Sciences et de la Technologie Houari Boumediene- Bab Ezzouar*

In this work, porous silicon (PSi) surface was functionalized by a multistep process in order to immobilize a specific enzyme, acetylcholinesterase (AChE). AChE hydrolyses acetylthiocholin (ATCh) or substrate in thiocoline and acetic acid. The modified AChE electrode is used for the electrochemical detection of organophosphorous compounds. The electrochemical detection using the modified electrode was perfomerd in presence of Malathion at different concentrations using Acetythiocholine Iodide (ATCl Iodide) as enzyme substrate. A decrease of oxidation peak current was observed, by increasing the Malathion concentrations, and this was due to the blocking of active sites of the AChE.

# Meyer-Neldel temperature on carrier transport of C70 molecular solid

**Thursday, 10th November - 13:30 - Poster Session - Gallery - Poster presentation - Abstract ID: 373**

***Mr. Sezaimaru Kouki*** [1]***, Mr. Nakashima Fumihiro*** [1]***, Prof. Yong Sun*** [1]***, Dr. Koichi Onishi*** [1]

***1.*** *Kyushu Institute of Technology*

Recently, the Meyer-Neldel rule was also observed on charge carrier mobility of fullerene materials such as C60 and C60/C70 mixture. At the Meyer-Neldel temperature, the charge carrier mobility becomes independent of the activation energy for carrier transport and temperature. Usually, the activation energy is a function of electric field and charge carrier concentration. Also, the Meyer-Neldel temperature depends only on structural properties of the disordered materials and can be used as an important material characterizing parameter. However, despite being one of the most abundant fullerenes, the Meyer-Neldel behaviors of the C70 material have not yet been studied in detail. In this paper, we report carrier transport properties of the C70 molecular solid at various temperature and electric field strength. To make a solid sample for measurement of the electrical properties, the C70 powder was pressed into a pellet at room temperature at pressure of 125 MPa. In measurements of the current-voltage characteristics of the C70 sample, the current passing through the sample was obtained using a digital electrometer (ADVANTEST R8252) with a current resolution of 1.0 fA at various d.c. bias voltages from 30 V to 200 V. The current measurements were carried out in the course of heating up and cooling down process between temperatures of 15 K and 450 K. The rate of heating up and cooling down process was 0.14 K/min with a stepwise increment of 1.0 K. The current-voltage (i-v) characteristics can be described conjecturally as a cubic polynomial of the voltage, i=avˆ3+bvˆ2+cv+d as shown in the figure. Moreover, the Meyer-Neldel temperature of the C70 solid was confirmed to be 310 K, at which a linear relationship between the current and voltage was observed. Also, at temperatures below the Meyer-Neldel temperature, the current increases with increasing voltage. On the other hand, at temperatures above the Meyer-Neldel temperature a negative differential conductivity effect was observed at high voltage side. The negative differential conductivity was related to the electric field and temperature effects on the mobility of charge carrier, which involve two variations in the carrier concentration and the activation energy for carrier hopping transport.

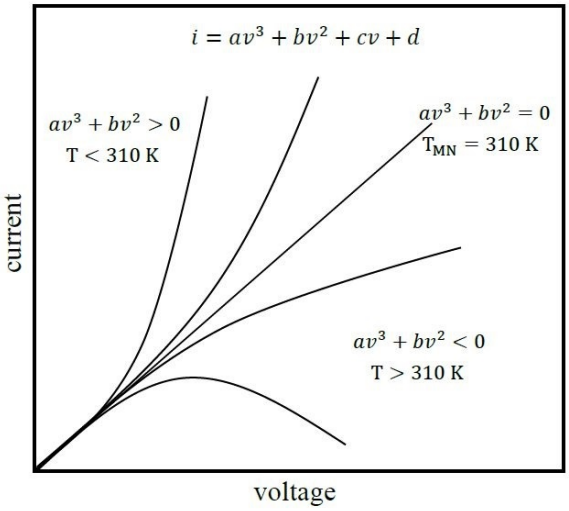


Schematic diagram of the i-v characteristics of the c70 sample near the meyer-neldel temperature of 310k..jpg

# Programmable artificial micro-swimmer

**Thursday, 10th November - 16:00 - Nanomedecine & Nanobiology - Room 1 - Oral presentation - Abstract ID: 408**

***Prof. Jinyao Tang*** [1]

*1. University of Hong Kong*

Introduction It has attracted much interest to design a self-powered artificial nanorobotic system which mimic the behavior of the motile bacteria due to both scientific merits as well as its potential applications. Previously, it has been demonstrated that asymmetric redox reaction on bi-metallic nanowire can produce the electric field and propel itself in solution. This autonomous motion shows that artificial inorganic nanomaterial can be used as nanomotor which harvests energy from the environment. Methods Here, we will present a rational designed micro-swimmer based on Janus nanotree which harvests energy from absorbed photons by photoeletrochemical (PEC) reaction. Our micro-swimmer incorporated both photocathode and photoanode. Upon illumination, the photoelectrochemical reaction on the swimmer surface generates the asymmetric ionic enviroments required to propel the migration of micro-swimmer. Results In this design, we focus on controllability and programmability of the micro-swimmer. The Individual Janus nanotree is designed that it can sense the direction of light vector and direct to illumination direction. Since the migration is regulated by the surface potential of micro-swimmer, we developed a simple chemical modification process to program the swimmer to show either positive phototaxis (migrates towards the light source) or negative phototaxis (migrate away from the light source). Discussion Two main advantages have been demonstrated in this light powered micro-swimmer. First, light can be used not only as the power source but also as a new method to control the migration of individual swimmer which provided another option besides magnetic control. Second, since the energy is provided from the light, it is easier to find a biocompatible redox shuttle to replace the widely used toxic H2O2, which would promise wider applications for micro/nanomotor. Reference: B. Dai, J. Wang , Z. Xiong, X. Zhan, W. Dai, C.C. Li, S. Feng, J. Tang, Programmable Artificial Phototactic Microswimmer, Nat. Nanotechnol. AOP Figure caption a. Schematic of micro-swimmer. b. The trajectory of a pristine nanotree spells ``nano'' as navigated by light. c. Sequential images of the green algae, E. Gracilis, pristine microswimmer, CSPTMS treated micro-swimmer suspension in aqueous solution with illumination from the right side

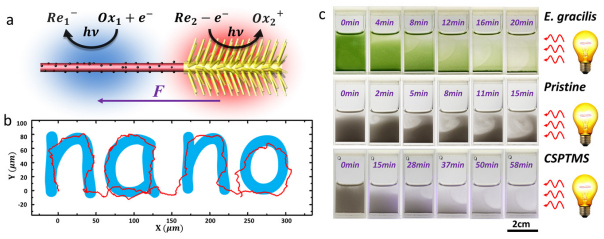


Picture1.jpg

# Saponin/lipid nanoparticles as an efficient adjuvant and delivery system for mucosal immunization

**Thursday, 10th November - 16:17 - Nanomedecine & Nanobiology - Room 1 - Oral presentation - Abstract ID: 527**

***Prof. Vladimir Berezin*** [1], ***Prof. Andrey Bogoyavlenskiy*** [1], ***Dr. Pavel Alexyuk*** [1], ***Dr. Aizhan Turmagambetova*** [1], ***Ms. Irina Zaitceva*** [1], ***Ms. Madina Alexyuk*** [1], ***Ms. Elmira Omirtaeva*** [1]

***1.*** *Institute of Microbiology and Virology*

Background: Mucosal surfaces are one of the major entrances for infectious diseases and mucosal immune response serve as a first line of defense. For reasons of safety, efficacy and cost, mucosal administration of vaccines is today a one of priorities for immunizing against many infectious pathogens penetrating through mucosal gates. Most commercial vaccines today are injectable and use aluminum salts as their adjuvant component. These vaccines are unable to induce high levels of immune response when delivered at mucosal sites. In order to make them more immunogenic and prepare vaccine for mucosal immunization, strong mucosal adjuvants/delivery systems are required. Recently purified triterpen saponins ``GlabiloxTM'' and ``AsgipanTM'' with low toxicity and high immunostimulatory activity were isolated from plants G. glabra and A. hippocastanum indigenous to Kazakhstan. Both saponins can interact with antigens and lipids resulting formation of nanoparticles 60-80 nm in size. Such nanoparticles can induce humoral and cellular immune responses through various routes of immunization, including intranasal, and provide protection against infection. Methods: Influenza virus external glycoprotein antigens (HA+NA) were isolated from purified influenza virus by non-ionic detergent treatment. Triterpen saponins GlabiloxTM and AsgipanTM were isolated from plant tissues by ethanol extraction and purified by HPLC fractionation. Nanoparticles incorporated HA+NA antigens, lipids and saponins GlabiloxTM or AsgipanTM were prepared by dialysis technique. Humoral and cellular immune responses and protection against influenza infection were studied in animal vaccination/challenge experiments after single intranasal immunization of influenza subunit vaccine prepared on the base saponin/lipid nanoparticles. Results: Intranasal immunization by subunit influenza vaccine on the base of nanoparticles contained HA+NA antigens, triterpen saponins GlabiloxTM or AsgipanTM and lipids stimulated formation of high levels of IgM, IgA, IgG1, IgG2a and IgG2b antibody and production of cytokines IL-2, IL-4, IL-10 and IFN-γ. Immunization/challenge experiments demonstrated 80-90% protection against influenza virus infection after single intranasal immunization of nanoparticulate influenza subunit vaccine in dose 5 μg per animal (Fig. 1). Conclusion: Saponin/lipid nanoparticles contained influenza virus HA+NA antigens, lipids and saponins GlabiloxTM or AsgipanTM can be used as an efficient adjuvant/delivery system for mucosal (intranasal) immunization against influenza.

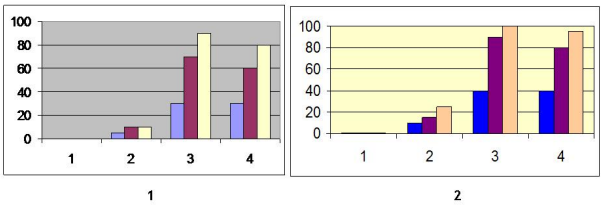


Fig 1. Protection against H1N1 influenza virus infection after single intranasal immunization of subunit influenza vaccine at intranasal (1) and subcutaneous (2) routes of immunization

On axis abscissa – groups of mice immunized vaccine preparations in various doses: 1,0; 3,0 and 5,0 ug/animal.
On axis ordinate – % protection against H1N1 influenza virus, strain A/Swine/Iowa/15/30 in dose 1000 $ELD_{50}$

1 – placebo
2 – subunit HA+NA vaccine without adjuvant
3 – nanoparticles incorporated HA+NA antigens, lipids and triterpen saponin Asgipan™
4 – nanoparticles incorporated HA+NA antigens, lipids and triterpen saponin Glabilox™

Fig 1.jpg

# Optical and electrochemical immunoassay for detection of superoxide dismutase 2 employing biocatalytic formation of quantum dots on the surface of microbeads

**Thursday, 10th November - 16:34 - Nanomedecine & Nanobiology - Room 1 - Oral presentation - Abstract ID: 533**

*Ms. Ruta Grinyte* [1], *Dr. Javier Barroso* [1], *Dr. Laura Saa* [1], *Dr. Valery Pavlov* [1]

*1. CIC biomaGUNE*

INTRODUCTION: Semiconductor nanocrystals known as quantum dots (QDs) are increasingly being used as photoluminescent materials in bio-imaging, photonics, and optoelectronic applications. Our group has pioneered the enzymatic in situ growth1-4 and etching 5 of fluorescent semiconductor CdS QDs, and on this base developed fluorogenic enzymatic assays. Those assays were much more cost efficient and demonstrated lower detection limits and better sensitivities than the standard assays based on organic substrates. In this study we developed new optical and electrochemical immunoassay for detection of tumor biomarkers such as superoxide dismutase (SOD2) employing enzymatic in situ generation and immobilization of CdS QDs onto microspheres. METHODS: Cadmium sulfide semiconductor nanoparticles were detected by fluorescence spectroscopy and square-wave voltammetry. Characterized by a wide field fluorescence microscope and a transmission electron microscopy equipped with an Energy Dispersive X-Ray Spectrometer. RESULTS AND DISCUSSION: In our immunoassay (Sheme 1) the target analyte (A) SOD2 mediates immobilization of alkaline phosphatase antibody conjugate on the surface of polyvinyl chloride microbeads. The enzymatic hydrolysis of para-nitrophenylphosphate by alkaline phosphatase triggered rapid formation on the surface of microbeads of phosphate-stabilized cadmium sulfide semiconductor nanoparticles which were detected by fluorescence spectroscopy and square-wave voltammetry. We have demonstrated that electrochemical and fluorogenic detection employing enzymatically generated CdS NPs yield new immunoassays with better detection limits in comparison with those of the previously published methods at least by three orders of magnitude. Our methodology allows for the detection of SOD2 in lysates from HepG2 (Human hepatocellular carcinoma) cells. REFERENCES: 1. L. Saa, A. Virel, J. Sanchez-Lopez and V. Pavlov, Chemistry, 2010, 16, 6187-6192. 2. L. Saa, J. M. Mato and V. Pavlov, Analytical chemistry, 2012, 84, 8961-8965. 3. L. Saa and V. Pavlov, Small, 2012, 8, 3449-3455. 4. G. Garai-Ibabe, L. Saa and V. Pavlov, Analytical chemistry, 2013, 85, 5542-5546. 5. R. Grinyte, L. Saa, G. Garai-Ibabe and V. Pavlov, Chemical Communications, 2015, 51, 17152-17155.

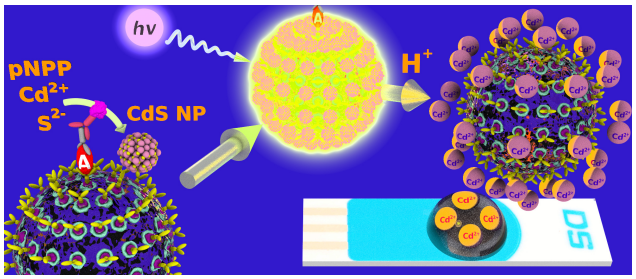


Scheme1.the principle of microbead-based elisa for detection of sod2 a .jpg

# Mussel Inspired Nanowire Platforms for siRNA delivery

**Thursday, 10th November - 16:51 - Nanomedecine & Nanobiology - Room 1 - Oral presentation - Abstract ID: 489**

***Dr. Baiju Govindan Nair*** [1]***, Prof. Yoshihiro Ito*** [1]

***1.*** *RIKEN*

Vertically aligned silicon nanowire (SiNW) substrates with efficient surface modifications are considered as three dimensional topological features for tissue engineering. The array of these high aspect ratio nanomaterials often act as a microenvironment for the exchange of a wide range of molecules between cells and culture substrates. High density nanowire array is found to be quite useful in reversible attachment of cells using a thermo-sensitive polymer and in vivo delivery of exogenous genes by supramolecular nanoparticles. The high density of SiNWs have significantly increased cell adhesion, proliferation and delivery of biomolecules. To achieve these goals, a proper functionalization that support cell growth and conjugation of biomolecules are required. In these contexts, mussel inspired surface chemistry using the oxidative polymerization of dopamine has secured role in the area of simple surface functionalization. Usually, 3, 4-dihydroxy-L-phenylalanine (DOPA) and lysine-rich proteins are known candidates that are responsible for the adhesion of mussels to any surface. Polymerized dopamine (PD) is capable of simply adhering to any substrates and expose prominent functional groups on the material surfaces. According to various research reports, PD coating is very stable and versatile due to covalent and non-covalent interactions. This ability of PD has opened up new opportunities for biomedical applications, including drug delivery and bio-sensing. In this bio-inspired approach, we deployed polydopamine (PD) assisted thin layer coating on high density SiNWs to anchor more siRNA. These adsorbed siRNA offered more surface concentration for substrate-mediated delivery. We have also found that there is a cell membrane perturbation during the cell-nanowire interaction which resulted in the effective delivery siRNA into cell and allows carrying out its biological function. Our results highlights the promising application of PD-coated high dense SiNWs as simple, fast, and versatile platforms for the transmembrane delivery of biomolecules.

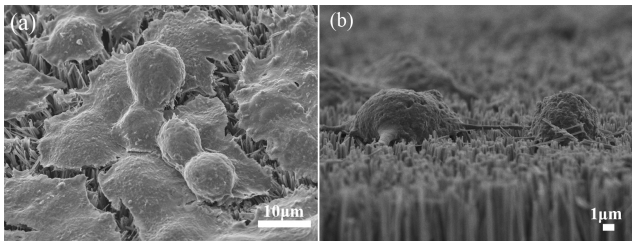


Figure.3.jpg

# Biodegaradable nanoporous microspheres by RAFT polymerization

**Thursday, 10th November - 17:08 - Nanomedecine & Nanobiology - Room 1 - Oral presentation - Abstract ID: 198**

***Prof. Ildoo Chung*** [1], ***Mr. Taeyoon Kim*** [1], ***Ms. Sorim Lee*** [1]

***1.*** *Pusan National University*

INTRODUCTION Spherical polymeric particles have been intensively studied and synthesized by a variety of methods such as spray drying, emulsification methods and so on. Controlled radical polymerizations (CRP) including RAFT, ATRP, SFRP have been studied for past few decades due to their tolerance of impurities, the ready availability of many kinds of initiators, catalysts and monomers, their mild reaction conditions, and their ability to produce polymers with predetermined molecular weights and narrow polydispersities In this study, nanoporous microspheres based on PMVK-b-PCL-b-PMVK block copolymers were fabricated by photodegradating PMVK blocks and evaluated their surfaces and internal structures by electron microscopies. METHODS Nanoporous nanoporous microspheres based on polycaprolactone (PCL) and photodegradable poly(methyl vinyl ketone) (PMVK) were synthesized and characterized. First, PCL based triblock copolymer was synthesized by RAFT polymerization followed by the fabrication of microsphere by emulsion method. Disk-shaped particles were then prepared by UV-irradiation with the microsphere. In order to polymerize by RAFT method, PCL based macro-CTA (chain transfer agent) was synthesized by reacting carboxylic acid-terminated CTA with PCL, and used for the synthesis of block copolymer with MVK. The morphology of the particles before and after UV irradiation were confirmed by SEM and TEM images and spherical microspheres were changed to disk-shaped forms, owing to collapsing of PMVK moieties by UV irradiation. RESULTS AND DISCUSSION As shown in Figure 1, fabricated microspheres had uniform size particles with approximately 5 um in diameter, and those from block copolymers had a nanoporous structures after UV exposure while PCL microspheres had kept the smooth surfaces. Spherical microspheres were gradually changed to disk-shaped forms as UV irradiation time increased, owing to collapsing of PMVK blocks by UV irradiation. CONCLUSIONS Nanoporous microshperes based on PCL and photodegradable polymethylvinylketone (PMVK) were synthesized and anticipated to enhance drug release and could find potential applications for biomaterials. ACKNOWLEDGEMENTS This work was supported by Basic Science Research Program (NRF-2014R1A1A4A01008897) through the Ministry of Education and National Research Foundation of Korea.

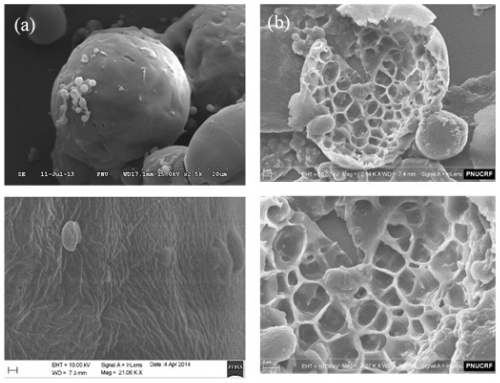


**Figure 1.** SEM images of the microspheres based on PMVK-b-PCL-b-PMVK (a) before and (b) after UV irradiation.

Figure 1.jpg

# Synergy of radiotherapy and chemotherapy delivered via gold nanostructures in glioblastoma multiforme

**Thursday, 10th November - 17:25 - Nanomedecine & Nanobiology - Room 1 - Oral presentation - Abstract ID: 309**

***Ms. Alexandra Vaideanu*** [1], ***Ms. Astrid Wendler*** [1], ***Dr. Colin Watts*** [1], ***Prof. Mark Welland*** [1]

***1.*** *University of Cambridge*

Glioblastoma multiforme (GBM) is reputable in its aggressiveness because of the inter- and intra- tumor heterogeneity which leads to resistance and recurrence. The aim of our work is to demonstrate the efficacy of a multimodal nanotechnology which exploits the chemical and physical properties of a system based on gold nanostructures combined with a tumor targeting element - in this case a tumor homing peptide, in eradicating GBM cell populations in vitro and tumour growth stagnation or reduction in vivo in an orthotopic xenograft model. We have showed previously (1) the synergistic effect of chemotherapy and radiotherapy in a construct based on spherical gold nanoparticles coated with mercaptoundecanoic acid (MUA) to which we attached cis-platinum drug. To further improve this technology we have used a modified construct in which we replace the MUA coating with mixed monolayer made of a small peptide and a polyethylene glycol linker/MUA. The peptide is designed such that it exploits the RGD motif targeting integrins associated with the newly formed blood vessels as well as the CendR rule motif (2) K/RXXK/R which is responsible for targeting of the particle to tumor cells due to binding to receptors such as neuropilin-1(VEGF168R). Furthermore, we are working towards synthesizing a stable porous superstructure built by self-assembly of the peptide and small gold cores, overall smaller than 50 nm which will allow the conjugation of more drug at the surface whilst incorporating the targeting element, therefore improving drug loading and sensitivity of targeting. This would also modify the radiosensitising properties of the system. The end goal of this work is to validate these findings in vivo and to ultimately submit this technology for clinical trials. One other remarkable point, is that even without targeting this technology is potentially deliverable in a stereotactic manner (directly into the brain) which would require a different animal model. (1) Setua, S., Ouberai, M., Piccirillo, S. G., Watts, C. & Welland, M. Cisplatin-tethered gold nanospheres for multimodal chemo-radiotherapy of glioblastoma. Nanoscale 6, 10865--10873 (2014) (2) Ruoslahti E., Bhatia S.N., Sailor M.J. Targeting of drugs and nanoparticles to tumors. J Cell Biol. 188(6):759-68 (2010)

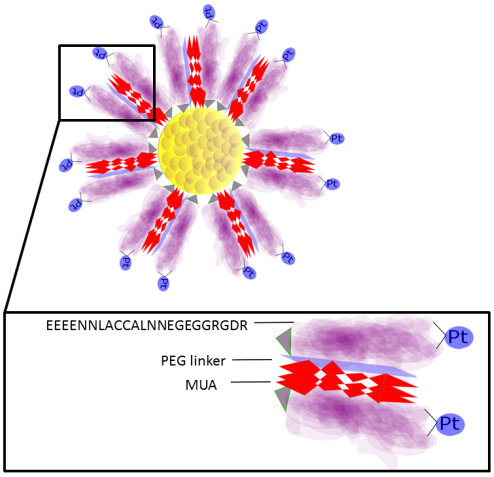


Annicfigure.png

# Activatable T1/T2 dual-mode MR imaging nanoplatform for enhancing accuracy by Fe/Mn oxide heteronanocrystals

**Thursday, 10th November - 17:42 - Nanomedecine & Nanobiology - Room 1 - Oral presentation - Abstract ID: 519**

***Mr. Myeong-Hoon Kim*** [1], ***Dr. Hye-Young Son*** [1], ***Ms. Ga-Yun Kim*** [1], ***Prof. Yong-Min Huh*** [1], ***Prof. Seungjoo Haam*** [1]

***1.*** *Yonsei University*

Introduction T1/T2 dual-mode contrast agents (DMCA) for magnetic resonance (MR) imaging have gained much interest for their ability to provide two complementary and reliable data within single instrument. However, most of the contrast agents are ``always ON'' systems exerting the MR contrast effect regardless of the interaction with biological targets; this can result in poor target-to-background ratios. Herein, we developed a redox-responsive activatable imaging nanosystem based on the Fe/Mn oxide core/shell heteronanocrystals functioning magnetic relaxation switch (MGRS) for T1/T2 dual-mode MR imaging. Mn3O4 shells were introduced to the nanoplatform to minimize the water proton interaction with the nanoprobe in normal condition before both immediate dissolution generating high-spin Mn2+ ions and MGRS activation under intracellular reducing environment. We investigated the OFF/ON operation mechanism of MGRS according to glutathione (GSH) levels on in vitro test, and confirmed the feasibility of the nanoprobes for in vivo T1/T2 MR imaging of tumor-bearing mice. Methods We synthesized Fe3O4@Mn3O4 core-shell heteronanocrystals through seed-mediated growth. As-prepared nanocrystals were encapsulated with PEG derivatives for the water-dispersibility and biocompatibility. MKN-45 gastric cancer cell line was used to evaluate feasibility of the nanoprobes for effective and activatable MR imaging performance. A xenograft tumor model was used to investigate in vivo tumor imaging with the nanoprobes. Results and discussion Fe3O4 and Mn3O4 were designed to be directly contacted as a core/shell heteronanocrystal structure to obtain efficient magnetic coupling between T2 and T1 materials. A popcorn-like shape and size (13.3 nm) after growth of Mn3O4 shells on the Fe3O4 nanospheres were confirmed in TEM and DLS results. Fe3O4@Mn3O4 nanoparticles were coated with polysorbate 80 to be dispersible in aqueous solution. We confirmed the redox-responsive ability of the nanoprobes by measuring its physicochemical changes (surface atomic composition, UV-vis absorbance, and MR contrast effects) after dispersion in the GSH solutions or cellular uptake. The nanoprobes showed highly enhanced T1/T2 relaxivities due to increased proton interactions and magnetic decoupling after dissolution of the Mn3O4 shells by redox reaction. We demonstrated potential utility of the nanoprobes as MR imaging agents in the animal studies showing clear T1/T2 contrast effects in the MR images.

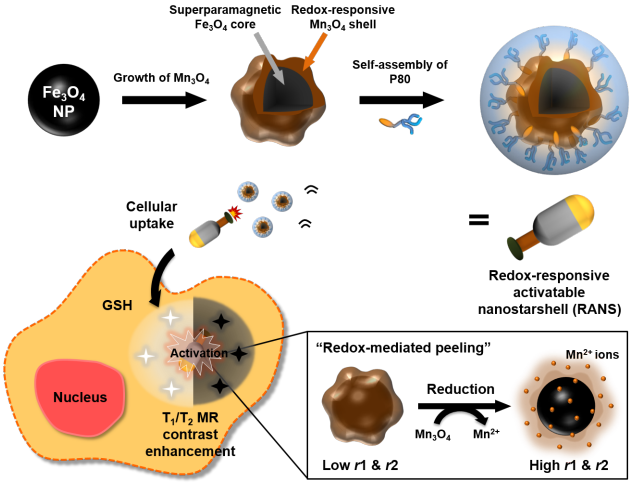
Superparamagnetic
$Fe_3O_4$ core
Redox-responsive
$Mn_3O_4$ shell
$Fe_3O_4$ NP
Growth of $Mn_3O_4$
Self-assembly of P80
Cellular uptake
Redox-responsive activatable nanostarshell (RANS)
GSH
Activation
Nucleus
$T_1/T_2$ MR contrast enhancement
"Redox-mediated peeling"
Reduction
$Mn_3O_4$
$Mn^{2+}$
$Mn^{2+}$ ions
Low r1 & r2
High r1 & r2

Figure.png

# Structural Investigation of the HS to LS Relaxation Dynamics in Spin Crossover compounds

**Thursday, 10th November - 16:00 - Electronics & Magnetics - Room 207 - Oral presentation - Abstract ID: 11**

***Ms. Teresa Delgado Pérez*** [1], ***Dr. Antoine Tissot*** [1], ***Dr. Céline Besnard*** [1], ***Dr. Laure Guénée*** [1], ***Prof. Andreas Hauser*** [1]

**1.** *University of Geneva*

Spin-crossover compounds are very topical, because of their possible applications in electronic and optical devices [1, 2]. Typically, d4-d7 transition metal ions can be converted from the low-spin (LS) to the high-spin (HS) state and vice versa with different external stimuli such as temperature, pressure, light or guest adsorption. At cryogenic temperatures, a photo-induced conversion from the LS stable state to the HS metastable state can be induced through the Light-Induced Excited Spin State Trapping (LIESST) effect [3]. Spin transitions are associated with large structural changes [1]. The metal-ligand bond lengths difference in iron(II) complexes of ~0.2 Å creates elastic interactions between the centres, resulting in cooperative effects that influence the thermal and light-induced spin crossover [2]. Therefore, structural analysis is very important for studying the thermal- and photo-induced spin-crossover phenomena. The investigation of the LS to HS photo-excitation and subsequent relaxation dynamics in the solid state is of particular importance for understanding the underlying physics associated with cooperative effects. In our studies Synchrotron X-Ray powder diffraction has been used to follow the structural changes of different compounds after photo-induced LS-to-HS conversion based on Light-Induced Excited Spin State Trapping (LIESST) at 10 K. In the case of the Hofmann clathrate [Fe(pz)Pt(CN)4] a complete study on the relaxation behaviour has been performed for six different particle sizes and a strong dependence of the relaxation mechanism with the particle size has been found [4]. In the case of the [Fe(n-Bu-im)3(tren)](PF6)2, for which two different spin crossover behaviours have been observed in the thermal transition depending on the sweeping rate of the temperature [5], spectroscopic studies show a plateau during the relaxation after LIESST when approximately half of the centres have relaxed back to the LS state indicating a specific structural feature at this composition. Synchrotron X-Ray powder diffraction reveals the occurrence of an order/disorder transition. In addition two different HS phases have been obtained by photoexcitation of the LS state at 10 and 80 K giving rise to different relaxation time scales.

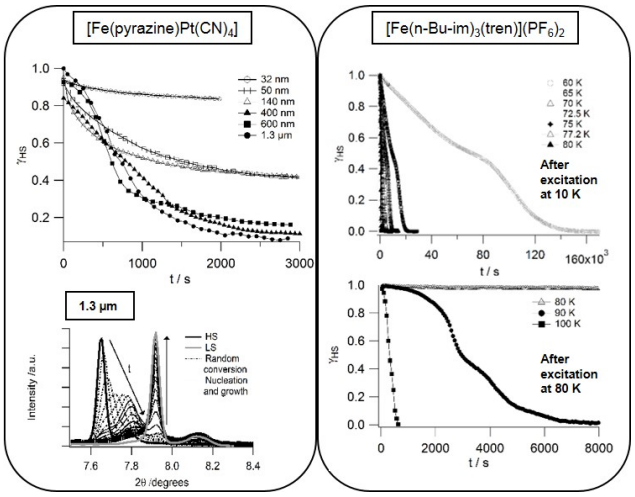
[Fe(pyrazine)Pt(CN)4]
32 nm
50 nm
140 nm
400 nm
600 nm
1.3 μm
γHS
t / s
1.3 μm
HS
LS
Random conversion
Nucleation and growth
Intensity /a.u.
2θ /degrees
[Fe(n-Bu-im)3(tren)](PF6)2
60 K
65 K
70 K
72.5 K
75 K
77.2 K
80 K
After excitation at 10 K
160x10^3
80 K
90 K
100 K
After excitation at 80 K

Picture.jpg

# Resistive switching in TiO2 nanocolumn arrays electrochemically grown

**Thursday, 10th November - 16:17 - Electronics & Magnetics - Room 207 - Oral presentation - Abstract ID: 498**

*Mr. Marian Marik* [1], *Dr. Alexander Mozalev* [1], *Dr. Jaromir Hubalek* [1], *Dr. Maria Bendova* [1]

*1. CEITEC - Central European Institute of Technology, Brno University of Technology*

Investigation of switching behavior of several metal oxides, which may have their resistance states modulated by voltage applied to or by current flowing through them, is nowadays a growing research field motivating researchers to prepare high-speed low-power nano-dimensional non-volatile Resistive Random Access Memory (ReRAM) devices. In such devices, a layer of metal oxide is usually sandwiched between two metallic electrodes for obtaining metal/semiconductor/metal structures. TiO2, among other metal oxides like Ta2O5, HfO2, ZrO2, ZnO, WO3, or NiO, is one of the most intensively used resistive switching materials because of many advantages, such as its versatile fabrication, wide band gap, and high dielectric constant.[1,2] Here we investigate the resistive switching behavior of TiO2 nanocolumn arrays prepared via the originally developed porous-anodic-alumina-assisted anodizing of Ti layers sputtered on a SiO2-coated Si wafer. The self-ordered TiO2 nanocolumns are fabricated using a one-step anodization procedure in oxalic acid at 40 V. This leads to growth of ~80 nm long columns embedded in the alumina matrix (Figure 1a). Thermal annealing is applied to alter electrical conductivity of the nanocolumns. For making a top electrical contact, the TiO2 columns are covered by gold electrochemically deposited into the pores. The electrode area is confined to about 104 μm2 by a combination of photolithography and chemical etching. The remaining Ti layer under the columns is used as the bottom electrode. Electrical characterization of the nanocolumn arrays by means of I(V) measurements shows resistive switching behavior after a formation cycle, manifested by a set process at negative polarization and a reset process at positive polarization of the Au electrode (Figure 1b). The ratio between the ON and OFF state resistivities ranges between 100 and 10000 whereas the set and reset voltage is temperature dependent. Thus, the TiO2 nanocolumn arrays developed here exhibit promising memristive properties. This research was supported by GAČR grant no. 15-23005Y and CEITEC 2020 (LQ1601). [1] W. B. Luo, et. al. Forming free resistive switching in Au/TiO2/Pt stack structure. Thin Solid Films, 2016, in press. [2] J. J. S. Yang, D. B. Strukov, D. R. Stewart. Memristive devices for computing. Nat. Nanotechnol. 2013, 8, 13--24.

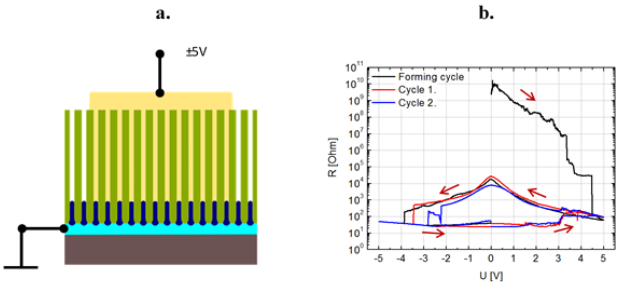


Figure 1. a and b.png

# SiAlON thin films on silicon and formation of nanofilaments with memristive properties

**Thursday, 10th November - 16:34 - Electronics & Magnetics - Room 207 - Oral presentation - Abstract ID: 352**

***Mr. Eduardo Marino*** [1], ***Prof. Blas Garrido*** [1], ***Dr. Sergi Hernandez*** [1], ***Mr. Oriol Blazquez*** [1]

**1.** *University of Barcelona*

Memristors are devices that change its resistance depending on the current that flows through. It is a reversible process where the material is typically cycled between two resistive states (ON conductive and OFF resistive) [1]. These changes are attributed to the generation of nanofilaments along the material, which can be interrupted and reconnected [2]. Silicon aluminum oxinitride (SiAlON) is well known for its mechanical and optoelectronic properties, and accidentally we found that nanolayers behaved like memristors. The purpose of this work consists in the study of SiAlON as a memristive material with outstanding properties. Devices were fabricated with a structure of a SiAlON thin film between two electrodes. The thin film of 165 nm was grown onto a Silicon substrate with the Pulsed Laser Deposition technique. Electrodes were obtained with the Electron Beam Evaporation by using a dark mask. Aluminum and Indium Tin Oxides (ITO) were used as electrodes; however the work was mainly focused in the use of aluminum. To measure changes in resistance, electrical tests were performed ramping up voltage and observing abrupt changes in intensity. The results showed an average resistance of 1 MΩ in the OFF state and 100 Ω in the ON; which represents a difference of four orders of magnitude between states (Figure 1.a). The conductive paths are very similar, except from the first process called the forming, which is more irregular due to the generation of nanofilaments. Resistive switching cycles were obtained by using alternate opposite voltages and the same voltage in both states. Apart from the two main states, it was possible to obtain different intermediate states by controlling the maximum voltage of the process (Figure 1.b). Devices maintained each state for a day and the processes may have characteristic repercussions in their surface. In conclusion, the formation of Al nanofilaments induces extremely good and controllable memristive properties in SiAlON. There is a change in more than four orders of magnitude of resistance between the two stable sates. The change between the states is very abrupt and extremely fast (faster than ns) and the devices appear ciclable without losing their memristive properties.

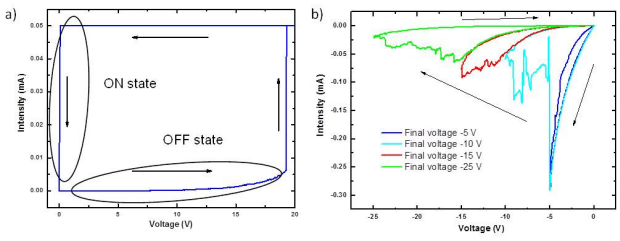


Figure1 abstract.jpg

# Comparative study of inorganic and hybrid ionogels as electrolyte for supercapacitors

**Thursday, 10th November - 16:51 - Electronics & Magnetics - Room 207 - Oral presentation - Abstract ID: 540**

***Ms. Ronak Janani*** [1], ***Dr. Heming Wang*** [1], ***Dr. Nicolas Farmilo*** [1], ***Dr. Alexander Roberts*** [2]

***1.*** *Sheffield Hallam,* ***2.*** *CATAPULT high value manufacturing, Warwick University*

Due to limitations of liquid electrolytes including toxicity, flammability and possibility of leakage, demand for a non-flammable solid electrolyte substitute for application in energy storage devices has increased drastically. Low temperature (<100°C) molten salts, also known as ionic liquids (ILs), have drawn attention of electrochemistry experts due to their great electrochemical properties and low volatility. In order to eliminate the possibility of leakage, ILs can be immobilized inside a solid/quasi-solid matrix. Such structure is referred to as ionogel. This work elucidates the physical, thermal and electrochemical characteristics of ionogels synthesized by different silica-based precursors with the aim of stressing how effective the choice of precursor can be. The herein reported ionogels have been synthesized through a straight forward in-situ sol-gel process. 1-ethyl-3- methylimidazolium trifluoromethanesulfonate, formic acid and various silica alkoxides were used as reactants. The prepared ionogels are categorized as either inorganic group or hybrid group. After completion of the gelation process, the ionogels were characterized using SEM, FTIR, Raman, and TGA. Their electrochemical performance for application in supercapacitors was also investigated using a combination of cycling voltammetry and EIS techniques. The findings evidenced a great influence of gel precursor on the morphology, pore structure and electrochemical behaviour of the gels. The SEM images, provided in Figure 1, show presence of a dense ``protective'' layer on the top surface of the hybrid gels while the morphology of the inorganic ionogels is shown to be homogeneous throughout their matrix. Furthermore, based on EIS analysis, inorganic ionogels have higher ionic conductivity ranging from 2 to 5 mS/cm while lower values are achieved with hybrid gel electrolytes (1-0.6 mS/cm). This difference in ionic conductivity resulted in capacitance values ranging from 60 to 20 F/g after 1000 voltammetric cycles while a capacitance of 70 F/g is achieved for a cell with pristine IL. Considerable difference in ionic conductivity can be attributed to diffusional barriers, poorly-connected pore structure and surface-hydrophobicity of hybrid electrolytes.

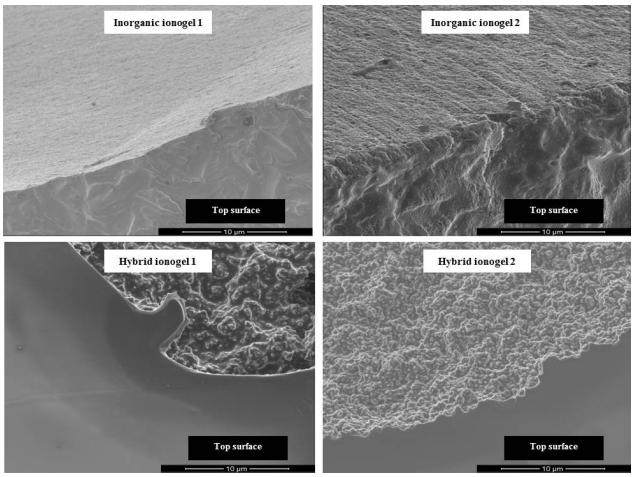
Inorganic ionogel 1
Top surface
10 µm
Inorganic ionogel 2
Top surface
10 µm
Hybrid ionogel 1
Top surface
10 µm
Hybrid ionogel 2
Top surface
10 µm

Figure 1.jpg

# Fabrication and characterization of ZnO/p-Si light-emitting devices by electron beam evaporation

**Thursday, 10th November - 17:08 - Electronics & Magnetics - Room 207 - Oral presentation - Abstract ID: 377**

***Mr. Pablo Vales [1], Mr. Oriol Blazquez [1], Dr. Julian López-vidrier [1], Dr. Sergi Hernandez [1], Prof. Blas Garrido [1]***

***1.*** *University of Barcelona*

ZnO is a direct and wide band-gap (Eg=3.37 eV) semiconductor with a large exciton binding energy (60 meV) and wurtzite crystalline structure under standard conditions. It is a non-toxic, earth-abundant, low-cost material compatible with silicon technology and transparent in the visible range, with tunable electrical conductivity depending on doping and post-annealing processes. It allows for a high-temperature and high-power operation, which gives this material a low noise generation and makes it suitable to sustain large electric fields. In this work we focused on the fabrication of light-emitting devices of ZnO thin films by electron beam evaporation, deposited on p-type silicon substrates [see Fig.1(a)]. ZnO thin films were fabricated using electron beam evaporation technique and subsequently annealed at 750 ºC for 1 hour in either N2 or air. Several characterization techniques were employed to determine their properties, such as SEM, XRD, Raman spectroscopy and PL. The electro-optical behavior of the devices was analyzed using optimized ZnO films by a probe station coupled to a monochromator. SEM images of the films displayed a textured surface with clear contrast in the grain boundaries, revealing that the thin films present a polycrystalline arrangement. XRD confirmed also that thin layers were highly oriented in the (002) direction and with a mean grain size of 40 nm. Raman scattering measurements revealed a good crystalline degree for all annealed samples. PL measurements exhibited optical emissions originated from defects and band-to-band exciton recombination processess. ZnO-based devices with a metal-oxide-semiconductor structure were fabricated from previous films by adding ITO and Al as top and bottom contacts, respectively. The devices present I-V curves that follow an exponential trend. Electrical measurements revealed higher conductivity in samples annealed in N2, attributed to a higher density of oxygen vacancies. The integrated electroluminescence exhibits an almost linear behavior with the injected current, which saturates at high injection regime [see Fig.1(b) and 1(c)]. Spectrally-resolved electroluminescence showed an emission related to defect states within the band-gap [see Fig.1(d) and 1(e)]. Finally, a photometric study revealed a CRI of 91.8 for our final devices. Thus, ZnO-Si heterostructures show potential to be used as an integrated light emitter.

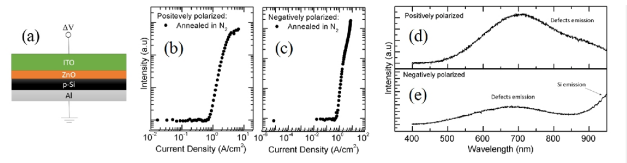


*Fig. 1.Scheme of the ZnO/Si device fabricated in the present work. (b) and (c) show the integrated EL as a function of current density for the samples annealed in $N_2$, for both positive and negative polarizations, respectively. (d) and (e) display the spectrally-resolved EL emission for the ZnO samples annealed in $N_2$, again for positive and negative polarizations.*

Figure1.jpg

# NATIVE FLUORESCENCE DETERMINATION OF TETRACYCLINE RESIDUES IN MILK PRODUCTS FOLLOWED BY SILICA-MODIFIED MAGNETIC NANOPARTICLES

**Thursday, 10th November - 17:25 - Electronics & Magnetics - Room 207 - Oral presentation - Abstract ID: 558**

***Mrs. Olena Khainakova*** [1], ***Prof. Vladymir Zaitsev*** [2], ***Dr. Natalia Kobylinska*** [2], ***Prof. Marta Elena Diaz Garcia*** [1]

***1.*** *University of Oviedo,* ***2.*** *Taras Shevchenko National University of Kyiv*

In recent years, antibiotics are widely used in food-producing animals not only for treatment of eat, but also therapeutically to maintain health and promot e growth. The presence of antibiotic's residues in food represents a risk for human health. The concentration of tetracycline in milk and milk products a maximum residue level of 100 μg/kg has been established. Various methods have been used for the determination of antibiotics: high-performance liquid chromatography, spectrophotometry, electrochemistry, fluorescence, mass spectroscopy and etc. Surface modified Fe3O4 are new kind functional materials, which have been widely used in sensing and biotechnology, etc. In this study, magnetite nanoparticles modified with ions Eu(III) was used for development of optical sensors for antibiotics determination. The magnetic nanoparticles coated with a thin silica oxide layer have been synthesized by combining co-precepitation and hydrothermal treatments. The TEM image of Fe3O4 nanoparticles prepared in aqueous medium reveals a size distribution in the range of 10.0±2.0 nm and silica shell about 2-3 nm. The magnetic dipole attraction decreases quickly with the increase of size of particles and thickness of silica shell. The using of sulfonate polyelectrolytes (polyvinyl and polystyrene sulfonic acids) allows to obtained core-shell particles with ion-exchange properties. The more high adsorption capacity of europium(III) was observed for magnetite modified polyvinyl sulfonic acids. Sorption of europium(III) was quite rapid (15 min). Increasing ionic straight (0.01 to 0.5 M) decreased the sorption extent only at higher sorbate to sorbent rations suggesting the dominance of inner-sphere type complexes at low equilibrium tetracycline concentrations. The optimum concentration of europium ions on surface magnetite nanoparticles for the determination of trace amounts of analyte in aqua solution is 2.5•10-5 mol/l for Tetracycline in concentration range 1.0•10-5 M--1.0•10-9 M. A preliminary series of experiments were obtained in water solution of tetracycline and showed that maximum intensity was achieved for pH close to 7-7.2. Similar measurements run on blank milk samples evidenced a different behavior. In the optimal experimental conditions, linear relationships were obtained, between intensity of fluorescence and concentration of tetracycline in milk samples. Thus magnetic nanoparticles with higher sorption capacity to the studied tetracycline were obtained.

# Magnetoresistance Aharonov--Bohm oscillations in type-II InAsSbP ellipsoidal quantum dots

**Thursday, 10th November - 17:42 - Electronics & Magnetics - Room 207 - Oral presentation - Abstract ID: 415**

***Prof. Karen Gambaryan*** [1]

*1. Yerevan State University*

The InAsSbP composition type-II ellipsoidal quantum dots (QDs) are grown on InAs(100) substrate from In-As-Sb-P quaternary liquid phase in Stranski--Krastanow growth mode. Device structures in the form of photoconductive cells are prepared for investigations. Magnetospectroscopy and high-precision capacitance spectrometry are used to explore the QDs structure's electric sheet resistance in magnetic field and the capacitance law at lateral current flow. Aharonov--Bohm (AB) oscillations with the period of δB=0.38±0.04 T are found on the magnetoresistance curve at both room and liquid nitrogen temperatures. The influence of the QDs size distribution on the period of AB oscillations is investigated. The values for both major and minor semiaxes of ellipsoidal QDs were theoretically calculated by the equation for the period of Aharonov-Bohm oscillations. Comparison of calculated and experimentally measured values shows that they are coincide with high accuracy. The magnetoresistance hysteresis equals to ~50 mΩ and ~400 mΩ is revealed at room and liquid nitrogen temperature, respectively. At increasing with continuously decreasing of applied voltage, the capacitance hysteresis (CH) and contra-directional oscillations are also detected. Behavior of the CH value versus applied voltage frequency in the range of f = 103--106 Hz is investigated. It is shown that the CH value decreases with increasing frequency up to 104 Hz, becomes constant (slightly increases) in the range of 104--105 Hz, continues decreasing and equals to zero at f0=7×105 Hz. The time constant for the QDs R--C parallel circuit (generator) is calculated.

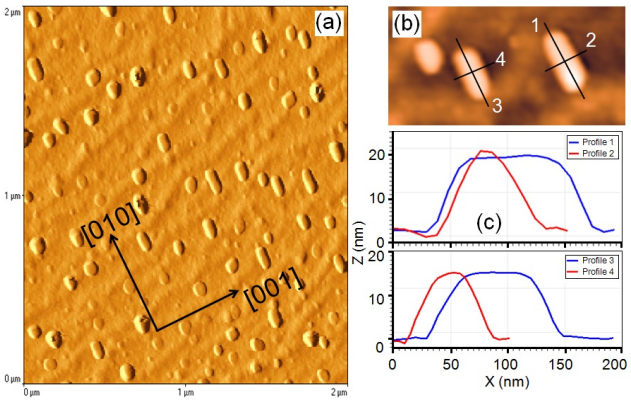


Ellipsoidal quantum dots.jpg

# The synthesis of N-doped TiO2/CdS nanocomposites for quantum dots-sensitized solar cells

**Thursday, 10th November - 17:59 - Electronics & Magnetics - Room 207 - Oral presentation - Abstract ID: 555**

***Ms. Cahyorini Kusumawardani*** [1]

***1.*** *Yogyakarta State University*

The N-doped TiO2/CdS nanocomposites had been synthesized by in situ formation of Cadmium Sulfide (CdS) quantum dots on N-doped TiO2 thin films through successive ionic layer adsorption and reaction (SILAR) method. The synthesis was done using (Cd(NO3)2 9 H2O) as Cd precursor and natrium sulfide (Na2S) as S source, which was performed by dipping the N-doped TiO2 thin film in the ethanolic precursor solutions as one synthesis cycle. The CdS contents and thicknesses were varied based on CdS synthesis cycle. The resulting N-doped TiO2/CdS nanocomposites were characterized using XRD, UV Vis Spectroscopy and SEM/EDX. The more cycles applied resulted in a higher CdS amount on N-doped TiO2 thin film which provided the more intense absorption in the visible light region. The N-doped TiO2/CdS nanocomposites with different CdS concentrations were then applied as photoanode of the quantum dots-sensitized solar cells (QDSSC) system. The results indicated that the concentration of CdS on TiO2/CdS nanocomposites highly influences the overall efficiency of the solar cell system.

# A Study on the Properties of Pure SnO2 Gas Sensors

**Thursday, 10th November - 18:16 - Electronics & Magnetics - Room 207 - Oral presentation - Abstract ID: 653**

***Dr. TARIK ASAR*** [1]***, Ms. Emine BOYALI*** [1]***, Mr. Burak KORKMAZ*** [1]***, Dr. Saime Şebnem ÇETİN*** [1]***, Prof. Süleyman ÖZÇELİK*** [1]

***1.*** *Gazi University*

1. Introduction -- SnO2 have been commonly used in its potential applications such as gas sensors, solar cells, display devices. It has also noteworthy characteristics such as high transmittance in the ultraviolet-visible region and high reflectance in infrared region, easy doping and easy tailoring. In this study, the structural, optical and electrical properties the SnO2 gas sensors have been investigated with changing SnO2 target power, butane gas concentration, applied voltage, and operating temperature. 2. Experimental -- SnO2 thin films were deposited on n-Si (100) and glass substrates with 50W and 100W SnO2 target power by using RF sputtering technique at room temperature. The other deposition parameters were kept constant at whole depositions. They were called as SnO2-1 (50W) and SnO2-2 (100W). After the deposition processes, the thicknesses of the thin films were confirmed by a stylus type profilometer. The structural and optical properties of the thin films were analyzed by the X-Ray diffractometer and UV-Visible spectrometer. Then, the fabrication processes were completed with the formation of the heaters and interdigital electrodes by the deposition of Pt metals with the thickness of 1000 nm and 500 nm, respectively. The gas sensors were tested with the different butane gas concentrations (0-750 ppm), applied voltages (0-5.0 V) and operating temperatures (100°C and 300 °C). 3. Results and Discussion -- The X-Ray diffraction measurements showed that the SnO2 thin films have SnO2 diffraction peaks at different peak positions. That means, the deposited SnO2 thin films have polycrystalline with tetragonal structure. It was obtained from the analyzing UV-Visible results that; the bandgap values were found around 3.8 eV. As can be seen from the Sensitivity - Gas Concentration graph that, the SnO2-2 gas sensor with 300 °C operating temperature has the best sensitivities at all butane concentrations. 4. Conclusions -- The results showed that the best gas sensors properties were obtained at 300 °C operating temperature for the SnO2-2 gas sensor which is deposited by using 100W target power. 5. Acknowledgments -- This work is supported by the MD and MSIT of Turkey with Project No: 2011K120290 and 0633.STZ.2014, respectively.

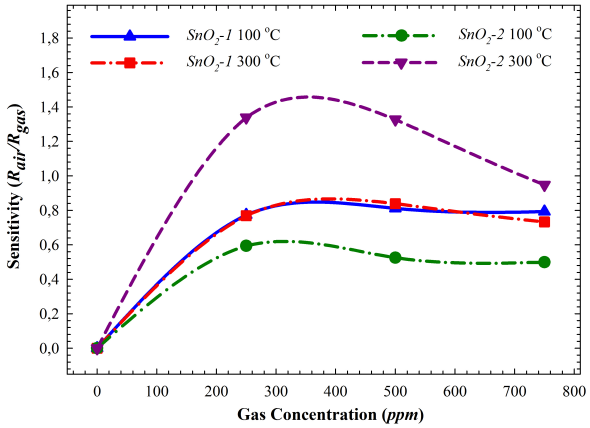


Sensitivity.jpg

# Fully Developed Mixed Convection Flow of a Nanofluid in a Vertical Channel

**Thursday, 10th November - 16:00 - Nanotechnology For Environment & Energy - Auditorium - Oral presentation - Abstract ID: 434**

***Dr. Fahad Al-Amri*** [1]

***1.*** *University of Dammam*

A closed form analytical solution of laminar mixed convection heat transfer of nanofluid inside two vertical parallel plates taking into account the Brownian motion and thermophoresis effects is presented in the fully developed region under the thermal boundary conditions of first and fourth kinds. Four different kinds of nano-sized solid particles which have different thermophysical properties suspended in water are considered. Closed form analytical expressions of velocity and temperature fields, pressure gradient, nanoparticle concentration profiles, and Nusslet number are illustrated. The effects of controlling parameters, namely buoyancy parameter, thermal conductivity solid/fluid ratio, and volume fraction on the hydrodynamic and heat transfer parameters such as pressure gradient and Nusslet number are in detail discussed. It is found that the Nusslet number increases with increasing buoyancy parameter and volume fraction. However, the pressure drop is found to increase with volume fraction and decrease with buoyancy parameter. In addition, the results show that, for upward mixed convection flow, the pressure drop due to the addition of nano-sized solid particles into the base fluid can be overcome by the buoyancy forces. The critical values of the buoyancy parameter at which the buoyancy forces balance the viscous forces are obtained and presented.

# Application of Graphene Based Nanoadsorbents in Produced-water Treatment for Removal of Dissolved Oil

**Thursday, 10th November - 16:17 - Nanotechnology For Environment & Energy - Auditorium - Oral presentation - Abstract ID: 337**

***Mr. Ahmad Diraki*** [1]***, Dr. Ahmed Abdala*** [2]

***1.*** *Qatar Foundation Research and Development (QR R&D), and Hamad Bin Khalifa University (HBKU),* ***2.*** *Qatar Environment and Energy Research Institute (QEERI), and Hamad Bin Khalifa University (HBKU)*

Co-produced water is the largest waste stream produced during oil and gas production. It contains a mixture of hydrocarbons, suspended and dissolved solids, inorganic substances and production chemicals. Current technology such as hydrocyclones and API gravity can remove suspended and dispersed oil from produced water down to 40 ppm. However, reducing oil content to few ppms is required to enable any beneficial use of produced water or to meet the recent strict environmental regulations for disposal of produced water. Therefore, post-treatment of produced water to remove emulsified and dissolved oil to acceptable levels is required. In this presentation, we test using different graphene based nanomaterials, including graphene nanoplatelet (GNP), graphene oxide (GO), thermally reduced graphene (TRG), and graphene-iron oxide nancomposite (G-Fe3O4) as adsorbents for removal of diesel from water. The nanomaterials are characterized by Scanning electron microscope (SEM), Transmission electron microscopy (TEM), X-ray diffraction (XRD), X-ray photospectroscopy (XPS), Thermal Gravimeteric analysis (TGA), and Brunnauer-Emmett-Teller (BET) surface area measurement. The initial diesel concentration was varied between 25-200 ppm, the diesel to adsorbent ratio ranged between 50 and 8000 mg/g, and the salinity (NaCl) was between 0 and 100,000 ppm. The concentration of diesel is measured using Total Organic Carbon (TOC). Our batch and column experiment results indicated that graphene based material has very rapid removal of diesel and more than 90% removal can be achieved in less than 5 min. More interestingly, the removal efficiency and the adsorption capacity increase significantly with salinity for all the adsorbents. The results were analyzed in light of the various adsorption isotherm. Our results indicate that graphene based nanomaterials are capable of reducing the oil content of high salinity produced water to less than 5 ppm. Moreover, different approaches for the regeneration of the graphene materials are tested and will be discussed.

# CTAB-coated magnetic nanoparticles for removal of direct yellow 12 from aqueous solutions

**Thursday, 10th November - 16:34 - Nanotechnology For Environment & Energy - Auditorium - Oral presentation - Abstract ID: 191**

***Dr. Alex Fabiano Campos*** [1], ***Mr. Paulo Henrique Michels Brito*** [2], ***Dr. Renata Aquino*** [1], ***Dr. Franciscarlos Gomes da Silva*** [1], ***Dr. Jerome Depeyrot*** [1]

***1.*** *Universidade de Brasília,* ***2.*** *Universidade de Brasila*

The textile and dye manufacturing industries produce large quantities of dangerous dyes, pigments and metals with a high potential to pollute wastewaters. In this context, some methods for color removal from waters and wastewaters are available such as membrane separation, biologic degradation, chemical oxidation, coagulation and flocculation [1]. More recently, some methods based on magnetically assisted chemical separation have been proposed to be more efficient and produce less waste [2]. In this work, we investigate the removal of direct yellow 12 (DY12) from aqueous solutions using magnetic nanoadsorbents based on ferrite nanoparticles (NP) modified with cetyltrimethylammonium bromide (CTAB). The nanoadsorbents were synthesized using the hydrothermal coprecipitation method in alkaline medium followed by a surface treatment with Fe(NO3)3 leading to CoFe2O4@gamma-Fe2O3 core-shell NP. The surface modification was carried out by mixing the NP and CTAB in aqueous solution at pH = 10 with sonication for 15 min. The influence of time, pH and initial dye concentration were evaluated from batch studies using 0.5 g/L of the nanoadsorbent. After chemical adsorption, the NP were separated using a hand-held magnet and the final concentration of DY12 in decanted solution was determined by UV-VIS spectroscopy at 395 nm. The results of the batch studies were analyzed in the framework of Langmuir and Freundlich models in order to evaluate the maximum adsorption capacity and the extent of affinity. The kinetics data were analyzed with pseudo-first order and pseudo second-order models. It was evidenced that the adsorption reached equilibrium within 30 min and it was independent of initial DY12 concentration. The maximum adsorption occurred at pH 5.0 leading to almost 100% of pollutant removal. The dye adsorption onto the magnetic adsorbents well followed the pseudo-second-order rate indicating that the rate-limiting step involves electrostatic forces between DY12 and nanoadsorbents. Finally, in the view of these results, the developed CTAB coated NP can be used as a low cost and effective adsorbents in removal of DY12 from wastewater. References: [1] M. Ghaedi et al, Chem. Eng. J. 187, 133 (2012) [2] N. M. Mahmoodi et al, J. Environ. Health Sci. Eng. 12, 96 (2014)

# Heavy metal adsorption by mercapto and amine functionalized silica aerogel-like materials

**Thursday, 10th November - 16:51 - Nanotechnology For Environment & Energy - Auditorium - Oral presentation - Abstract ID: 609**

***Mr. João Vareda*** [1]***, Prof. Luisa Durães*** [1]

***1.*** *CIEPQPF, Department of Chemical Engineering, University of Coimbra, Rua Sílvio Lima, 3030-790 Coimbra, Portugal*

The pollution by heavy metals is a serious problem of today's world. Both soils and water courses are affected by this issue as the two are very intertwined. In both media, heavy metals exist as cations in solution, the most dangerous form of these chemical elements, and adsorption appears as an adequate process to remove these contaminants. Silica based aerogels are incredible nanostructured materials that feature many interesting properties. Amongst them is the ability to tailor their surface chemistry, that allows the development of tailored new adsorbents for the removal of heavy metals from contaminated media. Using triethoxymethylsilane, tetraethyl orthosilicate, (3-aminopropyl) trimethoxysilane and/or (3-mercaptopropyl)trimethoxysilane the new adsorbents were prepared (Fig. 1) using sol-gel chemistry to remove the heavy metals most significant for Iberian soils. Because silica is a natural compound that exists in large amounts and forms in the environment, these new adsorbents are not armful in this context. The new adsorbents were ground into fine powders, sieved and assessed via batch sorption equilibrium and kinetic tests with Ni(II), Zn(II), Cd(II) and Cr(III) in single-metal solutions. The equilibrium tests reveal that the adsorbents show affinity towards these cations and that the removal of the contaminants via sorption is very efficient, achieving high values (results for metal uptake ranges from ~40 mg/g up to ~130 mg/g at an initial concentration of 500 ppm of cation with 0.09 g of adsorbent). The adoption process is very fast, being the equilibrium concentration achieved up to one hour for some metals and in about two hours for the remaining ones. Cation mixtures of these metals were also tested with these adsorbents. Acknowledgment: Work developed under the project ``AeroMCatch -- Silica Aerogels for Remediation of Soils Contaminated with Heavy Metals'' (Process No 141735), by João Vareda and University of Coimbra, funded by Fundação Calouste Gulbenkian (Portugal), through the ``Programa de Estímulo à Investigação 2015''. Keywords: Heavy metal; Aerogel-like materials; Adsorption; Organically-modified silica; Iberian Peninsula pollutants

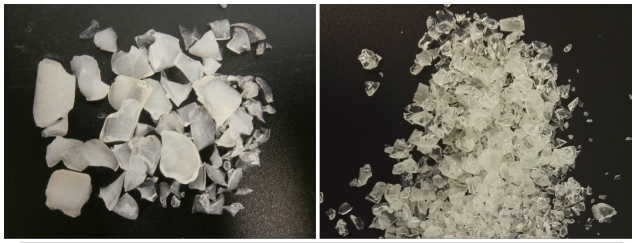

Fig. 1- Photograph of the two newly developed adsorbents (functionalized silica aerogel-like materials).

Fig1.png

# Design and fabrication of printed Graphene paper based micro-supercapacitor device with a Redox-active electrolyte

**Thursday, 10th November - 17:08 - Nanotechnology For Environment & Energy - Auditorium - Oral presentation - Abstract ID: 499**

***Ms. Bhawna Nagar*** [1]***, Dr. Deepak Dubal*** [1]***, Mr. Luis Pires*** [1]***, Prof. Arben Merkoçi*** [1]***, Prof. Pedro Gomez-romero*** [1]

***1.*** *Catalan Institute of Nanoscience and Nanotechnology (ICN2), CSIC and The Barcelona Institute of Science and Technology (BIST)*

Introduction Inspired by future needs of flexible, simple and low-cost energy storage devices, we designed smart graphene based micro-supercapacitors on ordinary paper substrates using redox-active aqueous electrolytes which can have great applications in portable electronics. This printed graphene device exhibited a maximum volumetric capacitance of 87.6 mF/cm3 (1.95 mF/cm2) at 3.2mA/cm3. Later, the performance was tested in hybrid electrolyte which was prepared by adding a redox-active species (potassium iodide, KI) in 1 M H2SO4. The results were remarkably improved with excellent volumetric capacitance of 813 mF/cm3 at 37.5 mA/cm3 (30.7 mF/cm2) (one order of magnitude higher). Method Briefly, graphene dispersion in water (2mg/ml) was printed over the two sides of conventional paper without any pre-treatment by stamping technique [1]. Further the printed electrodes were then soaked in either H2SO4 or H2SO4 containing different concentrations of KI (0.05 M, 0.1 M and 0.2 M) for 5 min and used for further measurements. All the values are given normalized per volume (cm3) of the total device. Results and discussion Figure 1a shows the TEM image of the graphene nanosheet which shows that the nanosheets are thin and transparent with extra-large size, inset is the electron diffraction pattern that confirms the formation of graphene. Figure 1(b) show the cyclic voltammetry (CV) curves in conventional H2SO4 and KI-doped H2SO4 electrolyte. It is revealed that area under the CV curves increases and is distorted from ideal rectangular shape (obtained from EDLC) suggesting increase in total capacitance and involvement of redox active KI. Galvanostatic charge/discharge curves are strongly in agreement with CV results (see Figure 1 c) and shows prolonged time for discharge indicating high energy and capacitance. The maximum volumetric capacitance was found to be 813 mF/cm3 for 0.1M KI+H2SO4 electrolyte which is one order of magnitude higher than the conventional H2SO4 electrolyte (Fig. 1d). The device achieved maximum energy and power densities of 0.29 mWh/cm3 and 73.6 mW/cm3, respectively, Figure 1(e). Finally, Figure 1(f) shows 97% capacitance retention over 1000 charge-discharge cycles for this device. References [1] Luis Baptista-Pires, Carmen C. Mayorga-Martínez, Mariana Medina-Sanchez, Helena Monton, and Arben Merkoci, ACS Nano 2016, 10, 853−860

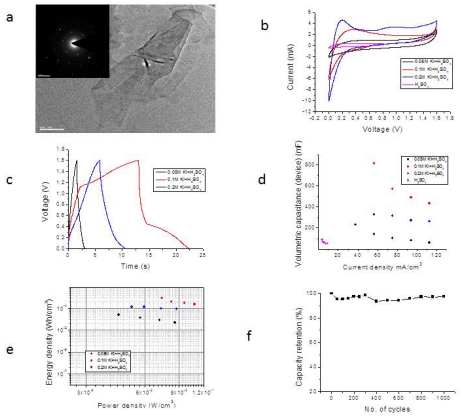


Fig. 1(a) TEM of graphene sheet, inset electron diffraction pattern (100 nm scale), (b, c) CV curves and CD cycles in different electrolyte, (d) Volumetric capacitance in different electrolytes, (e) Ragone plot and (f) Stability performance of the device upto 1000 cycle.

Abstarct image.jpg

# Effect of confinement inside CNTs for improving dehydrogenation from MXH4 clusters where M = Na, Li and X = Al, B

**Thursday, 10th November - 17:25 - Nanotechnology For Environment & Energy - Auditorium - Oral presentation - Abstract ID: 557**

***Dr. Hitesh Sharma*** [1], ***Mrs. Meenakshi Malhotra*** [1], ***Mrs. Kiranjeet Bedi*** [2]

***1.*** *IKG Punjab Technical University Jalandhar, Kapurthala,* ***2.*** *Punjab Agricultural University, Ludhiana*

Carbon nanomaterials such as fullerenes, CNTs and graphene have been reported as effective catalysts in improving the desorption behavior of complex metal hydrides. In comparison to catalytic effect, nanoconfinement plays dominant role in improving the dehydrogenation of LiBH4. We present results of our investigation into the effect of confinement of MXH4, where M = Na, Li and X = Al, B inside carbon nanotubes (CNTs). The calculations have been performed using density functional theory. NaAlH4, NaBH4, LiAlH4 and LiBH4 clusters were confined inside (9,0), (10,0) and (11,0) CNTs diameter of 7.47 Å , 7.87 Å , 8.73 Å respectively. The MXH4 interacts strongly with the surface atoms of CNT and CNT (11,0) is found to be the smallest stable system for confinement of MXH4 clusters. Hydrogen release energy(EHre) of NaAlH4 decreases sharply by 68.3%, w.r.t pure NaAlH4 cluster when confined inside CNT(11,0). Similarly, in CNT (11,0) EHre decreases by 38.1 % for LiAlH4, 12.7 % for NaBH4 and 19.1 % for LiBH4. The results can be interpreted in terms of charge transfer between the CNT and confined MXH4 clusters. Thus, resulting confinement had a profound effect in improving the energetics of complex metal hydrides without catalyst. The results provide an outline for extending the work to larger nanoparticles of metal hydrides inside CNTs of larger diameters and other carbon nanostructures.

# Effect of Undensified Silica Fume on the Dispersion of Carbon Nanotubes Within a Cementitious Composite

**Thursday, 10th November - 17:42 - Nanotechnology For Environment & Energy - Auditorium - Oral presentation - Abstract ID: 179**

***Mr. Salam Alrekabi*** [1], ***Prof. Andy Cundy*** [1], ***Dr. Andreas Lampropoulos*** [1], ***Prof. Raymond Whitby*** [2], ***Dr. Irina N Savina*** [1]

***1.*** *University of Brighton,* ***2.*** *Nazarbayev University*

The synergistic effect of multi-walled carbon nanotubes (MWCNTs) with different percentages (5%, 10%, 15%) of Undensified Silica Fume (USF) on the mechanical (compressive and direct tensile strengths) and microstructural properties (through Scanning Electron Microscopy) of cementitious composites has been studied. In the current study, USF was used to enhance the dispersion of nanotubes in the composite due to its small particle size, and to improve the bond between the nanotubes and the cementitious matrix. Ultrasonication techniques were employed to aid the dispersion of MWCNTs in water in the presence of superplasticizer as a dispersion agent. The experimental results indicate that incorporation of USF can considerably improve the dispersion of nanotubes (Fig.1), with subsequent enhancement of composite mechanical performance. This enhancement can be attributed to a reduction in the porosity of the cementitious composites, and improved crack arresting properties. Cementitious composites with hybrid incorporation of MWCNTs (0.025% by cement weight) and 10% USF showed a 36% and 22% increase in compressive strength at 3 and 28 days curing respectively.

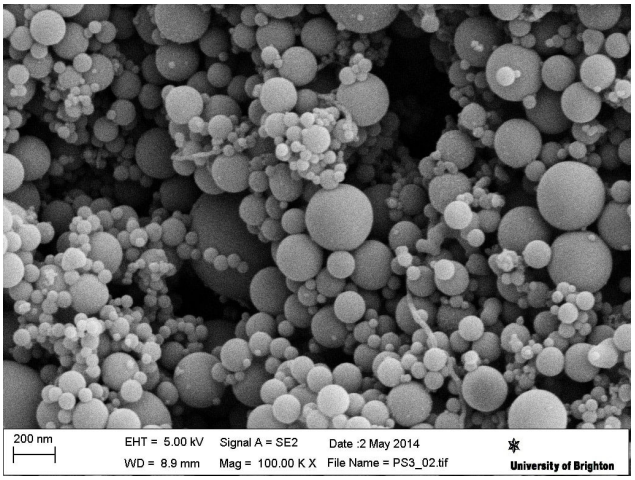


Fig-1.jpg

# Colloidal Au-Ag-Chalcogen-Based Ternary Nanocrystals for Energy Conversion Applications

**Thursday, 10th November - 17:59 - Nanotechnology For Environment & Energy - Auditorium - Oral presentation - Abstract ID: 59**

***Dr. Albert Figuerola*** [1], ***Ms. Mariona Dalmases*** [1], ***Dr. Maria Ibáñez*** [2], ***Mr. Pau Torruella*** [1], ***Dr. Víctor Fernàndez-Altable*** [1], ***Mr. Luis López-Conesa*** [1], ***Ms. Doris Cadavid*** [3], ***Ms. Laura Piveteau*** [2], ***Dr. Maarten Nachtegaal*** [4], ***Prof. Jordi Llorca*** [5], ***Prof. Maria Luisa Ruiz-González*** [6], ***Dr. Sonia Estrade*** [1], ***Prof. Francesca Peiró*** [1], ***Prof. Maksym V. Kovalenko*** [2], ***Dr. Andreu Cabot*** [3]

***1.*** *University of Barcelona,* ***2.*** *ETH Zurich,* ***3.*** *Catalonia Energy Research Institute (IREC),* ***4.*** *Paul Scherrer Institute,* ***5.*** *Universitat Politècnica de Catalunya,* ***6.*** *Universidad Complutense de Madrid*

The optimization of a material functionality requires both the rational design and precise engineering of its structural and chemical parameters. In this work, we show how colloidal chemistry is an excellent synthetic choice for the synthesis of homogeneous and compositionally complex novel nanostructured systems with potential application in the energy conversion field. Specifically, the Au-Ag-chalcogen system has been explored from a synthetic point of view, leading to a set of silver chalcogenide-based hybrid and ternary nanocrystals, including the synthesis of unusual ternary AgxAuyXz (where X = S, Se, Te) phases with different stoichiometry. A comprehensive structural and chemical characterization of all nanomaterials proved their homogeneity and the high degree of compositional control achieved. The work is complemented with the thermal and electric characterization of a ternary Au-Ag-Se nanocomposite with promising results: we found that the use of the ternary nanocomposite represents a clear improvement in terms of thermoelectric energy conversion, compared to a binary Ag-Se nanocomposite analogue.

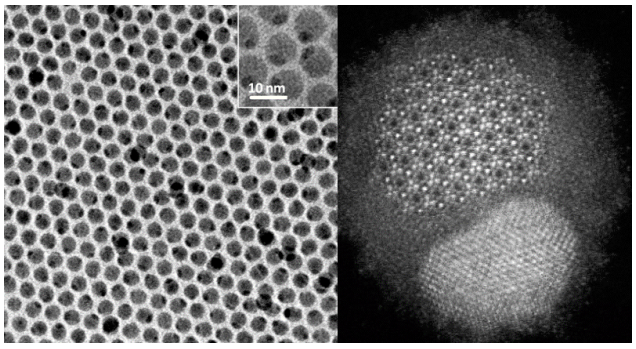


Figure.png

# Electrochemical Reduction of Carbon Dioxide on Nano-Copper Films Modified with Polymer of Intrinsic Microporosity

**Thursday, 10th November - 18:16 - Nanotechnology For Environment & Energy - Auditorium - Oral presentation - Abstract ID: 88**

***Mr. Sunyhik Ahn*** [1], ***Dr. Mariolino Carta*** [2], ***Prof. Neil Mckeown*** [2], ***Prof. Frank Marken*** [3], ***Prof. Andrew Barron*** [1], ***Dr. Enrico Andreoli*** [1]

***1.*** *Energy Safety Research Institute, Swansea University,* ***2.*** *University of Edinburgh,* ***3.*** *University of Bath*

Copper nanoparticles offer favourable activity and selectivity in reducing carbon dioxide into value added carbaneous products, but suffers from low material stability. Polymers of intrinsic microporosity (PIM) utilised as a protective layer for heterogeneous electro-catalysts can offer improved material stability by i) retarding Ostwald ripening effects in nanoparticle electrocatalysts, ii) protecting nanoparticles from poisoning effects by acting as a filter against large bio-molecules, and iii) immobilising catalysts which would otherwise leach out or dissolve in solution1-3. Here, a thin layer of PIM-EA-TB-H2 (BET surface area >1000m2g-1) is utilised as a protective film for copper nanoparticles. It is shown that the copper-PIM composite film results in significant improvements in catalyst stability under carbon dioxide electrolysis conditions. Effects on mass transport and host-substrate interactions resulting from the presence of the PIM surface layer are considered and the rate limiting process in the catalytic scheme is investigated. Figure 1. TEM image of nano-copper embedded in polymer of intrinsic microporosity. 1. D He, Y Rong, Z Kou, S Mu, T Peng, M Carta, NB McKeown, F Marken, Electroch. Commun. 59, p. 72, 2015 2. A Kolodziej, SD Ahn, M Carta, R Malpass-Evans, NB McKeown, F Marken, Electrochimica Acta, 160, p. 195, 2015 3. SD Ahn, A Kolodziej, M Carta, NB McKeown, A Buchard, F Marken, Electrocatalysis, 7, p. 70, 2016

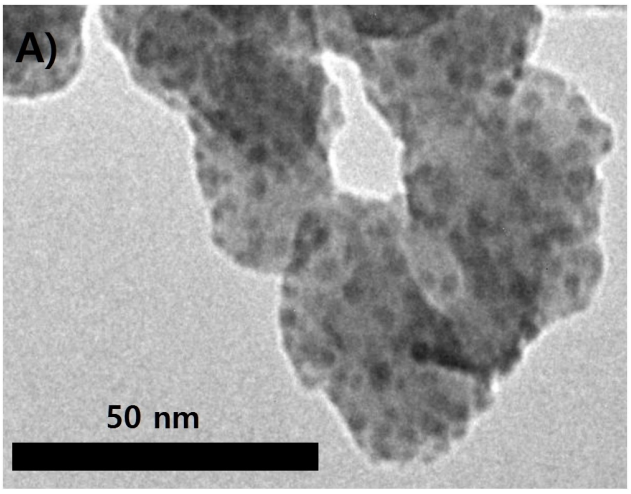


Figure 1 tem image.jpg

# Plasmonic nanostructures for catalysis and sensing

**Friday, 11th November - 09:00 - Plenary Speeches - Auditorium - Oral presentation - Abstract ID: 722**

***Prof. isabel pastoriza-santos*** [1]

***1.*** *University of Vigo*

Over the years, colloidal plasmonic nanoparticles have emerged as important building blocks of modern nanoscience and nanotechnology to deal with a wide range of applications including electronics, energy, medicine, catalysis, biosensing, imaging and therapy. The size- and shape-dependent optical properties of plasmonic nanoparticles make crucial the development of synthetic routes which lead to uniform nanoparticles with well-defined morphologies. On the other hand the assembly of nanoparticles has quickly evolved due to the resulting collective properties, which are highly enhanced over those of the individual particles. In this communication we report the fabrication of different SERS-active platforms based on plasmonic nanoparticles and assembies for catalysis and sensing. For instance, we will show a robust and recyclable ``dip-catalyst'' based on a gold nanoparticle (Au NP)--loaded filter paper composite, prepared by dip-coating. While acting as catalysts, the composites display excellent SERS efficiency, allowing the real-time monitoring of chemical reactions. Besides we present the self-assembly of highly uniform Au octahedra into uniform supercrystals (Figure 1) with the use of microevaporation, microfluidic technique, which controls the evaporation process spatially and temporally. Moreover, these plasmonic substrates made of supercrystals exhibit high and uniform SERS signals over extended areas with intensities increasing with the Au nanoparticle size. Finally, we demonstrate the fabrication of a novel plasmonic system based on Pd which show tunable optical response in the NIR region as well as good capabilities for catalysis and H2 sensing.

# Growth of nanowires with periodic morphologies via the vapor-liquid-solid mechanism

**Friday, 11th November - 09:35 - Plenary Speeches - Auditorium - Oral presentation - Abstract ID: 725**

***Prof. Chun-Sing Lee*** [1]

***1.*** *Center of Super-Diamond & Advanced Films (COSDAF), City University of Hong Kong*

The vapor-liquid-solid (VLS) process has been widely used to growth different one-dimensional nanostructures. Among these nanostructures, some show periodic changes in morphology (e.g. diameter oscillation). Our analysis show that the periodic morphological changes in a wide ranges of periodic 1D nanostructures can in fact be described by two simple linear relations: (1) inverse of the periodic spacing along the length direction follows an arithmetic sequence; and (2) the periodic spacing in the growth direction varies linearly with the diameter of the nanostructure (figure 1). These two simple relations can be explained by a surface curvature oscillation model in which the surface tension in a VLS growth system is strongly modulated by the nanometer size effect. Figure 1: Periodic Si nanodots obtained by VLS growth. (a) A TEM image of the product. (b) An HRTEM image of a nanodot in (a). (c) Plot of the 1/L against serial number. (d) Plot of diameter of Si nanodots against L.

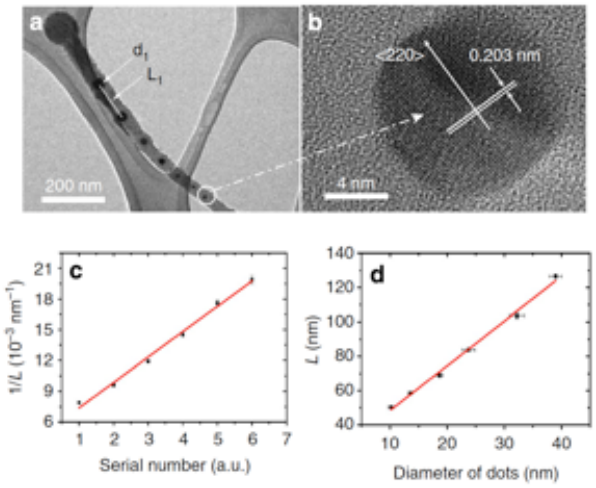


Figure 1.png

# Chemical, Structural and Surface Transformations in Nanocrystals

**Friday, 11th November - 10:45 - Plenary Speeches - Auditorium - Oral presentation - Abstract ID: 720**

***Prof. Liberato Manna*** [1]

***1.*** *Istituto Italiano di Tecnologia*

Nanocrystals (NCs) are among the most exploited nanomaterials to date due to their extreme versatility. A major focus of the talk will be on the recent progress on the study of chemical, structural and surface transformations in nanostructures, via both cation and anion exchange, as well as initiated by irradiation or by thermal annealing. Cation exchange is mainly operative in binary ionic compounds and involves replacement of the sublattice of cations with a new sublattice of different cations, while the sublattice of anions remains in place. Some of these transformations, as well as assembly, can now be followed in situ using dedicated transmission electron microscopes with new holder designs and new types of detection systems. An emerging area of research is that of anion exchange, especially in halide perovskites, in which the halide ions exhibit unusually high diffusivities. Mastering anion exchange in perovskite nanostructures, coupled with the possibility of preparing quantum confined structures, has opened new avenues in perovskite-based applications. Finally, new exciting directions have been uncovered recently through the development of plasmonic semiconducting nanoparticles and by the possibility to chemically adjust the density of free carriers in them. Applications of these materials range from catalysis to heavy metal recovery, sensing, photothermal and photodynamic therapy. The talk will also give an outlook on future developments in these various fields. Key Words: nanomaterials, nanocrystals, chemical and structural transformations, ion exchange

# Nanobiosensors for diagnostics

**Friday, 11th November - 11:20 - Plenary Speeches - Auditorium - Oral presentation - Abstract ID: 726**

***Prof. Arben Merkoçi*** [1]

***1.*** *Catalan Institute of Nanoscience and Nanotechnology (ICN2), CSIC and The Barcelona Institute of Science and Technology (BIST)*

Biosensors field is progressing rapidly and the demand for cost efficient platforms is the key factor for their success. Physical, chemical and mechanical properties of cellulose in both micro and nanofiber-based networks combined with their abundance in nature or easy to prepare and control procedures are making these materials of great interest while looking for cost-efficient and green alternatives for device production technologies. Both paper and nanopaper-based biosensors are emerging as a new class of devices with the objective to fulfil the ``World Health Organization'' requisites to be ASSURED: affordable, sensitive, specific, user-friendly, rapid and robust, equipment free and deliverable to end-users. How to design simple paper-based biosensor architectures? How to tune their analytical performance upon demand? How one can `marriage' nanomaterials such as metallic nanoparticles, quantum dots and even graphene with paper and what is the benefit? How we can make these devices more robust, sensitive and with multiplexing capabilities? Can we bring these low cost and efficient devices to places with low resources, extreme conditions or even at our homes? Which are the perspectives to link these simple platforms and detection technologies with mobile phone communication? I will try to give responses to these questions through various interesting applications related to protein, DNA and even contaminants detection all of extreme importance for diagnostics, environment control, safety and security.

# Some Features of Pressure Evolution in Systems ``Non-Wetting Liquid - Nanoporous Medium'' at Impact Intrusion

**Friday, 11th November - 13:30 - Poster Session - Gallery - Poster presentation - Abstract ID: 404**

***Dr. Victor Byrkin*** [1], ***Dr. Anton Belogorlov*** [1], ***Mr. Daniil Paryohin*** [1]

***1.*** *National Research Nuclear University MEPhI*

The last few decades systems consisting of nanoporous medium dispersed in a non-wetting liquid cause an increased interest from both the practical and theoretical points of view. Non-wetting liquid can infiltrate into the porous medium only with an excess pressure. Liquid infiltration tends to increase the solid-liquid interfacial energy and the absorbed energy is proportional to the specific surface area of the medium. Therefore this energy for nanoporous media can reach several orders of magnitude superior to traditional damping materials and shape-memory materials. As a consequence, the prospects of using devices based on systems consisting of a nanoporous medium immersed in a non-wetting liquid associated mainly with the absorption of mechanical energy of impact or explosion. The poster presents the results of experimental studies of impact filling the systems of industrially produced hydrophobic silicas Fluka 90 C18, Fluka 100 C8, Fluka 100 C18 and distilled water. With increasing the impact energies nontrivial pattern of pressure changes in the system over time is observed. A physical explanation is proposed for the observed phenomena.

# Complex defects in AlN/GaN interface

**Friday, 11th November - 13:30 - Poster Session - Gallery - Poster presentation - Abstract ID: 92**

***Dr. Yahor Lebiadok*** [1], ***Mr. Dzmitry Kabanau*** [1]

*1. SSPA "Optics, Optoelectronics & Laser Technology"*

The influence of complex defects (gallium, nitrogen and aluminum vacancies and corresponding interstitial atoms) in AlN/GaN heterointerface characteristics are discussed. The density functional theory calculations with the hybrid functionals B3LYP with Hay-Wadt effective core potentials for all the heavy atoms in a combination with Hay-Wadt valence basis were used. The model clusters of AlN/GaN interface with the mixing of gallium and aluminum atoms in the range of 0 - 100 % are under consideration. The energy dependence of AlN/GaN clusters on different extent of gallium and aluminum atoms mixing in the interface was calculated. It was ascertained that the complex defect nitrogen vacancy with interstitial nitrogen atom (illustrated in the figure) is more probably formed in the interface than in the gallium or aluminum part of the AlN/GaN heterostructure.

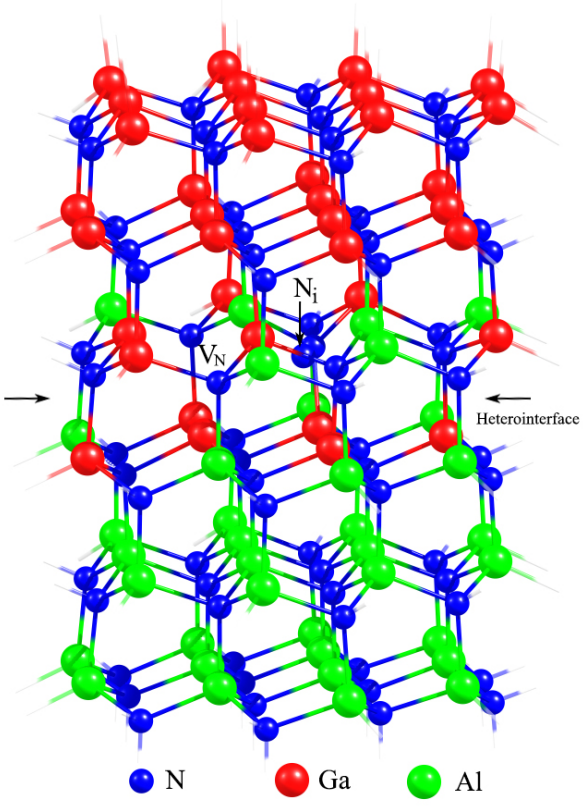


Forabstr.jpg

# Powerful Laser Diode Matrixes based on AlGaAs/GaAs heterostructures for Active Vision Systems

**Friday, 11th November - 13:30 - Poster Session - Gallery - Poster presentation - Abstract ID: 94**

***Dr. Yahor Lebiadok*** [1], ***Mr. Denis Shabrov*** [2], ***Mr. Dzmitry Kabanau*** [1]

***1.*** *SSPA "Optics, Optoelectronics & Laser Technology",* ***2.*** *B.I. Stepanov Institute of Physics*

The powerful laser diode matrixes (LDM) based on the AlGaAs/GaAs quantum heterostructures are used as illumination sources in the Active Vision Systems (AVS). The LDM lasing wavelength is in the range 790-880 nm (the atmosphere transparency spectral region), total optical output pulse power 6 kW. Achievement of AVS's high efficiency is connected with a high average power of illumination, which depends on the pulse duration and pulse repetition rate along with peak optical power. Effective realization of the principle of range gated active vision supposes usage of short light pulses. The LDM radiation pulse duration must be about 10-300 ns for the application in the AVS which are used for the distances from 100 m up to 10 km. To achieve such pulse duration (about 30 ns) and high pulse repetition rate (up to 100 kHz) values as well as requirements of AVS compactness special electric scheme and geometry of power supply is needed. Another problem related to using laser diode matrixes as illumination sources in AVS is LDM active layer heating as well as the LDM radiation divergence (and its concordance with objective field of view). The LDM passive cooling and method of radiation divergence control are also discussed.

# Removal of azo dye Orange II using nZVI catalyst supported on a natural fiber (Fique).

**Friday, 11th November - 13:30 - Poster Session - Gallery - Poster presentation - Abstract ID: 96**

***Mr. David Barinas [1], Mrs. Karen Bastidas [1], Prof. Hugo Ricardo Ramirez [1], Prof. Cesar Sierra [1], Mrs. Anamaria Barrera Bogoya [1]***

***1.*** *National University of Colombia (Bogota)*

Currently, nanoscale zero valent iron (nZVI) species are of interest for potential applications in soil remediation and wastewater treatment. Related studies have shown that nZVI has a high reactive surface allowing to improve sequestration capacity of heavy metals and other compounds difficult to treat as: chlorinated organic solvents, organochloride pesticides and organic dyes. This work carried out the preparation and characterization of nZVI catalyst supported on a natural fiber (fique) and its performance as wastewater treatment for organic dyes. The nanoparticles synthesis was performed by liquid phase reduction, in a first step the natural fibers were mixed with the precursor solution to form a mixture which was heated. To this mixture, a solution of ethanol and polyethylene glycol, were added with constant stirring. The reaction pH was adjusted using NaOH. And then, in a N2 atmosphere, sodium borohydride was added dropwise until the formation of the characteristic black precipitates. In order to characterize the synthesized catalyst. it was used, X-ray Diffraction (XRD). The catalytic activity of this bionanocomposite was studied for the removal of organic dyes in water samples, showing to be a very attractive and efficient technology for undeveloped countries like Colombia.

# Viscosity and thermal conductivity of aluminum nitride - ethylene glycol (AlN-EG) nanofluids

**Friday, 11th November - 13:30 - Poster Session - Gallery - Poster presentation - Abstract ID: 109**

***Dr. Gaweł Żyła*** [1]

***1.*** *Department of Physics and Medical Engineering, Rzeszow University of Technology*

The paper presents the results of experimental studies on basic thermophysical properties of aluminum nitride nanoparticles suspensions [1]. Ethylne glycol (POCH, Avantor Performance Materials Poland, Gliwice, Poland) was used as the base liquid for this nanofluids. Nanofluids were prepared with two step method with use of the commercial available AlN nanoparticles (PlasmaChem GmbH (Berlin, Germany), catalog number PL-HK-AlN) with average particle size 20 nm. Viscosity measurements were performed on HAAKE MARS 2 rheometer (Thermo Electron Corporation, Karlsruhe, Germany) Dynamic viscosity of the material in the range of shear rates from 0.01 to 1000 s-1 at constant temperature of 298.15 K was measured. The dependence of viscosity on temperature in the range from 273.15 to 323.15 K was also examined. To determinate thermal conductivity of AlN-EG nanofluids a KD2 Pro Thermal Properties Analyzer (Decagon Devices Inc., Pullman, Washington, USA) was used. Thermal conductivity was measured at a constant temperature of 298.15 K. It was presented that this material exhibits non-Newtonian nature and thermal conductivity increases linearly with the concentration of nanoparticles in suspension. [1] G. Żyła, J. Fal, Experimental studies on viscosity, thermal and electrical conductivity of aluminum nitride -- ethylene glycol (AlN--EG) nanofluids, Thermochimica Acta, 637, 11--16 (2016)

# Associative properties of diblock copolymers used in nanoparticle formation by Flash Nanoprecipitation.

**Friday, 11th November - 13:30 - Poster Session - Gallery - Poster presentation - Abstract ID: 124**

***Dr. Walid Saad*** [1], ***Prof. Robert Prud homme*** [2]

***1.*** *Amer,* ***2.*** *Princeton University*

Introduction: Flash Nanoprecipitation (FNP) is a nanoparticle (NP) formation technique that relies on amphiphilic diblock copolymer arrested growth of particles achieved through fast solvent/non-solvent mixing. FNP has been explored for the NP formation of hydrophobic drugs and imaging agents. A key feature of FNP is providing solvent conditions affording high solute supersaturation and polymer concentrations away from the critical micelle concentration (cmc). These conditions ensure solute nucleation and growth events are concurrent with polymer surface stabilization that arrests particle growth at the sub-micron level, resulting in controlled size NP of organic solutes. Locating the block copolymer cmc is of interest because the kinetics of nucleation and growth involved in the FNP process depend on the level of supersaturation. This study aims at determining the cmc for poly (ethylene glycol)-b-poly(ε-caprolactone) (PEG-PCL) in tetrahydrofuran/water mixtures, identifying the thermodynamic driving force for micellization, and elucidating the effect of the block length on micellization. Methods: Dynamic light scattering was used to locate the onset of micellization at various temperatures, and the closed association model to determine the standard thermodynamic functions. Cmc is identified as the point where an increase in light scattering intensity with respect to the signal obtained for dissolved block copolymer is observed. Values for the standard thermodynamic functions were estimated using the cmc values at different temperatures, and the effect of block length evaluated. Results: The cmc Vs. temperature results show the contribution of the hydrophobic block length on the free energy of micellization, with a free energy contribution of -0.024 KJ/mol per PCL monomer unit. A similar analysis reveals a weaker contribution for the soluble block at constant PCL block length, with a value of -0.0015 KJ/mol per PEG monomer unit. Discussion: Based on these results, modifying the insoluble block length is an effective approach for tuning cmc. The results map out the micellization domain and reveal the insignificant effect of the soluble block on micellization compared with the insoluble block. These results provide a framework for designing drug formulations via FNP, where high supersaturations of both the drug and the block copolymer are needed.

# Simulation and Visualization of Chirality-Dependent Thermal Conduction Phenomena in Carbon Nanotubes

**Friday, 11th November - 13:30 - Poster Session - Gallery - Poster presentation - Abstract ID: 142**

***Prof. Vadim A. Shakhnov*** [1], ***Prof. Lyudmila A. Zinchenko*** [1], ***Dr. Vladimir V. Makarchuk*** [1], ***Dr. Elena V. Rezchikova*** [1], ***Mr. Vadim Kazakov*** [1]

***1.*** *BMSTU*

In the paper, we present our approach to visual analytics support for research of carbon nanotube variation and its influence on thermal conduction phenomena. The outstanding thermal conductivity of carbon nanotubes attracts designers [1]. Carbon nanotubes FETs are promising candidates for the post silicon era. However, the fabrication of carbon nanotubes with the predefined properties is a big challenge [2]. Carbon nanotube specific variations, including nanotube diameter and chirality variations, influence the thermal conductivity of carbon nanotube [3]. A designer has to compare thermal properties of carbon nanotubes. However, carbon nanotubes are invisible for a human eye. Therefore, special efforts are required to find good design solutions [4]. In the paper, we focus on design solution with the predefined diameter. First, we find all possible chiral indices for the given diameter and then visualize all possible design solutions with their thermal properties. The corresponding statistical data is given as well. We illustrate our approach for research of thermal properties of single-walled carbon nanotubes. We discuss our results for the zigzag and the armchair nanotubes. Although nanotube devices are promising candidates for the coming post silicon era, more efforts for nanotube devices design automation are required. In the paper, we proposed a novel approach based on visual analytics. The approach supports a nanotube devices design process and simplifies a design solution choice. This work was partially supported by grant RFBR 15-29-01115 ofi-m. [1] G. Hills et al., ``Rapid Co-Optimization of Processing and Circuit Design to Overcome Carbon Nanotube Variations," IEEE Transactions on Computer-Aided Design of Integrated Circuits and Systems, 7, pp. 1082-1095, 2015. [2] B. C. Paul et al., ``Impact of a Process Variation on Nanowire and Nanotube Device Performance," IEEE Transactions on Electron Devices, 9, pp. 2369-2376, 2007. [3] A. M. Marconnet, M. A. Panzer, and K. E. Goodson, ``Thermal conduction phenomena in carbon nanotubes and related nanostructured materials'', Rev. Mod. Phys. 85, no. 8, pp. 1296 -1327, 2013. [4] V.A. Shakhnov et al., ``Simulation and Visualization in Cognitive Nanoinformatics'', International Journal of Mathematics and Computers in Simulation, 1, pp. 141-147, 2014.

# Influence of post-deposition annealing on the properties of nanostructured TiO2 thin films grown by RF magnetron sputtering for photonic applications

**Friday, 11th November - 13:30 - Poster Session - Gallery - Poster presentation - Abstract ID: 209**

***Dr. Tahar Touam [1], Prof. Azeddine CHELOUCHE [2], Mrs. Ilham Hadjoub [1], Mr. Djamel DJOUADI [2], Mr. Hammiche Laid [2]***

***1.*** *Université Badji Mokhtar-Annaba,* ***2.*** *université de Béjaia*

In this work, nanostructured TiO2 thin films were successfully grown on glass substrates at room temperature by using a RF magnetron sputtering technique. The effect of the post-annealing treatment for one hour at 400--600 °C on the structural, morphological, optical and waveguide properties were investigated by X-ray diffraction (XRD), Raman spectroscopy, scanning electron microscopy (SEM), atomic force microscopy (AFM), UV-Visible spectrophotometry and m-lines spectroscopy (MLS). The results show that all prepared films exhibit (101) XRD peak corresponding to the anatase phase of TiO2 and those annealed revealed an improvement in crystallinity. The latter being consistent with the clear Raman peaks observed around 144, 197, 399, 515, 519 and 639 cm−1, attributed to the Raman active modes of anatase phase with symmetries Eg, Eg , B1g , A1g, B1g and Eg , respectively. SEM micrographs and AFM images showed that as-grown TiO2 film displayed a homogeneous and smooth surface consisting of small grain size particles, while increasing the annealing temperature resulted in larger grain size and rougher surfaces. The UV-Visible transmittance results show that as-grown films were transparent with an average transmittance of more than 75 % in the visible region. Whereas a slight decrease in the transmission and a blue shift of the absorption edge from 3.50 to 3.56 eV were observed with annealing temperature. MLS measurements at 633 nm wavelength put into evidence that all TiO2 planar waveguides demonstrated a well-guided single mode for both transverse electric (TE) and transverse magnetic (TM) polarized light and their refractive indexes were found to increase with annealing temperature. Moreover, the ordinary and extraordinary refractive index and the birefringence values of the TiO2 thin film annealed at 600 °C were very close to the corresponding single-crystal anatase values indicating its higher degree of crystallinity.

# Investigation of Morphological and Optical Properties of Stain Etched Silicon

**Friday, 11th November - 13:30 - Poster Session - Gallery - Poster presentation - Abstract ID: 300**

***Dr. Maha Ayat*** [1], ***Dr. Sabrina Sam*** [2], ***Dr. Noureddine Gabouze*** [1], ***Dr. Rabah Boukherroub*** [3]

***1.*** *CMSI, Centre de Recherche en Technologie des Semi-conducteurs pour l'Energétique,* ***2.*** *Centre de Recherche en Technologie des Semi-conducteurs pour l'Energétique, Division Couches Minces Surfaces et Interfaces,* ***3.*** *Interdisciplinary Research Institute (IRI), IRI-IEMN, CNRS*

In the present work, we present the fabrication of ordered porous pyramids and silicon macropores by stain etching which is a low coast and simple chemical method. The etching of silicon surfaces is made in a solution based on vanadium oxide (V2O5)/hydrofluoric acid solution (HF). The goal of this work is to study the effect of metal catalyzer, such Palladium (Pd) and Silver (Ag), on the structures properties (morphological, structural and optical). For the metal assisted etching, we choose metals that differ with respect to their catalytic effect. Ag is a poor hydrogen recombination catalyst, though it is more effective than Si and Pd is an excellent hydrogen recombination catalyst. Thereby, we could confirm the self-cleaning effects of the fabricated structures as well as the optical properties. P-type silicon wafers with resistivity of 1 - 10 Ωcm, were used as substrate. The samples were divided into three groups: one group containing four Si samples, another group containing four Si samples with a thin film of Palladium (Pd) deposited and the last group containing four Si samples with a thin film of Silver (Ag) deposited. The three groups were etched in a mixture of HF (49%) and V2O5 (98%), for a period of 30, 60, 90, and 120 min. FTIR measurements of Si, Pd/Si and Ag/Si etched in HF/V2O5 solution revealed the presence of hydride species (SiHx) on the surface. The structures obtained by etching Si samples in HF/V2O5 for an etching time of 30 min show porous silicon layers which appear in form of islands separated by large channels. When the etching duration is extended to 1 h, the density of pyramids structure increases evidently. When Si surface is covered by a thin film of Ag, the structures obtained by increasing time of etching, are almost the same observed by etching Si surface covered by a thin Pd film which consists in a formation of macropores with pyramidal structures inside. The Ag/Si structures obtained showed a contact angle of 148.6 ±2° after organic treatment.

# Silicon Nanoparticles Coated with Chitosan for Using Anode of a Lithium Secondary Ion Battery

**Friday, 11th November - 13:30 - Poster Session - Gallery - Poster presentation - Abstract ID: 330**

*Ms. SUN MI JIN* [1], *Dr. Jong Sung Jin* [2], *Prof. Nam-ju Jo* [1]

*1. Pusan National University, 2. Korea Basic Science Institute(KBSI)*

Si has advantages such as high battery capacity, low discharge potential (below 0.5 V), and low cost by acting with lithium ion that can be represented as the following equation, but it is known to have lots of problems such as a capacity fading problem due to pulverization, low electrical contact, and large volumetric change according to solid electrolyte interphase (SEI) generation. This expansion is known to be carried out up to about 400 %. New materials such as Si-C and Si-Polymer are being actively progressed. If a metal such as Si is used as anode active material, lithium moves into the metal and takes up a gap between metals and reacts so that volume expansion occurs due to increased lattice constant. In this study, the Si-chitosan (CTS) was prepared by introduced from 3 molecular chitosan (low, medium, high) to Si nanoparticles. From these, the difference in battery efficiency was investigated when making lithium secondary battery half cell through the carbonization of Si based material by using low, medium and high molecular chitosan polymers. For the assessment of the physical properties of synthesized Si-CTS composite, FT-IR, TEM, SEM, XPS and elemental analyzer were employed for the characterization of physicochemical properties. The characteristics of the carbonized silicon anode active materials synthesized by using each method were electrochemically evaluated.

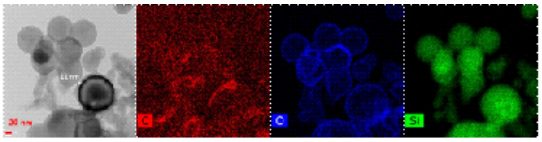

(a)

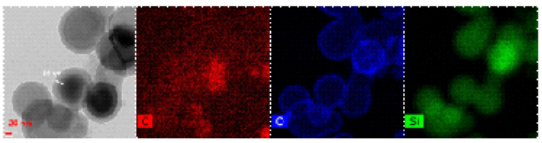

(b)

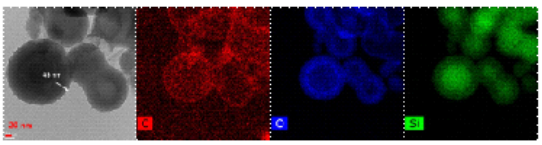

(c)

**Fig. 1** FE-TEM images of carbonized Si with low (a), medium (b) and high (c) chitosan.

Fe-tem.png

# Microanalysis of DDS Nanoparticle by Polarization Interferometric Nonlinear Confocal Microscopy

**Friday, 11th November - 13:30 - Poster Session - Gallery - Poster presentation - Abstract ID: 370**

***Prof. Chikara Egami*** [1]

***1.*** *Shizuoka University*

Nanoparticulate drug delivery systems (DDS) have attracted a lot of attention because of their size- and dopant-dependent properties. Nano formulations can be tailored to meet a wide range of product requirements dictated by disease condition, route of administration and considerations of cost, product stability, toxicity and efficacy. Researchers have an array of tools for DDS particle analysis, including scanning, transmission or atomic force microscopy (SEM/TEM/AFM); dynamic light scattering (DLS); nuclear magnetic resonance (NMR); and sundry spectrometry techniques, but they all have a variety of limitations, including complex sample preparation or the difficulty of analyzing enough particles to get a statistically significant result. Additionally, the analysis for sometimes must be performed even in preservation liquid solutions. Now, we focus on spectroscopic analysis of a single polymer DDS nanoparticle with a polarization-interferometric nonlinear confocal microscope to analyze the nanoparticle in high CTF (Contrast Transfer Function). Unlike fluorescent microscope, the microscope proposed has an advantage in nondestructive and noncontact evaluation without doping toxic dye probes. Introducing the Michelson-type polarization-vector interferometry enhances the spatial contrast resolution of the confocal system both in axial and lateral directions. There are two typical ways to use the interferometer: on the one hand, when the analyzer axis in front of a confocal pinhole is set at near 45°, the microscope functions as the positive-type one to add the signals of s- and p-scattering components; but, on the other hand, when the analyzer axis is set at near 135°, the microscope functions as the negative type one to subtract the signals of the two components. Here, in the negative type one, we set the confocal signal minimum while scanning the background; a tiny χ(3) area shines out against the dark background with high contrast. We measured three-dimensional inhomogeneous distribution in a single 200-nm particle with the microscope that performs the electric field subtraction of the scattered light from medium and the reference light. We have succeeded in evaluating dopant distribution in the DDS nanoparticle (see figure). Also, polarization analysis estimated the molecular density, molecular orientation and refractive index difference between major and minor axes.

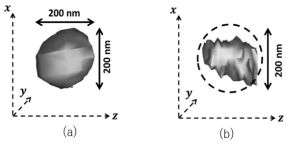


**Fig.** Three-dimensional images of a single nanoparticle: (a) surface image with conventional confocal microscope ($I$ = 1.0 W/cm2), (b) internal image with polarization interferometric nonlinear confocal microscope ($I$ = 8.0 W/cm2)

Figure.jpg

# CARBONIC ANHYDRASE INHIBITORS : 2-Substituted-1,3,4-Thiadiazole-5-Sulfamides act as powerful and selective inhibitors of the mitochondrial isozymes VA and VB over the cytosolic and membrane-associated carbonic anhydrases I, II AND IV

**Friday, 11th November - 13:30 - Poster Session - Gallery - Poster presentation - Abstract ID: 349**

***Dr. Fatma-Zohra SMAINE*** [1], ***Dr. Jean-Yves Winum*** [2]

***1.*** *1 Laboratory of ecocompatible asymmetric cataysis. Departement of Chemistry, Faculty of Sciences, Annaba-Badji- Mokhtar University, BP12 Annaba, Algeria.,* ***2.*** *Institut des Biomolécules Max Mousseron (IBMM) UMR 5247 CNRS-ENSCM-Université de Montpellier, Bâtiment de Recherche Max Mousseron, Ecole Nationale Supérieure de Chimie de Montpellier, 8 rue de l'Ecole Normale, 34296 Montpellier Cedex, France.*

A series of 2-substitutes-1, 3,4-thiadiazole-5-sulfamides was prepared ans assayed as inhibitors of several carbonic anhydrase (CA, EC 4.2.1.1) isoforms, the cytosolic CA I and II, the membrane-associated CA IV and the mitochondrial CA VA and VB. The new compounds showed weak inhibitory activitiy against hCA I (K1S of 102 nM- 7,42 µM), hCA II (K1S of 0,54-7,42 µM) and hCA IV (K1S of 4,32-10,05 µM) but were low nanomolar inhibitors of hCA VA and hCA VB, with inhibiton constants in the range of 4,2-32 nM and 1,3-74 nM, respectively. Furthermore, the selectivity ratios for inhibiting the mitochondrial enzymes over CAII were in the range of 67,5-415, making these sulfamides the first selective CA VA/VB inhibitors1. 1 Bioorganic and Medicinal Chemistry Letters 18 (2008) 6332-6335.

# Synthesis of zirconia-based Pyrochlore type photocatalysts

**Friday, 11th November - 13:30 - Poster Session - Gallery - Poster presentation - Abstract ID: 382**

***Mr. Yuta Kawakami*** [1], ***Dr. Takuya Suzuki*** [1]

***1.*** *The University of kitakyushu*

Photocatalyst is an environment purification material that can be removing organic or hazardous substances using solar energy. In recent year, Perovskite photocatalyst has been attracting attention as high performance solar cell's materials. Interference for electron orbital is important for improvement of photoactivity. Metal doping and increment of disorder has been conventional method for the band gap control of photocatalyst. This study focuses on the Pyrochlore structure of large distortion structure than the Perovskite structure. We expect that the large strain of the structure give effect for the electron orbit, therefore we tried the synthesis of Pyroclore type zirconia-based new photocatalyst. Pyrochlire has A2B2O7 composition consisting of A3+/B4+ or A2+/B5+. It is a big advantage of the combination using the difficult 3-4 valent pair or 2-5 valent pair to develop a new photocatalysts, however applications in zirconia have been not well known. Photoactivity of zirconia is lower than the titania is a common photocatalyst, however it has large band gap. We look forward to make easily insertion levels in its large band gap to develop new photocatalyst material. Therefore we select the zirconium as B site and 3-valent transition metal element (lanthanide element of La, Sm, Nd) as A site, to synthesize zirconia-based pyrochlore type photocatalyst. Identification of XRD was La2Zr2O7, Sm2Zr2O7, and Nd2Zr2O7. In observation crystalline shape, particles of sub-micron particles size has been confirmed in each sample by FE-SEM. La2Zr2O7 was the largest specific surface area, however it was very small value as 5.64m2/g. From UV-vis, respectively absorption edge 461nm (La2Zr2O7), 343nm (Sm2Zr2O7), and a value of each of the bandgap is 2.69eV (La2Zr2O7), 3.61eV (Sm2Zr2O7). Nd2Zr2O7's adsoeption edge could not identify cause, it has multiplex adsorption bands. We measured the CO2 production rate by acetic acid decomposition experiment as compared to commercial anatase titania (P-25).The photoactivities about 30% (Nd2Zr2O7), 23% (La2Zr2O7), 17% (Sm2Zr2O7) than P-25. From these results, Zirconia-based pyrochlore type photocatalyst addition of lanthanide element is considered to indicate a high photoactivity in this study.

# Peptide-functionalized Ultrasmall Gold Nanoparticles for Integrin Receptor Targeting

**Friday, 11th November - 13:30 - Poster Session - Gallery - Poster presentation - Abstract ID: 451**

***Ms. Usoa Aguilera Peral*** [1], ***Dr. Tom Coulter*** [1], ***Dr. Yao Ding*** [1], ***Ms. Cristina Espinosa Garcia*** [1], ***Dr. Sarah Hale*** [1], ***Mr. Alessandro Pace*** [1], ***Dr. Ketan Patel*** [1], ***Mrs. Angela Robinson*** [1], ***Dr. Dan Palmer*** [2], ***Dr. Phil Williams*** [1], ***Dr. Meike Roskamp*** [1]

***1.*** *Midatech Pharma Plc,* ***2.*** *Proficit Partners Ltd*

Cytotoxic chemotherapy is the standard of care for many types of cancer despite the frequently observed severe side effects. The targeted delivery of chemotherapeutics has great potential to reduce these effects by increasing drug concentrations within the target tissue, thereby reducing their required dose [1]. Compared to larger nanoparticles, Midatech's ultrasmall gold nanoparticles are less likely to form a protein corona due to their very small size and carbohydrate based ligand shell [2], which makes them especially interesting for active targeting strategies. Furthermore, their highly flexible organic ligand shell allows covalent attachment of functional molecules using several biocompatible coupling techniques. In this work we demonstrate the synthesis and analysis of a nanoparticle construct able to target cell surface α6 integrins. A laminin α1-derived synthetic peptide (SIKVAV) was covalently attached to carboxylated ultrasmall gold nanoparticles using EDC/NHS coupling chemistry (Figure 1). The resulting particles were analysed using dynamic light scattering (DLS) and high performance liquid chromatography (HPLC) amongst others. Assays were developed to measure the binding and uptake of the nanoparticle construct into cells by following the gold concentration. Using these assays, binding and an increased (roughly twofold compared to the base particle) uptake into HEPG2 cells, which overexpress the integrin receptor, was observed. Specificity of the binding was demonstrated by outcompeting the binding with free peptide. In conclusion, Midatech's SIKVAV-functionalized gold nanoparticles preferentially bind to integrin receptor expressing cells and are therefore interesting candidates for treating tumors that overexpress the integrin receptor, such as glioblastoma [3] or hepatocellular carcinoma [4]. References [1] S. M. Sagnella, J. A. McCarroll, M. Kavallaris, Nanomedicine 2014, 10, 1131. [2] K. Zarschler, L. Rocks, N. Licciardello, L. Boselli, E. Polo, K. P. Garcia, L. De Cola, H. Stephan, K. A. Dawson, Nanomedicine 2016, 12 (6), 1663-1701. [3] J. Lathia, J. Gallagher, J. M. Heddleston, J. Wang, CE. Eyler, J. Macswords, Q. Wu, A. Vasanji, R. E. McLendon, A. B. Hjelmeland, J.N. Rich, Cell Stem Cell. 2010, 6 (5), 421-32. [4] Y. Wu, X. Qiao, S. Qiao, L. Yu, Expert Opinion on Therapeutic Targets 2011, 15(4), 421-437.

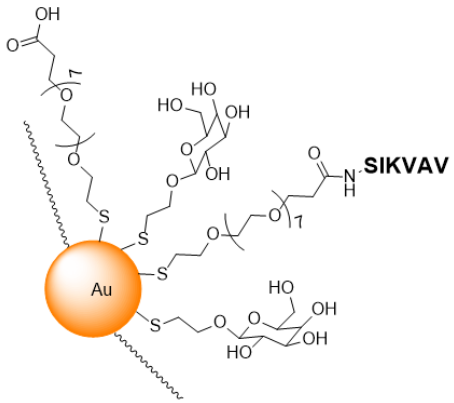


Figure 1. SIKVAV-functionalized gold nanoparticles for targeted drug delivery.

Figure 1. sikvav-functionalized gold nanoparticles for targeted drug delivery.png

# Microwave assisted hydrothermal synthesis of magnetite based nanoparticles for hyperthermia therapy

**Friday, 11th November - 13:30 - Poster Session - Gallery - Poster presentation - Abstract ID: 463**

***Mr. Milos Ognjanovic*** [1], ***Dr. Biljana Dojcinovic*** [2], ***Dr. Yue Ming*** [3], ***Dr. Hongguo Zhang*** [3], ***Dr. Bostjan Jancar*** [4], ***Dr. Sanja Vranjes Djuric*** [1], ***Dr. Bratislav Antic*** [1]

***1.*** *"Vinča" Institute of Nuclear Sciences, University of Belgrade, P.O.Box522, 11001 Belgrade,* ***2.*** *Institute of Chemistry, Technology and Metallurgy, University of Belgrade,Studentski trg 12-16, 11000 Belgrade,* ***3.*** *College of Materials Science and Engineering, Beijing University ofTechnology, Pingleyuan 100, Chaoyang District, Beijing 100124,* ***4.*** *Jožef Štefan Institute, Jamova 39, 1000 Ljubljana*

Superparamagnetic iron oxide nanoparticles (SPIONs) have great potential in theranostic applications due to their biocompatibility and unique magnetic properties. Magnetic hyperthermia is a therapeutic procedure based on the use of magnetic nanoparticles (MNPs) which activated by an externally applied AC magnetic field induces a temperature increase in tissues and organs where tumoral cells are present. In this work new synthesis route for doped magnetite with potential application in hyperthermia treatment is presented. The main goal was to analyze the influence of magnetite doping on morphological, structural/magnetic properties and heating efficiency of synthesized MNPs. Nanostructured spinel oxides of the formula MIIFe2O4 (MII=Fe2+, Zn2+, Mg2+ and Co2+) were prepared using two-stage procedure which include co-precipitation at room temperature accompanied by hydrothermal treatment in microwave field at 100°C. Structure of the samples was analyzed by the use of X-ray diffraction data. Particle size and their distributions were examined using transmission electron microscope images and ImageJ software. DC magnetization was measured by SQUID magnetometer. Heating abilities of MNPs were compared by calculating Specific Absorption Rate (SAR), and Intrinsic Loss Power (ILP), using DM100 Series device (nB nanoScale, Spain). An analysis of X-ray diffraction patterns showed good embedding of ions (Mg, Zn, Co) into parent magnetite compound. Different broadening of X-ray diffraction lines pointed to crystallite size dependence of dopant concentration. From TEM images it is clear that particles are well defined with size between 10 and 20 nm depending on the sample chemical composition. Calculated SAR values in the range of 90-150 W/g for 252 kHz frequency in 200 G magnetic field, indicated that samples show good heating efficiency. Both SAR and magnetization values depends on dopant and its concentration. The main conclusion is that examined magnetite based samples have sufficient heating efficiency to be potentially used in hyperthermia therapy. Future research will be focused on the using of different surface coatings to form more stable colloids.

# Recent Advances In Nano-Technology In Domain Of Agricultural Sciences And Food Industry

**Friday, 11th November - 13:30 - Poster Session - Gallery - Poster presentation - Abstract ID: 654**

***Mr. pejman ghelich*** [1], ***Mr. Ashkan Mohammadali Fam*** [1], ***Ms. Marjan Khorshidizadeh*** [1]

***1.*** *university of Tehran*

Nanotechnology is a new approach to the development of new tools in order to make the leap in agriculture and food industry for diagnose and treat diseases, increase the ability of plants to absorb nutrients, fight pests and microbial sources, increase bio fertilizer efficiency, reduce pollution and removed contaminants. Controlled environmental (Precision) agriculture / (CEA) can properly strengthen itself through Nano-technology by using Nano-devices, and Nano-sensors, improve the ability of the time-dependent Harvesting which would increase production and reduce chemical pesticides and pests. The most obvious application of nanotechnology in agricultural sciences, is use of Nano tools to supply pesticides and fertilizer for agricultural products. Controlled release of intended chemical substance, both in terms of time and location or even release after operation of a primer under certain conditions , has made this method very interesting for future development. The main challenges : (1) stabilizing underground conditions & (2) releasing ability of loaded substances in intended soil into or around the plants. This Nano-materials, from chemical point of view, can be classified into three main groups : (1) organic polymers, (2) inorganic compounds or polymers, and (3) compounds and composites, that can consist of materials of both preceding mentioned groups. Structures including Nano-capsules, Fullerenes and carbon Nano-tubes, and inorganic natural clay are some of promising alternatives. Nanotechnology can play an effective role in food storage in three ways: (1) Antimicrobial and Antiseptic surfaces (2) Antioxidant protection (3) Manipulation and control of enzymes' activities The application of nanotechnology in food production on the one hand in agriculture industry and in the other hand in inventing new methods for food production, which no longer depend on natural conditions, can be considered significantly important. Generally as follow: (1) Analysis and identification (2) GM food production as carriers (3) Pesticide/ drugs production and transportation (4) Food synthesis and production Biosensor is a detection device, containing a biological identifier part, and a transformer to convert the biological messages to electronic outputs. The prominent role of these devices has been shown in the Figure 1. This paper will review potential applications of Nanotechnology in these areas.

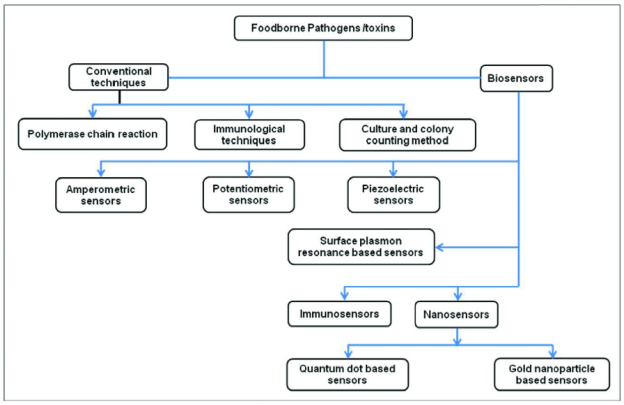


Abstract picture.png

# A soluble and fluorescent new type thienylpyrrole based conjugated polymer: optical, electrical and electrochemical properties

**Friday, 11th November - 13:30 - Poster Session - Gallery - Poster presentation - Abstract ID: 659**

***Ms. Tugba Soganci*** [1], ***Dr. Hakan Can Soyleyici*** [2], ***Dr. Metin Ak*** [1]

***1.*** *Pamukkale University,* ***2.*** *Adnan Menderes University*

Recently, increased attention has been focused on the synthesis of soluble and processable conducting polymers due to interest in their potential application. For this purpose a new type electroactive 2,5-di(2-thienyl)pyrrole derivative was synthesized and its novel solution-processable and fluorescent polymer, namely poly(N-(2,5-di(thiophen-2-yl)-1H-pyrrol-1-yl)-3,4,5-tris(dodecyloxy)benzamide) (P(TPDOB)), was electrochemically synthesized. Characterization of the monomer and the polymer was performed by 1H-NMR, 13C-NMR, cyclic voltammetry, and UV-vis and fluorescence spectroscopy. This soluble polymer has very well-defined and reversible redox processes in the acetonitrile--lithium perchlorate (ACN/LiClO4) couple. Moreover, P(TPDOB) shows multi-electrochromic behavior: blue in the oxidized state, caesious in the intermediate state and greenish in the neutral state. Also the copolymer consists of EDOT and TPDOB was synthesized by cyclic voltammetry. A copolymer film has superior electrochromic and electrical properties when compared with a homopolymer. Furthermore, the fluorescence features of the monomer and the polymer were investigated. Although the monomer is a violet light emitter, its polymer is a yellow light emitter. Synthesis of this new type solution-processable and fluorescent conducting polymer is an alternative to the conventional synthesis of soluble conducting polymers which allows the direct application of the conductive polymer to any desired surface for potential technological applications.

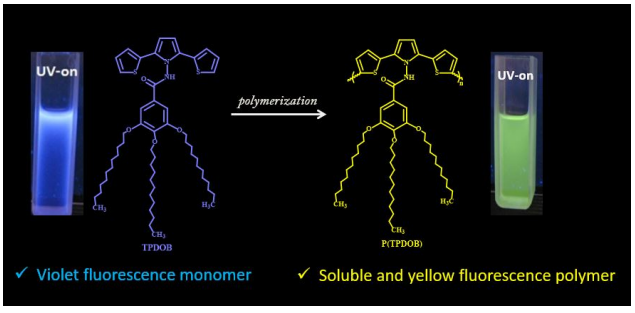


Ann c-ga.jpg

# Nanomaterials obtained by ruthenium immobilization on mesoporous

**Friday, 11th November - 13:30 - Poster Session - Gallery - Poster presentation - Abstract ID: 661**

***Dr. Violeta Niculescu*** [1]***, Dr. Radu Tamaian*** [2]***, Dr. Viorica Pirvulescu*** [3]

***1.*** *National Research and Development Institute for Cryogenics and Isotopes Technologies,* ***2.*** *National Institute for Research and Development for Cryogenic and Isotopic Technologies,* ***3.*** *Institute of Physical Chemistry, Romania*

Introduction. Since the discovery of the MCM-41 and FSM-16 in the early 1990`s of the last century, great and fascinating progress has been made in the design, preparation, characterisation and application of mesoporous silica materials. Methods. The mesoporous MCM-41 is successfully used as the support to immobilize transition metals like ruthenium by direct synthesis. UV-VIS spectroscopy and N2 adsorption are applied to characterizing these supported catalysts. Results and discussion. The synthesized material has high specific surface area, narrow pore size distribution, and large pore with high wall thickness which is very suitable for using as support material. Ruthenium can be dispersed effectively on MCM-41 by direct synthesis method and still keep the original 2D hexagonal mesostructure. The results of heterogeneous liquid oxidation (alcohols oxidation) reveal that these supported catalysts have high catalytic activity. Acknowledgments: this research was financed by The Executive Agency for Higher Education Research Development and Innovation Funding (UEFISCDI), Romania, on the Contract no. 210/2014, Project PN-II-PT-PCCA-2013-4-2075 and 34N/2016 NUCLEU Program, under Project PN 16 36 04 03 „Research on the development of new porous materials with high selective and catalytic properties for the reduction and stabilization of the pollutant concentrations in gaseous and liquid backgrounds''.

# Eco-toxicity of nanostructured ZnO, TiO2, Ce and Zr doped TiO2 developed for photocatalytic applications to Lemna minor and Sinapis alba

**Friday, 11th November - 13:30 - Poster Session - Gallery - Poster presentation - Abstract ID: 663**

***Dr. Ivana Troppová*** [1], ***Dr. Hana Sezimova*** [2], ***Prof. Stanislav Daniš*** [3], ***Dr. Pavlína Peikertová*** [1], ***Dr. Lenka Matějová*** [1]

***1.*** *VŠB-Technical University of Ostrava, Institute of Environmental Technology,* ***2.*** *University of Ostrava, Faculty of Science, Department of Biology and Ecology,* ***3.*** *Charles University in Prague, Faculty of Mathematics and Physics, Department of Condensed Matter Physics*

Introduction and scope of the work Eco-toxicological investigations of newly developed nanostructured materials for photocatalytic applications is a keen part of their development and introduction to practice. Highly photoactive material suspected to be risky to human health and environment should not be introduced to practical life at all. In our study several nanostructured materials based on TiO2 (pure as well as newly doped by Ce and Zr) and ZnO were developed for the photocatalytic reduction of CO2 and the photocatalytic decomposition of N2O. Those photocatalysts investigated in our eco-toxicological study showed the highest photocatalytic activity for both mentioned reactions. Thus, logically their eco-toxicity to plant species such as Lemna minor fronds and Sinapis alba roots was examined. Methods The advantage of performed tests compared to often used acute aquatic toxicity tests according to the OECD 201 methodology using freshwater green algae (Desmodesmus subspicatus, Chlorella vulgaris) is the fact that the nanostructured materials do not have to be dissolved in water, thus the sedimentation of the nanostructured material is excluded, and the concentration series before testing do not have to be prepared. Another fact is the evaluation method. In the test on Desmodesmus subspicatus the results being determined by counting the algal cultures under the microscope, using an automatic cell counting, and this process is highly influenced by turbidity of the material. In the tests that were used in our study, meaning tests on Sinapis alba and Lemna minor, reading of growth inhibition was feasible not with standing any turbidity of the tested nanostructured materials. Results The acute biological toxicity of ten developed photocatalytically-active nanostructured materials was determined. A large number of them showed no toxic effect to Sinapis alba and Lemna minor. The acute biological toxicity of developed materials was correlated either with their microstructural and structural properties, or their chemical stability. Acknowledgment Financial support from the Grant Agency of the Czech Republic (project reg. No.14-23274S) is gratefully acknowledged. This work was also financially supported by EU structural funding Operational Programme Research and Development for Innovation (project No. CZ.1.05/2.1.00/19.0388).

# Smart window application of a new hydrazide type SNS derivative

**Friday, 11th November - 13:30 - Poster Session - Gallery - Poster presentation - Abstract ID: 672**

***Mr. Ogun Gumusay*** [1], ***Ms. Tugba Soganci*** [1], ***Dr. Metin Ak*** [1], ***Dr. Hakan Can Soyleyici*** [2]

***1.*** *Pamukkale University,* ***2.*** *Adnan Menderes University*

In this article the smartwindow application of a new type of thienylpyrrole derivative is presented. For this purpose, the new type of 2,5-di(2-thienyl)pyrrole derivative, which is named N-(2,5-di(thiophen-2-yl)-1H-pyrrol-1-yl)-4-(vinyloxy)benzamide (TPVB), has been prepared by the reaction of 1,4-di(2-thienyl)-1,4-butanedione and 4-(vinyloxy)benzohydrazide. Using hydrazine instead of amine in the synthesis process has significantly improved the related polymer's optical properties. Spectroelectrochemical investigations revealed that P(TPVB) is more durable with better long-term stability and has the lowest band gap compared with the other SNS derivatives. A chronoamperometry experiment showed that the P(TPVB) polymer film has excellent redox stability, moderate switching time and high optical contrast. So it is possible to use this polymer with superior optical properties in smart window applications. A smart window based on P(TPVB) and poly(3,4-ethylenedioxythiophene) (P(EDOT)) was set up in a sandwich configuration. Optoelectrochemical investigations displayed that the reduced state of the device displays an orange color whereas it is blue for the oxidized state. The switching time and optical contrast (DT%) of the device at 625 nm are 1.0 s and 43%, respectively.

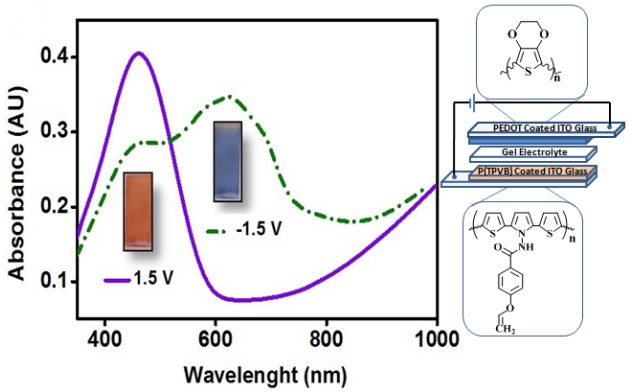


Graphical abstract.png

# Synthesis and Fluorescence Properties of Novel Asymmetric Star Shaped Polymer Containing Carbazole

**Friday, 11th November - 13:30 - Poster Session - Gallery - Poster presentation - Abstract ID: 673**

***Dr. Metin Ak*** [1], ***Dr. Erhan Karatas*** [2]

***1.*** *Pamukkale University,* ***2.*** *Selcuk University*

A fluorescent group containing novel asymmetric star shaped derivatives of 2,4,6-trichloro-1,3,5-triazine containing 2-hydroxy carbazole and (1,8-dihydropyren-1-yl)methanamine were designed, synthesized and characterized. Electrochemical polymerization of TPC was performed in acetonitrile (ACN)/LiClO4. Electrochromic properties of the conducting polymers were investigated via spectroelectrochemistry, kinetic and colorimetry studies. Spectroelectrochemical analysis of PTPC revealed electronic transitions at 308, 460 and 780 nm corresponding to π-π* transition, polaron, and bipolaron band formations, respectively. Moreover, PTPC illustrate electrochromic behavior: greenish in the oxidized state and transparent in the neutral state. Furthermore, fluorescence properties of this new type monomer were investigated.

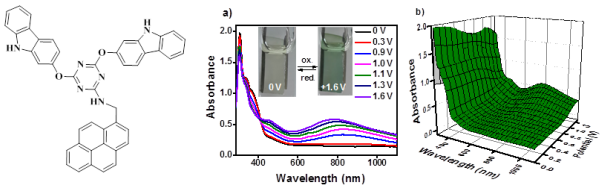


Erhan.png

# Processable Amide Substituted 2,5-Bis(2-thienyl)pyrrole Based Conducting Polymer and its Fluorescent and Electrochemical Properties

**Friday, 11th November - 13:30 - Poster Session - Gallery - Poster presentation - Abstract ID: 675**

***Mr. Yasin Abduloglu*** [1], ***Ms. Tugba Soganci*** [1], ***Dr. Hakan Can Soyleyici*** [2], ***Dr. Metin Ak*** [1]

***1.*** *Pamukkale University,* ***2.*** *Adnan Menderes University*

While majority of conductive polymers are insoluble and infusible, theirs solution processable derivatives are more desirable for preparing large size flat panel display and solid state applications because they are compatible with low cost, large area roll-to-roll manufacturing process. For this purpose, a solution processable fluorescent conjugated polymer (PDOB), consisting of electron rich N-(2,5-di(thiophen-2-yl)-1H-pyrrol-1-yl)-4-(dodecyloxy) benzamide (DOB) and its copolymer with 3,4-ethylenedioxythiophene P(DOB-co-EDOT) were synthesized by electrochemical polymerization technique. Electrochemical and optical properties of P(DOB) and P(DOB-co-EDOT) were investigated cyclic voltammetry, UV-vis absorption and fluorescence emission measurements, respectively. The optical band gap values of P(DOB) and P(DOB-co-EDOT) determined by spectroelectrochemical data were 1.92 eV and 1.62 eV, respectively. P(DOB) and P(DOB-co-EDOT) were exhibited favorable redox activity and electrochromic performance. Further kinetic studies demonstrated that the P(DOB) and P(DOB-co-EDOT) have high optical contrast ratios (60--25%), favourable coloration efficiencies (139.1 cm2.C-1 and 80.6 cm2.C-1), fast response time (1.5 s; 1.0 s), high stability. When compared to soluble poly (2,5-dithienyl pyrrole) derivatives in literature, P(DOB) have lowest oxidation potential and band gap and have highest optical contrast. As a result, these materials provide more plentiful electrochromic colours which useful for display application and hold promise for other solution-processable applications.

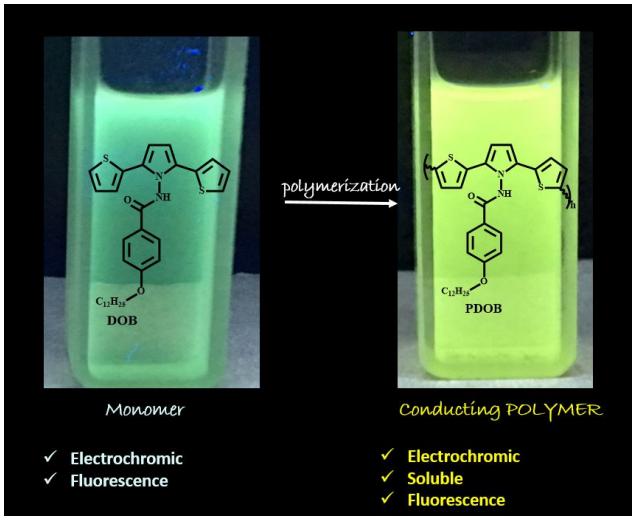


Graphical abstract.jpg

# Organic/inorganic nanoplatform for detection of cancer

**Friday, 11th November - 13:30 - Poster Session - Gallery - Poster presentation - Abstract ID: 677**

***Ms. Nikola Bugárová*** [1], ***Dr. Matej Mičušík*** [1], ***Dr. Zdenko Špitálsky*** [1], ***Dr. Peter Šiffalovič*** [2], ***Dr. Mária Omastová*** [1]

***1.*** *Polymer Institute, SAS, Dúbravská cesta 9, 845 41 Bratislava,* ***2.*** *Institute of Physics, SAS, Dúbravská cesta 9, 845 11 Bratislava*

A systemic toxicity of the patient organism is an important issues of the conventional chemotherapy treatment of cancer. The possible route to overcome the overall poisoning of organism is targeted delivery and controlled release of cytotoxins to the cancer cells. In recent years we witness accelerated research in the field of antibody-drug conjugates (ADCs). The specific and genuine interactions between the antibody and antigen directs the ADCs to the tumor cells. The controlled release of cytotoxins to tumor cells significantly lowers the systemic toxicity. The ADCs can be enhanced by a use of suitable platform [1]. With the invent of graphene and the other 2D materials their capabilities were extensively scrutinized for biomedical applications. Functionalized MoS2 layer exhibit extraordinary high sensitivity for detection of cancer related antigens. The rapid progress in covalent and non-covalent functionalization of exfoliated MoS2 layers opens new opportunities for binding of biocompatible molecules and proteins. In this work we prepared exfoliated MoS2 nanoplatelets and modified with suitable linker molecules to which the cytotoxins will be attached. The linker molecules allow controlled release of cytotoxin in cancer cells. The added value of MoS2 is the strong Raman signal and photoluminiscence in red part (above 600 nm) of visible spectrum. The alternative way would be to use graphene based nanoplatform. In particular, the hydrophilic character of GO permits the manufacture of reliable, highly sensitive and ultrafast biosensing (nano)platforms. Basic characterization of modified MoS2, GO and rGO, in terms of the degree of oxidation, exfoliation and nanoparticle size, are performed by SAXS and by XPS. The monoclonal antibodies (MAb) specifically obtained from the medium of hybridoma cells are proteins and the COOH group will be used for binding to nanoplatform with the amino groups on their surfaces. In the next step binding, internalization and effects of the functionalized GO-nanoplatform on the living cells using biological approaches will be studied. Acknowledgements This work was supported by the Slovak Research and Development Agency under the contract No. APVV-15-0641 and No. APVV-14-0120, and by project COST CA-15107. References [1] R. Duncan, Polymer conjugates as anticancer nanomedicines. Nat Rev Cancer 6, 688-701 (2006).

# A GREEN CHEMISTRY APPROACH TO SYNTHESIS OF Ce(IV) NANOPARTICLES USING ORIGANUM SYRIACUM

**Friday, 11th November - 13:30 - Poster Session - Gallery - Poster presentation - Abstract ID: 680**

***Dr. Birsen Öztürk*** [1], ***Mrs. Gozde Mediha Kamer*** [1], ***Dr. Dilek Ozyurt*** [1], ***Prof. Reşat Apak*** [2]

***1.*** *Istanbul Technical University,* ***2.*** *Istanbul University*

INTRODUCTION Cerium(IV) nanoparticles were synthesized using a green synthesis approach with co-precipitation method which relies on the oxidation of Ce(III) to Ce(IV) in basic medium. Green synthesis was carried out with a Middle Eastern herb called zahter (origanum syriacum), commonly found in Antakya region of Turkey, due to its high antioxidant and flavonoid capacity. METHODS Zahter extract was prepared at 60°C in 100 mL of deionized water in 1:1 dilution. 15 grams of Ce(III) nitrate was added to the extract at 60°C and the mixture was heated to 80°C with constant stirring. At 80°C, 1M Na2CO3 solution was added dropwise until a pH value of 9 was achieved. Then, the mixture was heated for 4-6 more hours at constant temperature. Synthesized particles were ultrasonicated for 30 minutes and washed using acetone/H2O mixture three times. SEM image of the synthesized particles was taken using FEI Quanta FEG 250 Scanning electron microscope. RESULTS Analysis of Zahter extract in terms of total antioxidant, phenolic and flavonoid content was performed using CERAC, Classical and modified phenolic content methods and Total flavonoid content method using AlCl3 [1-2] . All measurements were made using a Varian Cary 100 UV-Vis spectrophotometer. Results obtained from total Phenolic content and CERAC methods are represented as Gallic acid equivalents wheras the results obtained from total Flavonoid method are represented as Catechine equivalents. DISCUSSION To the best of our knowledge, origanum syriacum was used for the green synthesis of Ce(IV) nanoparticles for the first time. It is clear that due to its high antioxidant capacity, Zahter is capable of reducing Ce(IV) to Ce(III). Results represented in Table 1 show that CERAC is the most convenient and precise method for measuring total antioxidant capacity. REFERENCES 1. Singleton,V. L., Orthofer,R., Lamuela-Raventos,R.M. (1999). Analysis of total phenols and other oxidation substrates and antioxidants by means of folin-ciocalteu reagent. Methods Enzymol. 299, 152−178. 2. Berker,K.I., Ozdemir,F.A., Ozyurt,D., Demirata,B., & Apak,R. (2013). Modified Folin--Ciocalteu Antioxidant Capacity Assay for Measuring Lipophilic Antioxidants. J. Agric. Food Chem, 61(20), 4783-4791. Acknowledgments This research was supported by TUBITAK under project number TBAG 115Z887 and ITU-BAP research project number 39333.

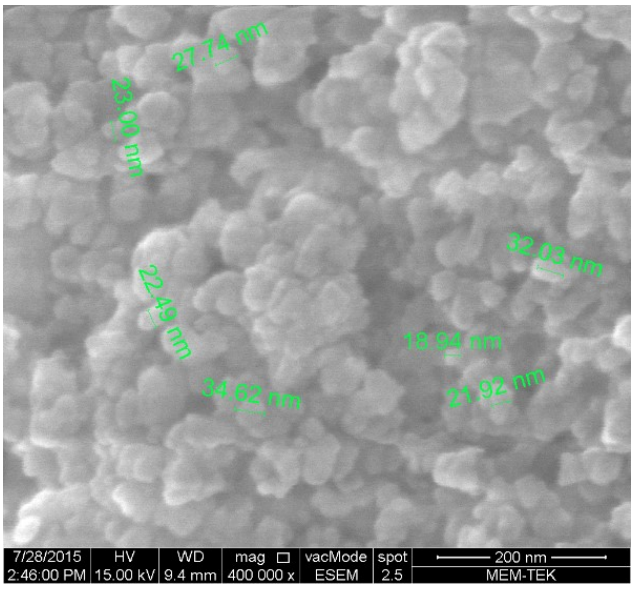


Sem image of nanoceria synthesized by origanum syriacum.jpg

# Porous Gold Nanoparticles for Nonresistant Inactivation of Influenza A Virus

**Friday, 11th November - 13:30 - Poster Session - Gallery - Poster presentation - Abstract ID: 521**

***Mr. Jinyoung Kim*** [1], ***Dr. Taeksu Lee*** [1], ***Ms. Minjoo Yeom*** [2], ***Ms. Aram Kang*** [2], ***Prof. Daesub Song*** [2], ***Prof. Seungjoo Haam*** [1]

***1.*** *Yonsei University,* ***2.*** *Korea University*

This article focuses on the inactivation of Influenza A viruses using porous gold nanoparticles (PoGNPs). Influenza virus have become resistant to the antiviral drugs such as Oseltamivir or Amantadine, because of their frequent genetic mutation. To prevent the antiviral treatment from building up the resistance, we first set the antiviral target which remains steady regardless of their subtype, disulfide bonds. As the disulfide bonds in hemagglutinin (HA) show regular pattern in entire HA protein sequence (1), we assumed that cleaving the disulfide bonds on HA could be an ideal target for influenza virus attenuation. PoGNPs, which has a large surface area due to its unique structure, had fabricated by surfactant-free emulsion method (2). The PoGNPs expected to show high affinity to the disulfide bonds because of the gold-thiol interaction. We demonstrated the decrease of the viral infectivity that was exposed to PoGNPs by the MDCK cell viability test with various subtypes of viruses (H1N1, H3N2, H9N2) whereas non-porous 130 nm gold nanoparticles and 130 nm silver nanoparticles showed much less effect on inactivation of viruses. The intracellular viral RNA quantification by realtime RT-PCR also demonstrated to ensure the mechanism of viral inhibition that the PoGNPs had blocked the viral entry process by deforming the HA, which resulted in membrane fusion. This PoGNP-utilized inactivation process proposes more convenient way for getting inactivated virus under laboratory-sized experiment. Moreover, PoGNPs can further be used in many ways such as photothermal lysis of virus or surface-enhanced Raman spectroscopy. Their versatility suggests the novel method for viral RNA extraction and detection. (1) M. S. Segal, J. M. Bye, J. F. Sambrook, M.-J. H. Gething. 1992. J. Cell Biol. 118: 227-244 (2) D. Bang, T. Lee, J. Choi, Y. Park, E. Kim, Y. Huh, S. Haam. 2015. Adv. Healthc. Mater. 4: 255-263

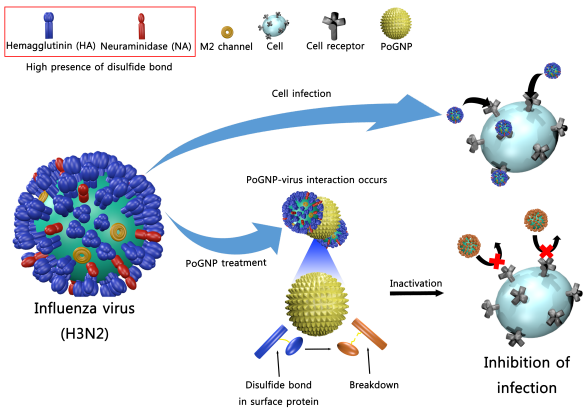


Porous gold nanoparticles for inactivation of influenza virus.png

# Homogeneous crystal nucleation kinetics in small closed systems

**Friday, 11th November - 13:30 - Poster Session - Gallery - Poster presentation - Abstract ID: 692**

***Dr. Zdenek Kozisek*** [1], ***Prof. Pavel Demo*** [1], ***Dr. Alexei Sveshnikov*** [1], ***Mr. Jan Kulveit*** [1]

**1.** *Institute of Physics, Czech Academy of Sciences, Prague*

Nuclei of a new phase are formed within metastable parent phase due to fluctuations. During this process it is necessary to overcome a certain nucleation barrier. At appropriate conditions the supercritical clusters (called nuclei) of nanometer size are formed. A better understanding to the nucleation and growth processes enables to develop materials with targeted properties. We have numerically solved the nucleation kinetic equations to determine the size distribution of nuclei and nucleation rates in small confined volumes. [1] As a model system crystal nucleation of Ni droplets was chosen due to availability of experimental data. [2] In smaller volumes one needs higher supercooling to form crystal nuclei and the depletion of liquid phase is not negligible. It is necessary to take into account the size dependence of the interfacial energy to explain satisfactorily experimental data. At lower supercooling number of formed nuclei is relatively low, as the nucleation barrier is higher, and the classical nucleation theory gives reasonable approach to nucleation rate. However in smaller volumes (< cubic micrometer) higher supercooling is needed to form nuclei and the decrease of the number of molecules within liquid phase plays important role in nucleation process. The number of nuclei increases with time, at a certain time reaches some maximum value, and continues to decrease as a consequence of liquid phase depletion. Similarly, nucleation rate reaches at a certain time some maximum value, which depends on nucleus size. This work was supported by the Project no. LD1504 of the Ministry of Education, Youth and Sports of the Czech Republic (COST Action CM1402). [1] Z. Kožíšek: CrystEngComm 15 (2013) 2269. [2] J. Bokeloh, R.E. Rozas, J. Horbach, G. Wilde: Phys. Rev. Lett. 107 (2011) 145701.

# Mechanical, electrical and antibacterial properties of polycrystalline ZnO films passivated with ZnS

**Friday, 11th November - 13:30 - Poster Session - Gallery - Poster presentation - Abstract ID: 641**

***Dr. Anna Baranowska-Korczyc*** [1], ***Dr. Mikołaj Kościński*** [2], ***Dr. Emerson L. Coy*** [1], ***Dr. Bartosz Grześkowiak*** [1], ***Dr. Małgorzata Jasiurkowska-Delaporte*** [3], ***Dr. Barbara Peplińska*** [1], ***Prof. Stefan Jurga*** [4]

***1.*** *NanoBioMedical Centre, Adam Mickiewicz University, ul. Umultowska 85, PL-61614 Poznań, Poland,* ***2.*** *NanoBioMedical Centre, Adam Mickiewicz University, ul. Umultowska 85, PL-61614 Poznań, Poland; Department of Physics, Life Sciences University, Wojska Polskiego 38/42, PL-60637 Poznań, Poland,* ***3.*** *NanoBioMedical Centre, Adam Mickiewicz University, ul. Umultowska 85, PL-61614 Poznań, Poland; Department of Soft Matter Research, Institute of Nuclear Physics PAS, ul. Radzikowskiego 152, PL-31342 Kraków, Poland,* ***4.*** *NanoBioMedical Centre, Adam Mickiewicz University, ul. Umultowska 85, PL-61614 Poznań, Poland, Department of Macromolecular Physics, Faculty of Physics, Adam Mickiewicz University, Umultowska 85, PL-61614 Poznań, Poland*

Zinc oxide (ZnO) nanostructures, due to their optical and electrical properties, are ideal systems for design of various devices such as: light emitting diodes, transistors or sensors of UV light, selected gases and biosensors. Among the various ZnO nanomaterials, the nanolayers obtained by the sol-gel process and subsequent calcination have attracted considerable interest in different applications as a result of their facile synthesis, polycrystalline nature and a high surface area to volume ratio. This study presents properties of polycrystalline ZnO nanofilms obtained by a spin-coating process followed by calcination in air and further passivation by a zinc sulfide (ZnS) layer in a gas-phase of H2S [1]. The ZnO/ZnS nanostructures were characterized by Fourier Transform Infrared and Raman spectroscopies, Scanning Electron Microscopy and Atomic Force Microscopy. The thin ZnS coating mimicked the shape of the ZnO crystals and did not significantly change the morphology of the ZnO film. Moreover, ZnS coating of ZnO films improved their stability in liquids, electrical conductivity and mechanical properties. ZnS as water-insoluble semiconductor enhanced the stability of ZnO layer in biological liquids. After sulfidation process ZnO/ZnS films were stable in water for over 7 days, while ZnO nanolayers were water soluble. Nanohardness and elastic modulus of the samples and nanowear tests were performed using nanoindentation methods and revealed improvement of mechanical properties after sulfidation process. The electrical conductivity of the ZnO nanolayers, investigated by Conductive-Atomic Force Microscopy and van der Pauw method, increased after ZnS coating formation as a result of surface defect passivation and removing oxygen molecules, which can trap free carriers. Additionally, ZnO and ZnO/ZnS films showed antimicrobial properties against Escherichia coli. Our findings indicate that ZnO surface passivation is required for designing future devices to improve its stability at different environments and enhance its mechanical, electrical and antibacterial properties. Acknowledgements Financial support from Polish Ministry of Science and Higher Education (Grant ``Iuventus Plus'' 0018/IP2/2015/73, 2015-2017) and Nation Centre for Research and Development (PBS1/A9/13/2012) is gratefully acknowledged. [1] The synthesis, characterization and ZnS surface passivation of polycrystalline ZnO films obtained by the spin-coating method, A. Baranowska-Korczyc et al., J. Alloy and Comp. (in press).

# Large-scale silver-modified nanofluorapatite -- bactericidal/cytotoxicity evaluation and physical characterization

**Friday, 11th November - 13:30 - Poster Session - Gallery - Poster presentation - Abstract ID: 667**

***Dr. Małgorzata Kus-Liśkiewicz*** [1], ***Mrs. Renata Wojnarowska-Nowak*** [1], ***Dr. Adriana Barylyak*** [2], ***Dr. Ganna Nechyporenko*** [3], ***Prof. Viktor Zinchenko*** [3], ***Prof. Danuta Leszczynska*** [4], ***Prof. Yaroslav Bobitski*** [5]

***1.*** *University of Rzeszow,* ***2.*** *Lviv National Medical University,* ***3.*** *Physico-Chemical Institute of NAS of Ukraine,* ***4.*** *Jackson State University,* ***5.*** *Lviv Politechnic National University*

In this report the physical and biological properties of new biomaterial: silver-doped fluorapatite were investigated. The aim of the study was to evaluate its bactericidal effect and the cytotoxicity on eukaryotic cells. Slightly modified method for the synthesis of apatite, doped with silver ions (for improving bactericidal efficacy) gives rise to the production of new promising biocomponent. The applications of fluor- and hydroxyapatites doped with silver occurred to be toxic to Staphylococcus aureus and have strongly indicated its antimicrobial activity. Importantly, material based on fluorapatite demonstrated highest biocidal effect in comparison to widely known hydroxyapatite. The structure of materials were studied by FTIR, Raman spectroscopy, TEM and Zeta potential analyses. The perspective of the future would be a using of such biomaterial as bone filler in medical industry e.g. implants or in dentistry with its bactericidal activity. Regarding to their use in medicine, this materials have not to be toxic to healthy cells. Thus, it have been also assessed the degree of cytotoxicity of modified apatites to eukaryotic cells.

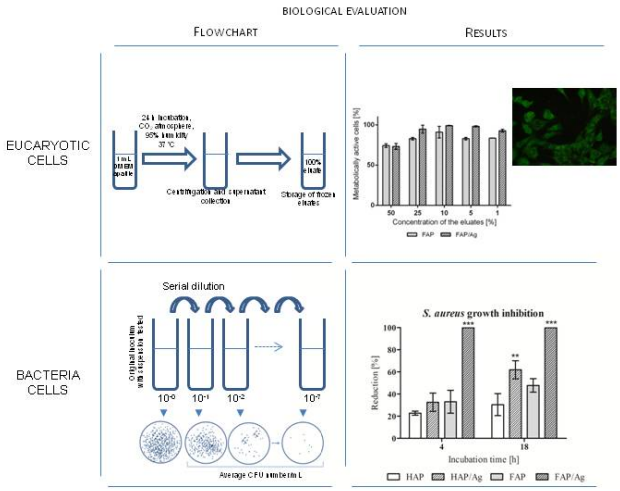


Fig 1 annic.jpg

# Microstructural investigation of hexagonal multilayered MoS2 nanoplatelets and their exposed edges role in gas-sensing

**Friday, 11th November - 13:30 - Poster Session - Gallery - Poster presentation - Abstract ID: 678**

***Dr. Geetanjali Deokar*** [1], ***Dr. Raul Arenal*** [2], ***Prof. Eduard Llobet*** [3], ***Dr. Dominique Vignaud*** [4], ***Mr. Jonathan Dervaux*** [5], ***Dr. Jean-Francois Colomer*** [1]

***1.*** *University of Namur,* ***2.*** *Universidad de Zaragoza,* ***3.*** *Universitat Rovira i Virgili,* ***4.*** *University of Lille,* ***5.*** *University of Mons*

MoS2 has attracted much attention owing to its excellent electrical, optical and other physical and chemical properties. Here we report, hexagonal MoS2 nanoplatelets growth on vertically aligned CNT substrates produced by chemical vapor deposition technique. Selective area synthesis of the nanoplatelets was achieved by pre-patterning of the source material for MoS2 growth. Surface morphologies and crystalline characteristics of the deposited MoS2 were examined by scanning electron microscopy, transmission electron microscopy, X-ray photoelectron spectroscopy, Raman spectroscopy and, UV-Visible spectroscopy. The MoS2 nanoplatelets with excellent crystalline quality exhibit hexagonal platelets-like morphologies, with the thickness and the length were measured to be around 20 - 30 nm and several hundred nanometers, respectively. The hexagonal MoS2 nanoplatelets with exposed edges shows selective and sensitive NO2 and NH3 detection. In future, the as-produced material could be potentially used for gas sensing applications.

# Platinum-free catalysts for low temperature fuel cells

**Friday, 11th November - 13:30 - Poster Session - Gallery - Poster presentation - Abstract ID: 714**

***Dr. Tatiana Lastovina*** [1], ***Ms. Julia Pimonova*** [1], ***Dr. Andriy Budnyk*** [1]

**1.** *International Research Center "Smart materials", Southern Federal University*

Introduction An efficiency of low temperature oxygen-hydrogen fuel cells is influenced by kinetic limitations of the oxygen reduction reaction (ORR). Platinum and its alloys with transition metals are usually used as cathodic catalysts for the ORR. However, platinum-based catalysts have some drawbacks such as high cost and high extent of degradation. Such situation stimulated recent investigations aiming on developing of platinum-free or low platinum content catalyst for ORR. Metal-organic frameworks (MOFs) and MOF-derived porous carbon materials may constitute a promising solution. This research is focused on the preparation of the porous MOFs that can be used as catalysts for oxygen reduction reaction. Methods Fe3O4@MOFs (MOF = ZIF-8, ZIF-68, HKUST-1) composites were prepared by sonochemical, solvothermal and microwave-assisted syntheses. At the first stage magnetic iron oxides nanoparticles were prepared by microwave-assisted modified co-precipitation method. They were characterized with X-ray diffraction (XRD), Fourier transformed Infrared spectroscopy (FTIR), transmission electron microscopy (TEM), dynamic light scattering (DLS). Then, magnetic nanoparticles were covered with MOFs. Final composites were additionally investigated using vibrating magnetometer and surface area and porosity analyzer. Furthermore, fractions of the samples were heat treated at 900 C under argon atmosphere to obtain catalytic active carbons. Results and Discussion According to XRD data the final composites contain both spinel phase of nanoparticles and the MOF's phase. It was shown that prepared materials are porous and magnetic; their surface area and porosity depends on synthesis conditions. To have an insight into applicability of obtained composites in ORR, they were investigated by cyclic voltammetry (CV) in three-electrode cell in phosphate buffered saline at pH = 6 (see Fig.1). In conclusion, we have obtained catalytic active composites, which might be suitable for applications in low temperature air-hydrogen fuel cells. This work was supported by Russian Foundation for Basic Research (grant № 16-33-00854).

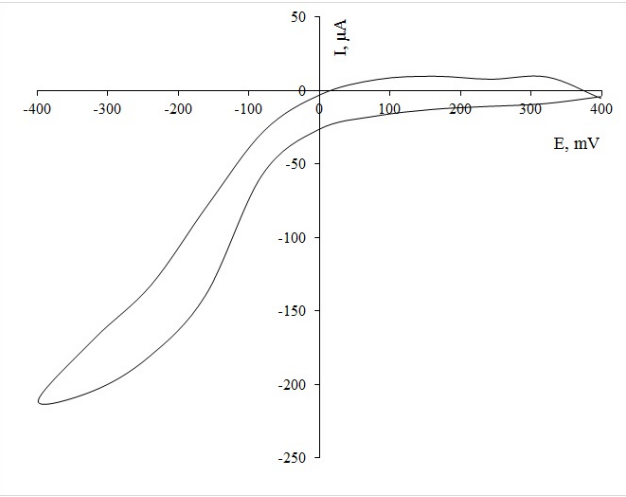


Cyclic voltammetry.jpg

# V2O5 nanorods as CO2 gas sensing devices

**Friday, 11th November - 13:30 - Poster Session - Gallery - Poster presentation - Abstract ID: 622**

***Ms. Ayouz katia*** [1]***, Mrs. Tala-Ighil Razika*** [2]***, Ms. Kawther Mhammedi*** [3]***, Dr. Sabrina Sam*** [4]***, Dr. Noureddine Gabouze*** [5]

***1.*** *CRTSE, 02 Bd Frantz Fanon B.P. 140 Alger 7 Merveilles, Algiers, Algéria / Institute of Electrical & Electronic Engineering, Université M'hamed Bougara Boumerdes, Rue de l'indépendance, Boumerdes 35000, ALGERIA,* ***2.*** *Institute of Electrical & Electronic Engineering, Université M'hamed Bougara Boumerdes, Rue de l'indépendance, Boumerdes 35000, ALGERIA,* ***3.*** *Thin layers and semiconductors, materials physics laboratory, University of Sciences and Technology Houari Boumediene BP 32 16111 BAB EL ALIA EZZOUAR ALGER,* ***4.*** *crtse Centre de Recherche en Technologie des Semi-conducteurs pour l'Energétique, Division Couches Minces Surfaces et Interfaces,* ***5.*** *SOAM, Centre de Recherche en Technologie des Semi-conducteurs pour l'Energétique*

In the present paper, a gas sensing device based on Vanadium oxide thin films (V2O5)/ Porous Si (PS) / Si structure has been used to detect CO2 gas at different concentration. Amorphous and crystalline vanadium pentoxide (V2O5) thin films were grown onto monocristalline silicon and porous silicon substrates using the Dip-coating method. The Vanadium oxide has been produced from vanadium alcoxide precursor. Different structures based on V2O5 / Porous Si/ Si have been realized and studied. Current-voltage (I-V) characteristics show that the sensor properties were modified due to CO2 gas presence. The structure sensitivity increases potential and concentration of CO2 increase. In addition, the structure exhibits fast response and 32s recovery time. The Obtained results are promising since the measured response and recovery time were lowered compared to CH/PS/Si structure.

# An Amide Substituted Dithienylpyrrole Based Copolymer: Its Electrochromic Properties

**Friday, 11th November - 13:30 - Poster Session - Gallery - Poster presentation - Abstract ID: 674**

***Ms. Simge Durur*** [1], ***Ms. Tugba Soganci*** [1], ***Dr. Hakan Can Soyleyici*** [2], ***Dr. Metin Ak*** [1]

***1.*** *Pamukkale University,* ***2.*** *Adnan Menderes University*

Electrochemistry of a new generation copolymer of N-(2,5-di(thiophen-2-yl)-1H-pyrrol-1-yl)-4-(vinyloxy) benzamide (TPVB) and 3,4-ethylendioxythiophene (EDOT) is presented. In this study, a novel copolymer based upon TPVB and EDOT is successfully synthesized and characterized in dichloromethane (DCM)/tetrabutylammonium hexafluorophosphate (TBP6) solution for different feed ratios of monomers via electrochemical methods. The copolymer film reveals three different colors (pale red color, green, midnight blue) under different potentials and it has good optical contrasts (44% at 555 nm and 75% at 1000 nm) and fast swiching times (1.5 s at 555 nm and 2.0 s at 1000 nm). Satisfactory results implied that the copolymer films (P(TPVB-co EDOT)) can be used in a wide variety of applications such as electrochromic devices, optical displays. We also describe a proposal for the determination of copolymer composition by means of the optical properties of P(TPVB-co-EDOT).

# Modified Denatured Lysozyme Effectively Solubilises Fullerene C60 Nanoparticles in Water

**Friday, 11th November - 13:30 - Poster Session - Gallery - Poster presentation - Abstract ID: 475**

***Ms. Marialuisa Siepi*** [1], ***Ms. Jane Politi*** [1], ***Ms. Angela Amoresano*** [1], ***Ms. Paola Giardina*** [2], ***Mr. Luca De Stefano*** [1], ***Ms. Daria Maria Monti*** [1], ***Mr. Eugenio Notomista*** [1]

***1.*** *University of Naples Federico II,* ***2.*** *National Research Council*

Carbon based nanomaterials, like fullerenes, nanotubes and graphene, have several applications in the medical field and engineering field, however the very low solubility of these materials both in organic solvents and in water poses serious limitations to their use. For example, fullerene C60, the most studied among fullerenes, can be dissolved in water in the form of nanoparticles of variable dimensions only through several weeks of sonication or using complex procedures involving organic solvents. For this reason the development of ``solubilizing agents'' for carbon materials is a very active research area. We have compared the efficacy as solubilizing agent of native and denatured hen egg white lysozyme, a highly basic protein. In order to obtain a denatured, yet soluble, lysozyme derivative, the four disulfides of the native protein were reduced and exposed cysteines were alkylated by 3-bromopropylamine, thus further increasing the already high positive charge of the native protein. Circular dichroism studies demonstrated that modified denatured lysozyme (amino-propyl-lysozyme, AP-LYS) is a random coil in water but can adopt a helical structure in organic solvents. Both native lysozyme and AP-LYS proved to be very effective solubilizing agents for C60 however dynamic light scattering, transmission electron microscopy and atomic force microscopy studies showed that AP-LYS allows to prepare more homogeneous and more stable C60 nanoparticles using lower amounts of protein. Preliminary studies shows that AP-LYS can be also used to solubilize in water other carbon allotropes.

# Gold nanoparticles as biocompatible surface for lipase adsorption: Physical-chemical study of the ``nano-bio'' interface

**Friday, 11th November - 13:30 - Poster Session - Gallery - Poster presentation - Abstract ID: 313**

***Ms. Heloise Ribeiro de Barros*** [1], ***Prof. Leandro Piovan*** [1], ***Prof. Izabel Riegel-vidotti*** [1]

***1.*** *Universidade Federal do Paraná*

As nanotechnology advances further, the developing of nanomaterials associated to biological components is increasing upward since the phenomena that occur in the ``nano-bio'' interface, are governed by driving forces of molecular and colloidal nature. The study of the interfacial interactions provides the understanding of the relationship between the materials structure. Also, the knowledge of their properties in different environments (for example, physiological media) is fundamental for the safe use of nanomaterials. In this context, gold nanoparticles (AuNPs) are of great interest since they offer a biocompatible surface for proteins and enzymes. Also, associate to their enhanced stability and low toxicity, AuNPs are very attractive for biomedical and biotechnological applications. Structural changes in proteins caused by the interaction with diverse ligands can affect their catalytic properties. Therefore it is mandatory the investigation about the effect caused in the protein conformation and their properties due to the adsorption on the AuNPs surface. Therefore, this work proposes the study of the interfacial interactions that occur in the adsorption of Candida antarctica type B (CALB) lipase on AuNPs surface and the impact in the catalytic activity. Two methodologies were analyzed: CALB added during the AuNPs synthesis (A-CALB/AuNP) and CALB added after the AuNPs synthesis (D-CALB/AuNP). In order to evidence this process, these systems were characterized by UV-Vis spectroscopy, transmission electron microscopy, zeta potential, dynamic light scattering, fluorescence spectrophotometry, circular dichroism and isothermal titration calorimetry. It was evidenced that changes in the conformation and catalytic properties of CALB depend on the AuNPs synthesis methodology. The main differences were attributed to the different sizes and shapes of the AuNPs obtained. Therefore, the presented work contributes to the understanding of surface interactions between CALB and AuNPs, providing useful information in the building-up of ``nano-bio'' interfaces.

# Periodical Surface Nanostructures Induced by Femtosecond Laser

**Friday, 11th November - 13:30 - Poster Session - Gallery - Poster presentation - Abstract ID: 693**

***Ms. Bogdan Calin [1], Ms. Catalina Albu [1], Dr. Laura Ional [2], Dr. Ekaterina Iordanova [3], Dr. Georgi Yankov [3], Dr. Aurelian Marcu [2]***

***1.*** *National Institute for Laser, Plasma and Radiation Physics, 077125 Bucharest, Romania,* ***2.*** *National Institute for Laser Plasma and Radiation Physics,* ***3.*** *'Georgi Nadjakov' Institute of Solid State Physics, 72 Tsarigradsko shosse 1784 Sofia Bulgaria*

Laser Induced Periodical Surface Structures -- LIPSS, commonly known as ripples, obtained in metals under femtosecond laser irradiation have been extensively investigated by many research groups. Depending on the irradiation conditions, such as laser fluence, number of laser pulses or laser wavelength, different morphology and ripples periods has been obtained: Low Spatial Frequency LIPSS (LSFL) with a periodicity close to the incident laser wavelength, λ, with orientation perpendicular to the laser polarization, and High Spatial Frequency LIPSS (HSFL) with a periodicity from λ/2 up to λ/10, with orientation parallel to the laser polarization. Such micro- and nano-textured surfaces have important applications such as fabrication of bio-mimetic substrates for cells growth and proliferation, surfaces with modified tribologic or wetting properties, security marking. Our previous experimental observations are complemented by calculations based on the classical interference theory, surface plasmon and surface harmonics generation theories. However, the mathematical model for surface harmonics generation involved in ripples formation doesn't provide reliable predictions and requires further investigations. In order to achieve this, using a large interval of wavelengths for the incident radiation provides a significant advantage. Our latest experiments are emphasized on finding whether there is a correlation between HSFL produced with wavelengths in the NIR region of the spectrum, and LSFL produced with UV radiation. Experimental results and the formation mechanisms of ripples structures are discussed.

# Statistically optimized preparation of catalase immobilized magnetic nanoparticles

**Friday, 11th November - 13:30 - Poster Session - Gallery - Poster presentation - Abstract ID: 119**

***Dr. Sandeep Kumar*** [1]***, Dr. Asim K Jana*** [2]

***1.*** *Department of Biotechnology, Dr. B R Ambedkar National Institue of Technology, Jalandhar,* ***2.*** *Department of Biotechnology, Dr. B R Ambedkar National Institute of Technology, Jalandhar*

Background / Aim: Immobilization of enzymes over magnetic nanoparticles (MNPs) of Fe3O4 can make this preparation easily recoverable (with applied external magnetic field). Materials and Methods: Catalase enzyme was immobilized over MNPs (C-G-A-MNPs) via 3-aminopropyl triethoxy silane (APTES) functionalization (A-MNPs) and glutaraldehyde activation over A-MNPs (G-A-MNPs) using statistical method for optimization i.e. response surface method (RSM) for optimization important variables. Results: Results obtained by experiment designed by RSM showed correlation coefficient 0.99, 0.97 and 0.98 (between actual and predicted value) was obtained with respect to catalase activity, protein loading and specific activity. Maximum catalase activity (32.1 ± 1.1 U mg-1 MNPs) and specific activity (97.7 ± 3.4 U mg-1 of loaded protein) was achieved with 64 mM of APTES, 10.97 µL of glutaraldehyde, 14.50 mg mL-1 of catalase enzyme, 67 min of time and 22.6 ºC of temperature. The stability studies showed the good retention of activity of C-G-A-MNPs (81.65±7.65 %) after 144 h at 4 oC in comparison to 7.87±2.15 % of free enzyme under similar conditions while there was retention of 64.34±8.15 % activity after 20 cycles. Discussion: RSM is a method supported the multi-variable non-linear model, it's helpful in evaluation and perceiving the interactions of the varied parameters influencing the method. This variable approach showed advantage in terms of reductions within the range of experiments, improved applied math interpretation and reduced time necessities. Conclusion: The enzyme immobilized preparation prepared by statistically optimization was found to be suitable and effective for reuse in its different applications. Key words: Magnetic nanoparticles, response surface methodology, enzyme immobilization, surface functionalization, central composite design, characterization, recyclability, stability

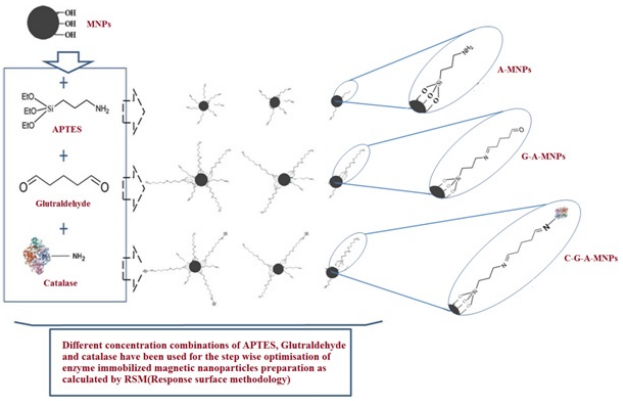


Scheme.jpg

# Pd2Sn vs. Au-Pd2Sn NPs: catalytic study for hydrogenation and Sonogashira coupling reactions

**Friday, 11th November - 16:00 - Nanocatalysis & Applications In The Chemical Industry - Room 1 - Oral presentation - Abstract ID: 125**

***Dr. Raquel Nafria*** [1], ***Mr. Zhishan Luo*** [1], ***Dr. Michaela Meyns*** [2], ***Prof. Jordi Llorca*** [3], ***Dr. Maria De La Mata*** [4], ***Ms. Sara Marti*** [4], ***Prof. Jordi Arbiol*** [4], ***Dr. Guillermo Muller*** [5], ***Dr. Arnald Grabulosa*** [5], ***Dr. Andreu Cabot*** [2]

***1.*** *Catalonia Energy Research Institute (IREC),* ***2.*** *Catalonian Energy Research Institute (IREC),* ***3.*** *Universitat Politècnica de Catalunya,* ***4.*** *ICN2,* ***5.*** *Universitat de Barcelona*

Multicomponent nanocrystals have become an important type of materials due to their ability to carry out multiple functions simultaneously. In this direction, colloidal synthesis allows to prepare nanoparticles (NPs) with a high level of control over size, geometry, phase and composition. Therefore the development of nanoparticles by colloidal synthesis is beginning to be used for the preparation and study of new catalysts, because their properties are strongly correlated with the design of their active centers. Additionally, catalysts based on well-dispersed colloidal nanoparticles, the so-called semiheterogeneous systems, combine the advantages of both homogeneous and heterogeneous catalysts. In this contribution we present the preparation of Pd2Sn and Au-Pd2Sn nanoparticles and the study of their catalytic behavior in hydrogenation and coupling reactions. Starting from Pd2Sn nanorods (NRs),1 Au-Pd2Sn heteronanorods (HNRs) were synthesized by a seed-mediated growth method.2 In order to obtain a thorough characterization of the HNRs and gain mechanistic insight into the Au growing process, TEM, HRTEM, XRD and XPS have been performed (Figure 1). The nanoparticles are active in hydrogenation of aromatic alkenes and alkynes under mild conditions, with an Au-effect on the catalytic outcome.3,4 The nanoparticles have also been tested in Sonogashira reactions.5 At low concentrations good activities towards the coupling product have been found. Unexpectedly, at high concentrations this product is catalytically reduced (Figure 2). Our preliminary study of the mechanism seems to indicate that the NPs also catalyze this reduction step without the involvement of molecular hydrogen. 1) Luo, Z.; Ibáñez, M.; Antolín, A. M.; Genç, A.; Shavel, A.; Contreras, S.; Medina, F.; Arbiol, J.; Cabot, A. Langmuir, 2015, 31 (13), 3952--3957. (2) Krylova, G.; Giovanetti, L. J.; Requejo, F. G.; Dimitrijevic, N. M.; Prakapenka, A.; Shevchenko, E. V. J. Am. Chem. Soc., 2012, 134 (9), 4384--4392. (3) Wu, Y.; Cai, S.; Wang, D.; He, W.; Li, Y. J. Am. Chem. Soc., 2012, (134), 8975−8981. (4) González de Rivera, F.; Angurell, I.; Rossel, D.M.; Erni, R.; Llorca, J.; Divins, J.N.; Muller, G.; Seco, M.; Rossell,O. Chem. Eur.J., 2013, 19 (36), 11963--11974. (5) González-Arellano, C.; Abad, A.; Corma, A.; García, H.; Iglesias, M.; Sánchez, F. Angew.Chem.Int.Ed, 2007, (119), 1558--1560.

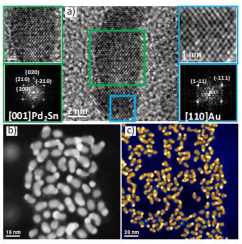


**Figure 1.** HRTEM micrograph of Au-$Pd_2Sn$ NRs (a), HAADF-STEM of Au-$Pd_2Sn$ (b) and false colored HAADF-STEM image of Au-$Pd_2Sn$ NRs (c).

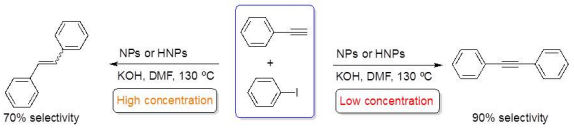


**Figure 2.** Products from the Sonogashira reaction at different concentrations.

Figure.jpg

# Water-Free Synthesis of Monodisperse Nickel(0) Nanoparticles

**Friday, 11th November - 16:17 - Nanocatalysis & Applications In The Chemical Industry - Room 1 - Oral presentation - Abstract ID: 171**

***Ms. Koyel Bhattacharyya*** [1], ***Prof. Nicolas Mézailles*** [1]

***1.*** *Université Paul Sabatier*

Nickel nanoparticles (Ni NPs) are valued for a variety of applications, ranging from catalysis[1] to magnetic properties[2] to the development of more complex nanomaterials[3]. The morphology of these nanoparticles plays a huge role in their behavior. Their size, shape, crystallinity, and surface state greatly affect their properties, and consequently their behavior in practical applications[4,5]. Previously, our lab developed a method for synthesizing size-tunable, monodisperse Ni NPs through the reduction of Ni(acac)2 (acac = acetylacetonate) at high temperature by oleylamine. An associated mechanistic study revealed that water was formed by the dehydration of the acac ligands during the reaction (Scheme 1: Reduction of Ni(acac)2 towards Ni NPs. This method produces water as a byproduct)[6]. Based on our understanding of the mechanism of reduction of Ni(II) into Ni NPs, we present a water-free method of synthesizing monodisperse Ni NPs (Scheme 2: Reduction of Ni(amide)2 to Ni(0)). This approach uses the thermal decomposition of the nickel(II) bis(oleylamide) precursor in the presence of the stabilizing ligand trioctylphosphine (TOP). Varying the ratio of TOP to nickel permits size tunability, resulting in nanoparticles ranging in size from 4 nm in diameter to 11 nm. The successful extension of this method to Fe and Co NPs will be presented. Finally, metal phosphide nanoparticles may be obtained by heating the metal NPs in the presence of white phosphorus (P4) (Figure 1: Synthesis of Ni2P NPs from Ni(0) NPs). [1] N. Mézailles, et al. Nano Today 2012, 7, 21--28. [2] R. D. Tilley, et al. J. Am. Chem. Soc. 2012, 134, 855--858. [3] (a) N. Mézailles, et al. Chem. Mater. 2011, 23, 2270--2277. (b) N. Mézailles, et al. Chem. Mater. 2012, 24, 688--697. [4] T. Zhang, et al. J. Phys. Chem. C 2010, 114, 3196--3203. [5] A. P. Alivisatos, et al. Nature 2005, 437, 664. [6] N. Mézailles, et al. Chem. Eur. J., 2012, 18(44), 14165--73.

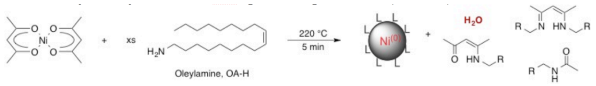


**Scheme 1.** Reduction of Ni(acac)$_2$ towards Ni NPs. This method produces water as a byproduct.

Scheme 1.png

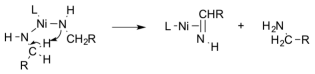


**Scheme 2.** Reduction of Ni(amide)$_2$ to Ni(0).

Scheme 2.png

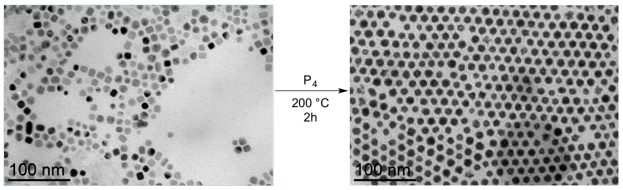


**Figure 1.** Synthesis of $Ni_2P$ NPs from Ni(0) NPs.

Figure 1.png

# Supported gold based bimetallic nanoparticles catalyzed oxidation and C-C coupling reactions

**Friday, 11th November - 16:34 - Nanocatalysis & Applications In The Chemical Industry - Room 1 - Oral presentation - Abstract ID: 64**

***Prof. Redouane Bachir*** [1], ***Dr. Nawel Ameur*** [1], ***Dr. Amina Berrichi*** [1], ***Prof. Sumeya Bedrane*** [1], ***Prof. Abderahim Choukchou-braham*** [1]

***1.*** *university of Tlemcen*

Since Haruta et al.[1] have shown that gold nanoparticles have catalytic activity for CO oxidation at very low temperature, a lot of research groups were interested in the preparation of new catalysts based on supported metal nanoparticules. The majority of these studies focuses towards development of methods for preparing nanoparticles increasingly smaller, preparation and design of supported bimetallic nanoparticles and exploits the characteristics of these nanoparticles to catalyze different reactions. Supported bimetallic nanoparticles have an important role to play as catalysts for different reaction. Indeed, according to the metal used, it is possible to prepare active, selective and stable catalysts for different reactions [2] In this paper we report an overview of studies, made by our research group, on the preparation and characterization of supported bimetallic nano-catalysts Au-M/support (M= Co, Fe, Cr, Cu, Ni) and (Support = Al2O3, SiO2, TiO2). Different strategies were used to synthesize the catalysts. These catalysts were fully characterized by TEM, DRUV-vis, DRX, BET, FTIR. The catalytic performances of these bimetallic nanoparticles were evaluated in the oxidation of cyclohexene[3] (scheme 1) Scheme 1: Oxidation of Cyclohexene and the synthesis of propargylamines via an A3 and AHA three component coupling reactions[4] (scheme 2) Scheme 2: Synthesis of propargylamines by three component coupling reaction [1] M. Haruta, T. Kobayashi, H. Sano, N. Yamada, Chem. Lett., 6 (1987) 405-408. [2] M. Sankar, N. Dimitratos, P. J. Miedziak, P. P. Wells, C. J. Kielye, G.J. Hutchings, Chem. Soc. Rev. 41 (2012) 8099-8139. [3] N. Ameur, A. Berrichi, S. Bedrane, R. Bachir, Adv. Mater. Res. (2014). [4] A. Berrichi, R. Bachir, M. Benabdallah, N. Choukchou-Braham, Tetrahedron Lett. 56 (2015) 1302-1306.

# Shape- and size-controlled synthesis of ligand free CeO2 nanoparticles and their catalytic performances: From nanospheres to nanostars

**Friday, 11th November - 16:51 - Nanocatalysis & Applications In The Chemical Industry - Room 1 - Oral presentation - Abstract ID: 488**

***Ms. Taisiia Berestok*** [1], ***Dr. Pablo Guardia*** [2], ***Dr. Raquel Nafria*** [1], ***Dr. Massimo Colombo*** [3], ***Dr. Sonia Estrade*** [4], ***Prof. Francesca Peiró*** [4], ***Dr. Andreu Cabot*** [1]

***1.*** *Catalonia Energy Research Institute (IREC),* ***2.*** *Centre Tecnològic de la Química de Catalunya,* ***3.*** *Istituto Italiano di Tecnologia,* ***4.*** *University of Barcelona*

Among the rare earth compounds CeO2 has become a technologically important material widely used in industrial applications and manufacturing processes[1]. Colloidal synthesis of nanoparticles (NPs) has attracted great interest due to possibility of a precise control over size and shape which would allow controlling the exposed crystallographic facets and hence the catalytic performance. Here we report on the synthesis of ceria NPs with control over size and shape resulting from a branching process. This process results from a kinetically controlled overgrowth due to the presence of surfactants that display preferential adsorption on particular crystallographic facets thus tuning the length and width of branches. CeO2 NPs were obtained through the thermal decomposition of cerium precursor in the presence of oleic acid, oleylamine, alkanediol and octadecene. Adjusting the experimental conditions allows us synthesizing NPs with different level of branching and shape evolving from spheres, flowers, cubes, kites and stars (Figure 1) all of them within the 7 to 45 nm size range. Some synthetic parameters allow tuning the final anisotropic degree of the NPs structure by controlling the branching events and growth. Tuning the amount of alkanediol molecules results on a shape evolution from irregular rombohedral NPs to branched structures. For the first time on ceria, organic ligands were replaced by shorter ones (Amino acids) or by inorganic ligands (Oxo- or polyoxometalates) which offer the advantage to stabilize NPs in polar solvents and decrease the steric hindrance of the organic once towards molecule absorbance[2,3]. The nanocryctals' surface was functionalized through the solution phase ligand exchange in acidic media with further exposing them to amino acids or oxometalates. This mild exchange process allows to keep constant the NPs' structure compare to other more aggressive treatments as for instance calcination. Finally, CO-CO2 conversion experiments were performed in order to test ceria branched structures as novel catalyst. Figure 1. (a)HRTEM micrograph of CeO2 octapod. (b)Reconstruction of the lattice by inverse Fourier transformation. (c)FFT obtained from the selected area. [1]C.Sun, et al, Energy & Environmental Science 2012, 5, 8475. [2]J.D.Roo, et al, Langmuir, 2016, 32 (8), pp 1962. [3]J.Huang, et al, ACS Nano 2014, 8(9), 9388.

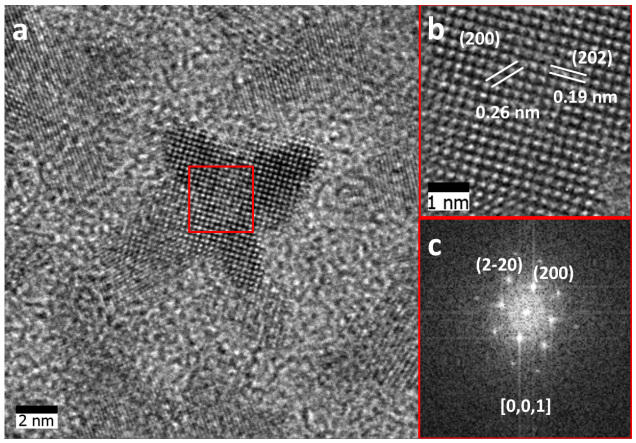


Hrtem stars abstract.png

# Simple approach towards few layers MoS2 nanorods/nanoflowers and their potential for piezo-photocatalytic rapid degradation activity

**Friday, 11th November - 17:08 - Nanocatalysis & Applications In The Chemical Industry - Room 1 - Oral presentation - Abstract ID: 514**

***Mr. Neeraj Kumar*** [1], ***Dr. Vyom Parashar*** [1], ***Prof. Suprakas Sinha Ray*** [2], ***Prof. Jane Catherine Ngila*** [1]

***1.*** *University of Johannesburg, Department of Applied Chemistry, Johannesburg,* ***2.*** *DST/CSIR National Centre for Nanostructured Materials, Council for Scientific and Industrial Research, Pretoria*

In the present scenario, energy demand and environmental remediation are the serious challenges for the worldwide scientific community. Photocatalysis has been extensively studied for its important applications in environmental purification and green energy. Various strategies (such as doping, co-catalyst loading, and hetero-structure formation) have been designed for the enhancement of degradation activity and for shifting UV light dependency to visible light. Still, the low efficiency and high process cost are the main hurdles for confronting the commercialisation of photocatalysis. Therefore, it is imperative to develop a new green approach to tackling conundrum of environmental remediation at the industrial level. Molybdenum disulfide (MoS2) has emerged as a promising semiconductor material for electronics, gas separation, energy conversation and storage due to its unique properties. However, its potential towards the water remediation has not fully explored. Herein, the defect-rich few layers MoS2 nanorods/nanorods were developed by a one-step hydrothermal approach using sodium dithiocarbamate as a sulphur source. The formation of few layers MoS2 nanorods/nanoflowers was concluded using different characterization tools such as XRD, SEM, HR-TEM, Raman, and AFM. The obtained sample exhibited rapid degradation activity towards methylene blue dye and Cr(VI) reduction to Cr(III) by introducing the ultrasonic wave in the dark/light. The rapid degradation rate in the dark is ascribed to the separation of electron and hole pairs in the presence of the electric field, which is formed due to the mechanical stress exerted on the MoS2 by ultrasonication. Almost 100% degradation ratio of both dye and reduction of Cr(VI) to Cr(III) was noticed in very short period of time. Furthermore, the plausible mechanism and various piezo-catalytic results will be discussed in greater detail during the presentation.

# Formation of nanostructured AlOOH film on Al alloys by steam coating toward corrosion protection

**Friday, 11th November - 16:00 - Nanofabrication & Nanomanufacturing - Room 207 - Oral presentation - Abstract ID: 550**

***Dr. Ai Serizawa*** [1], ***Prof. Takahiro Ishizaki*** [1]

***1.*** *Shibaura Institute Of Technology*

Al alloys have been used as advanced structural materials in automobile and railway industries because of excellent physical and mechanical properties such as low density, good heat conductivity, and high specific strength and ductility. Their low corrosion resistance, however, hinders their use in the corrosive environment. To improve the corrosion resistance of the Al alloys, the development of a novel coating technology has been highly desirable. In this presentation, we report a control method of corrosion protection for Al alloy using steam. The corrosion resistance of the composite film was also investigated. Al-Mg-Si alloy was used as the substrate. The substrates were ultrasonically cleaned in absolute ethanol for 10 min. The cleaned Al-Mg-Si alloys were set in the autoclave. The cleaned Al-Mg-Si alloy substrates were introduced in a Teflon-lined autoclave with a 100 ml capacity. 20 ml of ultrapure water was located at the bottom of the autoclave to produce steam. The autoclave was heated to a temperature of 373 to 453 K, and then held at this temperature for up to 48 h, and was subsequently cooled naturally to room temperature, resulting in the formation of anticorrosive films on magnesium alloys. The resultant films were characterized by XRD, XPS, FE-SEM and electrochemical measurements. FE-SEM image of film surface treated at 453 K for 48 h using steam were shown in Fig. 1. Plate-like nanostructure was densely formed on the surface. XRD patterns indicated that the film formed on two types of Al alloys by steam coating was mainly composed of crystal AlOOH. The corrosion resistance of the film was investigated using electrochemical measurements. The potentiodynamic polarization curves of the film coated and uncoated Al-Mg-Si alloy after immersion in the 5 wt% NaCl aqueous solution for 30 min revealed that the corrosion current density, jcorr, of the film coated Al-Mg-Si alloy decreased by more than two orders of magnitude as compared to the uncoated Al-Mg-Si alloy, indicating that the corrosion resistance of the Al-Mg-Si alloy were improved by the formation of the film via steam coating. This work was supported by JSPS Grant-in-Aid for Young Scientists (B) Grant Number 15K18237.

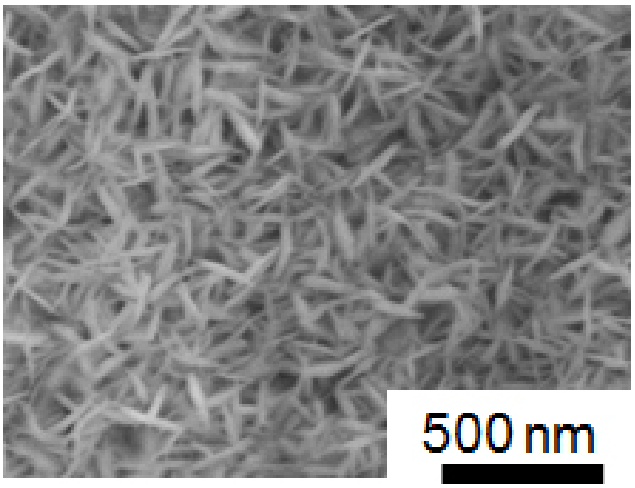


Fig1 serizawa.jpg

# Resizable nanopores

**Friday, 11th November - 16:17 - Nanofabrication & Nanomanufacturing - Room 207 - Oral presentation - Abstract ID: 543**

***Ms. Clemence Briosne-frejaville [1], Mr. Adrien Mau [1], Mr. Armandas Balcytis [2], Dr. Xijun Li [2], Prof. Saulius Juodkazis [2]***

***1.*** *Institut d'Optique Graduate School, Université de Bordeaux,* ***2.*** *Swinburne University of Technology*

Nanopores in solid-state membranes attract considerable interest due to their applicability in single molecule detection, identification and DNA/RNA sequencing. As this requires the ability to create holes on the molecular size-scale, significant fabrication challenges arise. Currently, focused ion beam (FIB) with helium ions enables the creation of single-nanometer sized openings with depth/diameter aspect ratios ranging in the hundreds. However, this type of milling is too slow to be practicable, hence, as a commercially viable option Ga FIB with subsequent hole resizing has to be pursued. FIB milling was used to open 30-100 nm diameter holes in Si3N4 membranes of comparable thickness. Holes and their arrays were milled in tens-of-seconds on the Si3N4-membrane on Si samples. Typically, the exit diameter was up to two times smaller than that at the beam entrance. Negligible resputtering of membranes took place and high fidelity holes were obtained. Thin metal coating sto prevent surface charging were implemented, however, through-holes can be milled even on as-received membranes at the smallest 6 pA ion currents. The smallest diameter holes of 30 nm were fabricated with a 10 nm spot-size beam (IonLiNE Raith). The opened holes were, next, subjected to electron beam for down-sizing. Following scaling rules were determined: (i) for the identical scan speed, the closure speeds in nm-per-second increase with the increasing of the magnification or the decreasing of the scan area size, (ii) hole closure speed in nm/s increases with the scan speed, and (iii) the closure speed in nm per area-scan decreases with scan speed. This indicates that material redeposition due to resputtering [1] is the most probable cause of hole rescaling. Hence, by material re-deposition it should be possible to fully close holes at the cost of thickness changes. Possible applications of nanoholes will include ion-transfer through cell membrane where the location and contact area can be controlled to unprecedented few-nm resolution. Frequency lifetime imaging (FLIM) technique will be employed for future ion transport experiments and provides a super-resolution capability due to precise knowledge of the hole position and geometry. [1] G. Seniutinas, et al., Beilstein journal of nanotechnology 4 (1), 534-541. 2013.

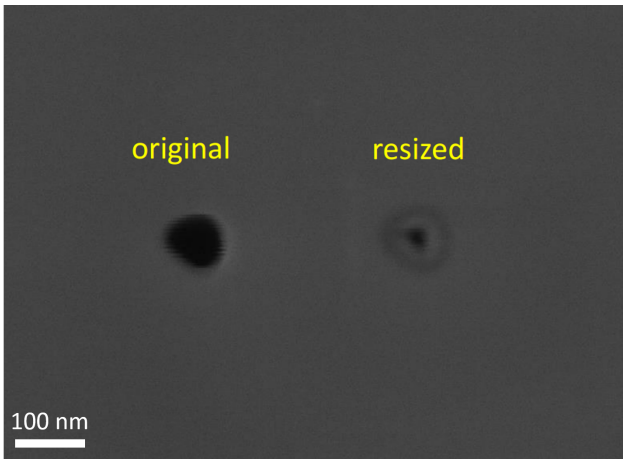


Img2.png

# The surface microstructure of SiC epitaxial films, grown by atom replacement.

**Friday, 11th November - 16:34 - Nanofabrication & Nanomanufacturing - Room 207 - Oral presentation - Abstract ID: 418**

***Mrs. Dina Bakranova*** [1], ***Prof. Sergey Kukushkin*** [2], ***Prof. Kair Nussupov*** [1], ***Dr. Andrey Osipov*** [2], ***Dr. Nurzhan Beisenkhanov*** [1]

***1.*** *Kazakh-British technical university,* ***2.*** *Institute for Problems of Mechanical Engineering RAS*

Such properties of silicon carbide (SiC) as high hardness, chemical resistance, high thermal conductivity, wide band gap (2.2 -- 3.7 eV) and high breakdown voltage [1] cause a great interest of that material in fabrication of semiconductor devices for various purposes. There are some difficulties for heteroepitaxial growth of β-SiC layers on silicon (Si) substrate. Primarily this growth suppressed by large lattice mismatches (~ 19%) [2] and thermal expansion coefficient mismatches (8%) between SiC and Si lattices. In [2] authors have been offered a new approach for SiC film formation onto Si substrate. The main idea of their work based on process of replacement some atoms of Si substrate by energetic C atoms, which leads to SiC layer forming. In this article, SiC films, obtained by influence of CO and SiH4 (264 Pa, 1250°C, 15 min) gases mixture on high-resistance single crystalline (111) oriented n-type Si substrate, were measured by X-ray diffraction (XRD), profilometry, atomic force microscopy (AFM), X-ray reflectometry (XRR) and Raman microscopy to study the phase composition, surface microstructure and surface roughness. It was revealed that SiC films contain both nanocrystalline and single crystalline 3C-SiC structures with highly perfection β-SiC crystallites. The surface of the film has a pyramidal or step-like structure with a distinct fragmentation of the faces and the height variations of up to 36 nm. It was found that the treatment of silicon substrates by acid mixture of HF: HNO3 (in 1:10 proportion) polishes their surface and leads to the appearance of the intensive oscillations of X-ray reflections, which allows to determine the thickness of the SiC film (about 100 nm). On the other hand, the chemical treatment causes emerging of etching pits and increases average roughness of surface, which results in decreasing of intensity of the main X-ray peak. [1] Wu W, Chen DH, Cheung WY, Xu JB, Wong SP, Kwok RWM, Wilson IH 1998 Appl. Phys. A 66 S539--S543 [2] Kukushkin SA and Osipov AV 2014 J. of Phys. D: Appl. Phys. 47 313001-41

# Study and analysis of composition variation influence for chemical reactions sequence and thermal effects in Al-Ni multilayered thermite materials

**Friday, 11th November - 16:51 - Nanofabrication & Nanomanufacturing - Room 207 - Oral presentation - Abstract ID: 82**

***Mr. Egor Lebedev*** [1], ***Prof. Dmitry Gromov*** [1], ***Mr. Yuri Shaman*** [2], ***Ms. Anna Presnukhina*** [1], ***Prof. Sergey Gavrilov*** [1]

***1.*** *MIET,* ***2.*** *Scientific-Manufacturing Complex "Technological Center"*

Over the recent years a reactive joining technology that uses nanostructured multilayer foils as local heat sources have attracted increasing attentions. Multilayer structures replaced the traditional powder thermite mixtures and opened up new possibilities of nano- and micro-scale surfaces and materials joining processes, based on self-propagating reactions in these foils providing rapid bursts of energy that can heat and melt the surrounding solder or braze layers and join materials at room temperatures and without additional external heating. The authors completed a detailed thermodynamic analysis of Al-Ni thermite system. As a result, the sequence of phase transformations and chemical reactions has been predicted, which allowed to optimize the stoichiometric ratio of the thermite mixture components. Mathematical modeling of the heat release process was allowed to estimate the speed of a chemical reaction front propagation, and to determine the minimum value of the structure total thickness for its initiation. Experimental samples of thermite multilayer Al/Ni foils of different total and bilayer thickness (from micro to nanosize) were fabricated by alternating magnetron sputtering of Al and Ni targets. For TGA and DSC measurements multilayer structures separated from the substrates by dissolving the sacrificial layer. The individual layers and the total structure thicknesses were controlled by cross-sections SEM measurements. Structural and elemental analysis was performed by XRD and XEDS measurements. The speed of chemical reactions propagation were evaluated using high-speed video camera. It was shown that the start temperature of the reaction can be varied in wide range changing the component layer thicknesses from micro- to nanosizes. Thus using this size effect it is possible to increase the sensitivity of the material to the initiation. Changing the atomic proportions of thermite structure components allows to change intensity and character of heat release. Thus, the multilayered thermite materials can be tailored to specific applications and tasks. X-ray phase composition studies was given the opportunity to make corrections in the thermodynamic calculations and to determine the sequence of phase transformations that allows to optimize the thermite material composition.

# Modelling of grain refinement around highly reactive interfaces in processing of nanocrystallised multilayered metallic materials

**Friday, 11th November - 17:08 - Nanofabrication & Nanomanufacturing - Room 207 - Oral presentation - Abstract ID: 571**

***Mr. Szymon Bajda [1], Prof. Dmytro Svyetlichnyy [1], Prof. Delphine Retraint [2], Prof. Michal Krzyzanowski [3]***

***1.*** *AGH University of Science and Technology,* ***2.*** *University of Technology of Troyes (UTT),* ***3.*** *Birmingham City University, AGH University of Science and Technology*

Duplex techniques are attempted to be developed combining nanocrystallisation processes with a subsequent thermomechanical processing in order to produce multilayered bulk structures with improved yield and ultimate tensile strengths, while conserving an acceptable elongation to failure. However, the impurities deposited on the surface of the materials cause bonding imperfections due to interfacial oxidation during the duplex process. The interfacial oxidation can lead to formation of the discontinuous oxides or continuous oxide layer at the interfaces. The interface oxidation occurring during duplex processes can influence the microstructure development around the interfaces depending on whether the oxide scale is a continuous layer or a layer of discontinuous oxide clusters with heterogeneous thicknesses. Effectively the oxide scale becomes a part of the microstructure development of such nano-crystallised multilayered structures. The behaviour of the highly reactive interfaces during the processing of nanocrystallised multi-layered materials has been investigated numerically using the developed multi-level thermomechanically coupled finite element based model. The macro level part of the model representing the multilayered nanocrystallised metallic material has been linked to the meso- level part representing the oxidised interface within the material. The results of the analysis supported the possibility of strain localisations formed around the oxide islets at the interface between nanocrystallised fcc 316L austenitic stainless steel plates during the hot rolling stage of the duplex processing technique. In this work, the meso- level model has been expanded into evolution of the microstructure using frontal 3D Cellular Automata (FCA) numerical approach. The modelling data reflecting the strain localisations around the oxide clusters allowed for calculation of the grain refinement. The simulations of the grain refinement and changes of the disorientation angle are presented in the paper. The evolution of the initial microstructure with randomly distributed not oriented grains around the scale clusters is simulated focusing on the distribution of the boundaries disorientation angle during rolling taking into consideration different rotation rates among other things. An appearance of new boundaries is accompanied with an increase of the number of low-angle boundaries. The obtained results are in good agreement with the available experimental data derived from the relevant microstructural investigation.

# Ions irradiation induced damage profile of metal nanowires

**Friday, 11th November - 17:25 - Nanofabrication & Nanomanufacturing - Room 207 - Oral presentation - Abstract ID: 456**

***Ms. Shehla Honey*** [1]***, Dr. Shahzad Naseem*** [1]***, Dr. Ishaq Ahmad*** [2]***, Mr. Force Tefo Thema*** [3]***, Dr. Malik Maaza*** [3]

***1.*** *Centre of Excellence in Solid State Physics, University of Punjab, QAC, Lahore, Pakistan,* ***2.*** *National Center for Physics, Quaid-i-Azam University, Islamabad 44000, Pakistan,* ***3.*** *UNESCO-UNISA Africa Chair in Nanosciences/Nanotechnology, College of Graduate Studies, University of South Africa, Muckleneuk ridge, P.O. Box 392, Pretoria-South Africa*

In this work, ions irradiation induced damage study of metal nanowires (Ag, Cu) at different energies, doses and ions species is presented. After irradiation, samples are characterized using scanning electron microscopy (SEM), x-ray diffraction (XRD) and transmission electron microscopy (TEM). The results of irradiated samples are then compared with un-irradiated samples. Finally, a database of effects of ion irradiation on metal NWs is made. Mechanism of damage creation in metal NWs by ions irradiation is explained by collision cascade effect and thermal spike model. This database will be useful for future design of metal nanowire based devices to be used under harsh environmental conditions such as upper space.

**Table:** Summary of $H^+$, $C^+$ and $Cu^+$ ions irradiation induced damage on Ag-NW at room temperatures

| Ions | Dose ions/cm$^2$ | Energy | Results |
|---|---|---|---|
| $H^+$ | 1 x $10^{14}$ | 100 keV | Defects created, Morphology stable, |
| | 1 x $10^{15}$ | 100 keV | Amorphous clusters created, Morphology stable, |
| | 1 x $10^{16}$ | 100 keV | Amorphous phase dominated, Morphology stable, |
| | 1 x $10^{17}$ | 100 keV | Deterioration of crystal structure , Morphology stable |
| | 1 x $10^{16}$ | 5 MeV | Improve crystal structure, morphology stable |
| | 1 x $10^{17}$ | 5 MeV | Improve crystal structure, morphology stable |
| $C^+$ | 1 x $10^{13}$ | 5 MeV | Defects created, Morphology stable |
| | 1 x $10^{14}$ | 5 MeV | Crystal damage, NWs diameter reduction |
| | 2 x $10^{13}$ | 5 MeV | Crystal damage, NWs diameter reduction, melting |
| | 1 x $10^{16}$ | 5 MeV | Crystal damage , melting, thinning and slicing of NWs |
| $Cu^+$ | 1 x $10^{13}$ | 5 MeV | Defects created, Morphology stable |
| | 1 x $10^{14}$ | 5 MeV | Crystal damage , melting and sputtering of NWs, NWs diameter reduction |
| | 1 x $10^{15}$ | 5 MeV | Crystal damage , melting, thinning and slicing of NWs |

Table.png

# Enhancement of electrochemical properties of micro/nano electrodes based on TiO2 nanotube arrays

**Friday, 11th November - 16:00 - Nanomedecine & Nanobiology - Room 412 - Oral presentation - Abstract ID: 136**

***Mr. Dhurgham Khudhair*** [1]***, Ms. Julie Gaburro*** [2]***, Mr. Sajjad Shafei*** [3]***, Prof. Saeid Nahavandi*** [1]***, Dr. Anders Barlow*** [4]***, Dr. Asim Bahatti*** [1]

***1.*** *Deakin university / Institute for Intelligent Systems Research and Innovation - IISRI,* ***2.*** *Australian Animal Health Laboratory - CSIRO, Vic 3219, Australia,* ***3.*** *Deakin university/ Institute for Frontier Materials,* ***4.*** *Center for material and surface science, Department of chemistry and physics, La Trobe University*

Abstract: Titanium oxide nanotube (TiO2 nanotube) arrays were produced by anodizing titanium foils in two different electrolytes. The first electrolyte consisted of ethylene glycol containing 0.5 wt% NH4F and 4 ml of distilled water to produce pure TiO2 nanotube arrays and the second consisted of HF aqueous solution (0.5% wt ) containing 0.5wt% polyvinyl alcohol to produce carbon doped TiO2 nanotube arrays. The fabricated TiO2 nanotube arrays were subsequently annealed in the atmosphere of nitrogen. The morphology and crystal structure of fabricated arrays were characterized by means of scanning electron microscopy and X-ray diffraction. The electrical conductivity and capacity of TiO2 nanotube arrays were investigated by electrochemical impedance spectroscopy (EIS) and cyclic voltammetry (CV).Water contact angle and biocompatibility of fabricated nanotube arrays were investigated. The results showed that carbon doped TiO2 nanotube arrays annealed in the atmosphere of nitrogen have higher conductivity and capacity than pure arrays annealed in the same atmosphere. Doping with carbon enhances the biocompatibility and wettability of TiO2 nanotube arrays. It has also noted that electrical conductivity and capacity of TiO2 nanotube arrays were directly proportional to the tube wall thickness.

# A Robust Scaffold for Multimodality Using a Plasmonic Gold Core and a Mesoporous Iron Oxide Shell

**Friday, 11th November - 16:17 - Nanomedecine & Nanobiology - Room 412 - Oral presentation - Abstract ID: 379**

***Ms. Aastha Kukreja*** [1], ***Mr. Byunghoon Kang*** [1], ***Dr. Eunji Jang*** [1], ***Dr. Hye-Young Son*** [1], ***Prof. Yong-Min Huh*** [1], ***Prof. Seungjoo Haam*** [1]

***1.*** *Yonsei University*

Introduction: Multifunctional nano-systems provide an alluring approach towards designing nanoparticles with desired characteristics, which emerge from the interaction between various components of the system. A combination of various imaging modalities augments the advantages and simultaneously overcomes the restrictions encountered by the individual technique. Nano-particles providing combined Magnetic resonance (MR) imaging and X-ray computed tomography (CT) are very promising. CT and MR image acquisition and registration are the foremost steps in radiation therapy planning. These provide valuable information in target definition and determination of radiation dosage. This report describes a simple one-pot approach for the development of multifunctional gold core/iron oxide porous shell nanoparticles (AuFe NPs) functionalized with matrix metalloproteinase (MMP) peptide for targeted multi-mode magnetic resonance (MR) imaging and computed tomography (CT) imaging of human gastric cancer cells (SNU-484 cells). The drug loading capacity of the porous iron oxide nanoshell was also demonstrated. Methods: We devise a modified one-pot solvothermal reaction to synthesize AuFe core-shell nanoparticles. Here, the Au seeds are first formed in the same reaction mixture, prior to iron oxide formation due to the lower reduction potential of gold compared to iron. By carefully controlling the reaction conditions, uniform AuFe core-shell particles were generated with a spherical Au core and mesoporous Fe3O4 shell. The particles are loaded with Doxorubicin (Dox) and the surface is protected with polyethylene glycol and coated with MT1-MMP peptide for targeting. Results: The as-obtained nanoparticles demonstrate excellent colloidal stability and biocompatibility. The gold core provides a strong X-ray absorption and the Fe3O4 shell enables the MR imaging and MMP peptide provides successful targeting. AuFe NPs were successfully loaded with Dox and a surface quenching effect of the gold nanoparticles is proposed and correlated with the release of Dox from the porous core/shell system. Discussion: The AuFe NPs successfully demonstrate a multifunctional platform for MR/CT dual imaging of gastric cancer cells in vitro. Also, the porous nanoshell can be loaded with an appropriate drug of choice for future applications in theragnosis. Morphological, magnetic, CT and cell experiments demonstrate the AuFe nanoparticles as possible candidates for advanced medical purposes.

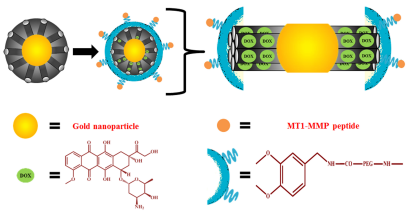


Aufe nps.jpg

# Infra-red laser pulse increases the expression of heat-inducible molecular cargo delivered via mesoporous silica nanoparticles

**Friday, 11th November - 16:34 - Nanomedecine & Nanobiology - Room 412 - Oral presentation - Abstract ID: 287**

***Ms. Lien Davidson*** [1], ***Dr. Natalia Barkalina*** [1], ***Dr. Marc Yeste*** [1], ***Mrs. Celine Jones*** [1], ***Dr. Kevin Coward*** [1]

***1.*** *University of Oxford*

INTRODUCTION: The use of nanocarriers for gene transfer into reproductive tissues, gametes, or embryos is gaining increasing capability as a non-invasive research tool for the manipulation and investigation of mechanisms underlying unexplained infertility. A significant limitation of current nanocarrier systems is the lack of controlled delivery to target sites, predominantly due to insufficient temporal and spatial control. Current literature describes several advances in specialized nanoparticles that respond to exogenous stimuli such as temperature and magnetic fields in order to assist controlled cargo release; however, such studies have yet to explore nanoparticle systems with thermo-controlled responsive molecular cargo. METHODS: A specialized molecular construct, featuring green fluorescent protein, and driven by the human heat-shock protein 70-1 promoter (HSP:GFP), was created as cargo for mesoporous silica nanoparticles (MSNPs). The cargo was electrostatically loaded onto MSNPs, and the MSNPs were delivered into HEK293T cells. Cargo expression following MSNP delivery was assessed with and without infra-red laser stimulus. Laser-treated cells were subjected to a single infra-red laser pulse (400mW, 1480nm) to stimulate a heat-shock response. RESULTS: MSNPs and infra-red laser treatment were not cytotoxic to HEK293T cells, both respectively and together. HSP:GFP cargo expression from MSNP delivery into HEK293T cells was increased two-fold following laser treatment, compared to delivery without laser treatment ($p<0.05$). DISCUSSION: We describe for the first time, the development of a laser-activated MSNP system with intrinsic heat-responsive cargo, capable of enhancing gene expression and providing spatial and temporal control. It is expected that this new approach for controlled and enhanced genetic expression could be applied to allow more refined spatio-temporal control of genetic manipulation for investigations into the pathophysiological mechanisms underlying unexplained mechanisms of infertility.

# Transparent conductive graphene-coated textile fibres: a platform for wearable electronics

**Friday, 11th November - 16:00 - Carbon & Graphene - Auditorium - Oral presentation - Abstract ID: 165**

***Dr. Ana Neves*** [1]

***1.*** *University of Exeter*

The concept of smart-textiles is witnessing a rapid development with recent advances in nanotechnology and materials engineering. Bearing in mind that the concept of textiles is much wider than clothes and garments, the potential is immense. While most current commercial applications rely on conventional hardware simply mounted onto fibres or fabrics, a new approach to e-textiles consisting in using functionalised textiles for several technological applications has the potential to change the paradigm of wearable electronics completely. Conducting fibres are an important component of any e-textile, nor only because they can be used as wiring for simple textile-based electronic component, but also because they can be used to build electronic devices directly on textile fibres. We have reported a new method to coat insulating textile fibres with monolayer graphene to make them conductive while preserving their appearance.[1] There are a number of factors that can greatly influence the sheet resistance achieved by graphene-coated textile fibres. In order to understand the influence of the topography of the fibres on the effectiveness of the graphene coating, an extensive study encompassing microscopy techniques like Atomic Force Microscopy and Scanning Thermal Microscopy, as well as Raman spectroscopy was performed.[2] This method has proven to be a versatile tool to achieve flexible, transparent and conducting fibres of different materials, sizes and shapes. The first applications of electronic devices built on such fibres are demonstrated, opening up the way for the realisation of wearable devices on textiles. [1] AIS Neves et al., Sci. Rep. 2015, 5, 09866 [2] AIS Neves et al. 2016 (in preparation)

# In vitro evaluation of carbon nanotube-based scaffolds for cartilage tissue engineering

**Friday, 11th November - 16:17 - Carbon & Graphene - Auditorium - Oral presentation - Abstract ID: 503**

***Dr. Jakub Rybka*** [1]***, Dr. Magdalena Richter*** [2]***, Mr. Eser Akinoglu*** [3]***, Dr. Tomasz Trzeciak*** [2]***, Prof. Jacek Kaczmarczyk*** [2]***, Prof. Michael Giersig*** [4]

***1.*** *Faculty of Chemistry, Wielkopolska Centre of Advanced Technologies, Adam Mickiewicz University in Poznań,* ***2.*** *Department of Orthopedics and Traumatology, Poznan University of Medical Sciences,* ***3.*** *Freie Universität Berlin, Department of Physics,* ***4.*** *Faculty of Chemistry, Wielkopolska Centre of Advanced Technologies, Adam Mickiewicz University in Pozn*

Introduction Cartilage injuries are one of the most common musculoskeletal disorders. Although a number of techniques have been designed to treat cartilage lesions, current research is focused on tissue engineering methods. Recent advances in molecular biology, biotechnology, and polymer science have led to both the experimental and clinical application of various cell types and biomaterials in the treatment of cartilage injuries. Methods This study reports an exceptionally good growth of chondrocytes on a 3D scaffold, based on multi-walled carbon nanotubes (MWCNTs). The MWCNT-based nanostructural scaffold was fabricated employing a plasma enhanced chemical vapour deposition technique. Articular cartilage specimens were taken from the distal femur of adolescent New Zealand White rabbits and chondrocytes were obtained by collagenase digestion. The quality of scaffolds was evaluated by the scanning electron microscope (SEM) and energy dispersive X-ray spectroscopy. Cell-seeded constructs were visualized with SEM. Results Chondrocytes adhered to the MWCNTs surface and were evenly distributed. After one week of culture, the number of cells was tripled than, when cultured in a plastic flask. These cells displayed multiple cytoplasmic extensions, which bend the nanotubes, and the cell morphology was altered by the MWCNTs surface structure (Figure: Morphology of the chondrocyte on the novel scaffold). Discussion Our study confirmed that the MWCNT-based surface provides a very good scaffold, which can be used to stimulate the formation of the cartilage tissue. Acknowledgment This work was supported by UMO-2012/06/A/ST4/00373 grant from the National Science Centre (Poland).

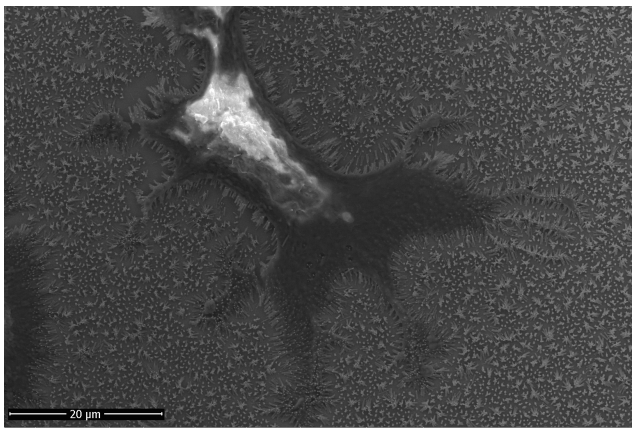


Figure 4.jpg

# Spice-based carbon dots: application to in vitro cancer growth inhibition

**Friday, 11th November - 16:34 - Carbon & Graphene - Auditorium - Oral presentation - Abstract ID: 602**

***Dr. Nagamalai Vasimalai*** [1], ***Ms. Vania Vilas-Boas*** [1], ***Dr. Juan Gallo*** [2], ***Dr. Cerqueira M.F.*** [3], ***Dr. Menéndez M*** [4], ***Dr. Costa J.M*** [4], ***Dr. Lorena Diéguez*** [1], ***Dr. Begona Espina*** [1], ***Dr. Maria Teresa Fernandez-arguelles*** [1]

***1.*** *Life Sciences Department, International Iberian Nanotechnology Laboratory (INL), Avenida Mestre Veiga, 4715-330 Braga, Portugal.,* ***2.*** *International Iberian Nanotechnology Laboratory (INL), Avenida Mestre Veiga, 4715-330 Braga, Portugal.,* ***3.*** *Center of Physics, University of Minho, 4710-057 Braga, Portugal.,* ***4.*** *Department of Physical and Analytical Chemistry, University of Oviedo Julian Clavería 8, 33006 Oviedo, Spain*

Synthesis and application of fluorescent carbon dots (C-dots) is emerging as a new alternative to inorganic semiconductor quantum dots due to their high photoluminescence, low photobleaching, high biocompatibility and excellent stability in aqueous media. All these features make them excellent candidates in biosensing, bioimaging, biomedical or catalysis applications. Nowadays multiple synthesis techniques are described to obtain C-dots, as well as different carbon sources as alternative for graphite source.1 In fact, natural source materials are being used for production of C-dots due to the simple, cost-effective and environmental friendly syntheses. However, when talking about the toxicity of C-dots, in vitro and in vivo results reported in the literature are inconsistent, and it is considered that the toxicity is mainly determined by the synthesis protocol.2 Therefore, due to the fascinating medicinal properties of certain compounds, in this work four different C-dots have been synthesized from spices including cinnamon, red chilli, turmeric and black pepper, by one-pot green hydrothermal method. They have been characterized with UV-Vis, Fluorescence, FTIR spectroscopies, DLS and TEM. These C-dots have been evaluated to study their toxicity to in-vitro human normal and cancer cells. Bioimaging studies confirmed that the C-dots inhibited cell viability dose-dependently, showing higher toxicity in cancer cells than in normal cells after 24 h incubation. Particularly, cell viability studies suggested that the growth of human cancer cells is suppressed up to 35%, 50%, 50% and 75%, when using cinnamon, red chilli, turmeric and black pepper respectively, whereas the growth inhibition of normal cells was not significantly affected. Conversely, C-dots synthesized from citric acid did not show any significant toxicity neither in normal nor in cancer cells, which suggests that the anticancer properties observed in the spice-derived C-dots can be attributed to the starting material employed for their fabrication. The interesting anti-cancer activity of the spice-derived C-dots along with the bioimaging applicability and excellent tolerability in normal HK-2 cells, suggests a promising future potential as efficient theranostic agents with minimal side effects in normal cells. 1. S. N. Baker et al., Angew. Chem. Int. Ed. 49 (2010) 6726-6744. 2. P. Pierrat et al., Biomaterials 51 (2015) 290-302.

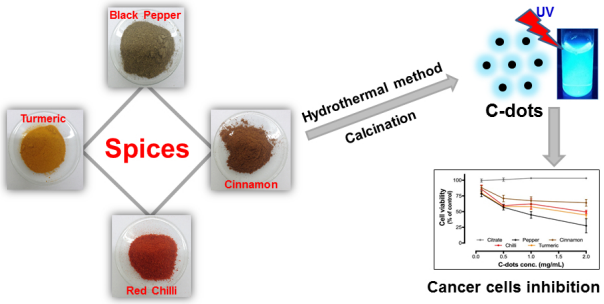


Graphical abstract v2 2 .jpg

# Role of hydrogen in affecting the growth trend of CNT on micron spherical silica gel

**Friday, 11th November - 16:51 - Carbon & Graphene - Auditorium - Oral presentation - Abstract ID: 225**

***Dr. Raja Nor Raja Othman*** [1], ***Ms. Amal Izzati Ismadi*** [1], ***Dr. Siti Nooraya Tawil*** [1], ***Dr. Kin Yuen Leong*** [1]

***1.*** *Universiti Pertahanan Nasional Malaysia*

Grafting CNTs onto substrates such as fibres and microparticles offers an alternative approach to tackle the issues associated with dispersion in a composite matrix, as well as additional benefits (hybrid effects) provided by these dual-filler systems. One approach to obtain such hybrid systems is the direct growth of nanotubes on the supporting fibre or particles. Previous study has shown that the CNTs would grow on the silica microparticles with the morphology closely related to the operating conditions such as temperature and time. However, the role of hydrogen in affecting the tube's morphology was not explored before. The particles were synthesized via chemical vapor deposition (CVD) method. Spherical silica gel with 40 -- 75 μm diameter was used as the substrate. Toluene and ferrocene were used as the hydrocarbon and catalyst source, respectively. The reaction time was kept for four hours while the temperature was maintained at 850°C. The morphology of the samples was further characterized by using FESEM and TEM, whilst TGA and Raman Spectroscopy measured the quality of the produced CNTs. The quality of the grafted CNTs was also compared with the conventional as purchased CNTs. The FESEM and TEM investigation proved that the flow hydrogen during reaction caused a tremendous difference in the outer diameter of the synthesized CNTs. Relatively thin CNT was observed under 50 ml/min of hydrogen flow compared to the particles synthesized without hydrogen. Raman spectroscopy of the CNTs revealed three bands; the disorder-induced D mode (~1321 cm-1), the tangential G mode (~1570 cm-1) and second order G' mode (~2642 cm-1). Raman analysis shows that the synthesized CNTs exhibited all these peaks, confirming the existence of CNTs. As G peak is more intense than D peak for all samples synthesized under hydrogen flow, it can be concluded that CNTs synthesized is indeed of high quality. The properties of grafted CNT on the surface of spherical silica gels were investigated. It can be confirmed that hydrogen plays an important role in influencing the morphology of the synthesized tubes.

# High-nitrogen graphene nanoflakes with iron functionalities: a viable catalyst for PEMFCs

**Friday, 11th November - 17:08 - Carbon & Graphene - Auditorium - Oral presentation - Abstract ID: 50**

***Mr. Pierre-Alexandre Pascone*** [1], ***Dr. Dimitrios Berk*** [1], ***Dr. Jean-Luc Meunier*** [1]

***1.*** *McGill University*

Introduction: A cost-effective alternative catalyst to platinum for the oxygen reduction reaction (ORR) in polymer electrolyte membrane fuel cells (PEMFCs) is iron deposited onto nitrogen-containing graphene. In this work, graphene nanoflakes were grown in-house with high levels of nitrogen (HN-GNFs) and iron functionalities to produce an active catalyst. The iron content was studied structurally and electrochemically. Methods: HN-GNFs are grown by the plasma decomposition of methane and nitrogen in a two-stage process using a thermal plasma torch. A wet-chemical method is used to incorporate iron nanoparticles into the graphene structure and the iron content is characterized by NAA, SEM, TEM, and XPS. Electrochemical studies by rotating disk electrode (RDE) are performed in different electrolyte solutions to determine catalytic performance towards the ORR. Results: Iron was successfully introduced at different levels into the HN-GNFs and the weight percent was measured by NAA; Fe-Low (1.25 wt%), Fe-Medium (3.77 wt%), and Fe-High (18.03 wt%). The introduction of iron did not change the qualitative surface conditions of HN-GNF, as verified by SEM. TEM shows iron nanoparticles with diameters between 10 to 35 nm within the graphene sheet layers (figure 1). With the iron imbedded into the HN-GNF, surface conditions are an incorrect indicator of overall iron content. XPS was performed on the limited amount of detectable iron; the deconvolution of the iron signal showed a mix of Fe, Fe(2+), and Fe(3+). An RDE study revealed that the addition of iron did not improve the catalytic performance in alkaline environments, with untreated HN-GNF already showing good activity towards the ORR. Iron proved to be beneficial in acid and neutral environments, with the Fe-Medium catalyst showing the best improvement to onset potential and current density. Discussion: The iron incorporation method used can be easily scaled to obtain whichever desired iron weight percent, with iron nanoparticles covered by the graphene sheets of the HN-GNFs. Catalysts with varying amounts of iron show no difference structurally to untreated samples while increasing the catalytic activity towards the ORR for acidic environments. The exact iron content still needs to be optimized to produce the best ORR catalyst for PEMFCs.

# Magneto-plasmonic-carbon-nanoscrolls with enhanced performances for sensitive biosensing applications

**Friday, 11th November - 17:25 - Carbon & Graphene - Auditorium - Oral presentation - Abstract ID: 280**

***Prof. Maria Benelmekki*** [1], ***Dr. Jeong-Hwan Kim*** [2]

***1.*** *NTNU,* ***2.*** *Yokohama City University*

Hybrid inorganic nanomaterials that combine two or more component into one nanostructure have experienced a substantial progress in terms of the design and synthesis processes. Such complex structures have the potential to combine magnetic, plasmonic, semiconducting and other physical or chemical properties into a single object, allowing enhanced and often new functionalities resulting from the synergetic combinations of parent properties. Herein, we present a novel method for generating magneto-plasmonic carbon-nanofilms and nanoscrolls using a combination of two gas-phase synthetic techniques. Ternary Fe@Ag@Si ``onion-like'' nanoparticles (NPs) are produced by a magnetron-sputtering-inert-gas-condensation source and are in-situ landed onto the surface of carbon-nanofilms, which were previously deposited by a DC-arc-discharge technique. Subsequently, a polyethyleneimine-mediated chemical exfoliation process is performed to obtain carbon-nanoscrolls (CNS) with embedded NPs (CNS-NPs). The carbon nanofilms undergo an interfacial transition upon deposition of NPs and become rich in the sp2 phase. This transformation endows and enhances multiple functions, such as thermal conductivity and the plasmonic properties of the nanocomposites. The obtained nanocomposites were evaluated as a Surface-Enhanced-Raman-Scattering (SERS) agents for ATP biomolecules, and showed a high Enhanced Factors (EF) allowing the detection of ATP molecules at concentrations of 10-10 M. In addition, CNSs-NPs showed an enhanced single- and two-photon fluorescence, in comparison with pristine CNSs and NPs. The photothermal response of CNSs-NPs suspension was monitored and showed higher performance as well as.

# Evaluation of a novel tool for the study of early metastasis based in B16F10 murine melanoma cells labeled with Cd-Te Quantum Dots.

**Friday, 11th November - 18:45 - Video Presentations - Video presentation - Abstract ID: 522**

***Mr. Víctor Díaz-García*** [1], ***Dr. Simon Guerrero*** [1], ***Dr. Marcelo J Kogan*** [1], ***Dr. Andrew Quest*** [1], ***Dr. José Pérez-donoso*** [2]

***1.*** *University of Chile,* ***2.*** *Universidad Andres Bello*

Many studies have proposed the use of fluorescent semiconductor nanoparticles or quantum dots (QDs) as new experimental tools to label cells and tumors due to their unique optical properties (high extinction coefficient, stability, increased brightness, etc.) in comparison with organic dyes. However, the use of QDs is limited by their toxicity in biological systems, mostly associated with Cd+2 release and reactive oxygen species (ROS) generation. Also, little is known about the effects of QDs on the metastatic capacity of cancer cells. With this in mind, we developed a methodology that permits obtaining viable B16F10 cells(syngeneic murine melanoma cells with C57BL/6 mice, widely used in metastasis studies) labeled with QDs to then study their behavior in migration and metastasis assays. The effects of QDs uptake on viability, proliferation, migration and invasiveness of B16F10 cells were determined in the absence or presence of N-acetylcysteine (NAC). Then, QDs-labeled B16F10 cells with in vitro migration parameters similar to control cells were selected and injected into C57BL/6 mice to evaluate their metastatic potential. Fluorescence levels associated with QDs uptake in different organs of the mice were determined at 5 min, 30 min, 1 h, 6 h and 24 h post injection. Our results suggest that QD-labeling of B16F10 cells severely reduces viability but that treatment with NAC significantly improves both labeling of cells and viability. Migration of QDs-labeled B16F10 cells was enhanced due to the production of ROS, but treatment of labeled cells with NAC prior to the assays reduced these parameters to control levels. On the other hand, proliferation and invasion by QDs-labeled B16F10 cells was reduced even following NAC treatment. In vivo assays show that QDs-labeling permits short-term tracking of B16F10 cells in the lung following intravenous injection into the tail vein(attached image), but these cells were unable to generate lung metastasis after 21 days. Our results suggest that B16F10 cells labeled with QDs could be used for monitoring early steps in the process of lung metastasis.

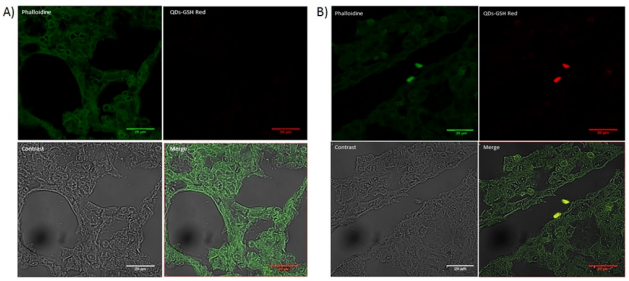


**Determination of QDs-labeled B16F10 cells present in lung of C57BL/6 mices.** By analysis of histological sections by confocal microscopy was determinated the presence of QDs-labeled B16F10 cells (Red) in lungs of C57BL/6 mice after 6 hours postinjection. Lung cells were labeled with phalloidine (green). A) Images of histological sections of lungs of C57BL/6 mice inoculated with B16F10 cells. B) Images of histological sections of lungs of C57BL / 6 mice inoculated with QDs-labeled B16F10 cells.

Qds-labeled b16f10 cells in lung.jpg

# Authors Index


Abd Elhafez, M. 80
Abdala, A. 162
Abduloglu, Y. 198
Acharyya, D. 45
Aguilera Peral, U. 188
Ahmad, I. 229
Ahn, H. 7
Ahn, S. 170
Ajarroud, A. 131
Ak, M. 193, 196--198, 209
Akinoglu, E. 40, 235
Al Amri, F. 161
Al Dosari, M. 80
Albu, C. 212
Alejo, T. 106
Alemu, H. 107
Alexyuk, M. 139
Alexyuk, P. 139
Alkama, R. 27
Alrekabi, S. 168
Ameur, N. 218
Amini Horri, B. 69, 112
Amoresano, A. 210
Andreoli, E. 170
Antic, B. 190
Anutgan, M. 121, 124
Anutgan, T. 121, 124
Apak, R. 200
Aquino, R. 163
Arbet, J. 116
Arbiol, J. 3, 18, 214
Arenal, R. 206
Arruebo, M. 106
Asar, T. 159
Atilgan, I. 121, 124
Avotina, L. 71, 123
Ayat, M. 120, 135, 183
Aydogdu, M. 15
Azizzadeh, f. 103

Bachir, R. 218
Bahatti, A. 230
Baik, M. 43
Baisariyev, M. 58
Bajda, S. 110, 228
Bakranova, D. 226
Balcytis, A. 66, 224
Baranowska Korczyc, A. 204
Barinas, D. 178
Barkalina, N. 233
Barlow, A. 230
Barrera Bogoya, A. 178
Barron, A. 170
Barroso, J. 141
Barylyak, A. 205
Bastidas, K. 98, 178
Bedi, K. 167
Bedrane, S. 218
Beisenkhanov, N. 226
Belhaneche Bensemra, N. 28
Belhousse, S. 28
Belli, V. 83
Belogorlov, A. 175
Bendova, M. 151
Benelmekki, M. 240
Benicek, L. 72
Berestok, T. 219
Berezin, V. 139
Berk, D. 239
Berouaken, M. 27
Berrichi, A. 218
Besnard, C. 149
Bhattacharyya, K. 216
Bhattacharyya, P. 45, 53
Biondi, M. 83
Blazquez, O. 152, 155
Bobitski, Y. 205
Bogoyavlenskiy, A. 139
Boudjouan, F. 50
Boukherroub, R. 183
Boyali, E. 159
Boyer, C. 129
Bozkurt, Y. 15
Brangule, A. 105

Braun, M. 12
Briosne Frejaville, C. 224
Brito, P. 163
Bruyere, S. 59
Budnyk, A. 207
Bugárová, N. 199
Bulyarskii, S. 96
Butoi, B. 71
Byrkin, V. 175

Cabot, A. 93, 169, 214, 219
Cadavid, D. 169
Calin, B. 212
Calin, M. 100
Campos, A. 163
Cantelar, E. 24
Cantisani, M. 83
Carsughi, F. 51
Carta, M. 170
Cavalli, S. 70
Chae, s. 134
Chelouche, A. 50, 182
Cheng Keong, C. 69
Chikhradze, M. 42
Chikhradze, N. 42
Chiriac, L. 132
Cho, M. 43, 49
Choi, Y. 49
Choukchou Braham, A. 218
Chung, I. 143
Cojocaru, G. 123
Colombo, M. 219
Colomer, J. 206
Constantinescu, C. 100
Corbi, P. 13
Cornelius, A. 55
Coulter, T. 188
Coward, K. 233
Coy, E. 204
Cundy, A. 168

Dalmases, M. 101, 169
Daniš, S. 195
Dao, D. 65
Darwish, S. 80
Davidson, L. 233
De La Mata, M. 214
De Wael, K. 82
Delgado Pérez, T. 149
Demitri, N. 123
Demo, P. 203
Deokar, G. 206
Depeyrot, J. 163
Dervaux, J. 206
Diaz Garcia, M. 156
Dinca, P. 71
Ding, Y. 188
Dinh, T. 65
Diraki, A. 162
Diéguez, L. 236
Djouadi, D. 50, 182
Dobosz, P. 94
Dogan, A. 68
Dojcinovic, B. 190
Drbohlavová, J. 16
Dronov, A. 11
Dubal, D. 165
Dubiel, B. 56
Dubkov, S. 96
Dudin, A. 9
Durur, S. 209
Durães, L. 164
Dutt, S. 88
Dyrnesli, H. 128
Díaz García, V. 241

Egami, C. 185
Ekren, N. 15
Elmarzugi, N. 80
Elomar, F. 61
Epple, M. 88, 114
Ersoz, A. 102
Esmaily, S. 5
Espina, B. 236
Espinosa Garcia, C. 188
Estrade, S. 101, 169, 219

Farcasanu, A. 132
Farmilo, N. 153
Fernandez Arguelles, M. 236
Fernàndez Altable, V. 169
Figuerola, A. 101, 169
Foisal, A. 65
Fujiki, A. 117
Fukunaga, H. 41
Fumihiro, N. 136

Furukawa, t. 126

Gabalis, M. 66
Gabouze, N. 27, 28, 120, 135, 183, 208
Gaburro, J. 230
Gago Fernandez, R. 59
Gaidau, C. 100
Galiceanu, M. 132
Gallo, J. 236
Galán Mascarósc, J. 18
Gambaryan, K. 157
García Juan, H. 106
Garrido, B. 152, 155
Gavasheli, T. 108
Gavrilin, I. 11
Gavrilov, S. 9, 11, 96, 227
Gegechkori, T. 108
Genç, A. 18
Ghelich, p. 191
Ghosh, J. 63
Giardina, P. 210
Giba, A. 59
Giersig, M. 40, 235
Gilles, P. 88
Gomes, V. 78
Gomez Romero, P. 165
Gong, H. 113
Govindan Nair, B. 142
Grabulosa, A. 214
Gracia, M. 24
Grigorescu, C. 123
Grinyte, R. 141
Gromov, D. 96, 227
Gross, K. 105
Grześkowiak, B. 204
Guardia, P. 219
Guarnieri, D. 83
Guerrero, S. 241
Gumusay, O. 196
Gunduz, O. 15
Gurbuz, M. 68
Guzel, R. 102
Guénée, L. 149

Haam, S. 37, 81, 86, 147, 202, 231
Hadjoub, I. 182
Hale, S. 188
Hallé, S. 73
Han, L. 18
Han, S. 81, 85, 86
Hassani, F. 5
Hauser, A. 149
He, Y. 18
Hedayatifar, L. 5
Hernandez, S. 152, 155
Honey, S. 229
Hong, T. 97
Horwat, D. 59
Hrubčín, L. 116
Hubalek Kalbacova, M. 12
Hubalek, J. 151
Hudaib, B. 78
Huh, Y. 37, 81, 147, 231
Hui Hui, L. 112
Huran, J. 32, 116
Hwang, H. 46

Ibáñez, M. 169
Ignat, M. 100
Ihara, H. 22
Indyka, P. 56
Ional, L. 212
Iordanova, E. 212
Ishii, T. 22
Ishizaki, T. 126, 222
Ismadi, A. 238
Issa, A. 61
Ito, Y. 142
Iwamoto, T. 8
Izquierdo Lorenzo, I. 61

J.M, C. 236
Jana, A. 213
Janani, R. 153
Jancar, B. 190
Jang, E. 86, 231
Jang, S. 39
Janíček, F. 32
Jasiurkowska Delaporte, M. 204
Jeon, D. 97
Jeong, J. 49
Jeong, K. 43, 49
Jin, J. 184
Jin, S. 184
Jo, N. 184
Jones, C. 233

Jradi, S. 61
Juodkazis, S. 66, 224
Jurga, S. 204
Jurjiu, A. 132, 133

Kabanau, D. 176, 177
Kaczmarczyk, J. 40, 235
Kaim, A. 34
Kamer, G. 200
Kang, A. 202
Kang, B. 81, 86, 231
Kang, H. 43
Kang, T. 109
Karatas, E. 197
Karuk Elmas, Ş. 102
Katia, A. 208
Kawakami, Y. 187
Kazakov, V. 181
Kechouane, M. 120, 135
Keffous, A. 120
Kermad, A. 135
Khainakova, O. 156
Khorsandi, D. 5
Khorshidizadeh, M. 191
Khudhair, D. 230
Ki, J. 86
Kim, D. 43, 109
Kim, G. 37, 147
Kim, H. 43
Kim, J. 202, 240
Kim, K. 46
Kim, M. 37, 85, 147
Kim, T. 143
Kim, Y. 46, 119
Kitsyuk, E. 96
Kobylinska, N. 156
Kogan, M. 241
Koh, W. 85
Korkmaz, B. 159
Kouki, S. 136
Kovalenko, M. 169
Kozisek, Z. 203
Kościński, M. 204
Kruk, A. 56
Krzyzanowski, M. 110, 228
Kukreja, A. 231
Kukushkin, S. 226
Kulveit, J. 203
Kumar, N. 221
Kumar, R. 55
Kumar, S. 213
Kurihara, S. 20
Kus Liśkiewicz, M. 205
Kusumawardani, C. 158
Kuwahara, Y. 20, 22
Kwiecien, M. 110

Laguna, M. 24
Laid, H. 182
Lampropoulos, A. 168
Lasmi, K. 28
Lastovina, T. 207
Lebedev, E. 227
Lebiadok, Y. 176, 177
Lee, B. 52
Lee, C. 43, 172
Lee, D. 52, 109
Lee, G. 46
Lee, K. 85, 134
Lee, S. 143
Lee, T. 202
Leong, K. 238
Leszczynska, D. 205
Li, X. 224
Liu, Z. 78
Llobet, E. 206
Llorca, J. 169, 214
Lokumcu, F. 103
Loreto, s. 82
Lovergine, N. 47
Lungu, C. 71, 123
Lungu, M. 123
Luo, Z. 214
López Conesa, L. 169
López Vidrier, J. 155

M De La Fuente, J. 24
M, M. 236
M.F., C. 236
Maaza, M. 229
Madadi, Z. 5
Magadzu, T. 26
Majta, J. 110
Makarchuk, V. 181
Malhotra, M. 167
Mamniashvili, G. 108

Maniecki, T. 96
Manna, L. 173
Mansour, S. 80
Marcu, A. 71, 123, 212
Marik, M. 151
Marin, A. 123
Marino, E. 152
Marken, F. 170
Marti, S. 214
Marzo, F. 47
Masoudi, A. 5
Masui, Y. 8
Mata, M. 18
Matsumoto, S. 22
Matějová, L. 195
Mau, A. 224
Mckeown, N. 170
Menari, H. 27, 120
Merinska, D. 72, 74
Merkoçi, A. 165, 174
Meunier, J. 239
Meynen, V. 82
Meyns, M. 214
Mhammedi, K. 208
Mierczyński, P. 96
Mikolasek, M. 32, 116
Min, J. 81, 86
Ming, Y. 190
Mitra, D. 63
Mičušík, M. 199
Mocioiu, A. 94
Moganedi, K. 26
Mohammadali Fam, A. 191
Molina, P. 35
Monti, D. 210
Morante, J. 1, 18
Moskalewicz, T. 56
Mozalev, A. 151
Muller, G. 214
Mun, B. 86
Muñoz, L. 35
Mézailles, N. 216
Mücklich, F. 59

Nachtegaal, M. 169
Nafria, R. 214, 219
Nagaoka, S. 22
Nagar, B. 165
Nahavandi, S. 230
Narayan, H. 107
Naseem, S. 229
Navidfar, A. 76
Nechyporenko, G. 205
Netti, P. 70, 83
Neves, A. 234
Ngila, J. 221
Nguyen, D. 129
Niculescu, V. 130, 194
Nomura, Y. 41
Notomista, E. 210
Nussupov, K. 226
Nuñez, N. 24

Ocaña, M. 24
Ognjanovic, M. 190
Oktar, F. 15
Omastová, M. 199
Omirtaeva, E. 139
Onaka, M. 8
Oniashvili, G. 42
Onishi, K. 136
Osada, M. 41
Osipov, A. 226
Ouadfel, M. 120
Oya, T. 44
Ozyurt, D. 200

Pace, A. 188
Packa, J. 32, 116
Palmer, D. 188
Parashar, V. 221
Park, G. 134
Park, J. 134
Park, S. 52, 119, 134
Paryohin, D. 175
Pascone, P. 239
Pastoriza Santos, i. 171
Patel, K. 188
Paun, N. 130
Pavlov, A. 9, 96
Pavlov, V. 141
Peeters, F. 91
Peikertová, P. 195
Peiró, F. 169, 219
Peksen, C. 68
Peplińska, B. 204

Perný, M. 32, 116
Pessine, F. 13
Petica, A. 100
Petruškevičius, R. 66
Phan, H. 65
Pigeat, P. 59
Pimonova, J. 207
Piotrowski, P. 34
Piovan, L. 211
Pires, L. 165
Pirvulescu, V. 194
Piveteau, L. 169
Polievková, E. 16
Politi, J. 210
Porosnicu, C. 123
Presnukhina, A. 227
Prete, P. 47
Prieto, M. 106
Profeta, M. 83
Profirio, D. 13
Prud Homme, R. 180
Pruna, A. 94
Pyatilova, O. 9
Páez, M. 35
Pérez Donoso, J. 241
Přikrylová, K. 16

Qamar, A. 65
Quest, A. 241

Raiola, L. 83
Raja Othman, R. 238
Ramirez, H. 98, 178
Rananga, L. 26
Ray, S. 221
Razika, T. 208
Retraint, D. 228
Rezchikova, E. 181
Rianna, C. 70
Ribeiro De Barros, H. 211
Richter, M. 40, 235
Riegel Vidotti, I. 211
Rinnert, H. 59
Roberts, A. 153
Robinson, A. 188
Rosato, R. 47
Roskamp, M. 188
Rossano, L. 70
Rotan, O. 88
Ruiz González, M. 169
Ruotolo, A. 94
Rybka, J. 40, 235
Ryglova, S. 12
Ryu, S. 109

Saa, L. 141
Saad, W. 180
Saito, K. 31
Salamati, B. 69, 112
Sam, S. 27, 28, 183, 208
Samori, P. 92
Sancak, A. 76
Sanchez, C. 90
Sanchez, s. 4
Sarwar, T. 65
Sasagawa, K. 126
Sasaki, R. 29
Sauerova, P. 12
Savina, I. 168
Savitskiy, A. 9
Say, R. 102
Schrader, T. 88
Sebastián, V. 106
Sedlacek, R. 12
Serizawa, A. 222
Sezimova, H. 195
Shabrov, D. 177
Shafei, S. 230
Shakhnov, V. 181
Shaman, Y. 227
Sharma, H. 167
Shi, J. 78
Shimada, I. 41
Shin, j. 97
Shin, M. 81, 86
Shin, m. 97
Shvets, I. 58
Siepi, M. 210
Sierra, C. 98, 178
Silva, F. 163
Skuratov, V. 116
Smaine, F. 186
Soganci, T. 193, 196, 198, 209
Sokolova, V. 88
Soldera, F. 59
Son, H. 37, 81, 86, 147, 231

Son, J. 97
Song, D. 202
Song, J. 43
Soyleyici, H. 193, 196, 198, 209
Stan, D. 100
Steenhaut, O. 11
Stefano, L. 210
Stevanato, E. 47
Sucharda, Z. 12
Suchy, T. 12
Suenaga, S. 41
Sugurbekova, G. 58
Sul, W. 46, 52
Sun, Y. 136
Sung Han, K. 119
Sunitha Vivek, Y. 69
Sunulu, A. 15
Supova, M. 12
Suzuki, T. 29, 31, 187
Sveshnikov, A. 203
Svyetlichnyy, D. 228

Takafuji, M. 22
Takahashi, N. 41
Takano, M. 44
Talbi, L. 27
Tamaian, R. 130, 194
Tamayo, L. 35
Tang, J. 138
Tang, P. 18
Tawil, S. 238
Tazerout, M. 50
Tefo Thema, F. 229
Terryn, H. 11
Tesarikova, A. 72, 74
Tighilt, F. 28
Tissot, A. 149
Torruella, P. 101, 169
Totani, K. 41
Touam, T. 50, 182
Toufaily, J. 61
Trabzon, L. 76
Trifonov, A. 96
Troppová, I. 195
Trzeciak, T. 40, 235
Tupy, M. 74
Turcu, F. 132
Turmagambetova, A. 139

Ualibek, O. 58
Ungureanu, R. 123
Urbonas, D. 66
Ursescu, D. 123
Ustarroz, J. 11

Vaideanu, A. 145
Vales, P. 155
Van Der Meer, S. 114
Vareda, J. 164
Vasimalai, N. 236
Vaškevičius, K. 66
Ventre, M. 70
Verdanova, M. 12
Vidal, A. 101
Viespe, C. 71
Vignaud, D. 206
Vilas Boas, V. 236
Vinches, L. 73
Vomiero, A. 2
Vranjes Djuric, S. 190
Váry, M. 116

Wada, M. 22
Wang, H. 153
Watts, C. 145
Welland, M. 145
Wendler, A. 145
Whitby, R. 168
White, M. 55
Wiley, D. 78
Williams, P. 188
Winum, J. 186
Wojnarowska Nowak, R. 205
Woo, Y. 109

Yaddaden, C. 135
Yamaguchi, Y. 20
Yamashita, K. 41
Yankov, G. 212
Yanxon, H. 55
Yeom, M. 202
Yeste, M. 233
Yildirim, K. 76
Yoo, D. 52
Yoo, H. 46, 52

Zaitceva, I. 139
Zaitsev, V. 156

Zaloudkova, M. 12
Zapien, J. 94
Zemzem, M. 73
Zhang, H. 190
Zhang, L. 18
Zhang, X. 18
Zinchenko, L. 181
Zinchenko, V. 205
Zulkifili, A. 117
ÇetİN, S. 159
Öztürk, B. 200
ÖzÇelİk, S. 159
ŞahİN, A. 15
Šiffalovič, P. 199
Špitálsky, Z. 199
Šály, V. 32, 116
Żyła, G. 179


Conferences, Events & Workshops